
The University Of Sheffield.

# Synthetic Polymers for Interaction with Vascular Endothelial Growth Factor

Louisa Jean Gilmore

Submitted for the degree of Doctor of Philosophy

Department of Chemistry, University of Sheffield

June 2009

## Declaration

This thesis is submitted to the University of Sheffield for the degree of Doctor of Philosophy, having not been submitted to any other University for any degree. I declare that all work contained herein is my own work, except where referenced and acknowledged accordingly.

.....

Louisa Gilmore

June 2009

## Acknowledgements

I would like to thank my supervisors, Dr Stephen Rimmer and Professor Sheila MacNeil, for their guidance and support throughout this PhD.

The BBSRC is gratefully acknowledged for providing the financial support for this project.

I am very grateful to Dr Tracie Whittle, Dr Sally McArthur, Mr Christopher Hill, Dr Heath Bagshaw, Mr Neil Bramall and Dr David Apperley for help with analysis of my materials. I would also like to thank Mrs Melanie Hannah for much appreciated technical assistance. Special thanks must also go to Dr Lynne Perlin and Dr Arthur Moir for advice on peptide synthesis, Dr Steven Carter for advice on polymer synthesis and Dr Louise Smith and Dr Emilia Krajewska for considerable help and support with cell culture.

I wish to thank the members of both the Polymer and Biomaterials Laboratory in the Chemistry Department and the Tissue Engineering group at the Kroto Research Institute and the related technical staff for help and support, as well as for providing an enjoyable environment in which to carry out my research.

Finally I would like to thank my family and Dan for their support and encouragement throughout.

## Abstract

Angiogenesis, the formation of new blood vessels from previously established blood vessels, is a vital process within wound healing and is regulated by a number of stimulators and inhibitors. A critical pro-angiogenic factor is Vascular Endothelial Growth Factor (VEGF), which stimulates cell growth, survival and proliferation upon binding with and activating two specific receptors on the endothelial cell membrane. This binding is influenced by interactions with heparin-like glycosaminoglycans.

The aim of this project was to synthesise a biomaterial dressing which would be able to bind and release the patient's own bioactive VEGF within a wound area, thereby stimulating angiogenesis through treatment with VEGF without the need to deliver external growth factors. Two systems were developed to meet this aim.

Core-shell molecularly-imprinted particles (CS-MIPs) with phosphate functionality were developed via the epitope approach to produce VEGF-binding particles. CS-MIPs were synthesised in the presence of a pentapeptide template (DKPRR) and were able to bind and release both this pentapeptide and $VEGF_{165}$, although a molecular imprinting effect was only observable upon peptide binding and release. Phosphate-functionalised core-shell particles were shown to bind and release $VEGF_{165}$, maintaining its biological activity for up to 48 hours.

Crosslinked hydrogels of N-vinyl-2-pyrrolidone and acrylic acid were functionalised with synthetic trilysine and triarginine peptides to produce materials capable of interacting with VEGF via heparin. These basic peptide sequences were able to interact with the highly sulphated heparin which in turn was able to interact with the heparin-binding domain of $VEGF_{165}$. These hydrogels were able to bind and release bioactive $VEGF_{165}$ and cytocompatibility was confirmed *in vitro* with primary human dermal fibroblasts and human dermal microvascular endothelial cells (HDMECs). VEGF- and heparin-bound triarginine-functionalised hydrogels stimulated HDMEC proliferation and had a significant directional effect on HDMECs, which formed tubules directed towards these materials in an *in vitro* angiogenesis assay.

# Contents Page

# Abbreviations

| | |
|---|---|
| AA | Acrylic acid |
| ADH | Alcohol dehydrogenase |
| AIBN | α,α'-azobisisobutyronitrile |
| ANOVA | Analysis of variance (statistical test) |
| BSA | Bovine serum albumin |
| CAM | Chick chorioallantoic membrane |
| COOH | Carboxylic acid |
| CS-MIP | Core-shell molecularly-imprinted particle |
| Cyt-C | Cytochrome C |
| DCC | Dicyclohexylcarbodiimide |
| DEGBAC | Diethyleneglycol bisallylcarbonate |
| DIPEA | Diisopropylethylamine |
| DKPRR | Aspartic acid-lysine-proline-arginine-arginine peptide |
| DMEM | Dulbecco's modified eagles medium |
| DMF | Dimethylformamide |
| DMSO | Dimethyl sulphoxide |
| DVB | Divinylbenzene |
| ECM | Extracellular matrix |
| EDC | 1-ethyl-3-(3-dimethylaminopropyl)carbodiimide |
| EDS | Energy dispersive spectroscopy |
| EGDMA | Ethylene glycol dimethacrylate |
| ELISA | Enzyme-linked immunosorbent assay |
| EtOH | Ethanol |
| EWC | Equilibrium water content |
| FACS | Fluorescence-activated cell sorting |
| FCS | Foetal calf serum |
| FGF | Fibroblast growth factor |
| GAA | Glycine-alanine-alanine peptide |
| GAG | Glycosaminoglycan |
| GC | Gas chromatography |
| HAEC | Human aortic endothelial cell |
| HBTU | 2-(1H-Benzotriazole-1-yl)-1,1,3,3-tetramethyluronium hexafluorophosphate |
| HCl | Hydrochloric acid |
| HDMEC | Human dermal microvascular endothelial cell |
| HOBt | N-Hydroxybenzotriazole |
| HPLC | High performance liquid chromatography |
| HS-GAG | Heparin/heparan sulphate glycosaminoglycan |
| HUVEC | Human umbilical vein endothelial cell |
| ICP-AES | Ion-coupled plasma atomic emission spectroscopy |
| IL-8 | Interleukin-8 |
| IPA | Isopropyl alcohol (Propan-2-ol) |
| KGF | Keratinocyte growth factor |
| KKK | Trilysine peptide |
| KKKKKK | Hexalysine peptide |
| MES | 2-Morpholinoethanesulfonic acid |
| MIP | Molecularly-imprinted polymer |
| MTT | 3-(4,5-Dimethylthiazol-2-yl)-2,5-diphenyltetrazolium bromide |

| | |
|---|---|
| MW | Molecular weight |
| NHS | N-hydroxysuccinimide |
| NMR | Nuclear magnetic resonance |
| NVP | N-vinyl-2-pyrrolidone |
| OPHP | Oleyl phenyl hydrogen phosphate |
| PBS | Phosphate buffered saline |
| PDGF | Platelet-derived growth factor |
| PIGF | Placenta growth factor |
| PLG | Poly(lactide-co-glycolide) |
| PND | Poly(NVP-co-DEGBAC) hydrogel |
| PNDA | Poly(NVP-co-DEGBAC-co-AA) hydrogel |
| PNDKKK | Poly(NVP-co-DEGBAC-co-AA) hydrogel functionalised with KKK peptide |
| PNDRRR | Poly(NVP-co-DEGBAC-co-AA) hydrogel functionalised with RRR peptide |
| PVP | Poly(N-vinyl pyrrolidone) |
| PRKRD | Proline-arginine-lysine-arginine-aspartic acid peptide |
| RGD | Arginine-glycine-aspartic acid (cell adhesion peptide) |
| RRR | Triarginine peptide |
| SDS | Sodium dodecyl sulphate |
| SEM | Standard error of mean |
| SIMS | Secondary ion mass spectrometry |
| SSSSSSSS | Octaserine peptide |
| TCP | Tissue culture polystyrene |
| TEMED | N,N,N',N'-Tetramethylethylenediamine |
| TGF | Transforming growth factor |
| THF | Tetrahydrofuran |
| TNBS | Trinitrobenzenesulphonic acid |
| TNF | Tumour necrosis factor |
| ToF-SIMS | Time-of-flight secondary ion mass spectrometry |
| UV | Ultra-violet |
| VEGF | Vascular endothelial growth factor |
| VPF | Vascular permeability factor |
| Wt% | Weight percent |
| XPS | X-ray photoelectron spectroscopy |

# 1 Introduction

## 1.1 The Skin

The skin is the largest organ of the human body and plays a crucial role through the regulation of water and electrolyte balance, thermoregulation, and by acting as a barrier to external agents[1]. The skin consists of two principal layers, the epidermis and the dermis (Figure 1.1).

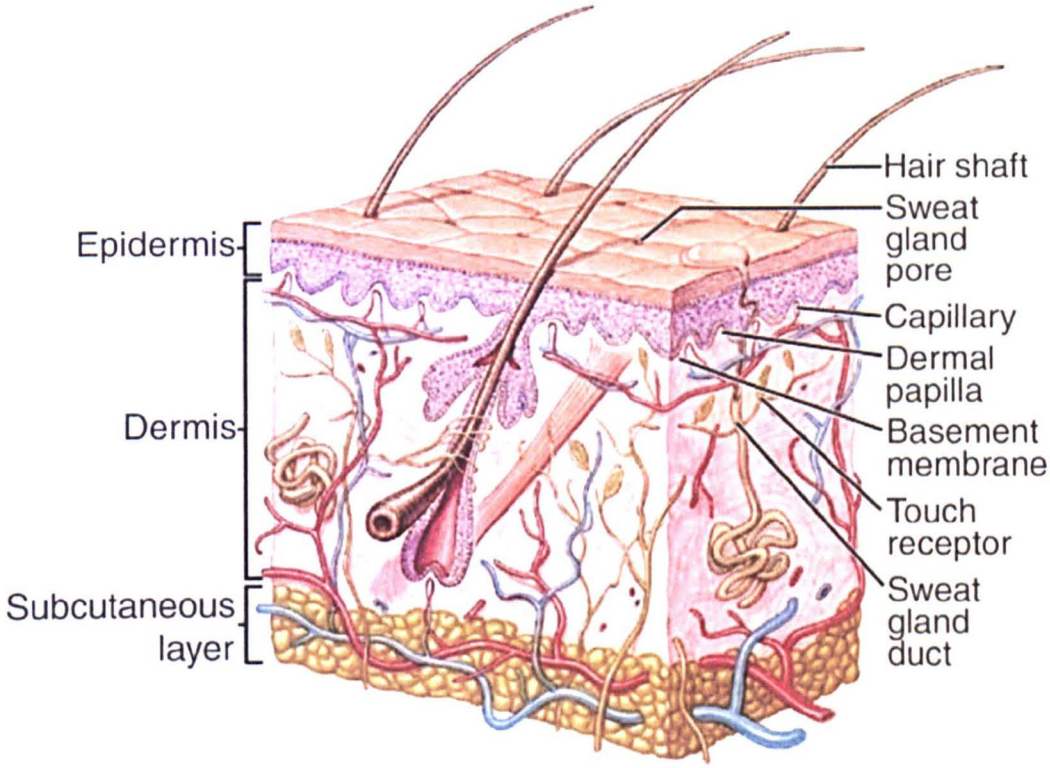


**Figure 1.1: The structure of human skin†**

The epidermis is the outer layer of skin, comprising four layers, primarily consisting of stratified squamous epithelium. The basal cell layer is the deepest layer of the epidermis and is the location of keratinocyte mitosis, the process of cell division, supplied with nutrients from blood vessels in the adjacent dermis. As mitosis occurs, cells migrate upwards to replenish outer layers of cells. At any given time, up to 30% of the keratinocytes in this layer are preparing to divide[2]. Above the basal cell layer are the spinous layer, the granular cell layer and the stratum corneum. These layers reflect the visible changes along the continuous process of keratinocyte maturation from basal

† Adaptation of Figure 6.2 reprinted from *Hole's Human Anatomy & Physiology,* 8th Edition, Shier, David; Butler, Jackie; Lewis, Ricki, Copyright1999 McGraw-Hill. Permission requested 15/05/09

layer to stratum corneum (reviewed by Powell et al[2]). In the spinous layer the cells are connected by spine-like cohesive desmosomes. In the granular cell layer the cells flatten and contain granules, lysozymes which cause cell death by destroying the cell's organelles, including the nucleus. Finally, in the stratum corneum, the keratinocytes are flat, dead cells. The cells overlap and have thick cell membranes which adhere to each other to provide the barrier functionality of skin. Gradually these cells are removed and are replaced with cells from the underlying layers of epidermis.

Below the epidermis is the basement membrane, a layer which adheres the two layers, supports the basal cells and allows nutrients and cells to move to the epidermis from the dermis[2]. Below the basement membrane is the dermis which contains a number of cell types including fibroblasts, macrophages, mast cells and white blood cells[3]. This layer consists of dense, fibrous connective tissue, predominantly collagen and elastin. The texture of the collagen fibres gives rise to two layers within the dermis, the papillary layer and the reticular layer[3]. The papillary layer at the top of the dermis makes up approximately 20% of the dermis thickness and consists of loosely woven collagen and elastin fibres and numerous blood vessels. The reticular layer consists of larger, coarser connective tissue with a network of blood vessels present between the dermis and the subcutaneous layer. The dermis has numerous functions including mechanical strength, a substrate for diffusion of nutrients and waste and immune system functions[2]. Finally, the innermost layer of the skin is the subcutaneous layer[4]. It contains fat cells which vary in number depending on the area of the body. This layer loosely binds skin to the underlying organs.

The skin can be disrupted due to a number of different problems, including ulcers, burns and trauma, resulting in the loss of barrier function of this crucial organ. A major loss of barrier function can result in bacterial entry, sepsis and death in, for example, severe burns injuries. It is clear therefore that it is of great importance to restore skin integrity as soon as possible.

## 1.2 Wound Healing

A wound is "a defect or break in the skin which occurs as a result of physical or thermal damage, or an underlying medical or physiological condition"[5]. Severe wounds can be classified by the repair process and are described as acute or chronic. Acute wounds (generally tissue damage caused by external forces) will usually heal completely over a reasonable time-frame unless extensive skin loss occurs, whereas chronic wounds are those which fail to heal in the normal manner, or become fixed in any stage of the healing process for six weeks or more[6]. Chronic wounds are predominantly venous, pressure or neuropathic ulcers[7].

Wound healing is a complex, dynamic process involving the coordinated actions of both resident and migratory cell populations which repair injured tissue and restore skin functions. The process of wound healing is often described as having three to five main stages (depending on how the events are linked by the author) which overlap in time. In this thesis a brief overview of wound healing is provided as detailed discussions of wound healing can be found in a number of review articles[8-11]. The process occurs with the four main events of haemostasis, inflammation, proliferation and maturation.

1. Haemostasis

Upon injury, blood vessels are ruptured, activating haemostasis, the stoppage of bleeding by platelet aggregation, clot formation and vasoconstriction[7]. Cytokines and growth factors are released during this phase, promoting clotting and enlisting critical cellular elements for wound healing.

2. Inflammation

Inflammation occurs almost simultaneously with haemostasis. This stage often occurs from a few minutes to 24 hours after the initial injury and lasts for around 3 days[5]. This stage is triggered by the mediators released in the haemostasis process as well as by injured tissue and capillaries. Vasodilation allows infiltration by immune cells and phagocytosis occurs, with neutrophils present to contain any microorganisms and macrophages present to ingest necrotic tissue[12]. Macrophages also release further cytokines which regulate the wound healing process[10]. After this stage the wound should be clean, bleeding should have been halted and the proliferation stage can begin.

3. Proliferation

The proliferation stage consists of a number of events[9]. Fibroblasts migrate from surrounding tissue and deposit granular tissue, consisting of numerous substances including fibronectin, hyaluronan and other extracellular matrix (ECM) compounds. This process is known as granulation, which replaces the fibrin clot and provides the skin with strength and form. The flow of blood to the tissue is restored through the process of angiogenesis, the formation of new blood vessels via the migration of endothelial cells into the site of injury. Re-epithelialisation then occurs as keratinocytes completely cover the wound. This involves keratinocyte proliferation and migration from the edges of the wound bed. Migration stops once the cells from opposite sides of the wound bed meet. The reepithelialisation which occurs re-establishes the skin barrier.

4. Maturation

Finally, maturation, or remodelling, of the granular tissue occurs to produce mature connective tissue, and the density of cells is reduced by apoptosis[9]. This process is important as the rate, quantity and total amount of matrix deposition determines the strength of the scar tissue[11].

## 1.3 Angiogenesis: The Formation of New Vasculature

The growth of new blood vessels through angiogenesis is a fundamental requirement for a developing embryo but is less common in adults[13], occurring primarily in the female reproductive cycle and in wound healing. It has been related to pathological conditions including diabetic retinopathy, rheumatoid arthritis and tumour development[14].

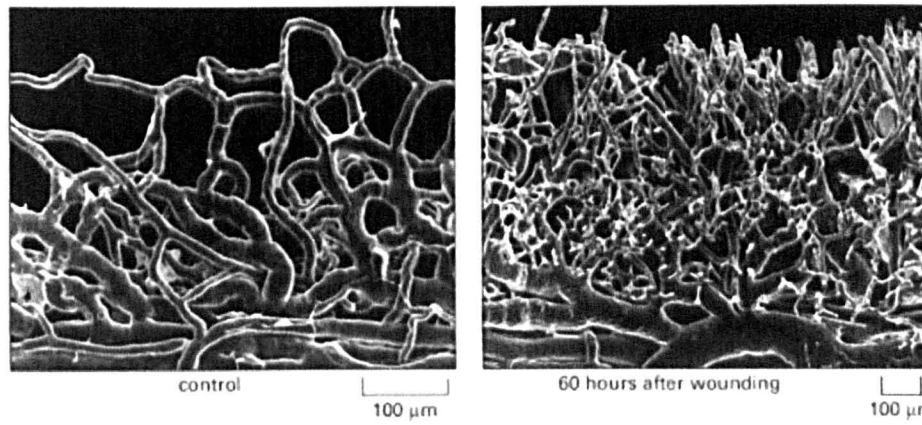


**Figure 1.2: New capillary formation in response to wounding. Scanning electron micrographs of casts of the system of blood vessels surrounding the margin of the cornea. Sixty hours after wounding new capillaries sprout toward the site of injury, just above the picture, showing the response of the endothelial cells to an angiogenic factor released at the wound†.**

Healing in wounds occurs as a sequential cascade of overlapping processes that requires the coordinated completion of a variety of cellular activities. As previously discussed, wound angiogenesis occurs during the proliferative stage of wound healing and such healing, other than the most superficial, could not occur without this process. Damaged vasculature must be repaired in the wound site to allow epithelialisation and the cellular activity required by wound healing would not be possible without the nutrient supply from the restored bloodstream[15]. Therefore angiogenesis is a critical early stage component of wound healing.

Angiogenesis involves a number of sequential events, closely regulated by a number of angiogenic stimulators and inhibitors. Stimulators include vascular endothelial growth factor (VEGF), fibroblast growth factor-1 (FGF-1), fibroblast growth factor-2 (FGF-2), transforming growth factor-α (TGF-α), transforming growth factor-β (TGF-β), platelet-derived growth factor (PDGF), tumor necrosis factor-α (TNF-α), pleiotropin,

† Reproduction of figure 22-27 reprinted from *Molecular Biology of the Cell,* Alberts, Bruce; Johnson, Alexander; Lewis, Julian; Raff, Martin; Roberts, Keith; Walter, Peter, 4th Edition, Garland Science, New York, USA, Copyright 2002. Permission requested 15/05/09

angiogenin, and interleukin-8 (IL-8). Inhibitors include thrombospondin, cartilage-derived inhibitor, angiostatin, platelet factor 4, and interferon-α and interferon-β[13]. Angiogenesis is controlled by the balance between stimulators and inhibitors, and in health there is an exact and coordinated balance between the two.

The process of angiogenesis involves a number of coordinated events[16] (Figure 1.3). Firstly angiogenic growth factors are released by injured tissue, diffuse into nearby tissue and bind to specific endothelial cell receptors on pre-existing blood vessels, initiating a cascade of events. Vasodilation occurs, increasing vascular permeability in response to vascular endothelial growth factor (VEGF). This allows release of plasma proteins which produce a provisional scaffold for endothelial cell migration[17, 18]. Vasodilation is followed by proteolytic degradation of the basement membrane and extracellular matrix[19]. The endothelial cells then proliferate and migrate towards the injured tissue, regulated by chemotactic, haptotactic and mechanotactic stimuli, with further ECM degradation to accommodate the sprouting vessel[20]. The sprouting blood vessels, initially present as a solid cord, subsequently form a lumen and are able to increase vessel diameter and length by thinning of the endothelial cells, intercalation or by fusion with other blood vessels[21]. Finally maturation of the blood vessel occurs, including the introduction of mural cells (pericytes or smooth muscle cells), production of basement membrane, specialisation for a specific function or vascular regression[22].

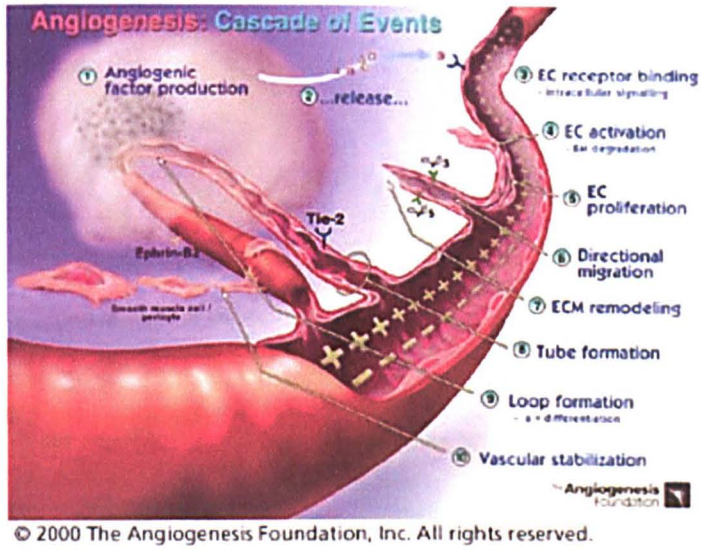



**Figure 1.3: Schematic representation of the events occurring during angiogenesis†**

† Reproduction of an image from the Angiogenesis Foundation. Permission requested 16/04/09. Image from http://www.angio.org/understanding/understanding_archive.html on 18/05/09.

## 1.4 Vascular Endothelial Growth Factor (VEGF)

VEGF (also known as VEGF-A) was identified in media conditioned by bovine pituitary follicular cells by Ferrara et al[23] in 1989. This protein was shown to be the same as Vascular Permeability Factor (VPF) which was identified in 1983 by Senger et al[24]. Ferrara et al[23] showed that the growth factor is heparin-binding, cationic and heat stable, with a molecular weight of approximately 45,000 Da under non-reducing conditions. Under reducing conditions, a molecular weight of ~23,000 Da was determined, suggesting that VEGF is a dimer, comprised of two units with identical molecular weight. It was found to have a unique N-terminal amino acid sequence of Ala-Pro-Met-Ala-Gly and to be a potent mitogen to vascular endothelial cells only.

Since the identification of VEGF there have been numerous publications in this area, detailing its structure as well as its influence in physiological and pathological angiogenesis, and there are many review papers available[13, 21, 25-27]. It is beyond the scope of this thesis to discuss in detail the exact role of VEGF within physiological

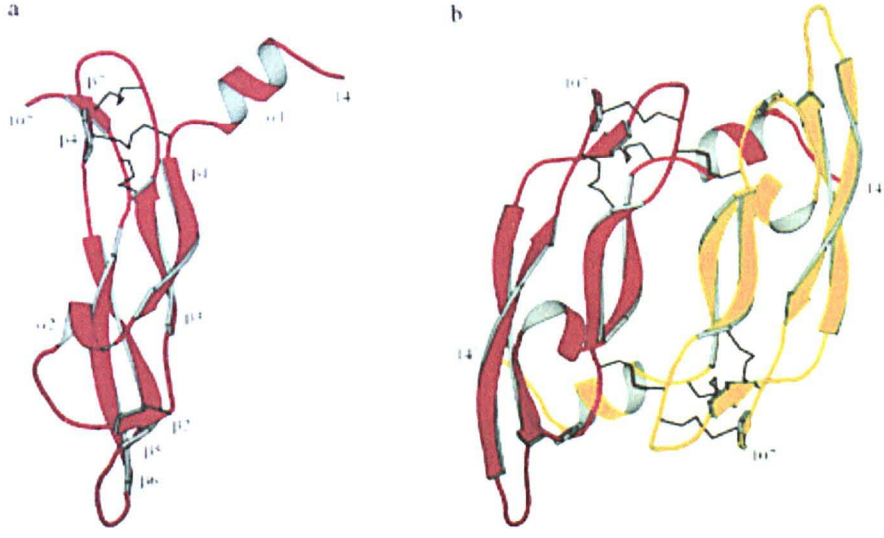


**Figure 1.4: Ribbon representation of a) the receptor-binding domain of VEGF and b) a VEGF dimer. The two disulfide bonds are shown as black lines. Helix a1 consists of residues 16 to 24, and the central four-stranded b-sheet is formed by b1 (residues 27–34), b3 (51–58), b5 (73–83), and b6 (89–99), with the characteristic cysteine knot motif at one end [strands b4 (67–69) and b7 (103–105)], and a short three-stranded b-sheet [strands b2 (46–49), b5, and b6] at the other end. Reproduced from Hoeben et al†**

† Reproduction of figure 1 reprinted from *Pharmacological Reviews*, Vol. 56 no. 4, Hoeben, Ann, Landuyt, Bart, Highley, Martin S., Wildiers, Hans, Van Oosterom, Allan T., De Bruijn, Ernst A., "Vascular Endothelial Growth Factor and Angiogenesis", 549-580, Copyright 2004, with permission from The American Society for Pharmacology and Experimental Therapeutics.

angiogenesis but VEGF is known to play a pivotal role in this process, inducing endothelial cell proliferation and migration, as well as stimulating vascular permeability and hexose transport and playing a role in endothelial cell survival[28]. VEGF is also a regulator of pathological angiogenesis. This was confirmed by Kim et al[29], who demonstrated that monoclonal antibodies for VEGF inhibited the growth of tumours in nude mice.

This protein belongs to a family of VEGF proteins, also including the physiological subtypes; VEGF-B, VEGF-C, VEGF-D and placenta growth factor (PIGF), and the exogenous subtypes; VEGF-E (viral VEGF) and VEGF-F (derived from snake venom)[30]. VEGF was shown to belong to the cysteine knot growth factor superfamily[31]. This family consists of dimeric growth factors which are characterised by a cysteine knot motif at one end of a conserved four-stranded β-sheet within each unit[32]. The 3D structure of VEGF is represented in Figure 1.4.

The human gene for VEGF is present on chromosome 6p21.3[33]. It exists as a number of different molecular species[28], including proteins with 121, 145, 165, 183, 189 or 206 amino acid residues, the molecular heterogeneity being caused by alternative splicing from a single human VEGF gene containing 8 exons. VEGF is produced by many different cell types, including macrophages and T-cells, smooth muscle cells, kidney cells, keratinocytes, mesangial cells, astrocytes, osteoblasts and tumour cells (discussed by Klagsbrun et al[13]), which preferentially express $VEGF_{121}$, $VEGF_{165}$ and $VEGF_{189}$. $VEGF_{183}$ is also widely distributed throughout the body but $VEGF_{145}$ and $VEGF_{206}$ are more rare and seem to be restricted to placental cells[28].

Muller et al[34] reported that VEGF comprises two identical polypeptide chains which are joined together covalently by a pair of disulphide bonds between Cys-51 and Cys-60[34]. They report that the main feature of the protein is a cystine knot motif consisting of an eight residue ring formed by disulphide bridges between Cys-57-Cys-102 and Cys-61-Cys-104 with a third disulphide bond between Cys-26-Cys-68 passing through it. Fairbrother et al[35, 36] reported that various isoforms all share a common amino-terminal receptor-binding domain of 115 residues, with crystal structure of the VEGF species varying in the length of the carboxy-terminal end.

The mitogenic activity of VEGF to vascular endothelial cells involves the growth factor binding with two receptors on the surface of endothelial cells which make up the blood vessels (reviewed by Ferrara et al[26]). These receptors are VEGFR-1 (Flt-1), a fms-like tyrosine kinase[37] and VEGFR-2 (KDR/Flk-1), the kinase domain region[38]. These receptors have a high affinity for VEGF and are also receptors for other similar growth factors.

It was reported by Ferrara et al[23] in 1989 that VEGF is a heparin-binding growth factor. Heparin and heparan sulphate are members of the glycosaminoglycan (GAG) family, a family of linear polysaccharides present on most animal cell surfaces, basement membranes and in the extracellular matrix[39]. Heparin/heparan sulphate glycosaminoglycans (HS-GAGs) comprise a linear chain of 10-200 disaccharide units of N-acetyl-D-glycosamine linked to D-glucuronic acid. Modifications of this disaccharide unit occur, including *N*- and *O*- sulphation, and epimerisation of β-D-glucuronic acid to α-L-iduronic acid, resulting in high heterogeneity of the HS-GAG family[40]. Heparin is a highly sulphated polysaccharide, with an average of 2.7 sulfo groups per disaccharide unit, and the highest negative charge density of any known biological macromolecule, whereas heparan sulphate has less sulphation with a highly varied sequence, often found in the ECM and attached to the cell surface[41]. This family is known to play an important role in the regulation of a number of physiological processes, including cell growth and differentiation, blood coagulation and cell-cell and cell-matrix interactions, and is subsequently widely studied (reviewed by Capila et al[41]). It has been shown that the more basic $VEGF_{189}$ and $VEGF_{206}$ bind heparin with high affinity and are found in the extracellular matrix, whereas $VEGF_{121}$ is an acidic polypeptide, is not heparin binding and is therefore freely diffusible. $VEGF_{165}$ displays intermediate properties, it is heparin-binding and is found in the extracellular matrix, attached to the cell surface and is also secreted[42, 43]. Of particular relevance to this research, all of the heparin-binding forms of VEGF share a 50 amino acid heparin-binding region at the carboxy-terminus[35].

The binding of VEGF with VEGFR-1 and VEGFR-2 has been shown by a number of groups to be significantly influenced by heparin-like GAGs, associated with the cell surface, as well as exogenous heparin and heparan sulphate, and thus the interaction of VEGF with HS-GAGs is vital in the process of angiogenesis[44-47]. Research by Keyt et

al[48] has determined that the binding of $VEGF_{165}$ to heparin is localised to 55 amino acid residues present at the carboxy terminal. Plasmin cleavage of $VEGF_{165}$ was carried out and produced a homodimer which is composed of 2 disulphide-linked amino terminal regions (1-110) ($VEGF_{110}$) and two identical carboxy-terminal fragments (111-165). With the heparin binding domain (111-165) missing, $VEGF_{110}$ lacked the ability to significantly bind to heparin but maintained the ability to bind with the VEGF receptors. However, the carboxy-terminal fragment (111-165) was able to bind with heparin with the same affinity as intact $VEGF_{165}$, demonstrating that the carboxy-terminal is the heparin-binding domain. Further tests on $VEGF_{110}$ showed that removal of the carboxy-terminal fragment substantially decreases the mitogenic potency of VEGF towards the endothelial cell. This suggests that the heparin binding domains influence VEGF-receptor interactions, which are vital for effective signal transduction and stimulation of endothelial cell proliferation.

The extracellular matrix, including glycosaminoglycans as well as collagens, laminin and fibronectin[49], is therefore thought to play an important role in the regulation of heparin-binding growth factors. Associations occur between heparin-binding growth factors and heparan sulphate proteoglycans in the ECM, followed by release of the growth factors, including VEGF, as the ECM is degraded by proteases in a highly localised manner at the cell surface. This association is able to prevent diffusion of the growth factors from the localised area, control the release of the growth factor and modulate the stability and bioactivity of many important angiogenic growth factors, including VEGF[50, 51].

## 1.5 Therapeutic Applications of VEGF

The process of angiogenesis is vital and therefore therapeutic strategies to control angiogenesis by administering angiogenic regulators have become an important research area[52]. A number of growth factors are capable of inducing blood vessel formation and, although research is available detailing administration of synthetic molecules which are reported to induce angiogenesis[53], most strategies employed to achieve this involve the administration of known biological angiogenesis stimulators, primarily VEGF or acidic and basic fibroblast growth factors. The previous discussion of angiogenesis shows the complex biological processes involved, and it is suggested that the therapeutic administration of a combination of angiogenic regulators may lead to the most successful results. Despite this, research has shown that the simplified approach of administering single growth factors, including by bolus injection or polymeric implants, has been trialled for various conditions, and some successes in stimulating angiogenesis in animal and small-scale clinical studies have been reported[54-61].

The simplistic approaches of intravenous or intra-arterial bolus delivery or delivery of VEGF directly into the localised area could lead to a number of potential problems, especially at high doses. Potential hazards (extensively reviewed by Epstein et al[62]) include the development of new blood vessels in non-target tissue, an increase of vascular permeability in non-target tissue and the growth of tumours. This knowledge leads to the widely accepted opinion that low and localised doses of angiogenic growth factors give better results than one-off large doses. Therefore considerable research efforts are currently directed towards synthetic and natural biomaterials which are able to act as protein carriers and provide local and controlled delivery of proteins. This approach is expected to have numerous advantages over bolus injections of the growth factor. Such localised delivery could minimise unwanted side effects and provide a sustained release of growth factor to the target area, thus optimising the therapeutic potential. Release of VEGF from a biomaterial should also be able maintain the bioactivity of the protein in comparison to bolus delivery where the half-life is reported to be less than one hour[63-66]. This approach is expected to lead to safer, more successful treatment, as well as enabling the use of low quantities of growth factor which would be economically advantageous as the VEGF protein is expensive to make or buy.

### 1.5.1 Requirements for Delivery System

In order to produce successful delivery vessels for growth factors it is prudent to mimic the extracellular matrix which is known to regulate the localised release of growth factors in biology. It is also thought to retain growth factors in the local environment, stabilise the active conformation of the growth factors and protect them from inactivation[50, 51]. Thus, numerous biomaterial delivery methods aim to mimic the ECM to deliver bioactive growth factors to specific locations.

When producing a material for a biological application, the material must be non-immunogenic, it must not produce toxic byproducts, it must be suitable for sterilisation and be free of pathogens. For a biodegradable application it must also degrade into non-toxic products which can be removed from the body. For delivery of a growth factor, the material and synthesis route must also protect the growth factor to ensure it remains biologically active. Finally, for clinical applications, the material should be relatively easy to produce and handle, it should also be of reasonable cost and should be a socially accepted approach[51].

### 1.5.2 Current Approaches

A variety of approaches to deliver growth factors are currently under investigation, including diffusion-controlled systems and environmentally-responsive materials. There are already a number of detailed reviews in this area[50, 51, 67, 68], providing many examples of biomaterials for angiogenic growth factor delivery. In this thesis, an overview of the different material approaches will be provided to give an insight into current developments in this area.

#### *Natural Materials*

Natural materials have been used extensively in this area of research, in many cases due to their similarities to the ECM and their biocompatibility. A variety of materials have been investigated including agarose[69] and chitosan[70], but the majority of delivery vessels are based around fibrin, collagen and gelatin, alginate and hyaluronic acid.

The natural presence of fibrin within a wound means that it is a common material for angiogenic growth factor delivery[57, 71, 72]. In a case study reported by Kipshidze et al[57]

of a patient with an ischemic limb, new blood vessels were formed after treatment with VEGF in a fibrin matrix. The fibrin matrix slowed the release of the growth factor and thereby sustained angiogenesis. Wong et al[72] also utilised fibrin in their approach, and showed the binding and release of bFGF, $VEGF_{165}$ and $VEGF_{121}$ from fibrin sealant clots. Delivery of the growth factors alone in a chick chorioallantoic membrane assay led to an angiogenic response, but the blood vessels produced were leaky and immature, whereas more mature vessels were observed as a combination of the growth factors were applied. Ehrbar et al[71] recently covalently bound VEGF to fibrinogen implants utilising a variant of VEGF which crosslinks to fibrinogen by the transglutaminating activity of factor XIII during polymerisation. The protein can then be released by proteolysis rather than diffusion. Histology of an *in vivo* assay at a three week timepoint revealed that VEGF released by proteolysis promoted blood vessel growth significantly more than diffusion-based release. In this method VEGF should only be released when required, thus having a more pronounced effect.

Collagen and gelatin, a natural polymer derived from collagen, are also commonly used biomaterials which have been employed in angiogenic growth factor delivery[73-78]. Collagen hydrogels were produced by Tabata et al[75] with varying amounts of crosslinker to study the release of VEGF and the effect on angiogenesis *in vivo*. They concluded that bioactive VEGF was released upon hydrogel degradation and that the rate of release was determined by the amount of crosslinking. A prolonged angiogenic effect was observed upon VEGF release when subcutaneously implanted in mice. Gelatin microparticles were employed by Patel et al[76] to release VEGF *in vitro* and *in vivo*. Again, release kinetics were shown to be dependent on crosslinking. The microspheres were able to maintain the bioactivity of the VEGF over 14 days, determined by an *in vitro* cell based assay; this was a significant improvement over the bioactivity of VEGF in bolus injections.

Alginate, an anionic polysaccharide derived from algae, forms a hydrocolloid gel when mixed with divalent cations (eg. $Ca^{2+}$)[79]. Simple aqueous gelation which can entrap molecules makes this material popular as a delivery system[65, 80-82]. Elcin et al[82] reported the effect of VEGF release from calcium alginate microspheres on neovascularisation at the subcutaneous site of the rat model, and showed that this system promoted vigorous angiogenesis. More recently Jay et al[65] were able to tune VEGF release by varying the

divalent cation employed and found that VEGF bioactivity could be retained for at least 15 days.

Hyaluronic acid, a non-sulphated GAG, has also been employed in growth factor delivery systems. A considerable amount of the research in this area has been carried out by the groups of Peattie and Prestwich[64, 83-86], who have recently been investigating copolymers of hyaluronic acid and other polysaccharides, which will be discussed further in a later section of this introduction. In 2004 Peattie et al[85] released VEGF and bFGF from hyaluronic acid hydrogels. Release of the growth factors individually *in vivo* resulted in an increase in blood vessel growth in comparison to the hydrogel alone. Interestingly, a synergistic interaction was observed between the GAG and VEGF and as a result, a significantly larger effect was observed for the VEGF-releasing GAG than the other treatment groups. In 2006 Peattie et al[86] analysed the release of VEGF and keratinocyte growth factor (KGF). In this case *in vivo* studies showed the hydrogel containing both KGF and VEGF produced the greatest angiogenic response out of all the treatment groups.

***Synthetic Materials***

There are a number of potential advantages to using synthetic delivery devices over the natural alternatives. Using synthetic materials may reduce the risk of infection and immunogenicity issues in comparison to natural substances and also allows the synthesis of reproducible materials with controllable properties[50]. A variety of different synthetic biomaterials are available today which allow for numerous different approaches to be undertaken.

A number of research groups have investigated the use of poly(lactide-co-glycolide), a well-known biomaterial due to favourable degradation into non-toxic byproducts[87-91]. Release of the encapsulated growth factor should be related to this degradation, offering control of release kinetics by modification of the chemical composition of the material[92]. An interesting study by Richardson et al[89] details the release of $VEGF_{165}$ and PDGF-BB from a porous poly(lactide-co-glycolide) (PLG), synthesised through a high pressure $CO_2$ fabrication process. The growth factors were released with individual release kinetics, made possible by different incorporation methods for each growth factor. The results of the *in vivo* study in the subcutaneous tissue of Lewis rats (a strain

of rat frequently used as an animal model) revealed that PDGF alone led to blood vessel maturation but no increase in blood vessel density, and VEGF alone led to an increase in the number of blood vessels, but the vessels were small and immature, whereas the combined release of the two growth factors led to the formation of mature blood vessels. Kanczler et al[90] produced poly (D,L-lactic acid) scaffolds using supercritical $CO_2$ to release VEGF. The resultant VEGF release led to increased tubule formation in an *in vitro* Matrigel study. Poly(lactide-co-glycolide) microspheres with acid end groups were synthesised by Cleland et al[91] to release VEGF. The growth factor release was sustained over a 21 day period, probably due to association of the acid end groups and the heparin-binding domain of VEGF, and generated a dose-dependent angiogenic response in a corneal implant assay.

The use of hydrogels as delivery devices is also popular due to their favourable properties (further discussed in section 1.8). Release of bFGF was sustained for up to 28 days from degradable dextran hydrogels, synthesised by Hiemstra et al[93] from dextran vinyl sulfone conjugates and tetrafunctional mercapto-poly(ethylene glycol) (Figure 1.5).

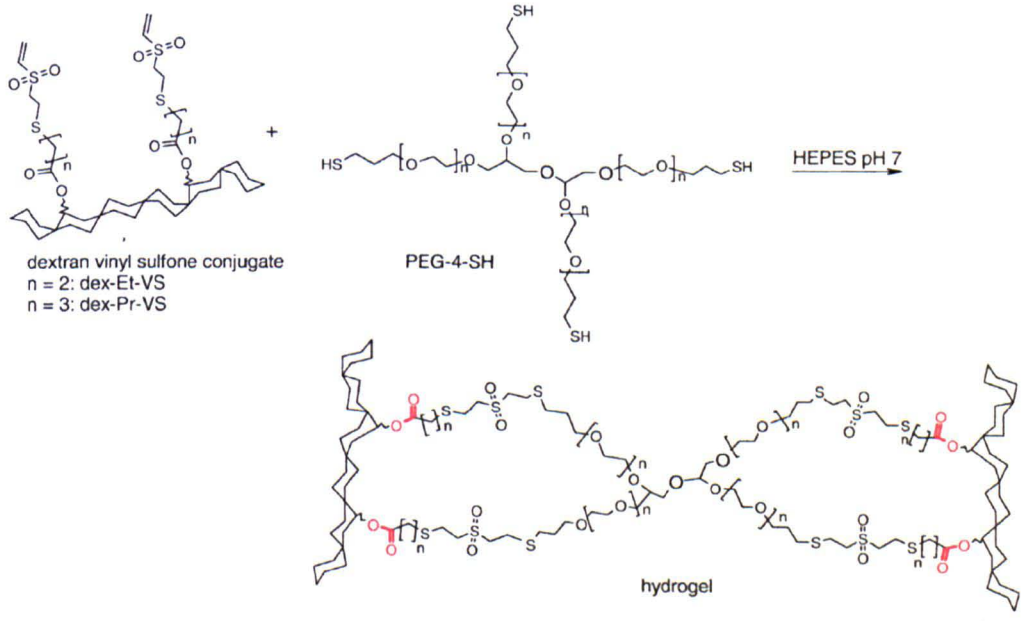


**Figure 1.5: *In situ* hydrogel formation carried out by Hiemstra et al by Michael addition of dextran vinyl sulfone conjugates (dex-Et-VS or dex-Pr-VS) with tetrafunctional mercapto PEG (PEG-4-SH). Reproduced from Hiemstra et al†**

† Reproduction of scheme 1 reprinted from *Journal of Controlled Release*, Vol. 122 no. 1, Hiemstra, Christine; Zhong, Zhiyuan; Van Steenbergen, Mies J.; Hennink, Wim E.; Feijen, Jan, "Release of model proteins and basic fibroblast growth factor from in situ forming degradable dextran hydrogels", 71-78, Copyright 2007, with permission from Elsevier.

Norton et al[94] reported hydrogels containing 2-hydroxyethyl methacrylate, N-vinyl-2-pyrrolidone and poly(ethylene glycol), which also contained microspheres. This dual material approach allowed controlled release of VEGF as well as an anti-inflammatory drug with individual release kinetics. Poly(ethylene glycol)-based hydrogels were also produced by Zisch et al[95]. These innovative hydrogels allowed cell adhesion by the incorporation of pendant RGD-based peptides, as well as the incorporation of crosslinking matrix metalloproteinase substrate peptides to allow cell-mediated remodelling of the matrix. $VEGF_{121}$ and $VEGF_{165}$ were covalently incorporated and in a chick charioallontoic membrane assay new blood vessel formation was observed in the presence of the hydrogels. An *in vivo* investigation in rats saw these biomaterials remodelled into native, vascularised tissue. An alternative monomer, *N*-isopropylacrylamide (NIPAM), was employed by Kavanagh et al[96] to produce thermosensitive copolymer films for delivery of VEGF to human aortic endothelial cells (HAECs). Films loaded with VEGF were shown to release 30 ng of VEGF over 7 days *in vitro*, increasing HAEC proliferation by 18.2% over the control.

An elegant approach to growth factor delivery was recently reported by Ehrbar et al[97]. A genetically engineered bacterial gyrase subunit B (Gyr B) was coupled to polyacrylamide (Figure 1.6). Gyr B could then be dimerised by the addition of coumermycin, an antibiotic, resulting in gelation of the hydrogel. $VEGF_{121}$ with a hexahistidine motif at the N-terminus was incorporated into the hydrogel to determine release characteristics. Release of the protein occurred only as increasing concentrations of novobicin were added, resulting in dissociation of the hydrogel. Novobicin concentrations were able to control the release of $VEGF_{121}$ and the $VEGF_{121}$ released in this way was shown to increase proliferation of human umbilical vein endothelial cells (HUVECs). This approach shows the considerable potential of pharmacologically controlled hydrogels for drug delivery.

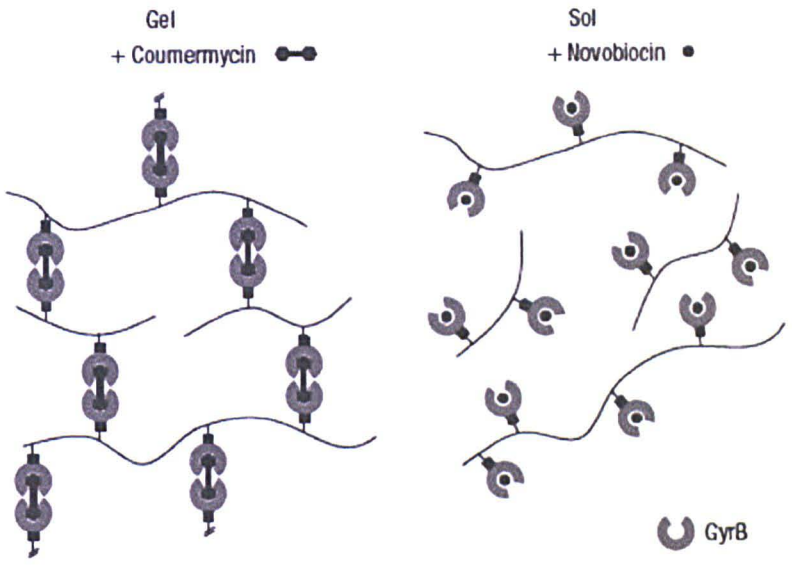


**Figure 1.6: Schematic of drug-sensitive hydrogel adapted from Ehrbar et al†. GyrB coupled to an acrylamide polymer is dimerised by coumermycin, resulting in gelation of the hydrogel. In the presence of novobiocin, GyrB is dissociated, resulting in dissolution of the hydrogel.**

***Heparin Incorporation***

As mentioned previously, heparin and heparan sulphate GAGs play a significant role in regulating angiogenesis. A number of natural and synthetic routes to a heparin-mimic have been detailed which are able to release bioactive growth factors but they are generally unable to truly offer the spatial localisation, stability and controlled release offered by heparin in the ECM. Considerable research efforts have therefore turned to the incorporation of heparin into many of the materials discussed previously, including heparin in alginate systems[58, 98], heparin in poly(ethylene glycol) gels[49, 99] and in fibrin matrices[100], thus combining the advantages of heparin regulation with support offered by the materials.

The effectiveness of heparin incorporation was nicely demonstrated by the group of Peattie[64] who produced chemically modified hyaluronan and gelatin hydrogels containing very low quantities of heparin of 3% w/w and below. Their heparin-containing hydrogels were able to regulate the release of VEGF and bFGF for up to 42

† Adapted by permission from Macmillan Publishers Ltd: *Nature Materials*, Vol. 7, Ehrbar, Martin; Schoenmakers, Ronald; Christen, Erik H.; Fussenegger, Martin; Weber, Wilfred, "Drug-Sensing Hydrogels for the Inducible Release of Biopharmaceuticals", 800-804, Copyright 2008.

days and *in vivo* studies in mice showed that the presence of heparin allowed sustained vascularisation over 28 days. Most recently this group utilised their hydrogels to release VEGF, angiopoietin-1 (Ang-1), KGF and PDGF in an *in vivo* study in the *Balb/c* mouse ear pinna[83]. Dual growth factor delivery was found to produce the best results, resulting in more mature vasculature. They also recorded more mature vessel formation for the heparin-containing hydrogels than for those without heparin. Dual growth factor delivery from a heparin-based biomaterial was also shown to give the most successful results in a study by Nillesen et al[101]. In this case, VEGF and FGF were released from collagen-heparin scaffolds and, when subcutaneously implanted in rats, a combination of the two growth factors resulted in the highest density of blood vessels and the most mature blood vessels of all the treatment groups.

The release of single growth factors has also elicited positive results in heparin containing materials. Biodegradable Pluronic/heparin hydrogels to deliver bFGF were produced by Yoon et al[102] and resulted in release over one month which enabled neovascularisation *in vivo*. Steffens et al[103] utilised heparin to modulate the angiogenic potential of their collagen matrices. Heparin was covalently incorporated into the matrices using 1-ethyl-3-(3-dimethylaminopropyl)-carbodiimide (EDC) and *N*-hydroxysuccinimide (NHS) and an increase in endothelial cell proliferation was observed in the presence of heparin in comparison to the collagen matrices alone. A further increase in proliferation was observed as VEGF was loaded in to the matrices.

A two-component delivery system was reported by Jeon et al[104]. Heparin was incorporated covalently into poly(L-lactide-co-glycolide) nanospheres in the presence of EDC to enable long-term zero-order delivery of bFGF. No burst release was observed with this delivery method and the bFGF was released over three weeks. When these nanospheres were further incorporated into fibrin gels the release period was extended to four weeks, with release dependent on fibrinogen concentration in the fibrin gel. The bFGF was shown to be bioactive *in vitro* and led to microvessel formation *in vivo* in a mouse ischemic limb.

***Summary of Current Growth-Factor Delivery Approaches***

The synthesis of ECM-mimics by a variety of routes has been described, employing both natural products and synthetic materials, as well as a combination of the two. These results demonstrate that stimulation of angiogenesis is significantly more successful with growth factors delivered via a biomaterial than when growth factors are delivered by bolus injection. This is expected to be due to stability of the growth factor within the biomaterial and its sustained release over a longer time period. A number of approaches showed improvements when more than one growth factor was released, but stimulation of angiogenesis was also observed when only one growth factor was delivered. Finally, results of studies incorporating heparin into the biomaterial suggest that the presence of heparin is advantageous and is able to further improve the ability of growth factor delivery vessels to stimulate angiogenesis.

Despite a number of impressive reports detailing significant improvements in angiogenesis upon localised growth factor delivery, no single material is currently able to fulfil all roles of the ECM whilst meeting the requirements for a biomaterial, particularly regarding a simple, reproducible and cost-effective synthesis.

## 1.6 Project Aim

The aim of this research is to synthesise a cost-effective, simple and reproducible biomaterial which could mimic the ECM and bind and release VEGF to stimulate angiogenesis for wound-healing applications. The biomaterial should be biocompatible and be able to be stored, as well as being stable and able to release bioactive VEGF. It should also be easy to remove after use without disruption of the healed tissue.

In contrast to the previous examples of growth factor delivery systems, we plan to stimulate angiogenesis using the VEGF produced within the wound bed. In this study a biomaterial is designed which could act as a "VEGF reservoir" within a wound bed; binding, storing and releasing the patient's own VEGF to aid angiogenesis. Utilising a patient's own VEGF would have a number of advantages over the application of exogenous growth factor including:

- Prevention of protein inactivation during the synthetic procedure
- Avoidance of the high cost of growth factors
- Avoidance of clinical issues related to the delivery of exogenous growth factor
- Avoidance of complex regulatory issues related to the delivery of exogenous growth factor

The intention is to produce biomaterials for future use as an external wound healing material, designed to be removed after use. For this reason the materials are not designed to be biodegradable. Instead, the required properties for an external wound healing dressing include a robust, flexible and easy to handle biocompatible material which is neither light nor temperature sensitive, and which is compatible with standard sterilisation procedures and easy to remove.

Two approaches are investigated to meet these requirements; a VEGF-specific molecularly-imprinted polymer system and a heparin-binding peptide-functionalised hydrogel. An initial introduction to the background of the two techniques is provided in this section. Detailed information regarding the methodologies and the specific chemical compositions for each approach employed is provided in the following chapters.

## 1.7 Strategy 1: Core-Shell Molecularly-Imprinted Particles

In this approach, core-shell particles were designed utilising molecular imprinting to interact directly with vascular endothelial growth factor (VEGF).

### 1.7.1 Molecular Imprinting

The concept of molecular imprinting is based on the principle of molecular recognition, described as the preferential binding of a chemical to its "receptor". This binding is highly selective and occurs favourably in comparison to the binding of structural analogues of the chemical. It is well known that molecular recognition occurs within nature and an example of this is the highly specific recognition between antibody and antigen. Proteins are complex macromolecules which are able to achieve highly specific molecular recognition with target molecules as a result of attractive forces between complementary functionality on the protein and the target molecule.

Such recognition observed in nature has led chemists to attempt to produce synthetic receptors, crosslinked polymers containing functionalised cavities, which can mimic the molecular recognition and operate with the same degree of selectivity. The production of such molecularly-imprinted polymers is a challenging goal, but it would also be extremely rewarding as these materials would be able to complement the current biological recognition tools, such as antibodies, and would also be able to provide significant advantages, as they could be more robust and more cost-effective.

Since the introduction of molecularly-imprinted polymers (MIPs) by Wulff[105] this technology has grown rapidly in popularity. Only a brief literature search is required to reveal the versatility of this approach. Potential applications for highly selective molecularly-imprinted polymers are widespread and could include drug delivery, immunoassays, drug screening, enantioseparation, solid phase extraction, capillary electrophoresis, chromatographic and membrane separation and catalysis[106-115], and there are already a number of excellent reviews in this area[116-122].

#### *Basic Principles*

The principle behind molecular imprinting is to allow a template molecule to interact with a functional monomer, producing a template-monomer complex. The monomer

present is then polymerised with a suitable cross-linker to produce a rigid polymer. The template is removed to leave cavities with a memory for the template in terms of size, shape and functionality. Upon the reintroduction of the template molecule to the polymer, it should rebind to these cavities with high selectivity over any other compounds present. This method is illustrated schematically in Figure 1.7.

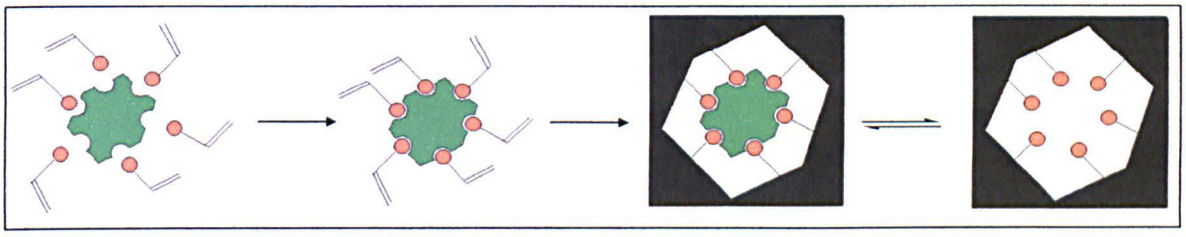

**Figure 1.7: A schematic representation of molecular imprinting**

The synthesis of molecular recognition units in this manner could have many possible advantages over the use of antibodies. Synthetic recognition materials may be cheaper to produce and more robust than an antibody, with increased stability to temperature, pH and organic solvents. Natural antibodies are generally incompatible with organic solvents and so cannot be used successfully within such media.

***Preparation of Molecularly-Imprinted Polymers***

The association between the template molecule and the binding monomer can be covalent or non-covalent, including, for example, hydrogen bonding, hydrophobic interactions and Van der Waal interactions. The type of interaction will affect the ease of synthesis and the selectivity of the produced polymeric species.

The covalent approach, initially reported by Wulff et al[105] in 1972, is thought to be able to produce MIPs with high selectivity. There are a number of drawbacks to this method[123]; often the synthesis is difficult and time consuming, it is only appropriate for certain templates, the recognition speed is slower and the removal of the template requires harsh conditions as it involves the cleavage of a covalent bond. The alternative approach of non-covalent imprinting, first realised by Mosbach et al[124, 125], would be expected to result in less selective polymers due to the weaker non-covalent interactions employed but may also have a number of advantages[123]. The synthesis of non-covalent

polymers is more straightforward and this method is compatible with a large range of templates. The template can be removed under mild conditions, which is vital for a drug delivery application, and template rebinding may be faster than in the covalent approach.

The advantages and disadvantages of these approaches mean that it is important to consider which type of molecular imprinting is suitable for the aim of the project. Considerations necessary include the class of template molecule, the required selectivity, the timescale and cost[123]. Hybrid techniques may also be employed, such as the combination of the covalent and non-covalent approach[126, 127] or the use of a template immobilised on a solid support[128].

***Format Considerations***

Molecularly-imprinted polymers are traditionally produced as a macroporous polymer in one step. This procedure is relatively straightforward and involves bulk polymerisation in non-polar solvents followed by grinding and sieving of the solid MIP to produce the required particle size. The majority of literature on molecular imprinting describes such an approach, but the synthesis of a macroporous monolith often leads to difficulty in the removal of the template molecule, as cavities can be formed throughout the entire polymer. There are numerous alternative preparations for various physical configurations that have been discussed to date[120], including uniform beads, microspheres, membranes, rods and polymer monolayers. It is important to select the monomer and polymerisation procedure not only with regard to the template molecule, but also with consideration to the required format for the desired application.

***Solvent Considerations***

The solvent is an important consideration[123]. It must simultaneously dissolve the reagents, act as a porogen to allow the synthesis of accessible cavities, disperse the heat of reaction and allow the formation of the template-monomer complex. The solvent must also be compatible with the application of the imprinted polymer. In most cases, the solvent utilised in the imprinting step is the same solvent used when rebinding the template, which is an important consideration for MIPs with specific applications.

The majority of the research in this area has been performed entirely in organic solvents as this is traditionally the solvent choice for molecular imprinting, especially for non-covalent imprinting techniques. This is primarily due to the non-covalent interactions which are possible within an organic medium. The most appropriate interaction for precise molecular recognition between template and monomer is hydrogen bonding. This interaction is thought to be the most effective for the synthesis of selective MIPs as it is dependent on distance and direction of the monomer and template[123]. Hydrogen bonding can occur with minimal interference within organic solvents, such as toluene and dichloromethane, and so the use of organic solvents is popular to optimise the selectivity through such interactions[129]. In order to truly produce versatile receptors for use within both academia and industry, MIPs are required which are able to function within water.

### 1.7.2 Peptide and Protein Imprinting

Protein imprinting has become more popular recently as successful polymers would be extremely rewarding. A number of reviews are now available for protein-imprinted polymers[120, 130-137]. Current protein binding relies upon antibodies for various applications such as assays, extraction and biosensors[132] but these are very expensive and fragile. These drawbacks provide a niche for more inexpensive, robust and reusable materials. It is thought that such polymers could have applications within protein purification, diagnostics, biosensors and drug delivery[131, 136].

#### *Difficulties in Protein Imprinting*

The nature of large, flexible peptides and proteins leads to a number of synthetic difficulties when producing an imprinted polymer for this type of template molecule, which renders the standard procedure of bulk imprinting in non-polar solvents and the subsequent grinding and sieving ineffective. One of the synthetic challenges encountered within this type of situation is diffusion. In a nice overview of molecular imprinting, Flam[138] highlighted the fact that a bulky protein will not be able to move in and out of a polymer network with the same ease as a low molecular weight compound. This can lead to permanent entrapment of the protein in the polymer material[131]. Although porogens can be added to improve the situation by increasing the surface area, for the usual bulk polymerisation method grinding would most likely still be necessary

to free the template and make the binding sites accessible. Grinding this material could damage any binding sites produced.

Another synthetic consideration is the flexibility of polypeptides and proteins, which is not experienced for the traditional low molecular weight templates used in molecular imprinting. The conditions for polymerisation must be considered as some conditions could denature the protein which would render it inactive. The use of such flexible templates can yield less well-defined recognition sites as a protein could alter conformation to fit into an imprint formed for a different template, or it may no longer fit into its imprinted cavity in different conditions[132]. Thermodynamic considerations for the design of a MIP, including consideration of more flexible templates, have been discussed in detail by Nicholls[139].

Finally, and probably the most significant challenge of protein imprinting, is the poor stability and solubility of proteins in organic solvents and the necessity for a polymer which is capable of operating in an aqueous environment for biological applications[131]. Imprinting in an aqueous environment is discussed in more detail in the following section because of the extra considerations required.

In recent years there have been a number of different approaches suggested for the binding of macromolecules to overcome these difficulties. A number of groups have attempted to utilise conventional bulk polymerisation procedures with water-soluble monomers. However, as will become apparent, the majority of imprinting techniques discussed for biomacromolecules utilise surface imprinting techniques to avoid the aforementioned diffusion difficulties. The challenges of imprinting these templates within an aqueous environment are also met by a number of different interactions including the use of functional groups capable of strong interactions such as metal-chelating, as well as hydrophobic and electrostatic interactions and also reliance on shape specificity, combined with multiple weak interactions including hydrophobic and hydrogen-bonding interactions in water.

***Imprinting in an Aqueous Environment***

The techniques available for imprinting in aqueous media are limited in comparison to those available for organic solvents. There are difficulties associated with the use of water as a solvent, primarily the incompatibility with hydrogen bonding, an interaction of vital importance for the organisation of template and functional monomer within the majority of non-covalently imprinted polymers produced in organic media[140]. Water, due to its hydrogen donor and hydrogen acceptor abilities, prevents the hydrogen bonding between template and functional monomer occurring, instead forming such bonds itself with both the template and monomer species[141]. As the solvent in an imprinted polymerisation is generally present in large quantities in comparison to the other components, the solvent-template and solvent-monomer interactions render conventional hydrogen bonding useless in aqueous media and so it is generally accepted that imprinted polymers relying on such hydrogen bond interactions alone are incompatible in aqueous systems. This means that other non-covalent interactions become more important within aqueous imprinting, including hydrophobic interactions and electrostatic interactions. The most successful aqueous imprinting systems would be expected to utilise a combination of non-covalent interactions.

A large number of different approaches have been trialled to achieve molecular imprinting in an aqueous environment. These include the use of a combination of organic and aqueous solvents[142-145], although work by Nicholls et al[141] suggests that in order to achieve specific interactions in aqueous media it is advantageous to carry out the imprinting process within the media required for recognition.

A number of innovative approaches to an entirely aqueous MIP have been recorded including covering a pre-formed MIP with a thin film of mineral oil[146], the use of cyclodextrin as a novel monomer[147] and imprinting at the air-water interface[148]. The sol-gel technique has also been used extensively, and is discussed in a review by Diaz-Garcia et al[149].

A popular approach to aqueous imprinting is the synthesis of molecularly-imprinted particles by emulsion polymerisation and mini-emulsion polymerisation. Mini-emulsion polymerisation for molecular imprinting has been employed extensively by G. Tovar et al[150-153] and has been shown to enable the production of selective MIPs. Core-shell

molecularly-imprinted particles (CS-MIPs), in which the functional monomer is present in the outer-shell of the particle, have also been reported by a number of research groups. A considerable amount of work in this area was carried out by Perez-Moral et al[154-156]. Research published by Perez et al[154] produced cholesterol-binding particles via a two-stage aqueous emulsion polymerisation of a poly(styrene-co-divinylbenzene) core and an outer shell consisting of a specially designed template-surfactant, pyridinium 12-(cholesteryloxycarbonloxy)dodecane-sulfate, which allowed the template to be positioned at a predefined distance from the surface of the polymer, and a polymerisable surfactant, pyridinium 12-(4-vinylbenzyloxycarbonyl)dodecanesulfate. Results illustrated that the hydrophobic cavities were able to rebind cholesterol from a 0.5 mM solution in 60:40 2-propanol:water. No rebinding of cholesterol was observed when the rebinding experiments were carried out in isohexane, a nonpolar solvent. This demonstrates that the interactions involved are hydrophobic in nature as cholesterol is reasonably soluble in isohexane and will therefore tend to remain in solution rather than rebind to the hydrophobic cavities. Perez-Moral et al[155] also employed the core-shell methodology to bind propranolol through non-covalent interactions in the presence of an organic solvent porogen. Results suggested that the presence of a porogen during shell synthesis increased the level of uptake of propranolol in both aqueous and organic media. As expected, it was also demonstrated that particles imprinted with a larger amount of template showed a higher rebinding capacity in both aqueous and organic environments. More recently, the same group have also imprinted propranolol, morphine and naproxen into core-shell nanoparticles using non-aqueous surface-initiated living-radical polymerisation[156].

Carter and Rimmer[157] reported the synthesis of core-shell molecularly-imprinted particles (CS-MIPs) by emulsion polymerisation in aqueous media, which were shown by selective extraction and saturation binding experiments to be able to differentiate between the template, caffeine, and theophylline, a structurally similar analogue. The particles utilised both hydrophobic interactions as well as a phosphate binding system, previously employed by Takagi et al[158], leading to electrostatic interactions between the phosphate binding monomer and the template molecule. Core particles of poly(styrene-co-divinylbenzene) were coated by an outer layer of a long chain alkyl phosphate and ethylene glycol dimethacrylate (EGDMA) in the presence of the template. The presence of phosphate within the shell was confirmed by ion-coupled plasma mass spectrometry

(ICP-MS) of acid digests of the latexes produced. Competitive binding studies demonstrated the selectivity of the caffeine-imprinted particles, although imprinting with theophylline did not lead to a product which was able to selectively extract theophylline. The competitive binding studies were carried out in both water and a buffer solution, and results revealed that particles produced in this way performed better in water. Radiotracing experiments were carried out to prove that, in such surface-imprinted particles, all of the caffeine template could be successfully removed in the extraction process. Further research showed that this technique was also able to produce MIPs which could differentiate between close structural analogues (S)-propranolol and (S)-atenolol[159], as well as a system which could selectively bind the Gly-Gly sequence in the tripeptides Tyr-Gly-Gly and Gly-Gly-His whilst excluding the sequence Met-Leu-Phe[160].

From these examples it is obvious that molecular imprinting in aqueous environments is possible and that a variety of approaches can be utilised depending on the required application. Consideration of each individual template will allow for determination of the most suitable technique to achieve the most successful results.

### 1.7.3 Current Approaches to Protein Imprinting

Recently this area has become popular and so an ever increasing number of publications are available. The imprinting of the standard low molecular weight template molecules has previously relied upon a small number of strong interactions between template and functional monomer. The nature of proteins and polypeptides and their large quantities of functional groups over large surface areas suggests that the imprinting of these biological materials would likely result in large numbers of less specific interactions which could possibly produce less specific polymers. The type of interactions required and therefore the polymerisation method, the monomers and the format of the produced polymer, are all highly dependent on the desired template and application of the MIP. For this reason a number of techniques are discussed, with examples of two different approaches to protein imprinting; whole protein imprinting and the epitope approach.

***Whole Protein Imprinting***

A number of different approaches have been reported for the imprinting of whole proteins, all of which attempt to overcome the specific difficulties observed for large, multifunctional templates. The majority of the approaches fall within the following three categories.

*3D Polymer Gels*

Firstly research continues to focus on 3D matrices, as bulk systems are able to contain numerous binding sites and therefore have a high potential binding capacity. Hjerten et al[161] have polymerised acrylamide and N,N'-methylene bisacrylamide in the presence of various proteins including ribonuclease and myoglobin from horse to produce a gel. The imprinted polymers were packed into chromatography columns and were able to specifically absorb all of the proteins tested, and showed that the absorptive properties were highly dependent on ionic strength and gel concentration. An interesting point discussed was that gels could be produced which were capable of recognising several proteins simultaneously and were able to discriminate between two proteins differing by only twenty amino acid residues. Hjerten et al have since employed this type of polymer to recognise viruses and bacterial cells[162-164]. Polyacrylamide gels were also produced by Ou et al[165] with methacrylic acid and 2-(dimethylamino)ethyl methacrylate to imprint lysozyme. The imprinted polymer was able to absorb 85% more lysozyme than the non-imprinted polymer although a number of problems were encountered. The polymer was shown to be not specific for the template and more than a quarter of the template could not be extracted from the polymer. This may be due, in part, to the use of a gentle elution method. It was suggested that a higher crosslinking density leads to a more selective and compact gel from which diffusion of the protein is more problematic. This is expected to be similar for many of the gels produced by bulk polymerisation for protein recognition. The ease of template removal and subsequent accessibility with a lightly crosslinked material must be balanced against the superior imprinting efficiency of a highly crosslinked material.

Pang et al[166] produced protein-imprinted beads from acrylamide and N,N'-methylene bisacrylamide by inverse-phase suspension polymerisation. The beads were imprinted with BSA and it was observed that the MIP had a much higher capacity than the non-imprinted polymer. The MIP was also shown to be selective for BSA over ovalbumin.

Binding was attributed to complementary cavities for BSA with multiple electrostatic interactions and an enhanced imprinting effect was observed when the surface zeta potential for the template and beads were equal.

The use of molecularly-imprinted hydrogels has also become popular (reviewed by Bergman et al[131] and Byrne et al[167]). Several advantages, including compatibility with an aqueous environment and swelling capabilities, which minimise diffusion difficulties, make hydrogels promising materials for protein delivery. The hydrogel approach for binding biologically relevant materials has been utilised by a number of groups, but the majority of work has been aimed towards the imprinting of small molecules including nitrophenyl esters[168] and norephedrine[169]. Uysal et al[170] have produced a molecularly-imprinted hydrogel for haemoglobin from *N*-t-butylacrylamide, acrylamide and itaconic acid. They found that preparation pH was critical for materials with an isoelectric point. The resultant hydrogels were selective for haemoglobin over fibrinogen and myoglobin and the imprinted polymer absorbed 1.5-2.2 times more haemoglobin than the non-imprinted equivalent.

Stimuli responsive molecularly-imprinted hydrogels were produced by Hua et al[171] to bind bovine serum albumin (BSA). The use of "smart" hydrogel materials could lead to drug delivery applications, as altering environmental conditions could allow release of the template. The hydrogel relied upon interaction of the acidic BSA with a basic monomer *N*-[3-(dimethylamino)propyl]-methacrylamide (DMAPMA) and the stimuli-responsive properties of *N*-isopropylacrylamide (NIPAM). It was possible to remove the template in mild conditions with sodium chloride by disruption of electrostatic interactions. The use of sodium chloride also inhibited the significant non-specific absorption experienced. The selectivity observed when removing the template from a protein mixture, and the control offered by external stimuli such as temperature and ionic strength suggest that there is some potential for this technique.

An interesting approach was also described by Miyata et al[172] who produced a MIP consisting of a functionalised lectin and polyclonal anti-AFP antibody crosslinked with N,N'-methylene bisacrylamide in the presence of AFP, a tumor-specific marker glycoprotein. The hydrogel was shown to shrink as AFP was rebound and caused reversible crosslinking, whereas the non-imprinted hydrogel was found to swell slightly

upon addition of AFP. No change in the MIP was observed for the addition for ovalbumin, a control protein. The use of an antibody would be expected to make this approach less robust than a synthetic alternative but it does have potential as a sensing device.

The use of 3D gels to imprint whole proteins has the advantages of a high binding capacity together with the flexibility and high porosity required for a macromolecular template. The negative aspect of this approach is an inherent lack of stability and mechanical strength compared to standard bulk imprinting methods[132], as well as diffusion difficulties. The high crosslinking required to improve stability would make the diffusion of proteins more difficult and so a balance must be met. Improving the issue of mechanical strength could make the use of 3D gels attractive for protein binding. One method to improve mechanical strength was shown by Guo et al[173] by incorporating a matrix of macroporous chitosan beads to polyacrylamide gels. The imprinted polyacrylamide gel was formed in the pores of the chitosan beads to provide mechanical strength. Haemoglobin-MIPs were shown to absorb considerably more haemoglobin than a non-imprinted equivalent and were selective for haemoglobin over BSA, which is a protein with a different shape. It was reported that the MIP could be reused but that acetic acid and sodium dodecyl sulphate were required to remove the bound protein. This suggests that this approach is more suitable for a sensor application than a protein delivery system.

*Surface Imprinting*

An alternative approach to overcome diffusion difficulties is the use of a surface-imprinting approach, generally achieved by producing a thin film or polymerising on a supporting surface. The first reported MIP for proteins was produced by Glad et al[174] who utilised organic silanes polymerised on the surface of porous silica particles in aqueous solution. A boronate silane functional monomer was incorporated to produce a polymer capable of recognising the glycoprotein transferrin. When compared to MIPs produced from the same monomers but via bulk polymerisation the beads were shown to offer superior recognition, demonstrating the advantages of surface imprinting for proteins.

The use of sol-gel chemistry has been discussed together with surface-imprinting by Zhang et al[175] to produce a human serum albumin (HSA) MIP film on the surface of a piezoelectric quartz crystal gold-electrode. At the most effective binding temperature of 20-35°C, the film was selective for the template against guest compounds, haemoglobin horseradish peroxidise, egg yolk, egg white and trypsin, and was relatively stable to pH. The binding capacity of the films produced was shown to be highly dependent on the salts and solvents employed. Wang et al[176] have also employed surface-imprinting to produce a sensor for myoglobin and haemoglobin. In this synthesis a gold-coated silicon chip was coated with a protein-containing self assembled monolayer of alkanethiol, able to attach to the gold surface via sulphur-metal bonds and to the protein via the hydroxyl group. Again, the use of a surface imprinting technique allowed the synthesis of a MIP sensor capable of selectively detecting a target protein.

Metal interactions used to bind proteins have been described by Shnek et al[177] and involves the attachment of the protein to an artificial lipid membrane using metal ion coordination. In this system, $Cu^{2+}$, a divalent transition metal ion, is immobilised onto a solid support through chelating agents. The desired target compound is used as a template to position the metal. The chelating agents bind the metal tightly yet leave a coordination site available for the formation of a complex with the protein. Imidazole moieties in histidyl residues, present on the surface of proteins, coordinate to the $Cu^{2+}$, immobilising it to the surface. This method is obviously only suitable for proteins containing an exposed histidine residue at its surface.

Surface-imprinting techniques have also been employed by Bossi et al[178] to coat polystyrene microplate wells with MIPs specific for various proteins including microperoxidase, horseradish peroxidase, lactoperoxidase and haemoglobin. They discuss that the imprinted polymer consists of 3-aminophenylboronic acid which attaches to the polystyrene surface through "aromatic ring electron-pairing interactions", presumably $\pi$-$\pi$ interactions. A strong imprinting effect was observed for all proteins reported with little cross-reactivity. It was shown that utilising the grafted MIP considerably improved the affinity to the template in comparison to the equivalent free-standing MIP, probably due to the formation of highly accessible binding sites and a stabilised polymer.

Polypyrrole based MIPs were produced by Ramanaviciene et al[179] for label-free detection of bovine leukaemia virus glycoproteins. The polymer was produced by electrochemical deposition onto the surface of a platinum black electrode in the presence of the template. The template was finally extracted with sulphuric acid. Pulsed amperometric detection was then used to detect the protein and showed that the protein could be bound, removed and rebound over several cycles, but that the polymer became less effective with each repeat cycle.

Work has also been carried out for protein binding to a lipid monolayer on a solid support or at the air/liquid interface[180]. Binding of the acidic protein ferritin was expected to interact with cationic/non-ionic lipids and induce charge patterns in the fluid monolayer. Interestingly, monolayers on a solid support saw ferritin adsorption reduce as the charge in the monolayer reduced, whereas at the air/water interface binding was increased as the amount of non-ionic lipid increased and the amount of charged lipid decreased. These results demonstrate the influence of lipid mobility at the air/water interface. The practicality and stability for this approach for use in a specific application needs to be further investigated.

The surface-imprinting approach avoids difficulties associated with diffusion and offers obvious mechanical advantages. Utilising a surface-imprinting technique means the shape-selectivity offered by a 3D cavity may not be provided and so these materials may exhibit less selectivity. A surface technique could also require less protein but will therefore also have a lower binding capacity.

*Surface-Imprinting via Template-Immobilisation*

A number of groups are also carrying out surface-imprinting using a template-immobilisation approach where the template is attached to a solid support and the polymer is formed around it before removal of the template on the support. This approach has the advantages of being compatible with insoluble templates, minimising protein aggregation and allowing the formation of homogeneous binding sites[130]. It may also be a cost effective approach as it could minimise the amount of protein required in the imprinting step.

In a report from Chou et al[181] thin imprinted polymer films were formed on glass supports (Figure 1.8). In this study, a monolayer of protein was formed on a glass support, on to which a polymer was formed by UV initiation. The glass support and template were removed to leave a polymer with surface recognition cavities for a protein, in this case C-reactive protein, a marker of inflammatory response. This so-called "micro-contact" imprinting meant that the template could be easily removed, avoided diffusion problems of the macromolecule through a bulk polymer and also meant that only a small quantity of expensive template was required. In this procedure, a phosphorylcholine (PC) derivative was used as a functional monomer as PC is a natural ligand for the pentaprotein. The 10 μm film MIP produced was shown to be selective to the template over HSA and lysozyme. Recently this group have used the "micro-contact" approach to produce MIPs for lysozyme, ribonuclease A and myoglobin[182], creatine kinase[183] and ovalbumin[184].

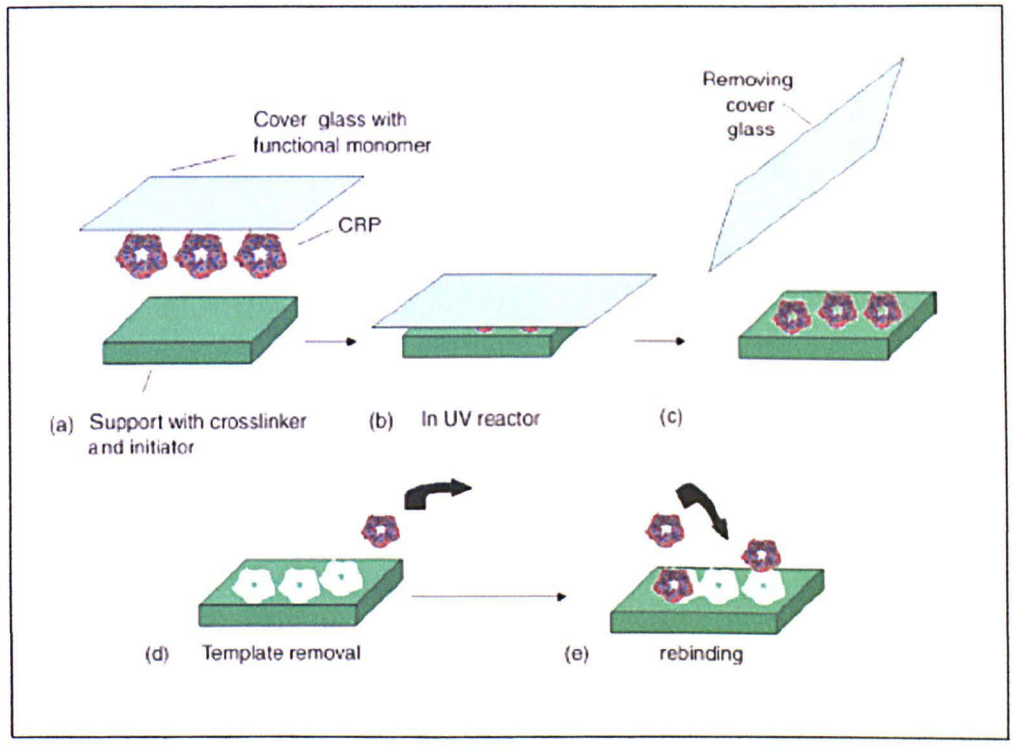


**Figure 1.8: A schematic of the "micro-contact" approach utilised by Chou et al† (a) the protein is adsorbed onto a cover glass together with the functional monomer; (b) the cover glass is combined with the support containing the crosslinker and initiator and placed in a UV reactor; (c) the cover glass is removed; (d) the template is extracted; (e) rebinding of the template occurs.**

† Reproduction of figure 1 reprinted from *Analytica Chimica Acta*, Vol. 542, Chou, Pei-Chen; Rick, John; Chou, Tse-Chuan, "C-reactive protein thin-film molecularly imprinted polymers formed using a micro-contact approach", 20-25, Copyright 2005, with permission from Elsevier.

Radio-frequency glow-discharge plasma depositions were used by Shi et al[185] to produce thin film MIPs around proteins which had been coated with disaccharide molecules (Figure 1.9). The protein was deposited onto a mica surface and then coated with disaccharide, allowing formation of multiple hydrogen bonds. Polymerisation of $C_3F_6$ was carried out, reacting with the disaccharide molecules to produce polysaccharide-like cavities for recognition of various templates including albumin, and streptavidin. The polymer film produced was mounted onto a solid support and the mica and protein were removed. It is reported that non-specific protein binding should be minimal due to the highly directional nature of a hydrogen bond. Protein recognition for these particles was evident in competitive adsorption studies, suggesting that the required selectivity could be possible with this approach. It is thought that firstly proteins are adsorbed non-specifically. In this case the template protein would be retained more successfully on the surface whereas an adsorbed protein with low affinity for the cavity would be exchanged with a dissolved protein in solution. Although the results suggest that non-specific protein adsorption occurs, the ability to preferentially

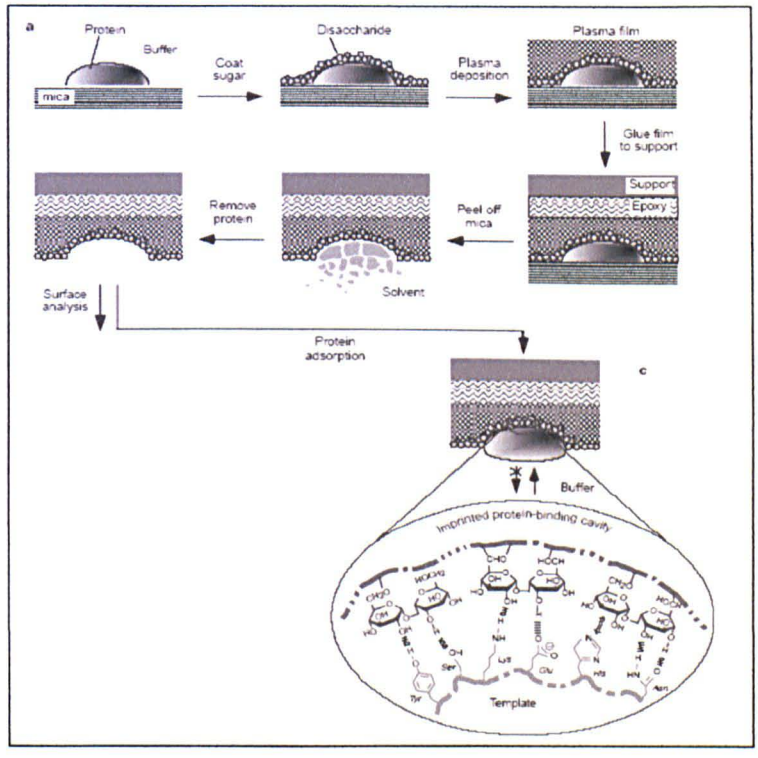


**Figure 1.9: Schematic of the imprinting approach employed by Shi et al†. The protein was deposited onto a mica surface and then coated with disaccharide. Plasma polymerisation of $C_3F_6$ was carried out around the disaccharides. The polymer film produced was mounted onto a solid-support and the mica and protein were removed to produce disaccharide-based recognition cavities.**

† Adapted by permission from Macmillan Publishers Ltd: *Nature*, Vol. 398, Shi, Huaiqiu; Tsai, Wei-Bor; Garrison, Michael D.; Ferrari, Sandro; Ratner, Buddy D., "Template-imprinted nanostructured surfaces for protein recognition", 593-597, Copyright 1999.

retain the template protein is key, and this could lead to selective polymers through dynamic adsorption-exchange.

An immobilised template was also utilised by Shiomi et al[186] to form molecularly-imprinted silica surfaces. Haemoglobin was immobilised covalently via imine bonds between the protein and aldehyde groups on the silica. Organic silane monomers, 3-aminopropyltrimethoxysilane and propyltrimethoxysilane, were then polymerised onto the haemoglobin-silica surface. The template was removed by treatment with oxalic acid to produce polymers with cavities selective for haemoglobin over myoglobin, transferrin and chymotripsinogen. The results showed that polymers produced with immobilised templates were more successful than those produced with the protein in solution and also demonstrated that the selective absorption of haemoglobin onto the MIP was dependent on the isoelectric point and the molecular weight of the protein as well as the shape and hydrophobicity of the cavities.

Li et al[187] have developed polymer nanowires with surface recognition sites for possible applications such as affinity chromatography. The target molecule was immobilised on the pore walls of nanoporous alumina, a technique analogous to the immobilised templates on porous beads previously discussed by Mosbach[128]. The nanopores were then filled with acrylamide and N,N'-methylenebisacrylamide and polymerisation occurred to produce selective polymer nanowires which were able to recognise protein molecules including albumin, haemoglobin and cytochrome c in pH 7.0 PBS solution.

Matsunaga et al[188] discussed an interesting approach using crystallised lysozyme. Crystallised proteins are regularly oriented with no mobility, thus reducing difficulties related to conformational changes of macromolecules in the imprinting process. Crystallised lysozyme on a cellulose membrane was coated with a pre-polymerisation mixture of acrylic acid (functional monomer), 2-(methacryloyloxy) ethylphosphonylcholine (co-monomer), N,N'-methylene bisacrylamide (crosslinker) and poly(ethylene glycol). A sensor chip was placed on top of the mixture and polymerisation was then carried out. Removal of the cellulose membrane and template left a lysozyme-imprinted polymer-coated sensor chip. The crystallised lysozyme-MIP showed a higher selectivity than the free-lysozyme MIP and the non-imprinted polymer and suggests that such an approach may lead to successful MIPs for protein recognition.

Core-shell particles were employed by Tan et al[189] to recognise bovine serum albumin. The particles were formed by a two-stage miniemulsion polymerisation. Firstly core particles were produced and the template was then immobilised to the core particle via a spacer chain containing an imine bond. The shell of methyl methacrylate and EGDMA was then polymerised around the core, producing core-shell particles with surface cavities after removing the BSA template by hydrolysis of the imine group. In agreement with other studies, the immobilised BSA MIP had a higher binding capacity than the free BSA MIP and a non-imprinted version. Selectivity studies showed that only the immobilised BSA MIP was able to selectively bind BSA.

***Epitope Approach***

The nature of proteins and the large quantities of functional groups over a large surface area suggests that the imprinting of such materials would likely result in large cavities with large numbers of less specific interactions which could produce less specific polymers. The true selectivity of these MIPs is of interest as a number of proteins of similar size and with similar functionality would generally be present within a biological sample. Without highly selective functionality it is unclear as to whether such a cavity could provide the selectivity observed for a more size-selective binding site.

A very interesting approach towards protein imprinting and a much cited report was published by Rachkov[190] detailing an "epitope approach" to the imprinting of peptides (Figure 1.10). This name refers to the biological interaction of an antibody with an antigen, as when an antibody binds with an antigen it interacts only with a small section of it, known as the epitope (the antigenic site of the protein). This approach utilises a short peptide chain as the template, which is an amino acid sequence present on the target protein or polypeptide. The cavity formed should then be specific for that amino acid sequence and should therefore be able to bind both the short peptide as well as the larger protein. Rachkov et al[190] showed this approach to be successful in the imprinting of a tetrapeptide, producing MIPs capable of selectively recognising both the tetrapeptide and oxytoxin, a nonapeptide containing the tetrapeptide sequence. Bulk radical copolymerisation of methacrylic acid (MAA) and ethylene glycol dimethacrylate (EGDMA) produced macroporous MIPs, which were then ground and sieved to give the desired peptide-imprinted MIPs. Some selectivity was demonstrated with this system but the polymers performed best in a mixed-aqueous mobile phase.

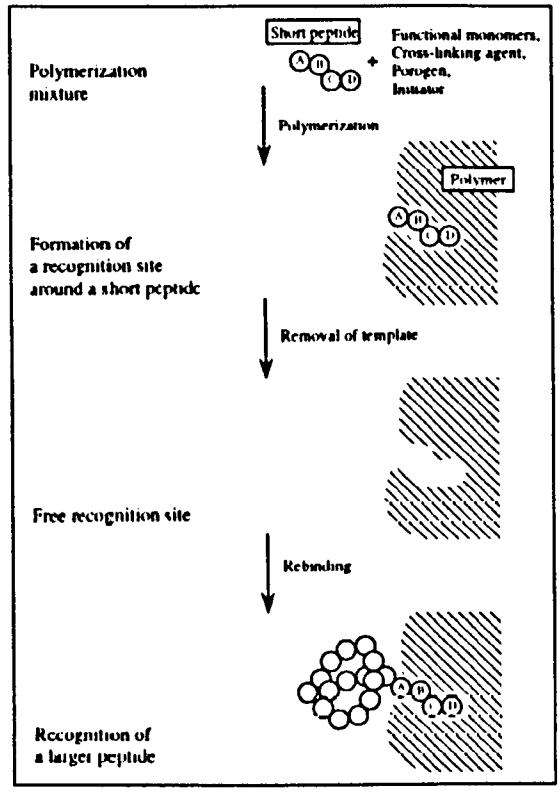


**Figure 1.10: Schematic of the epitope approach, reproduced from Rachkov et al†**

The possible advantages of this approach, including cost and reduction of problems associated with a flexible protein template, have meant that the epitope approach has been investigated by a number of researchers.

The epitope approach was combined with a solid support in a study by Titrici et al[191]. A crude peptide was synthesised on a silica support and then used as the template. The pores of the silica support were then filled with MAA and EGDMA and polymerisation was initiated. The silica mould was dissolved by $NH_4HF_2$ to give organic imprinted polymer beads. In chromatographic binding experiments a heptadecapeptide nociceptin H-FGGFTGARKSARKLANQ-OH was retained twice as strongly on a particle imprinted with P(H-Phe-Gly-Si) (the correct sequence for this peptide) than P(H-Gly-Si), again demonstrating that the epitope approach described can produce highly selective MIPs for polypeptides. From the Sellergren group, Emgenbroich et al[192] also report the use of the epitope approach to recognise short peptide sequences, this time via the phosphate group on phosphorylated tyrosine. With their system it was possible to produce MIPs containing a diaryl urea monomer which were selective for peptides

† Reproduction of figure 1 reprinted from *Biochimica et Biophysica Acta*, Vol. 1544, Rachkov, Alexandre; Minoura, Norihiko, "Towards molecularly imprinted polymers selective to peptides and proteins. The epitope approach", 255-266, Copyright 2001, with permission from Elsevier.

containing phosphorylated tyrosine, with significantly higher binding observed for the target peptide on the MIP than for the non-imprinted equivalent. These systems demonstrate success with the epitope approach but do not truly show whether this methodology can be applied to larger proteins.

Nishino et al[193] successfully combined template immobilisation with the epitope approach to produce MIPs selective for cytochrome c, alcohol dehydrogenase and bovine serum albumin. Nonapeptide sequences reproduced from the respective proteins were tethered to a functionalised silane surface, followed by polymerisation of a mixture of acrylamide, N,N-ethylenebisacrylamide and poly(ethylene glycol) 200 diacrylate around the peptide template. Surface-imprinted cavities were formed which were highly selective for the target proteins. The success of this study was attributed to collective hydrogen bonding within the cavities which could only offer very low binding strength to non-target proteins.

Tai et al[194] have also employed the epitope approach to produce a MIP film able to detect the dengue virus protein. This system was produced as a sensor with a quartz crystal microbalance chip. A 15-mer peptide from the protein was selected as a template and was present as the monomers, acrylic acid, acrylamide and N-benzylacrylamide, were copolymerised onto the chip by UV initiation. The use of the epitope approach meant that the proteins had to orientate in a specific way to bind to the chip. Although no information regarding selectivity of the MIP was provided, this approach was able to provide quantitative detection of the dengue virus protein.

Very recently an interesting report was published by Xue et al[195], who imprinted staphylococcus aureus protein A (SpA) to produce MIPs which could then recognise the bacteria staphylococcus aureus. The imprinted polyacrylamide gel beads were able to selectively bind SpA in the presence of four competitor proteins (ovalbumin, β-lactoglobulin, lysozyme and bovine serum albumin) and staphylococcus aureus over two competitor bacteria (E. coli and S. thermophilus).

***Summary of Current Protein Imprinting Techniques***

Protein imprinting is currently an area of considerable research interest but there are a number of difficulties associated with this technique, including compatibility with aqueous media, flexibility of the target molecule and diffusion difficulties. There have been a variety of approaches suggested to overcome these difficulties, including utilising 3D gels, surface imprinting techniques and the epitope approach. All of the techniques discussed are able demonstrate protein binding, often with impressive selectivity, but differences between the approaches, templates and potential applications makes it very difficult to truly compare the results. As shown in this section, excellent progress in this area has been made in the last few years, and there are now many innovative approaches to producing a MIP for a protein target. It is expected that research in this area will continue, combining current approaches as well as finding new solutions to this challenge.

From consideration of the literature it is clear that in order to produce a protein-imprinted polymer for a specific application, it is necessary to consider the target protein, the material requirements and the potential application before determining the most effective imprinting approach.

## 1.8 Strategy 2: Peptide-Functionalised Hydrogels

An alternative approach to producing a VEGF-binding polymer is to utilise the VEGF-binding ability of heparin itself. Hydrogels were designed to bind heparin which could then bind VEGF, thus mimicking the extracellular matrix.

### 1.8.1 Hydrogels

Wichterle and Lim[196] first proposed poly(2-hydroxyethyl methacrylate) (p(HEMA)) hydrogels for use in contact lenses in 1960. This class of material was defined in 1986 by Peppas and Mikos[197] as "water-swollen networks (crosslinked structures) of hydrophilic homopolymers and copolymers". Hydrogels are 3D materials with crosslinks that may be chemical; ionic, covalent or non-covalent (e.g. hydrogen bonding or Van der Waal forces), or physical due to entanglement or crystallites[198]. The crosslinker then provides the network structure and physical integrity of the resultant hydrogel. Hydrogels are able to achieve very high water contents, absorbing amounts of water from 10-20% (an arbitrary lower limit) of their dry weight up to thousands of times their dry weight[199], in comparison to the much more limited water absorption of hydrophobic polymer networks such as poly(lactic acid) and poly(lactide-co-glycolide) of less than 5-10 wt%[200]. Design of an appropriate synthetic approach as well as consideration of the chemical composition of a hydrogel (including choice of monomers, crosslinking method and crosslinker density) allows control of vital properties such as equilibrium water content, mechanical strength and degradation, as well as response to external stimuli.

### 1.8.2 Hydrogels for Biological Applications

Duncan[201] describes biomaterials as "any material, natural or synthetic, that comprises the whole, or a part, of a living structure or biomedical device and performs, augments, or replaces a natural function". The most important feature of a biomaterial is that it is biocompatible to allow the material to be used successfully for the specific application. The desired biological response to a biomaterial may vary depending on its function. For some applications it may be desirable to have a material which does not interact with the biological system and so would be inert. Alternatively, it may be necessary to

produce a material which interacts with the cells close to the material. Marchant[202] suggests that biocompatibility can be considered as a "dynamic two-way process that involves the time-dependent effects of the host on the material and the material on the host".

Hydrogels are now important materials for pharmaceutical and medical applications. The extremely high water contents achievable with hydrogels leads to unique physiochemical properties as the water content of these materials, and their resulting soft and rubbery consistency, enable hydrogels to resemble natural living tissue more closely than other synthetic biomaterials[203]. These properties are advantageous in many biological applications including drug delivery, tissue engineering, diagnostics and cell attachment, and a number of reviews of this area are available[198, 199, 204-209].

It is possible to produce hydrogels from both natural and synthetic polymers and both types of materials have advantages and disadvantages (Table 1.1). Natural polymers have advantages of inherent biocompatibility, biodegradability and may also contain moieties which are able to support cellular activities[200]. The possible disadvantages of insufficient mechanical properties and the chance that they may evoke an immune or inflammatory response must be weighed up against the advantages. Similarly, synthetic hydrogels may have the advantages of being well-defined structures and therefore have controllable degradation and functionality, but have no inherent bioactive properties. The properties required for a particular application must be considered when selecting the basic hydrogel formulation.

| Natural Materials | Synthetic Materials |
|---|---|
| Alginate | Acrylic acid (AA) |
| Chitosan | 2-Hydroxyethyl methacrylate (HEMA) |
| Collagen | *N*-(2-hydroxypropyl) methacrylate (HPMA) |
| Dextran | Methacrylic acid (MAA) |
| Fibrin | *N*-isopropyl acrylamide (NIPAM) |
| Gelatin | *N*-vinyl-2-pyrrolidone (NVP) |
| Hyaluronic acid | Poly(ethylene glycol) acrylate/methacrylate (PEGA/PEGMA) |
| | Poly(ethylene glycol) diacrylate/dimethacrylate (PEGDA/PEGDMA) |
| | Vinyl acetate (VAc) |

**Table 1.1 Monomers commonly employed in hydrogel synthesis (adapted from Lin et al[200])**

### 1.8.3 Hydrogels as Wound Dressings

Dressings for wound healing have been used throughout history, with traditional dressings including natural or synthetic bandages, lint, gauzes and cotton wool[5]. These traditional approaches aimed to keep the wound dry and free from bacteria. It is now known that wounds heal faster and more effectively in a moist environment. A review by Menaker et al[210] discusses that a moist environment can prevent tissue loss, promote enzymatic activity to clear residual debris in the early stages of wound healing and facilitate keratinocyte migration. All of these factors mean that a wound able to heal in a moist environment can develop greater breaking strength and is cosmetically superior[210]. There are a number of requirements for a successful wound dressing. These include being able to maintain a moist environment, allowing gaseous exchange whilst being impermeable to exogenous micro-organisms, being able to remove excess exudates, maintaining a suitable temperature and pH, having appropriate mechanical strength and allowing easy removal without trauma[5, 10, 211]. Many different types of dressings are available to meet these criteria for different applications[211] (Table 1.2).

| Dressing categories | Sub-categories |
|---|---|
| Non-adherent fabrics | |
| Absorptive fabrics | Foam, gauze |
| Occlusive dressings: | |
| Non-biologic | Alginates, Films, Foams, Hydrocolloids and Hydrogels |
| Biologic | Amnion, Homograft, Skin substitutes and Xenograft |
| Creams, ointments and solutions | Antibacterial, Enzymatic and others |

**Table 1.2: Types of dressings (adapted from Lionelli et al[211] with additions from Menaker et al[210])**

Occlusive dressings, those dressings that maintain a moist wound surface when in place[212], can be defined in two categories, biologic and non-biologic, with the non-biologic category further divided into five major groups; films, foams, alginates, hydrocolloids and hydrogels[210-212].

There are many types of hydrogels currently on the market including Vigilon, Cutinova, Gelfolie, Nu-gel, Tegagel, Flexigel, Curagel, Flexderm, Aquaform, Granugel, Hypergel, Intrasite gel and Purilon gel[210, 211, 213]. Suitable hydrogels are made from a variety of polymers including poly(ethylene oxide), poly(propylene glycol), carboxymethylcellulose,poly(methacrylate) and poly(N-vinyl-2-pyrrolidone)[5, 210, 211, 213].

Hydrogels are well suited to application as an occlusive dressing and are available as gels, sheets or impregnated gauze[211]. Due to the high water contents discussed earlier, they are able to maintain a moist environment but are not always able to absorb much wound exudate, generally limiting their application to light and moderately exuding wounds[5]. The flexibility of hydrogel sheets means that they can be cut to fit a wound and will follow the wound contours. They are non-adherent and so are easy to remove but therefore also require a secondary cover to secure them. A secondary cover also provides a barrier to bacteria as hydrogels themselves are poor bacterial barriers[210]. Hydrogels are also non-reactive with biological tissue, non-irritant and permeable to air and water[5]. An advantageous property of hydrogel-based dressings is a cooling effect that occurs. Hydrogels have a high water content, which has a high specific heat capacity and is therefore able to absorb excess heat from the epidermis, thus cooling the skin. The application of a hydrogel is able to cool the skin surface by up to 5°C and maintain the temperature reduction for up to six hours, thereby helping to reduce pain and inflammation[212]. Due to numerous advantageous characteristics, hydrogels are thought to be suitable for use at all stages of wound healing except for infected or heavily-exuding wounds[214].

### 1.8.4 Hydrogels for Drug Delivery

As previously discussed, protein delivery by bolus injection is not optimal due to short half-lives of the proteins and proteolytic degradation, leading to short circulation times and fast renal clearance[200]. This has led to development of many polymeric protein delivery devices (as detailed in section 1.5). Hydrophilic hydrogels have many unique properties which make them suitable for drug or biomolecule delivery. The use of hydrogels often allows mild synthetic and encapsulation procedures, and these materials are flexible and as such they are able to conform to a required shape. Crucially, hydrogels are generally biocompatible due to their high water content and resultant physiochemical similarity to the ECM[203]. The fact that hydrogels are hydrophilic in nature also provides an advantageous "stealth" characteristic *in vivo* through avoidance the host's immune response, thereby causing a reduction in phagocytosis (reviewed by Lin et al[200]).

The highly porous structure of hydrogels can be easily controlled by altering the chemical composition of the material which allows loading of the drug or biomolecule into the matrix and subsequent release. Many hydrogel formulations also offer a stimuli responsive character which is used extensively in drug delivery. It is possible to produce hydrogels which exhibit dramatic changes in swelling behaviour, network structure, permeability and mechanical strength when presented with an external stimulus, such as temperature, electric field, light, pressure, magnetic fields, pH and the presence of ions[215]. This responsive characteristic is ideal for a delivery system as the reversible swelling allows controlled release.

Modification of the chemical composition of a hydrogel also provides a number of attractive properties. Addition of a functional group (e.g. acrylic acid) allows bioadhesiveness[200] and control of the concentration of a particular functionality allows incorporation of the desired quantity of drug into the hydrogel matrix. It is also possible to design hydrogels to be biodegradable via a variety of mechanisms, including enzymatic, hydrolytic or environmental degradation due to pH or temperature[204].

***Loading and Delivery Mechanisms***

The loading of drugs or biomolecules into a hydrogel matrix is thought to be performed by two approaches; post loading and *in situ* loading[200]. In post loading the compound is absorbed after the hydrogel has been formed. In this case absorption occurs via diffusion and is also influenced by any functionality in the hydrogel which interacts with the compound. *In situ* loading occurs simultaneously with hydrogel matrix formation and encapsulates the compound as the hydrogel is formed around it.

Methods to deliver drugs or biomolecules from hydrogels range from very simple to more sophisticated approaches, the major types of which are as follows, as discussed by Baldwin et al[216]. If hydrogel systems are only physically crosslinked the compound will be released upon polymer dissolution. Degradation of chemically crosslinked hydrogels can occur by a number of mechanisms and for these systems the release can occur at a rate dependent on this degradation. For those hydrogels containing functionality for interaction with the compound (e.g. ionisable groups), the release rate may be determined by the binding release rate between the polymer and drug or biomolecule. Release from hydrogels with covalently incorporated compounds will be dictated by

cleavage of the covalent bond. Release rates can also be determined by the swelling characteristics of hydrogels which are chemically crosslinked. These different mechanisms lead to a wealth of delivery methods which can be tuned for a specific application. Chemical composition including choice of monomer and crosslinking density can be modified to provide the desired rates of dissolution and degradation, as well as determining the stimuli responsiveness of a system.

### 1.8.5 Current Approaches for Hydrogel-Based Protein Delivery Systems

There is a wealth of literature available detailing protein drug release from hydrogels, a number of which, developed by Tabata et al[75], Peattie et al[64, 83, 85, 86], Hiemstra et al[93], Norton et al[94], Zisch et al[95], Kavanagh et al[96], Ehrbar et al[97] and Yoon et al[102], have already been discussed in section 1.5.2 for the delivery of angiogenic growth factors. There are number of recent reviews available[204, 217, 218] and the reader is directed to these for a detailed insight into this area. Here a few recent examples will be provided to demonstrate the variety of hydrogels currently available for protein delivery.

Various pH sensitive systems have been well researched and there are a number of examples available. A pH sensitive system was reported by George et al[219], synthesised from alginate and guar gum, a non-ionic polysaccharide, crosslinked by glutaraldehyde, for intestinal delivery of BSA. Such materials could minimise release in the acidic stomach and then release the drug upon swelling as pH increases in the intestinal tract. Alginate, the pH sensitive component, dissolves fast at high pH and so it was combined with guar gum and crosslinker to control the release. Guar gum was expected to retard release as it swells when hydrated, forming a viscous layer. The optimum ratio of 3:1 alginate to guar gum with 0.5% crosslinker was shown to release the drug at pH 7.4 due to hydrogel swelling. At pH 1.2 only 22% of BSA was released, in comparison to 94% at pH 7.4. Very recently Xiao et al[220] produced a pH sensitive hydrogel from carboxymethyl pachyman, a β-D-glucan, crosslinked with epichlorohydrin. This hydrogel was found to be biodegradable and the release of two model proteins, BSA and lysozyme, in simulated intestinal media was found to be due primarily to diffusion but also due to degradation of the matrix. Encouragingly, when released from the hydrogel, the stability and enzymatic activity of the protein was retained, presumably because the hydrogel is able to shield the proteins from proteolytic attack.

Temperature can also be used to control protein release. Wu et al[221] employed poly(N-isopropylacrylamide) (poly(NIPAM)) hydrogels to release BSA and insulin in a thermosensitive system. Poly(NIPAM) hydrogels have a lower critical solution temperature (LCST) at approximately 32°C. Below this LCST, the hydrogel is swollen and hydrophilic but above this temperature the hydrogel shrinks into a collapsed hydrophobic state. In this case poly(NIPAM) was crosslinked with varying concentrations of N,N'-methylene bisacrylamide and release was shown to be dependent on the size of the protein as insulin, the smaller protein, was released faster than BSA and over 48 hours almost 94% of the insulin loaded was released in comparison to only 57% of the BSA.

A number of hydrogels are designed to be injectable, gelling upon introduction to the body. Tae et al[222] prepared physically crosslinked hydrogels produced by poly(ethylene glycol) modified with fluorocarbon end groups. This composition results in an injectable liquid which became a hydrogel upon introduction to an aqueous environment due to hydrophobic interactions between the end groups. Their results showed that when human growth hormone (hGH) is complexed with $Zn^{2+}$, release is prolonged up to two weeks from these hydrogels with no destabilisation, aggregation or burst release. BSA, hGH and γ-globulin were all found to be released by diffusion, but surface erosion of the hydrogel also occurs and it was suggested that larger proteins would only be released as the material is degraded. Injectable amphiphilic poly(ethylene glycol) based hydrogels were also synthesised by Huyng et al[223] from pentablock copolymer containing poly(β-aminoester), poly(ethylene glycol) and poly(ε-caprolactone). This system is temperature and pH sensitive. At low temperatures and low pH the polymer is in solution and interacts with the protein, insulin, ionically. After injection into the body, and resultant increase in temperature and pH to 37°C and pH 7.4, a micellar gel is formed, containing the insulin by ionic interactions with the aminoester functionality. Release of the insulin then occurs by diffusion and also by degradation of the poly(β-amino ester). Other injectable and biodegradable hydrogels include poly(ethylene glycol) hydrogels produced from acrylated poly(lactic acid)-b-poly(ethylene glycol)-b-poly(lactic acid) macromonomers. These hydrogels were produced by Piantino et al[224] to control the release of Neurotrophin-3 by degradation via ester hydrolysis of the crosslinks. *In vitro* analysis showed that release could be controlled by chemical

composition, with the optimised composition allowing release over 2 weeks. *In vivo* analysis showed that the released Neurotropin-3 was biologically active.

Natural polymers are also used extensively in systems controlled by diffusion and degradation. Carvalho et al[225] discuss dextrin hydrogels which are produced by derivatising dextrin with vinyl acrylate groups. These hydrogels were shown to release BSA over various time frames as release was diffusion-based and was dependent on crosslinking density. Two natural, hydrophilic polymers; sodium alginate and hydroxypropyl methylcellulose (HPMC), were used to produce hydrogel beads for release of BSA by Nochos et al[226]. A high BSA loading was exhibited for all hydrogel formulations. The incorporation of HPMC into alginate hydrogel beads resulted in an increased degree of swelling, due to high hydrophilicity, which in turn resulted in improved BSA release in a physiological saline solution. 42% of BSA was released from the HPMC-alginate system in 7 hours, in comparison with the 5% released for sodium alginate only.

Enhanced corneal epithelial wound healing was achieved by controlled release of epidermal growth factor by Hori et al[227]. Cationic gelatin hydrogels, crosslinked with glutaraldehyde, were used and release of the growth factor was as a result of biodegradation of this material. *In vitro* the release was shown to be biphasic with an initial burst followed by slow release. *In vivo* analysis showed that release of the growth factor from these hydrogels led to accelerated wound healing in a rabbit corneal epithelial defect model.

The release of multiple growth factors was discussed in section 1.5 and was shown to be beneficial in the examples given. The release of two different proteins was also reported by Lee et al[228] from hyaluronic acid and tyramine hydrogels. They showed that release was related to the mechanical strength of the hydrogel, with weaker hydrogels releasing proteins faster than stronger ones. Release was also shown to be dependent on the interaction of the protein with the hydrogel. Negatively charged α-amylase was released by diffusion from the hydrogel, whereas lysozyme, a positively charged protein, interacted with hyaluronic acid and therefore was released only due to degradation of the hydrogel, resulting in unique release kinetics for each protein.

### 1.8.6 Hydrogel Summary

Hydrogels have been used extensively as drug delivery systems due to many advantageous properties including biocompatibility, mild synthetic procedures and the wide range of formulations possible. A significant property of hydrogels is the release control that can be achieved depending on the chemical composition selected. Drug release can be controlled by swelling of the materials, often in response to an external stimulus, and degradation of the polymer, thus material design can be tailored to achieve the release kinetics required. As discussed previously, hydrogels have already been investigated to release growth factors and the successes reported suggest that there is considerable scope to develop new hydrogel formulations for specific growth factor-delivery applications.

## 1.9 Summary

The vital role of angiogenesis within the wound healing process has been discussed and the important role of angiogenic growth factors has been highlighted. VEGF, a potent angiogenic stimulator, was discussed in detail, as well as the influence of heparin-interaction. The potential of VEGF for therapeutic application was considered and a number of current approaches were discussed for delivery of exogenous angiogenic growth factors. Whilst impressive results have been presented by a number of groups, no material is currently able to fulfil all roles of the ECM whilst remaining simple to produce, reproducible and cost-effective. In order to produce a successful ECM-mimic, two approaches to protein delivery have been introduced, molecularly-imprinted polymers and hydrogel delivery systems. In both cases a number of impressive systems have been detailed, showing the potential of these approaches for protein delivery in a wide range of applications.

## 1.10 Project Overview

As discussed in section 1.6, this thesis details the development of a biocompatible system that is capable of binding and releasing a patient's own VEGF in a wound healing application. An approach utilising a patient's own growth factors is expected to be more cost-effective than exogenous protein delivery, as well as easier to develop and get regulatory approval for moving to the clinic. It also removes the risk of protein denaturation during the synthetic procedure.

Two approaches are investigated: VEGF-specific molecularly-imprinted particles and a heparin-bound peptide-functionalised hydrogel for interaction with heparin-binding growth factors. These materials were designed to mimic the ECM, binding growth factors non-covalently to allow release within a wound, whilst fulfilling the clinical requirements of being relatively simple to produce, easy-to-handle, stable, cost-effective and socially-acceptable as they would not require delivery of exogenous growth factor.

***Project Objectives***

***Approach 1: Molecularly-Imprinted Polymers***

1. Design a suitable MIP system for binding and release of VEGF
2. Optimise synthetic procedure
3. Synthesise and characterise MIP and a false-imprinted and non-imprinted comparison
4. Analyse the VEGF binding and release characteristics

***Approach 2: Heparin-Bound Peptide-Functionalised Hydrogels***

1. Design a hydrogel system capable of binding and release of VEGF through interaction with bound heparin.
2. Synthesise and characterise a heparin-binding hydrogel
3. Analyse VEGF binding and release characteristics
4. Analyse hydrogel cytocompatibility with relevant skin cells
5. Analyse hydrogel potential to stimulate angiogenesis with an *in vitro* angiogenesis model

# 2 Strategy 1: Core-Shell Particles

## 2.1 Consideration of VEGF as a Target for Molecular Imprinting

The crucial role of VEGF within both physiological and pathological angiogenesis makes this protein an intriguing template for molecular imprinting. As discussed in the introduction to this report, there are a variety of approaches utilised to imprint such biological materials into molecularly-imprinted polymers, each with advantages and disadvantages. It is thought that to produce a selective MIP, the synthetic route undertaken should consider the application of the material produced, time and cost constraints, the type and format of polymeric material and the nature of the template itself.

As discussed in section 1.7, core-shell molecularly-imprinted particles (CS-MIPs) have been produced previously in our research group. These particles consist of a poly(styrene-co-divinyl benzene) core with a molecularly-imprinted outer shell of oleyl phenyl hydrogen phosphate crosslinked with ethylene glycol dimethacrylate. Research carried out with these particles by Carter et al[157, 159, 160] prior to this project concentrated on hydrophobic, low molecular weight organic compounds. The use of such compounds as templates enabled electrostatic interactions and hydrogen bonding with the phosphate functional monomer, as well as hydrophobic interactions, to produce successful recognition polymers. These materials meet many of the criteria discussed for the imprinting of biomacromolecules, such as the location of the cavities in the outer shell only and the compatibility with aqueous medium. Prior to this project, such particles had been imprinted with tripeptide sequences and the results suggested that recognition of short peptide sequences is possible[160]. As mentioned previously, Rachkov et al[190] have reported the "epitope approach" for the imprinting of proteins; a promising approach involving the imprinting of peptides consisting of a specific amino acid sequence which is also found on the protein of interest (Figure 2.1). The resulting polymer would then be able to recognise the protein through the amino acid sequence imprinted. This approach is thought to be cost-effective as it allows the use of synthetic peptide sequences rather than expensive protein, and could potentially produce imprinted polymers with higher selectivity than whole-protein systems due to the use of unique peptide sequences, allowing size and shape selectivity, instead of relying on multiple hydrogen bonds alone.

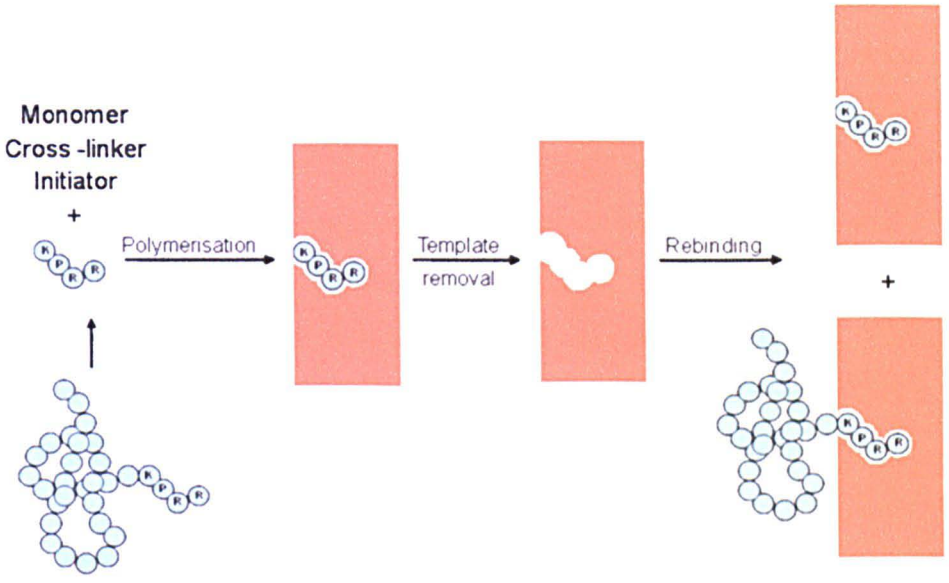


**Figure 2.1: Schematic of the epitope approach to molecular imprinting. An amino acid sequence from a protein is selected and this amino acid sequence is used to synthesise a peptide. The peptide is then imprinted into the polymer. Following removal of the template, an imprinted cavity is then present in the polymer which is able to bind both the peptide as well as the original protein (adapted from Rachkov et al[190]).**

Heparin and cell surface-bound heparin-like glycosaminoglycans (GAGs) bind with VEGF *in vivo*, influencing the interaction of VEGF with endothelial cell receptors and therefore VEGF's ability to induce angiogenesis[44, 46]. This research initially attempts to produce a polymer capable of interacting with the protein as a "heparin-mimic", meaning it should interact with the protein via its heparin binding region and through similar interactions. Whereas heparin is able to bind electrostatically with basic amino acids present on VEGF through its sulphate moieties, the core-shell particles produced would be designed to interact electrostatically through the phosphate-based functional monomer present in the shell of the particles. Sulphate-based monomers have been investigated previously in unpublished work by S. Carter and were shown to produce less effective CS-MIPs than the phosphate alternatives.

The previous success reported for the imprinting of short peptide sequences in these core-shell particles, as well as the advantages expected for the epitope approach meant that this approach was selected for this project. Core-shell particles with phosphate functionality in the outer shell were targeted for interaction with a peptide sequence containing basic amino acids from the heparin-binding region of VEGF.

## 2.2 Methodology

Core-shell particles molecularly-imprinted with biological materials were produced via emulsion polymerisation. An emulsion is defined by IUPAC as being a "fluid colloidal system in which liquid droplets and/or liquid crystals are dispersed in a liquid"[229]. This type of polymerisation requires a dispersing medium (in this case water), a water-insoluble or only slightly water-soluble monomer, a water-soluble initiator and a surfactant, which is employed above the critical micelle concentration (CMC) to allow formation of micelles[230]. Polymerisation then occurs within these micelles, generally resulting in polymer particles with diameters ranging from 50-500 nm[231].

The core-shell particles for this application were produced following the general procedure described by Carter et al[157, 159, 160]. The particles were prepared via a two-stage batch emulsion polymerisation process leading to a core-shell structure (Figure 2.2). The core particles were synthesised from a styrene/divinylbenzene monomer feed in the presence of surfactant to produce crosslinked poly(styrene-co-divinylbenzene) nanoparticles. A second polymerisation phase was then initiated in the presence of a template to coat the core particles with an outer shell of crosslinker, EGDMA and functional monomer, oleyl phenyl hydrogen phosphate (OPHP).

The functional monomer employed in this research, oleyl phenyl hydrogen phosphate, originally isolated by Takagi et al[158], is a long chain alkyl phosphate, combining surface-active functionality with the ability to interact electrostatically with nitrogen donor atom-containing templates via the phosphate group. This allows the formation of core-shell molecularly-imprinted particles containing easily accessible imprinted cavities within the outer shell, offering advantages including ease of template removal, accessibility of imprinted cavities and compatibility with water, but it is also acknowledged that, as for most techniques, this methodology is not without its disadvantages. Consideration of the functional monomer reveals that it has disadvantages due to its polymerisability. The location of the double bond, internal to the long alkyl chain, renders it relatively unreactive and it is suggested that the monomer is not truly copolymerised but is instead incorporated into the EGDMA network through transfer of the radical via hydrogen abstraction[157].

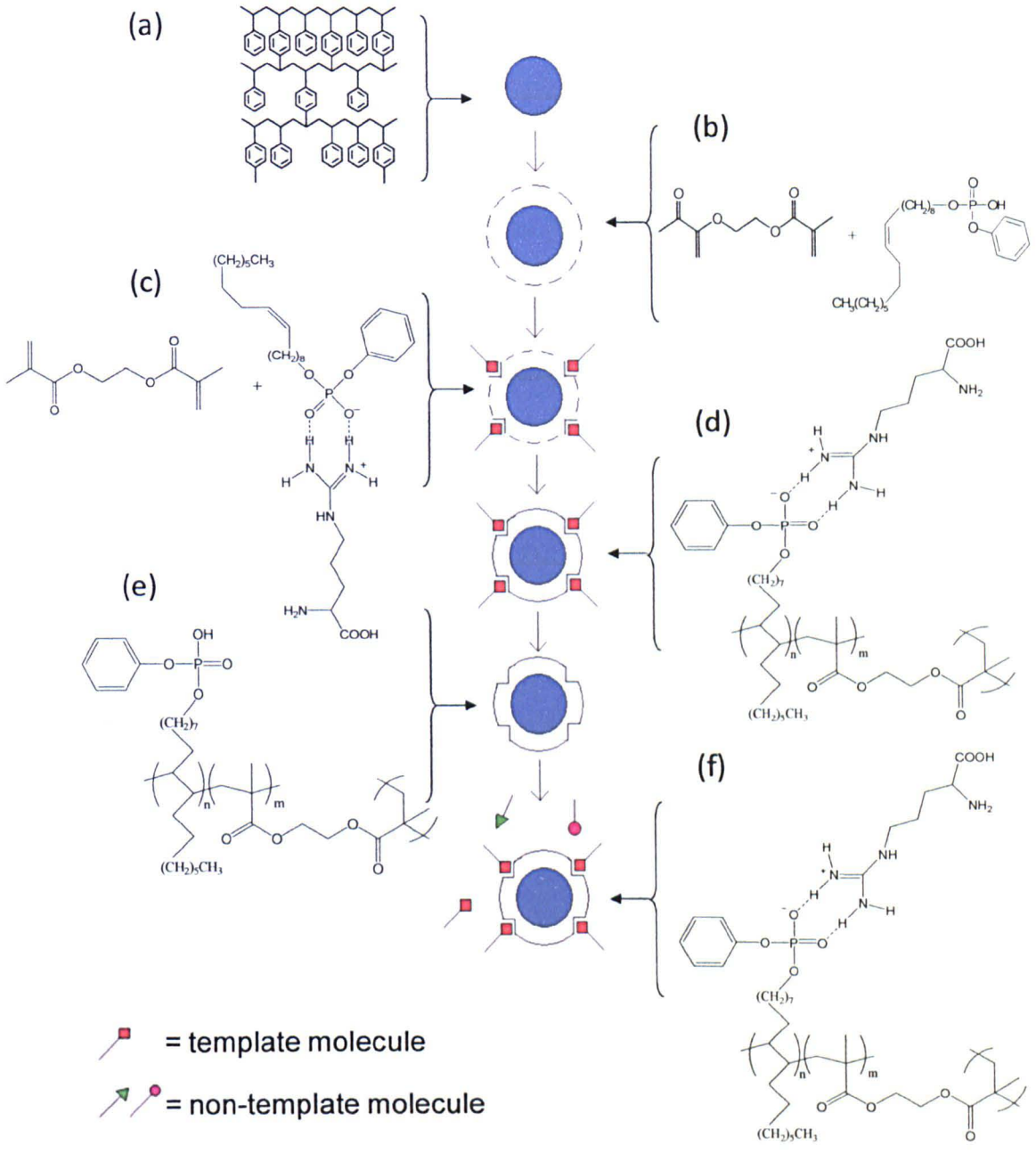


**Figure 2.2: Methodology of core-shell molecularly-imprinted particle synthesis (shown with arginine as an example template). (a) Synthesis of crosslinked polystyrene core particles. (b) Equilibriation of shell monomers around core particles. (c) Interaction of template molecule with functional monomer. (d) Polymerisation of the outer shell in the presence of the template molecule. (e) Removal of the template molecule. (f) Reintroduction of the template molecule to the molecularly-imprinted core-shell particle.**

## 2.3 Optimisation of Synthesis

In this work, a basic amino acid sequence from the heparin binding region of VEGF was selected as the template for imprinting (discussed in Chapter 3). It was thought that selecting a basic region should allow optimum selective binding with the phosphate groups of the CS-MIP. It was hypothesised that peptides which contain more hydrophobic or neutral amino acids, such as those trialled previously by Carter et al[160], will be imprinted more readily than those containing highly basic and hydrophilic moieties, as charged sequences may not be influenced by the hydrophobic effect and will therefore rely upon electrostatic interactions with the functional monomer alone to incorporate the peptide into the shell of the particles. It was therefore considered necessary to attempt to optimise electrostatic binding between the CS-MIP and template species in this case, to improve molecular imprinting of a basic peptide. Non-covalent interactions, such as the hydrophobic effect and electrostatic binding, are thought to be strongest in lower temperature environments and lower temperature synthesis routes have been shown to produce MIPs with higher selectivity[232]. The initial attempt at optimising the process was therefore to consider the possibility of carrying this reaction out at a low temperature to optimise the non-covalent interactions.

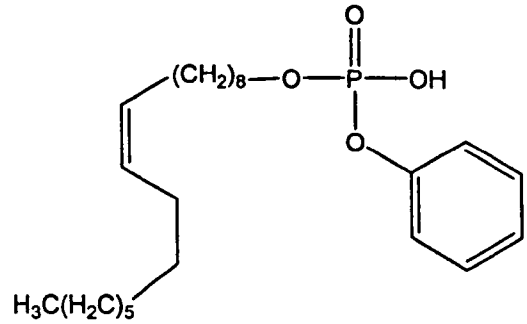


**Figure 2.3: Structure of oleyl phenyl hydrogen phosphate**

Another area for consideration was the functional monomer, oleyl phenyl hydrogen phosphate (Figure 2.3). The surfactant-like properties of this monomer were thought to locate imprinted cavities at the surface of the core-shell particles, but as discussed previously, the location of the double bond internal to the alkyl chain renders oleyl phenyl hydrogen phosphate fairly unreactive in radical polymerisation. The location of cavities at the particle surface is vital in epitope imprinting to allow access of the larger protein, and so it was decided to continue using this monomer despite its low reactivity and attempt to optimise incorporation of this monomer into the core-shell particles.

## 2.4 Redox Initiation Study

Potassium persulphate and ascorbic acid were selected as a redox initiator system to allow polymerisation to occur at a low temperature. Research by Gafurov et al[233] showed that ascorbic acid is a promising component of a redox initiator system, as it retains a high reducing power at a wide range of pH, and demonstrated its use at 30°C. The decomposition of the potassium persulphate is thought to be accelerated by the dienol group of ascorbic acid through the following donor-acceptor interactions which allows the reaction to occur at lower temperatures (Figure 2.4).

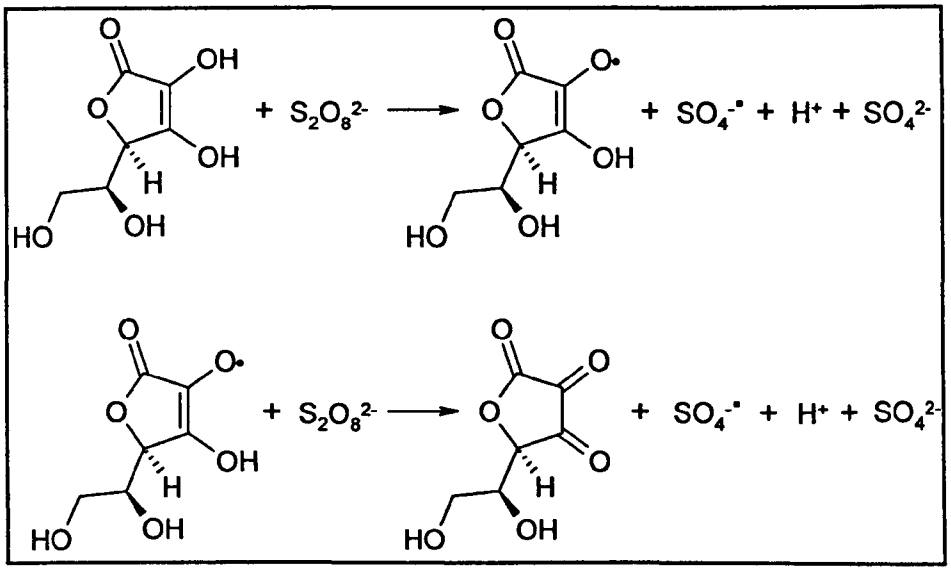


**Figure 2.4: Suggested interaction between potassium persulphate and ascorbic acid (from Gafurov et al[232])**

A number of experiments were carried out to determine whether this redox system could be used to produce core-shell particles at 30°C, as well as the effect of ascorbic acid on the stability of the resulting latex.

### 2.4.1 Results of Redox Initiation Trials

Different latex formulations for the synthesis of cross-linked polystyrene core particles were trialled both to investigate the effect of this initiator system on the latexes produced, and to optimise the polymerisation with this initiator system.

| Sample | Styrene (g) | DVB (g) | Molar Ratio | SDS (g) | Temp (°C) | Potassium Persulphate (g) | Ascorbic acid (g) | Molar Ratio |
|---|---|---|---|---|---|---|---|---|
| 1 | 4.64 | 5.82 | 1:1 | 1.00 | RT | 0.105 | 0.068 | 1:1 |
| 2 | 8.36 | 1.16 | 9:1 | 1.00 | RT | 0.105 | 0.068 | 1:1 |
| 3 | 8.36 | 1.16 | 9:1 | 0.50 | 30 | 0.105 | 0.068 | 1:1 |
| 4 | 8.36 | 1.16 | 9:1 | 2.00 | 30 | 0.105 | 0.068 | 1:1 |
| 5 | 8.36 | 1.16 | 9:1 | 1.00 | 30 | 0.105 | 0.068 | 1:1 |
| 6 | 8.36 | 1.16 | 9:1 | 1.00 | 30 | 0.209 | 0.068 | 2:1 |
| 7 | 4.50 | 0.50 | 11:1 | 1.00 | 30 | 0.209 | 0.068 | 2:1 |

**Table 2.1: Latex formulations for poly(styrene-co-divinylbenzene) core particles (RT = room temperature SDS = sodium dodecyl sulphate surfactant)**

All latexes produced followed the method described in section 10.3.3 with varying conditions (Table 2.1), with the aim of synthesising a latex with little or no coagulum.

| Formulation | Solids Content (%) | Particle Diameter (nm)[a] | Comment |
|---|---|---|---|
| 1 | 5.9 | 23 | Coagulated |
| 2 | 12.2 | 68 | Significant coagulation |
| 3 | 10.4 | 33 | Significant coagulation |
| 4 | 13.4 | 37 | Significant coagulation |
| 5 | 12.3 | 33 | Significant coagulation |
| 6 | 13.1 | 42 | Slight coagulation |
| 7 | 7.2 | 43 | No coagulation |

**Table 2.2: Physical properties of poly(styrene-co-divinylbenzene) latexes (a) average particle diameter determined by light scattering**

Initially a 1:1 molar ratio of styrene to divinylbenzene was employed, as in sample 1, but this ratio led to a low viscosity emulsion with large amounts of coagulum forming within the reaction vessel. Switching from 1:1 to 9:1 styrene to divinylbenzene reduced the quantity of coagulum produced significantly, although it was only when the solids

content within the emulsion was halved, for sample 7, that an emulsion free from coagulation was produced.

The solids contents of the latexes were analysed, which suggested that the overall yield of the reaction was largely unaffected by factors such as surfactant quantity, molar ratio of potassium persulphate to ascorbic acid or monomer ratio. Formulations from 2 to 6 were found to have solids contents from 10.4% to 13.4% after coagulation and washing. The latex produced in sample 1 was found to have a solids content of only 5.9%, due to the extremely high amount of coagulum observed. A 7.2% solids content was observed for sample 7, a latex with half of the initial monomer content. It is acknowledged that these values are inaccurate as they do not take into account the solids present as coagulum, and for this reason no final monomer conversion values are available.

The particle diameters of these latexes, both for the core particles discussed here and the core-shell particles which are discussed later, are very small, in the region of 20-70 nm. The particle sizes observed are smaller than would be anticipated from a standard emulsion polymerisation technique (generally 50-500 nm), and instead bear resemblance to particles produced by microemulsion polymerisation (generally 10-100 nm), which can occur when either the surfactant concentration is very high or the monomer concentration is very low[231, 234]. In this case it is expected that the formation of such small particles is due to the large quantities of surfactant. This high level of surfactant was employed following the general procedure previously described by Carter et al[157, 159, 160]. The formation of particles with small diameters is thought to be advantageous as this will lead to an increased surface area of the resultant polymer; which is important for surface-imprinting techniques.

After the alteration of monomer composition from 1:1 styrene/divinyl benzene to 9:1 styrene/divinyl benzene, the particle size increased from 23 nm to 68 nm. This is most likely to be due to the coagulation of the larger particles present in sample 1, leading to a lower particle size for this sample. Altering the monomer composition in this way would not be expected to significantly affect the particle size of the latexes produced. No significant effect on particle size was observed as surfactant level was varied in samples 3, 4 and 5. At such a high level of surfactant, any further increases in surfactant concentration would be expected to have a minimal effect on the particle size observed.

In sample 6, the quantity of potassium persulphate was doubled to give a 2:1 molar ratio of potassium persulphate to ascorbic acid as suggested in research by Gafurov et al[233]. This had little effect on the overall solids content of the latex, but led to an increase in particle size and a decrease in coagulation. This is likely to be due to minimising the quantity of unreacted ascorbic acid present in the latex, thereby increasing the colloidal stability of the system. Finally, halving the monomer content of the reaction in sample 7 produced the most successful latex with a solids content of 7.2%. No coagulation was observed for this system and particles of 43 nm diameter were produced. It was this system that was chosen as the optimised procedure for further investigations into core-shell synthesis.

## 2.5 Investigation into Alternative Initiator Systems

It was thought that to optimise the imprinting efficiency of this polymer system it would be important to achieve the highest incorporation of the functional monomer, OPHP, as possible in the outer shell of the particles. This should lead to improved recognition properties as it may enable interaction with more template molecules, or especially where templates with more than one functional group are concerned, the template may interact with more than one functional monomer, possibly producing a more specific recognition cavity. Five formulations were trialled for core-shell synthesis, both redox and thermal systems, using the optimised formulation of sample 7, varying only in the choice of initiator. The systems trialled were potassium persulphate and ascorbic acid (system 1), 4,4'-azobis-(4-cyanovaleric acid) (system 2), hydrogen peroxide and ascorbic acid (system 3), ammonium persulphate and N,N,N',N'-tetramethylethylenediamine (TEMED) (system 4) and potassium persulphate (system 5). All of these were used successfully to produce latexes of core particles with solids contents of 7.2%, 7.8%, 6.9%, 6.8% and 7.3% for initiator systems 1 to 5 respectively.

The effect of outer shell formation around the core particles (i.e. core-shell synthesis) was then analysed with respect to particle size, zeta potential and incorporation of oleyl phenyl hydrogen phosphate as determined by ion coupled plasma atomic emission spectroscopy (ICP-AES). ICP-AES was carried out at the Centre for Analytical Sciences, University of Sheffield.

Initially initiator system 1 was analysed to determine whether it was possible for the outer shell polymerisation to occur at a low reaction temperature. ICP-AES was employed to investigate the practicality of such a system with a relatively unreactive monomer such as oleyl phenyl hydrogen phosphate. Particle size analysis of the core and core-shell particles produced by initiation with potassium persulphate and ascorbic acid showed a significant increase in particle size as the shell is formed, as would be expected. An increase of approximately 7 % in diameter is observed from the core to the core-shell particles, from 44 nm to 47 nm. Although these results infer that a shell is formed on the surface of the poly(styrene-co-divinylbenzene) core particles, it does not provide any information on the incorporation of the functional monomer. ICP-AES analysis revealed that 59.3 mg/kg of phosphorous was found within the core-shell particles, equating to the incorporation of only 1.9% of the functional monomer introduced to the reaction mixture. Absence of phosphorous in the core particles was confirmed by ICP-AES analysis, which showed that, as expected, the poly(styrene-co-divinylbenzene) particles contain less than 4.45 mg/kg phosphorous, which is below the threshold of the technique. This confirms that phosphorous in the core-shell particles was due to the phosphate monomer. Such a low incorporation of functional OPHP monomer into the outer shell of the particles suggests that this initiator system may not be suitable in this case.

In order to determine whether oleyl phenyl hydrogen phosphate could be successfully incorporated into the core-shell particles in a low temperature reaction, the other two redox initiator systems were trialled; hydrogen peroxide with ascorbic acid at 35°C (initiator system 3), and ammonium persulphate with N,N,N',N'-tetramethylethylenediamine (TEMED) at 30°C (initiator system 4) (Table 2.3). Particle size analysis of both systems showed a significant increase in particle size (Figure 2.5) upon formation of the outer shell, inferring that a shell had been formed on the particles. However, as for the potassium persulphate redox system, these low temperature systems afford relatively low functional monomer incorporation of 3.5% and 1.9% for hydrogen peroxide system and ammonium persulphate system respectively. When considering the functional monomer incorporation, these results suggest that hydrogen peroxide and ascorbic acid is the most successful initiator system for a low temperature reaction, but the limited incorporation of OPHP for all of the low temperature systems suggests that, for this monomer, this approach may not be suitable.

| Initiator System | 1 | | 2 | | 3 | | 4 | | 5 | |
|---|---|---|---|---|---|---|---|---|---|---|
| Initiators | Potassium persulphate & ascorbic acid | | 4,4'-azobis-(4-cyanovaleric acid) | | Hydrogen peroxide & ascorbic acid | | Ammonium persulphate & TEMED | | Potassium persulphate | |
| Particle Type | Core | Core-shell | Core | Core-shell | Core | Core-shell | Core | Core-shell | Core | Core-shell |
| Temp. (°C) | 30 | 30 | 60 | 60 | 35 | 35 | 30 | 30 | 70 | 70 |
| Average Particle Diameter (nm)[a] | 44.0 | 47.2 | 42.1 | 45.5 | 51.1 | 53.8 | 47.4 | 51.9 | 28.7 | 111.7 |
| Average Zeta Potential (mV) | -46.3 | -47.7 | -46.8 | -47.9 | -42.2 | -47.5 | -39.6 | -44.7 | -44.2 | -52.6 |
| Phosphorous content (mg/kg)[b] | - | 59.3 | - | 201.3 | - | 101.5 | - | 56.6 | - | 350.2 |
| Functional monomer incorporation (%) | - | 1.9 | - | 6.5 | - | 3.5 | - | 1.9 | - | 11.7 |

**Table 2.3: Results of initiator trial (a) average particle diameter determined by light scattering (b) phosphorous content determined by ICP-AES**

As discussed previously, the internal double bond present within the alkyl chain of oleyl phenyl hydrogen phosphate is thought to be fairly unreactive and so this monomer does not copolymerise very successfully. The monomer is most likely incorporated into the shell of the core-shell particles via transfer[157], the reaction between a radical and a non-radical species in which a hydrogen atom is abstracted from oleyl phenyl hydrogen phosphate leaving a radical present on the monomer. The radical can be stabilised through resonance with the double bond present, subsequently decreasing the reactivity of the radical. A transfer reaction between a radical and a non-radical species may have a higher activation energy than a standard propagation reaction which could make this reaction strongly temperature-dependent[235]. It is suggested that at the temperatures previously trialled, 30-35°C, the activation energy had not been overcome and therefore the incorporation of the functional monomer into the shell of the particles was minimal. Any phosphate monomer present within the shell was unlikely to have been covalently bound and was therefore removed during the vigorous washing steps undertaken prior to ICP-AES analysis.

Although it is thought that the use of low temperature systems could optimise non-covalent reactions between the template and functional monomer employed in molecular imprinting, it is necessary to incorporate as much of the functional monomer as possible to produce molecularly-imprinted polymers capable of recognition. The two thermal initiator systems were then trialled, 4,4'-azobis(4-cyanovaleric acid) (initiator system 2) and potassium persulphate (initiator system 5) (Table 2.3). It was hypothesised that a higher temperature would enable the activation energy for a transfer reaction to be reached, and therefore should lead to an increase in the incorporation of OPHP. The ICP-AES results confirmed this hypothesis, as incorporations of 6.5% and 11.7% for 4,4'-azobis(4-cyanovaleric acid) and potassium persulphate respectively were achieved. Although still relatively low values, they represent a significant improvement compared to those at low temperature. As for the low temperature systems, an increase in particle diameter for both systems was observed once the shell had been formed, from 42 nm to 46 nm for 4,4'-azobis(4-cyanovaleric acid) and from 29 nm to 112 nm for potassium persulphate (Figure 2.5).

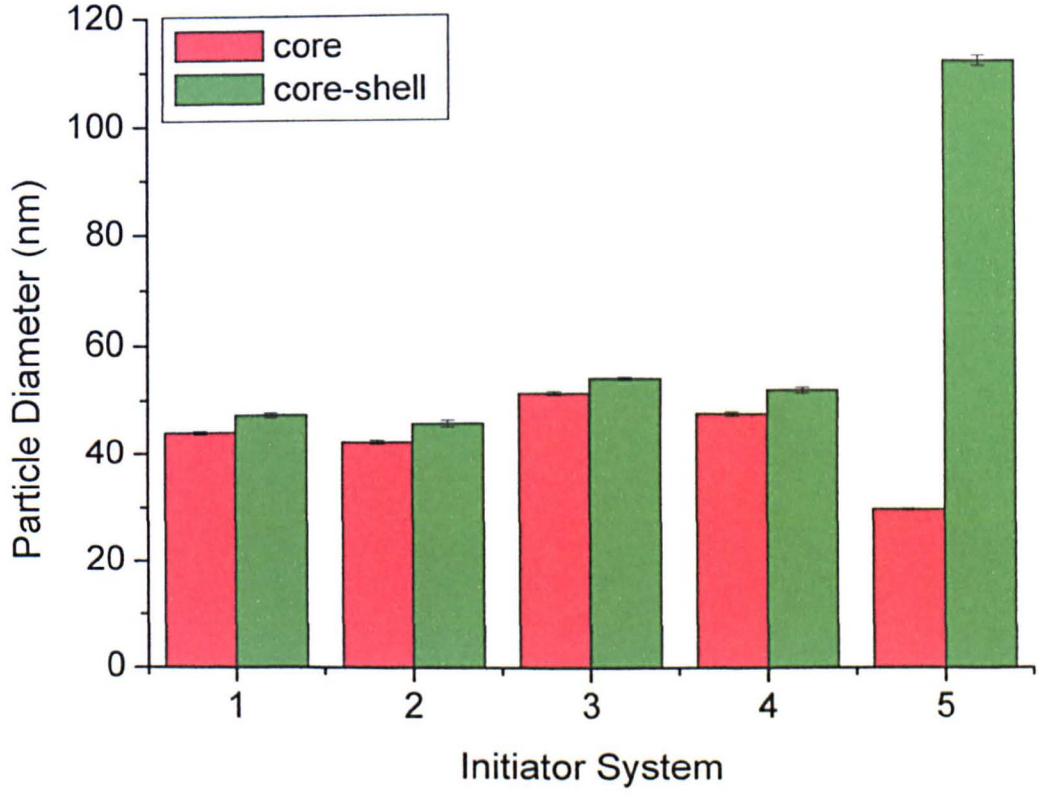


**Figure 2.5: Particle diameter increase upon outer-shell formation for different initiator systems. Values shown are mean ± SEM.**

Unlike initiator systems 1-4, for which the particle diameter increase upon shell formation is as would be expected for these particles, the extremely large increase in particle size from core to core-shell for the potassium persulphate initiator trial (system 5) is obviously not due to increased shell thickness. In this case, the monomer feed in the shell formation reaction could obviously not lead to such a large increase. Instead this increase is expected to be as a result of partial flocculation within the sample, leading to a multimodal particle size distribution, which is confirmed by the increased viscosity of this sample. Although flocculation is complex it is suggested that this may be due to the large amount of potassium persulphate utilised. This could cause the polymerisation rate to be too high, as well as affecting the pH of the system and the ionic strength, all of which would be expected to have a significant effect on latex stability.

Finally, the zeta potentials of all latexes in the initiator trial were analysed. Zeta potential is a physical property exhibited by particles in suspension. A net charge at a particle surface affects the ion distribution in the surrounding interfacial region[236]. This results in an increased counter-ion concentration adjacent to the particle surface. The liquid layer surrounding the particle therefore consists of two layers, referred to as an

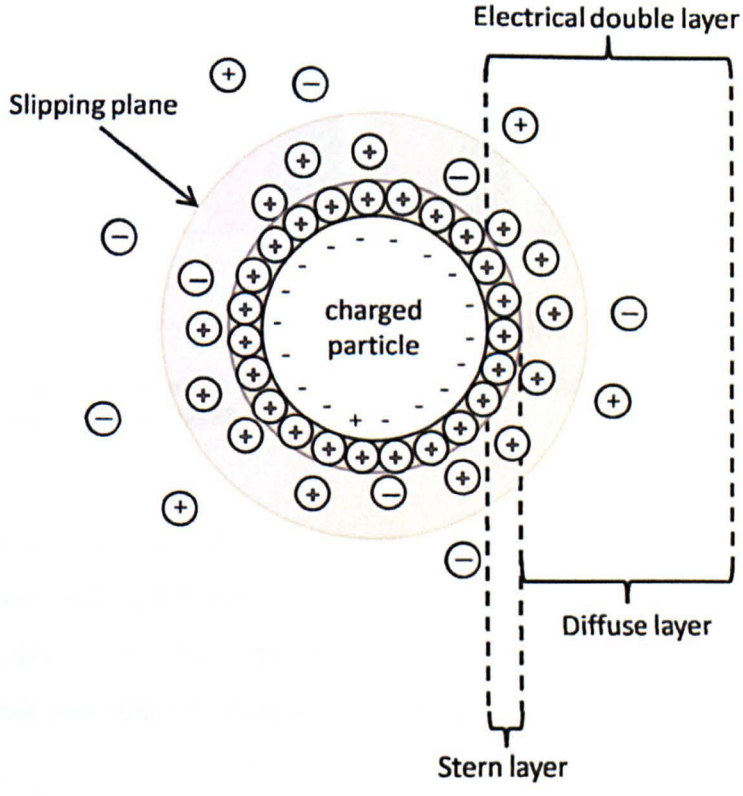


**Figure 2.6: Schematic showing the electrical double layer surrounding a charged particle and the slipping plane, the boundary at which the zeta potential is measured.**

electrical double layer. The inner region, known as the Stern layer, is where the ions are strongly bound to the particle, and the outer region (the diffuse layer) contains ions which are less firmly associated[236, 237]. There is a notional boundary within the diffuse layer, known as the surface of hydrodynamic shear, or the slipping plane[238]. When the particle moves, ions within this boundary move with it and those ions outside of this boundary remain with the bulk solution. Zeta potential is the potential which exists at this boundary. The magnitude of the zeta potential indicates the stability of the colloidal system[239]. If the particles are highly charged, either positively or negatively, they will repel each other and are unlikely to coagulate.

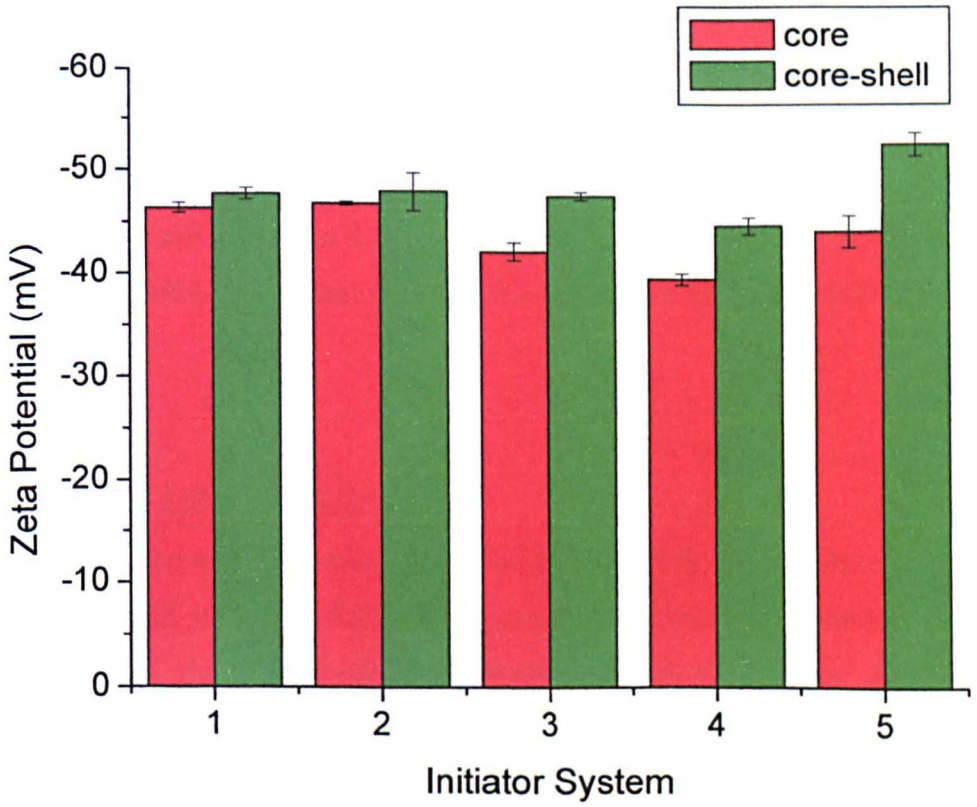


**Figure 2.7: Change in zeta potential upon formation of outer-shell for different initiator systems. Values shown are mean values ± SEM.**

Due to the large amounts of surfactant present in the latexes, as well as the fact that the crude latexes were analysed, thereby leading to varying pH and ionic strength values for the individual latexes, the zeta potential results are utilised primarily to compare with ICP-AES data and consider the change in zeta potential upon shell formation.

Results from the latexes produced during the initiator trials show that, as hypothesised, the formation of a charged shell around the core particles leads to an increase in the zeta potential of the particles (Figure 2.7). The overall zeta potentials for the core particles were negative due to the presence of sodium dodecyl sulphate at the surface of the particles. The zeta potentials measured for the core particles were all fairly similar, ranging from -39.6 mV to -46.8 mV. Although all particles for all five initiator systems showed an increase in zeta potential upon shell formation, the increases observed for the potassium persulphate and ascorbic acid system and the 4,4'-azobis-(4-cyanovaleric acid) system were not statistically significant (two sample student t-test). The other systems all demonstrate a statistically significant increase in zeta potential when the shell is present on the core particle (two sample student t-test, $p < 0.05$). Initiation by the hydrogen peroxide and ascorbic acid and the ammonium persulphate and TEMED systems led to a zeta potential increase of 13% as the outer shell was formed. As expected, initiation by potassium persulphate at 70°C gave the largest zeta potential increase from -44 mV to -53 mV, an increase of 18%. This is in agreement with the ICP-AES results, which show that this system leads to the highest phosphorous content in the polymer.

### 2.5.1 Summary of Initiator Study

Initially it was thought that the optimum polymerisation procedure for peptide-imprinted core-shell particles would involve a low temperature initiation method, in order to optimise the non-covalent interactions between template and functional monomer. From the three redox initiator systems trialled it was determined that such an approach led to very low incorporation of the functional monomer, which is believed to be due to the low reactivity of OPHP. It was thought that improving incorporation of the functional monomer would be vital for the molecular imprinting process, and so thermal initiators, potassium persulphate and 4,4'-azobis-(4-cyanovaleric acid), were also trialled. Both thermal systems allowed formation of the core-shell particles and led to increase in particle size and zeta potential as the outer shell was formed. Initiation by potassium persulphate at 70°C gave the highest incorporation of oleyl phenyl hydrogen phosphate of 11.7%, and so this system was used for further investigations involving this monomer, despite the weak flocculation observed in this technique.

## 2.6 Optimisation of Thermal Potassium Persulphate Initiation

Initiation by potassium persulphate at 70°C allowed the highest incorporation of functional monomer but also resulted in a partially flocculated system, which is more difficult to handle in the next stage of the process and also decreases the latex surface area. It was therefore necessary to determine a formulation which minimises flocculation before this procedure could be used for molecular imprinting. Two approaches were trialled, reduction of initiator content and replacing the batch process with a starve-fed emulsion polymerisation.

Starve-fed emulsion polymerisation refers to a method of monomer addition where the monomer is gradually introduced into the reaction vessel at a specific rate in order to allow the majority of the monomer to be polymerised before further monomer is added. In a batch emulsion polymerisation (as carried out previously), the polymer particles are swollen with monomer which makes them "soft", and so upon collision these particles are likely to flocculate. It was hypothesised that carrying out the reaction using a starve-fed approach for the optimised system of initiation by potassium persulphate at 70°C would avoid the presence of heavily swollen polymer particles and would thereby reduce the amount of flocculation. Reduction of the initiator concentration was also expected to reduce aggregation. Although flocculation is a complex process, it is known that latex stability is affected by the rate of polymerisation and also the pH and ionic strength, all of which could be influenced by a high concentration of potassium persulphate.

| Properties | Core | Core-shell Batch | Core-shell Starve-fed | Core-shell Reduced Initiator |
|---|---|---|---|---|
| Average Particle Diameter (nm)[a] | 30 | 112 | 33 | 44 |
| Particle Diameter Increase (%) | - | 273 | 10 | 47 |
| Phosphorous content (mg/kg)[b] | < 4 | 350.2 | 260.3 | 338.7 |
| Phosphate monomer incorporation (%) | 0 | 11.7 | 8.7 | 11.2 |

**Table 2.4: Physical properties of core and core-shell particles produced in the optimisation of a thermal potassium persulphate initiated core-shell synthesis (a) average particle diameter determined by dynamic light scattering (b) phosphorous content determined by ICP-AES**

The hypotheses above were confirmed when comparing the same formulation for both batch and starve-fed reactions and reaction with reduced initiator concentration (Table 2.4). The core latexes produced had average particle diameters of approximately 30 nm

but a considerable difference was observed when the core-shell particles were formed. For the batch reaction, as used in all previous experiments, a particle diameter of 112 nm was measured for the core-shell particles, whereas under starve-fed conditions and with reduced initiator particle diameters of 33 nm and 44 nm were determined. Although the use of the starve-fed approach is able to completely eliminate the problem of flocculation, ICP-AES analysis of the particles showed that the phosphorous content of the sample was reduced. Phosphorous contents of 11.7% and 8.7% were obtained for the batch and starve-fed reactions respectively. A possible explanation for this observation is that in the batch reaction there is a higher concentration of monomer present at all times, which may result in a slightly higher rate of the transfer reaction, and thus slightly higher functional monomer incorporation. By halving the initiator concentration it was possible to produce core-shell particles with an average diameter of 44 nm with no significant change in phosphorous content, and therefore this optimised formulation was selected for the imprinting experiments.

## 2.7 Final Summary

A core-shell approach to molecular imprinting developed by Carter et al[157, 159, 160] was chosen for this project. It was thought that the use of a redox initiation system would allow the synthesis to be carried out close to room temperature, thus optimising the non-covalent interaction between the template and functional monomer that is required in molecular imprinting. An initial study with the redox system of potassium persulphate and ascorbic acid enabled the formulation to be optimised for this approach. It was determined that synthesis of the core-shell particles was possible with redox initiation, but that incorporation of the functional monomer was very low. This was also shown to be the case for two alternative redox systems, hydrogen peroxide with ascorbic acid and ammonium persulphate with TEMED. From these results it was determined that it would not be possible to carry out the molecular imprinting technique with redox initiation, as it was vital to maximise functional monomer incorporation and thereby increase interaction between template and functional monomer. Thermal initiation was then considered, with the most successful incorporation of OPHP observed with potassium persulphate initiation at 70°C. Finally, optimisation of initiator concentration allowed a synthetic procedure to be developed to produce a stable latex, which could then be employed in molecular imprinting studies.

# 3 Core-Shell Molecularly-Imprinted Particles

Following optimisation of the core-shell synthesis procedure, the next step in the epitope imprinting of VEGF requires the determination of a suitable peptide sequence to be imprinted during the formation of the outer shell. In this chapter the choice of template is rationalised and the ability of the resultant core-shell molecularly-imprinted particles to bind both peptide sequences and VEGF is discussed.

## 3.1 Determination of Peptide Sequence

A discussion of VEGF was provided previously (section 1.4) and the structure and folding of this protein, together with information available relating to the activity of different regions of the protein, must be carefully considered in order to determine which amino acid sequence is chosen as the peptide template for epitope imprinting. It is also necessary to ensure that the sequence chosen is located in an accessible region of the protein if recognition of the protein by the polymer is to be achieved.

VEGF consists of two identical polypeptide chains which are covalently linked by a pair of disulfide bonds[35]. A number of different isoforms exist, but $VEGF_{165}$, the most common isoform, will be considered here. It is known that all heparin-binding isoforms share the same 50 residue C-terminal, termed the heparin-binding domain (Figure 3.1 & Figure 3.2 & Figure 3.3)[35].

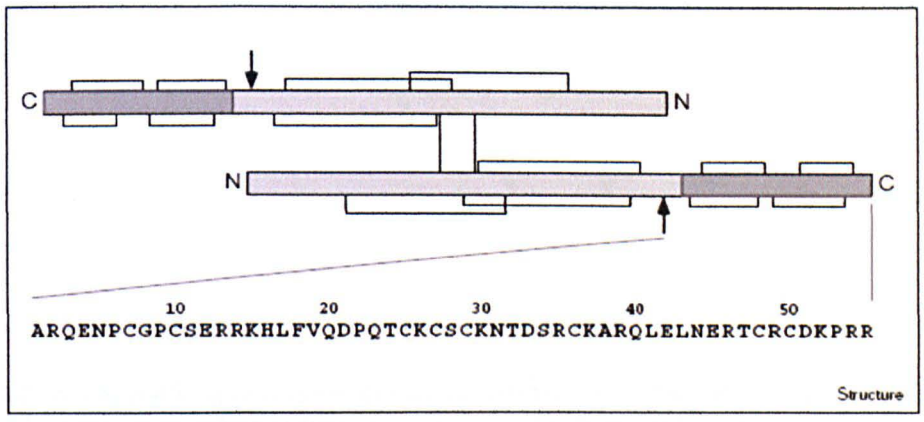


**Figure 3.1: A schematic representation of $VEGF_{165}$. The darker regions represent the heparin-binding domain. Disulphide bridges are represented by lines. Reproduced from Fairbrother et al†.**

† Reproduction of figure 1 reprinted from *Structure*, Vol. 6 no. 5, Fairbrother, Wayne J., Champe, Mark A., Christinger, Hans W., Keyt, Bruce A., Starovasnik, Melissa A., "Solution structure of the heparin-binding domain of vascular endothelial growth factor", 637-648, Copyright 1998, with permission from Elsevier.

The 50 residue heparin-binding region of $VEGF_{165}$, after plasmin cleavage, can interact with heparin with the same affinity as $VEGF_{165}$ but does not interact with cell receptors for VEGF[48]. Conversely, $VEGF_{165}$ with this 55 residue fragment removed will bind to cell receptors but not heparin. Moreover, upon binding with cell receptors the mitogenic potency of VEGF is significantly reduced in comparison to $VEGF_{165}$.

It is thought that the heparin-binding region of VEGF must be relatively accessible to allow interaction with large polysaccharides like heparin and cell surface-bound heparin-like GAGs and so it is postulated that this region would also be accessible for binding with phosphate groups on the surface of the CS-MIPs produced.

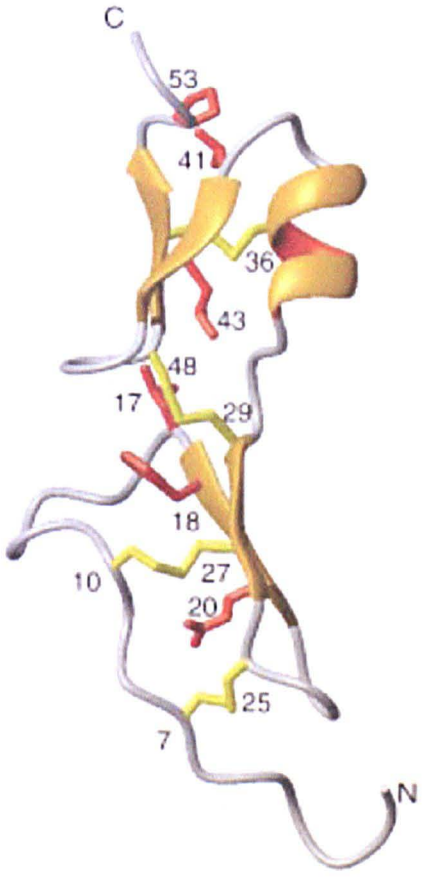


**Figure 3.2: A schematic stereo representation of the structure of the 55-residue heparin-binding region of $VEGF_{165}$, highlighting secondary structure, disulfide bridges and hydrophobic packing of selected sidechains. Adapted from Fairbrother et al†**

† Adaptation of figure 5 reprinted from *Structure*, Vol. 6 no. 5, Fairbrother, Wayne J., Champe, Mark A., Christinger, Hans W., Keyt, Bruce A., Starovasnik, Melissa A., "Solution structure of the heparin-binding domain of vascular endothelial growth factor", 637-648, Copyright 1998, with permission from Elsevier.

The high negative charge density of heparin suggests that an excess of positive charge would be present on any specific heparin-binding site on $VEGF_{55}$. The areas of positive charge on the heparin binding region can be seen when considering the solvent-accessible molecular surface of $VEGF_{55}$ (Figure 3.3)[35]. Thus it is expected that the heparin binding site on $VEGF_{55}$ will include Arg13, Arg14, Lys15, Lys30, Arg35, Arg39, Arg46 and probably also Lys52, Arg54 and Arg55.

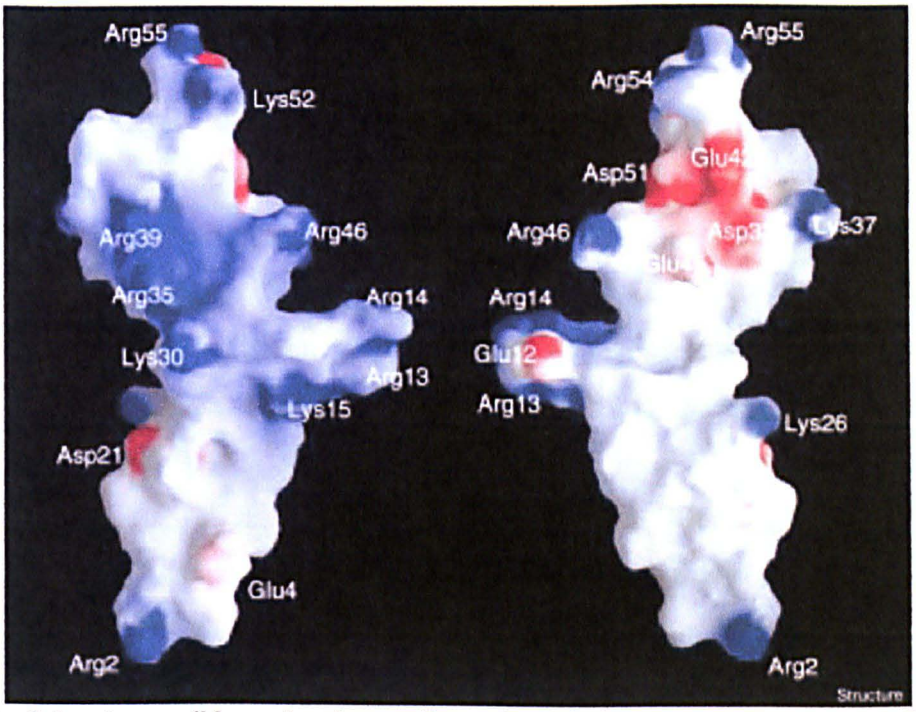


**Figure 3.3: Solvent-accessible molecular surface of minimised mean structure of 55-residue heparin-binding region of $VEGF_{165}$. Colour code: red = acidic residue, white = no charge, blue = basic residue. The two views are related by 180° rotation about the vertical axis. Reproduced from Fairbrother et al†**

In order to replicate heparin binding it was therefore decided to select an amino acid sequence rich in basic residues. Research by Rachkov et al[190] suggests that the most suitable template size for epitope imprinting is 3-6 amino acid sequences with a surface area in the region of 650-900 $Å^2$. For an unfolded polypeptide chain, the total accessible surface area, $A_t$, is directly proportional to its molecular weight, Mw

$$A_t = 1.45Mw$$

† Reproduction of figure 7 reprinted from *Structure*, Vol. 6 no. 5, Fairbrother, Wayne J., Champe, Mark A., Christinger, Hans W., Keyt, Bruce A., Starovasnik, Melissa A., "Solution structure of the heparin-binding domain of vascular endothelial growth factor", 637-648, Copyright 1998, with permission from Elsevier.

A 3-6 amino acid residue was therefore required from the heparin-binding region for initial investigations. Although a number of highly basic residues of a similar size exist within this region it is acknowledged that these regions are likely to be involved in folding and hence it may be difficult to replicate the 3D conformation of these residues in the protein when imprinting only the short peptide sequence. This could have a negative effect on the recognition properties of the polymer produced, as the sequence of interest on the protein may not have the correct conformation to fit into the previously formed recognition cavity. In order to avoid this complication, a sequence from the end of the carboxy terminus was selected as this is unlikely to be affected by folding.

The sequence selected was the pentapeptide Asp-Lys-Pro-Arg-Arg (DKPRR), residues 51-55 (Figure 3.4). This residue has an approximate total accessible surface area of 973 $Å^2$ and offers a number of advantages. Firstly, it is a highly charged species containing three basic amino acids. Secondly, this sequence includes two adjacent arginine residues, Arg54 and Arg55, which is also observed in another part of the heparin-binding sequence, Arg13 and Arg14. This may mean that different areas of the heparin-binding region of the protein could also interact with the recognition cavity. As mentioned previously, this sequence is not involved in protein folding (shown in Figure 3.2) and also contains a proline residue. The distinctive cyclic structure of proline's side chain locks its φ backbone dihedral angle at approximately -60°, giving proline an exceptional conformational rigidity compared to other amino acids[240]. This introduces rigidity into the peptide and therefore is expected to reduce the number of conformations possible for this peptide in relation to other less rigid pentapeptide sequences.

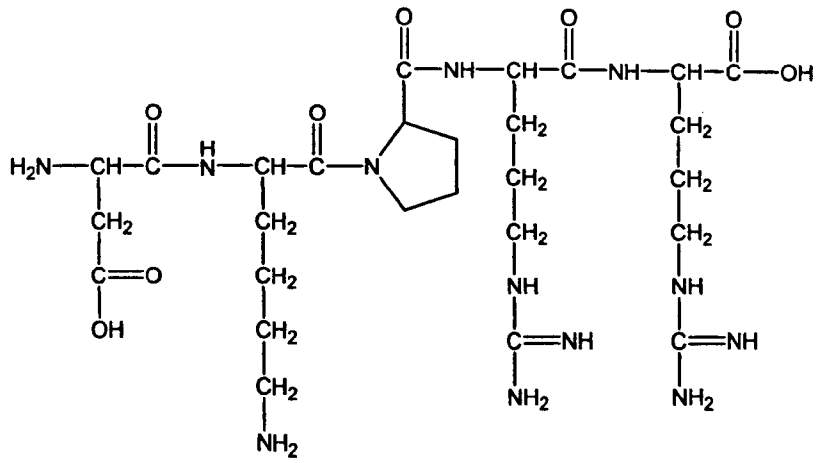

**Figure 3.4: Structure of DKPRR peptide**

The high proportion of basic amino acid residues in this sequence is expected to be highly beneficial for this application. Interactions between basic amino acid residues, including lysine and arginine, and acidic phosphate groups, such as those present on the core-shell particles, are known to play an important role in nature. A significant example is the formation of ionic bonds between these groups in DNA-binding proteins[241]. In particular, arginine, characterised by its basic guanidinium group, is capable of forming electrostatic and hydrogen bonds of a highly specific nature with anions, primarily phosphates, sulphates and carboxylates[242]. The exceptional ability of arginine to form strong non-covalent bonds is based on its guanidine moiety. This guanidinium functionality is able to use "Y-delocalisation" for stability, sharing the positive charge evenly over the three nitrogen atoms (Figure 3.5), and possesses a number of potential hydrogen bond donors[242]. Arginine is highly water-soluble and has a pKa of 12.48[243].

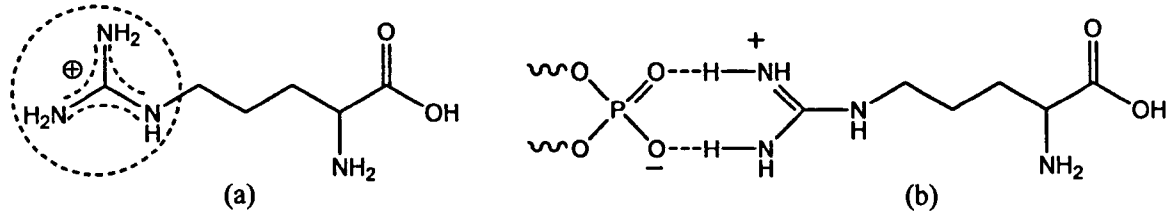


**Figure 3.5: (a) Structure of arginine. The guanidine moiety is highlighted and shown in the singly protonated form utilising Y-delocalisation (b) Suggested phosphate-arginine interaction**

Research by Fromm et al[244] details the high frequency of arginine residues in heparin-binding regions of proteins and shows that stronger hydrogen bonding and more exothermic electrostatic interactions between the sulphate and carboxylate groups on GAGs with arginine side chains, rather than other basic amino acids, contributes significantly to the strong protein-GAG interaction. It is therefore thought that the use of an anionic phosphate functional monomer and an arginine-based template molecule could lead to more specific interactions between the polymer produced and the template due to a possible reduction in non-specific hydrophobic binding and an increase in more specific electrostatic interactions.

## 3.2 Synthesis and Characterisation

Four types of particles were produced to determine the ability of core-shell molecularly-imprinted particles (CS-MIPs) to bind and release VEGF. Firstly, core particles were produced as previously discussed in Chapter 2 and these particles were analysed for their recognition ability. A second emulsion polymerisation step was then carried out to produce three further samples; DKPRR-imprinted CS-MIPs, imprinted with the peptide sequence present on VEGF, GAA-imprinted CS-MIPs, imprinted with an unrelated peptide sequence for comparison and blank-imprinted CS-MIPs, core-shell particles produced without the presence of a peptide.

The samples were produced by the procedure determined in Chapter 2. After synthesis of the core particles, the functional monomer and crosslinker were added to the emulsion and allowed to equilibrate around the core particles. The template was then added in pH-adjusted buffer, and was left for one hour to interact with the functional monomer to form the desired template-monomer complex. The reaction was then initiated by potassium persulphate at 70°C and the reaction was carried out for 16 hours. After the polymerisation, the template was washed from the particles prior to peptide and protein binding and release studies.

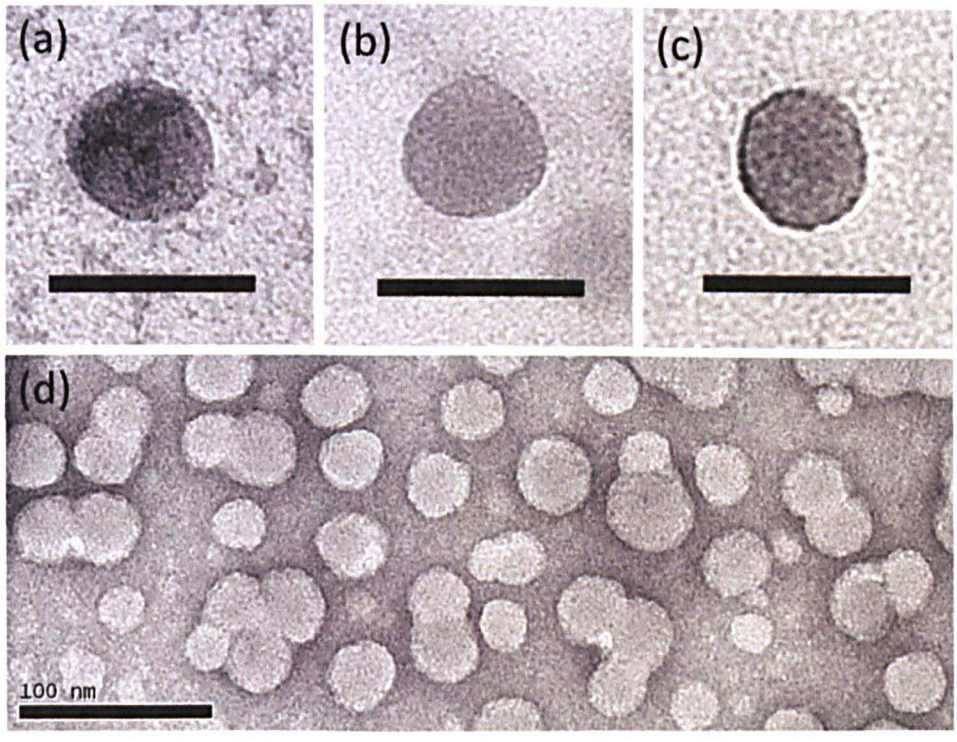


**Figure 3.6: TEM images of (a) blank-imprinted CS-MIP (b) GAA-imprinted CS-MIP (c) DKPRR-imprinted CS-MIP and (d) core particles. Scale bar for core-shell particles = 50 nm.**

This synthetic procedure allowed the formation of core-shell particles. It was observed that coagulum formed during the synthesis of the peptide-imprinted particles, but in all cases the stable portion of the latex was analysed.

By this method, core particles of 35 nm were produced with a zeta potential of –38 mV. Formation of the outer shell led to changes in the physical properties, as would be expected (Table 3.1). As the outer shell was formed an increase in particle diameter was observed in all cases. The increase in particle size was accompanied by a small increase in zeta potential from -38.0 mV to -41.6 mV, -42.9 mV and -42.7 mV for the blank CS-MIP, DKPRR CS-MIP and the GAA CS-MIP respectively, but this zeta potential increase was not shown to be significant.

| Sample | Particle Diameter (nm) [a] | Zeta Potential (mV) [b] | Phosphorous content (mg/kg) [c] |
|---|---|---|---|
| Core | 34.9 ± 0.2 | -38.0 ± 1.6 | < 10 |
| Blank CS-MIP | 44.4 ± 0.8 | -41.6 ± 0.9 | 347.4 |
| DKPRR CS-MIP | 48.2 ± 0.1 | -42.9 ± 1.1 | 390.0 |
| GAA CS-MIP | 45.4 ± 0.3 | -42.7 ± 1.3 | 344.6 |

**Table 3.1: Physical properties of core and core-shell particles. (a) Particle diameter as determined by dynamic light scattering. (b) Zeta potential determined after dialysis to remove template from the core-shell particles. (c) Phosphorous content determined by ICP-AES after washing procedure.**

The incorporation of the functional monomer is vital for a molecularly-imprinted monomer as it is this functional group that would provide the recognition site for binding the target molecule. The presence of the functional monomer was analysed by ICP-AES, considering total phosphorous content. The location of the phosphate monomer at the surface of the particles was then investigated by X-ray Photoelectron Spectroscopy (XPS) and Energy-Dispersive Spectroscopy (EDS). Prior to analysis by any of these techniques, the samples were vigorously washed, either by coagulation with isopropyl alcohol and subsequent washing or by dialysis, to remove any unbound monomer and template material. This meant that their phosphorous content is assumed to be from monomer bound into the core-shell particles.

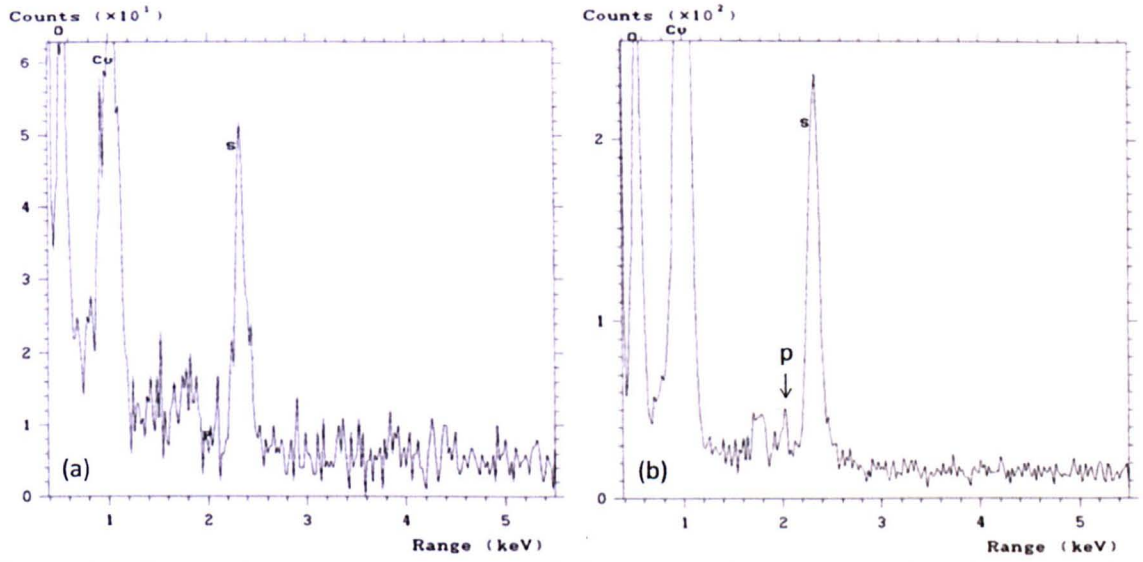


**Figure 3.7: Energy-Dispersive Spectroscopy (EDS) spectra of (a) core and (b) DKPRR-imprinted core-shell particles showing the presence of a phosphorous peak (p). The presence of a phosphorous peak is seen in all of the core-shell particles.**

Qualitative confirmation of the presence of the monomer in the shell was provided by EDS (Figure 3.7) and XPS (Figure 3.8). For both techniques, no phosphorous was observed for the core particles and phosphorous peaks were observed for all core-shell particles (core-shell images shown are representative of all core-shell images produced). Quantitative analysis by ICP-AES showed no phosphorous present on the core particles. As the outer shell is formed it is possible to detect phosphorous with 347.4 mg/kg present within the blank CS-MIPs. Similar quantities of 390.0 mg/kg and 344.6 mg/kg were observed for the DKPRR CS-MIP and the GAA CS-MIP respectively. These results are comparable to the results shown in Chapter 2 for core-shell particles produced in the same manner and confirm that the functional monomer is present in the outer shell of the material.

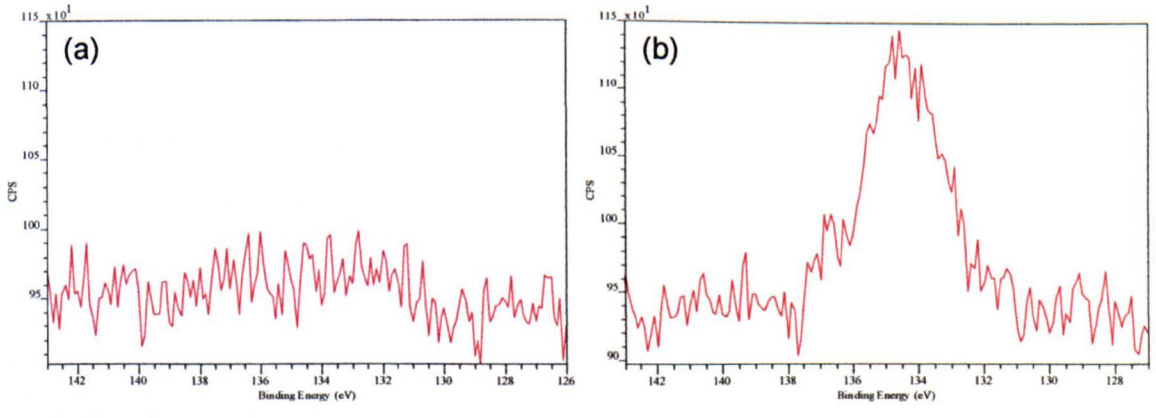


**Figure 3.8: X-ray Photoelectron Spectroscopy (XPS) spectra of the phosphorous 2P region of (a) core and (b) DKPRR-imprinted core-shell particles. Phosphorous presence was confirmed for all core-shell particles.**

## 3.3 Peptide Binding Studies

The molecularly-imprinted particles in this study were produced to recognise, bind and subsequently release VEGF. The particles were first tested to determine their ability to recognise and rebind the peptide template, DKPRR. Due to the high costs involved when working with a synthetic peptide and a biological protein, only small quantities of the particles were produced, and therefore binding studies were carried out on a small scale. Two approaches to a peptide binding study were used to investigate whether the molecular imprinting would influence selectivity: a colorimetric study and a zeta potential study. The particles were analysed for their ability to bind DKPRR, the template of interest, PRKRD (proline-arginine-lysine-arginine-aspartic acid), a scrambled version of the peptide, and SSSSSSSS (octaserine), an unrelated and relatively inert peptide sequence.

### 3.3.1 Colorimetric Peptide Binding Study

Due to the low quantities of CS-MIPs available, it was thought that a colorimetric study would allow easy assessment of the binding abilities of the different particles. A number of molecularly-imprinted polymers have been previously reported in which the recognition process can be optically analysed using a variety of sophisticated approaches, including incorporation of fluorescent or chemiluminescent compounds within the MIP[245-247] and the use of fluorescent templates and labels[248-250]. MIPs have been produced for which binding can be analysed by UV/Vis, infrared and surface plasma resonance[251]. Fewer reports are available which result in a visual colour change. Analysis of binding by colour change has been achieved in a variety of ways. A change in yellow colour intensity was reported by Manesiotis et al[252] upon binding of Z-glutamate with a 1-(4-styrl)-3-(3-nitrophenyl)urea functional monomer, and Gräfe et al[250] utilised the azo dye 4-trifluoroacetyl-4'-[N-(methacryloxyethyl)-N-(ethyl)amino] azobenzene which exhibits a colour change from red to yellow upon covalent binding with amines in organic solvent.

In order to conduct a colorimetric study, it was decided to produce the peptide sequences required for the binding study with a suitable chromophore at the end of the sequence. It was thought that this would allow both qualitative analysis of the peptide when bound to the particles, as well as provide quantitative data about the binding by analysis of the peptide solutions before and after exposure to the polymer samples. A

similar approach was previously used by Chow et al[249] who analysed homocysteine-imprinted MIPs using fluorescently-tagged homocysteine.

Methyl red was selected as the chromophore for this work. Methyl red is a weakly basic azo dye with a $pK_a$ of 4.8[253] which is known to undergo a colour change from yellow to red when pH is lowered within an aqueous solution. Methyl red is employed as a pH indicator in the range of 4.4 to 6.0[254]. It is widely documented that the colour change observed is due to the azo form, which exists in neutral conditions, being converted into a tautomeric equilibrium of the protonated ammonium species and the azonium species[255, 256].

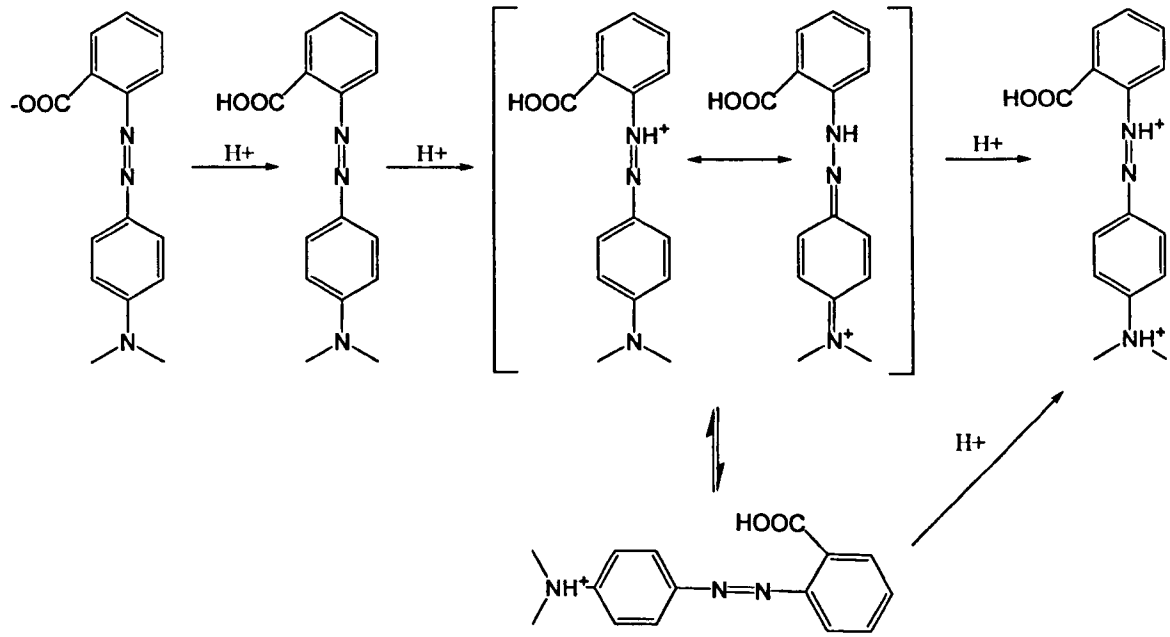


**Figure 3.9: Protonation equilibria for methyl red (as discussed by Tawarah et al[256])**

Ueno et al[257, 258] discuss the use of methyl red-modified cyclodextrin to demonstrate guest selective binding. In this work, methyl red is attached to the wall of a β-cyclodextrin, present in a cavity, and a binding study was carried out in an acid solution. Even in acid the modified cyclodextrin remains yellow as the methyl red is inside the cavity and therefore protected from protonation. An organic guest compound then displaces the methyl red from the cavity and a colour change from yellow to red is then observed. It was hypothesised that producing methyl red-modified peptide sequences to analyse the effect of molecular imprinting may allow a colorimetric assessment of the quantity of peptide binding but also a method to detect the presence of binding regions

or cavities. It was suggested that binding regions or cavities in the outer shell of the particles may be able to interact with the imprinted peptide through numerous electrostatic interactions, thus preventing the structural changes occurring during protonation and preventing, or at least minimising, the colour change usually observed upon decreasing the pH for a methyl red moiety in solution. The selectivity of the binding regions would then be demonstrated, since unrelated peptide sequences, despite being bound to the particle, may not be tethered by as many electrostatic interactions and would therefore be susceptible to structural change, and therefore also colour change, upon lowering the pH of the solution.

The methyl red-tagged peptides (methyl red-SSSDKPRR (MRSSSDKPRR), methyl red-SSSPRKRD (MRSSSPRKRD) and methyl red-SSSSSSSS (MRSSSSSSSS)) (Figure 3.10) were synthesised by solid phase peptide synthesis to allow colorimetric binding and release analysis of the imprinted polymers. The methyl red moiety possesses a carboxylic acid group which enabled incorporation by the formation of an amide bond between this and the terminal amine present on the peptide sequence. The methyl red molecule could therefore be attached to the peptide at the end of the standard peptide synthesis programme. Three serine spacer units were added between the DKPRR sequence and the methyl red molecules for two reasons. Firstly, the methyl red molecule is relatively hydrophobic and so the water-soluble serine units were added to keep the peptide water-soluble. Secondly, the serine units were added as a spacer unit, to prevent the methyl red molecule affecting the ability of the DKPRR sequence to bind with the CS-MIPs.

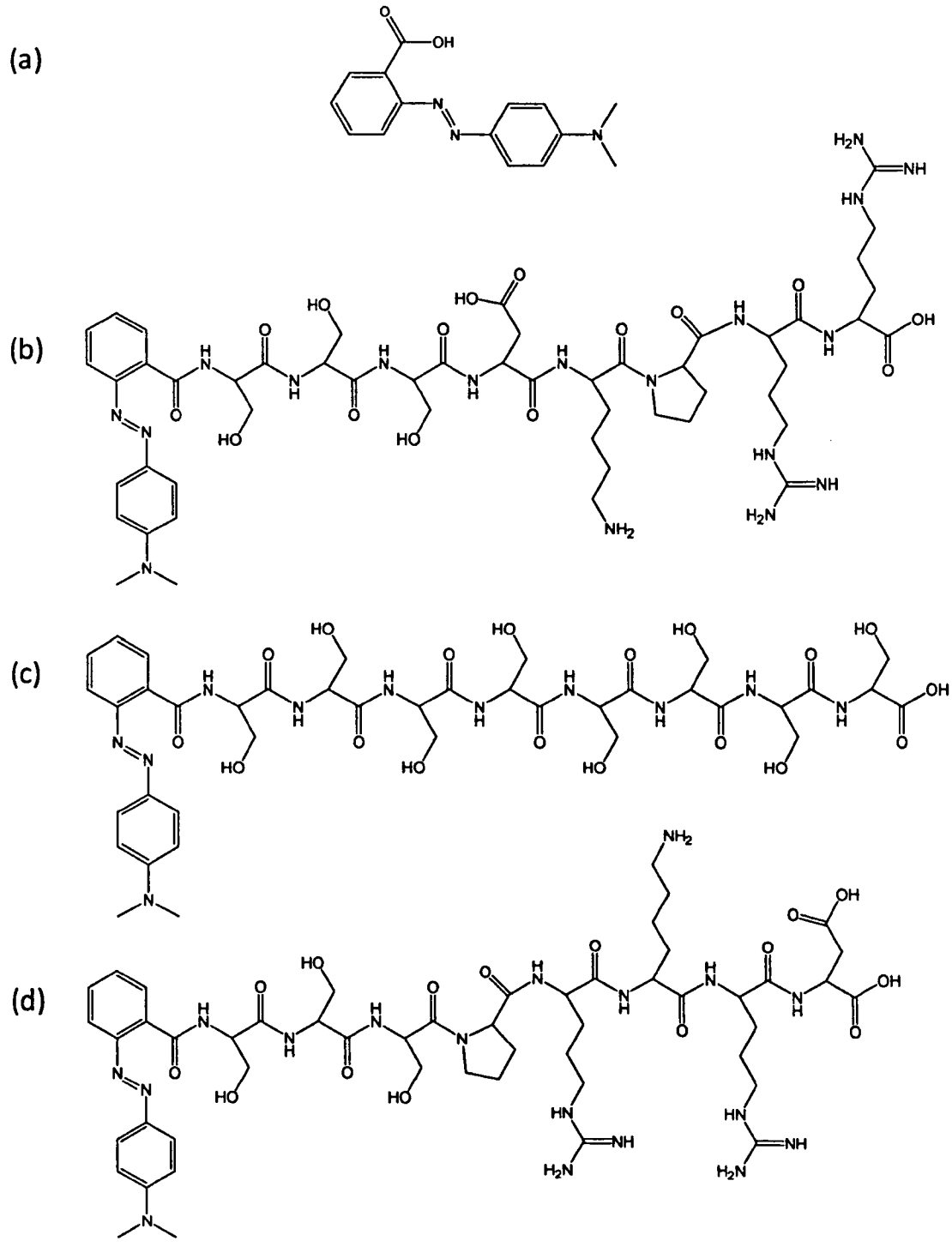


**Figure 3.10: Structures of (a) methyl red; (b) MRSSSDKPRR; (c) MRSSSSSSSS; (d) MRSSSPRKRD**

Firstly, the modified peptides were analysed in solution to confirm that the expected colour changes occurred as for the methyl red moiety alone. The structural changes from the azo species, in alkaline and neutral pH, to the tautomeric equilibrium of the protonated ammonium species and the azonium species are also observed with UV/Vis spectroscopy in aqueous solution for methyl red-modified peptides employed in this study. The azo form of the methyl red peptides produces two main absorption maxima

at 270 nm and 470 nm. Following the research published on *p*-methyl red by Tawarah et al[256], the peak at 470 nm is attributed to the π-π* transition of the azo group and the maximum at 270 nm is due to the n-π* transition of the amide group. As the pH is lowered, and the structure is converted to the protonated ammonium species and the azonium species, the maximum at 270 nm is gradually replaced by an absorption maximum at 315 nm and the peak at 470 nm is shifted to 510 nm (Figure 3.11a). This shift is visible by eye as the colour changes from orange to red (Figure 3.11b).

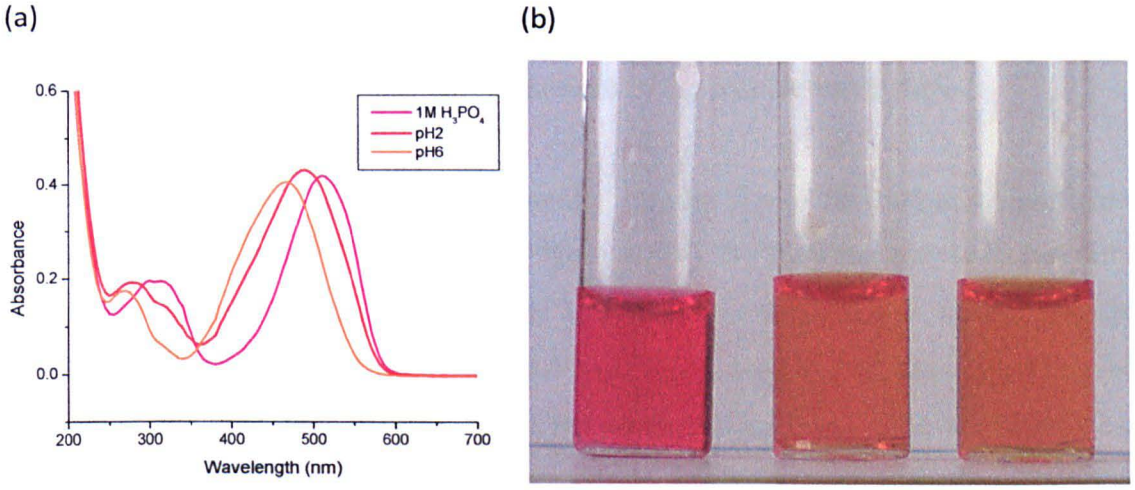


**Figure 3.11: Results of a visible absorption spectroscopy pH study on MRSSSDKPRR. (a) UV/Vis spectrum of MRSSSDKPRR at different pH values showing the colour change upon protonation. (b) Visual colour change image of MSSSDKPRR at different pH values (L-R) 1 M $H_3PO_4$, pH 2 and pH 6.**

***Peptide Binding Study Results***

The ability of the core and core-shell particles to bind peptide sequences was analysed by three different methyl red-tagged peptides; MRSSSDKPRR, the peptide sequence of interest, MRSSSPRKRD, a scrambled version of the peptide, and MRSSSSSSSS, an unrelated peptide sequence with different functionality. Prior to peptide binding all polymer samples were coagulated and washed thoroughly to remove any template (Section 10.3). 0.1 ml of each latex (equating to 4.6 mg, 4.2 mg, 3.6 mg and 2.8 mg of core, blank CS-MIP, GAA CS-MIP and DKPRR CS-MIP, respectively) was then exposed to solutions of the three different peptides to determine whether there was any selectivity observed in non-competitive studies.

In all cases, the introduction of methyl red-tagged peptide solution to the polymer resulted in 100% peptide bound to the polymer. This strong binding was attributed to the presence of the methyl red moiety, a hydrophobic group which binds preferentially

to the organic polymer rather than remaining in solution. This interaction between the methyl red moiety and the core and core-shell particles meant that it was not possible to determine a binding constant by this method. Instead it was decided to remove the peptide bound only by hydrophobic interactions, and thereby determine the amount of peptide interacting with the particles via electrostatic interactions with the polymer. In order to remove peptide bound entirely by this hydrophobic interaction, a series of washes was employed with increasing concentrations of isopropyl alcohol (IPA) from 0% to 100% alcohol. It was anticipated that introducing isopropyl alcohol would minimise hydrophobic interactions, resulting in peptide bound only through electrostatic interactions with the phosphate monomer present in the particle outer shell.

When considering the MRSSSDKPRR peptide, introduction of IPA led to a significant decrease of peptide on the core material (Figure 3.12d). By 80% isopropyl alcohol only 8% of the initial peptide loading remained bound to this polymer. No further peptide was removed from this material despite washes to 100% isopropyl alcohol being carried out. Much higher quantities of MRSSSDKPRR were retained on the core-shell particles, thereby demonstrating binding through interaction of the peptide with the phosphate functionality of the polymer. 88% of the MRSSSDKPRR exposed to the GAA-imprinted polymer remained on the polymer, even in a 100% isopropyl alcohol solution (Figure 3.12a). A similar result was observed for the DKPRR-imprinted polymer (Figure 3.12b), with 83% of MRSSSDKPRR remaining on the polymer after the washing steps. The blank CS-MIP (Figure 3.12c), produced in the absence of the template, bound 92% of the peptide binding to the polymer even in 100% isopropyl alcohol. It is hypothesised that the high binding observed for the blank-imprinted particles may be due to the random distribution of functional monomer in the outer shell of the particles. This could lead to a high number of less selective binding sites, or binding sites with a 1:1 functional monomer to peptide interaction, in comparison to imprinted core-shell particles which may contain fewer binding sites but with a higher affinity for the peptide due to higher functional monomer concentration in the imprinted cavities.

The selectivity of binding was tested by comparing MRSSSDKPRR with MRSSSPRKRD, a scrambled sequence, and MRSSSSSSSS, an unrelated peptide sequence. The binding study with MRSSSPRKRD resulted in a similar binding pattern

to that obtained with MRSSSDKPRR (Figure 3.12). By an 80% isopropyl alcohol solution only 10% of the peptide remained on the core particles, compared to a final value of 94% for GAA-imprinted particles, 95% on the blank-imprinted particles and 84% on the DKPRR-imprinted polymer.

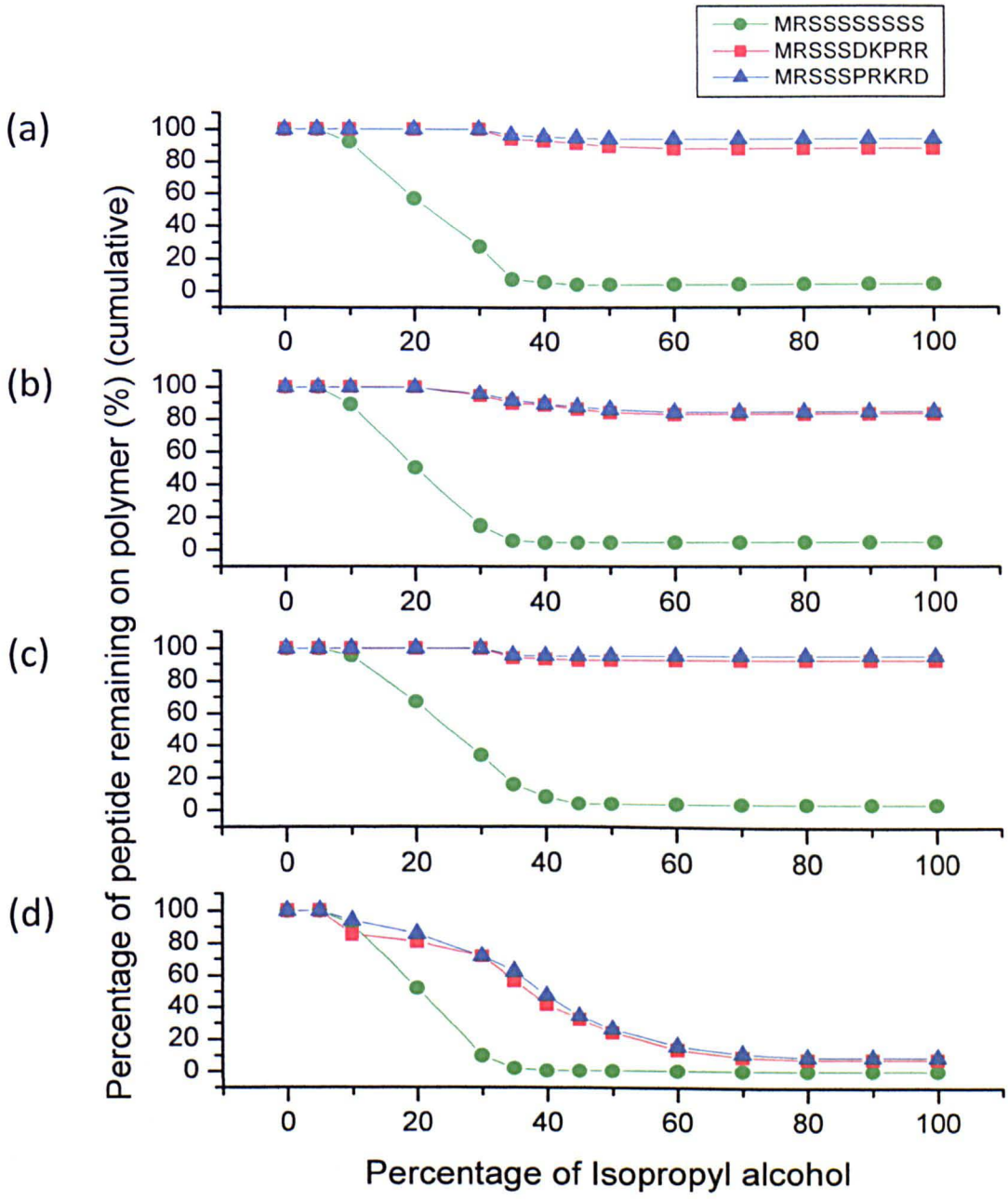


**Figure 3.12: Results of peptide binding studies showing peptide release with increasing isopropyl alcohol percentage for the four different polymer samples; (a) GAA CS-MIP (b) DKPRR CS-MIP (c) Blank CS-MIP (d) Core particles.**

It is hypothesised that any binding occurring between peptide and core-shell particles would be due to electrostatic interaction of the anionic phosphate functionality in the

polymer with the cationic amine or guanidinium functionality on the peptide sequences. Using this hypothesis, it was anticipated that the methyl red-tagged serine peptide (MRSSSSSSSS) would show minimum interaction with the polymer, other than hydrophobic interactions due to methyl red. Experimental results agreed with this hypothesis, with only 1% of the total MRSSSSSSSS peptide exposed to the polymer remaining on the core particles after isopropyl alcohol washes (Figure 3.12d). Low quantities of peptide after washing were also observed for the core-shell particles. 4% of total peptide was found remaining after washes for the DKPRR CS-MIP, the blank CS-MIP and the GAA CS-MIP (Figure 3.12a-c). In all cases with this peptide, any peptide that was removed had been recovered by 50% isopropyl alcohol, suggesting that hydrophobic interactions were indeed responsible for the initial binding observed.

| | **Amount of peptide remaining on polymer after IPA washes (μg/mg polymer)** | | | **Selectivity (S)** | |
|---|---|---|---|---|---|
| | MRSSSDKPRR (U1) | MRSSSPRKRD (U2) | MRSSSSSSSS (U3) | U1/U2 | U1/U3 |
| Core particles | 0.26 | 0.30 | 0.02 | 0.85 | 11.80 |
| Blank CS-MIP | 3.19 | 3.18 | 0.15 | 1.00 | 21.25 |
| GAA CS-MIP | 3.53 | 3.67 | 0.18 | 0.96 | 20.16 |
| DKPRR CS-MIP | 4.29 | 4.23 | 0.24 | 1.02 | 17.59 |

**Table 3.2: Selectivity of methyl red-tagged peptide binding experiments. U = amount of peptide remaining per milligram of polymer after all washes where 1 = MRSSSDKPRR, 2 = MRSSSPRKRD and 3 = MRSSSSSSSS.**

Consideration of the final quantity of each of the peptides on the polymers after all isopropyl washes reveals binding selectivities (Table 3.2). The selectivity value, S, for each binding experiment could be determined (S = amount of target molecule bound/amount of competitor peptide bound). A value of 1 shows no selectivity to either compound, a value higher than 1 denotes selectivity towards MRSSSDKPRR, the target molecule, and a value lower than 1 shows selectivity towards the competitor compound. When comparing MRSSSDKPRR to MRSSSPRKRD the blank particles show no selectivity to either peptide, as would be expected, with a value of 1.00. A value of 1.02 for the DKPRR CS-MIP shows very weak selectivity towards the target peptide, whereas a value of 0.96 for the GAA CS-MIP shows that particles imprinted for GAA are slightly selective towards the scrambled competitor, MRSSSPRKRD. It is not too surprising that the selectivity values in this experiment are insignificant since the two compounds are identical in terms of their charge and functionality, varying only in the sequence of five of the amino acids. From these results, it was confirmed that both basic

peptides could bind to the core-shell particles, with no significant differences between the two.

When comparing the results from MRSSSDKPRR with MRSSSSSSSS, strong selectivity was observed in all cases. Selectivities of 11.80, 21.25, 20.16 and 17.59 were determined for the core particles, GAA CS-MIP, blank CS-MIP and DKPRR CS-MIP respectively.

***Peptide Release Studies***

The best way to determine the effects of molecular imprinting may not be just to consider binding, but to also consider the release of the target molecule, especially for drug delivery applications. The molar ratio of monomer to target molecule was 1:1 in the synthesis, but it is likely that more than one monomer could interact with one peptide moiety due to the high functionality of the peptide sequence employed. If this is the case, it may be that high selectivity would not be immediately observed on binding, as all polymers with phosphate functionality in the shell would be expected to bind with basic peptides to some degree. It is suggested that, upon binding into a molecularly-imprinted cavity, the target molecule is bound by numerous simultaneous electrostatic interactions, resulting in stronger binding and therefore possibly having a significant effect on the release characteristics.

*Colour Change*

The methyl red-modified peptide sequences were bound to the polymer as described in the peptide binding study discussion above. After the peptide binding and isopropyl washes, an acid release study was carried out, with washes of 50% isopropyl alcohol and 50% phosphoric acid of increasing molarity, until the peptide had been removed by interrupting the electrostatic interactions between the phosphate groups in the polymer and the amine and guanidine groups in the peptides. As the bound methyl red peptides were exposed to an increasingly acidic environment, a colour change for the polymer-peptide material was confirmed by the naked eye.

In the MRSSSDKPRR study for the non-specific polymers, core, GAA-imprinted and blank-imprinted particles, the bound-peptide changed colour immediately from orange to red, whereas the peptide bound to the specific DKPRR-imprinted polymer remained orange (Figure 3.13).

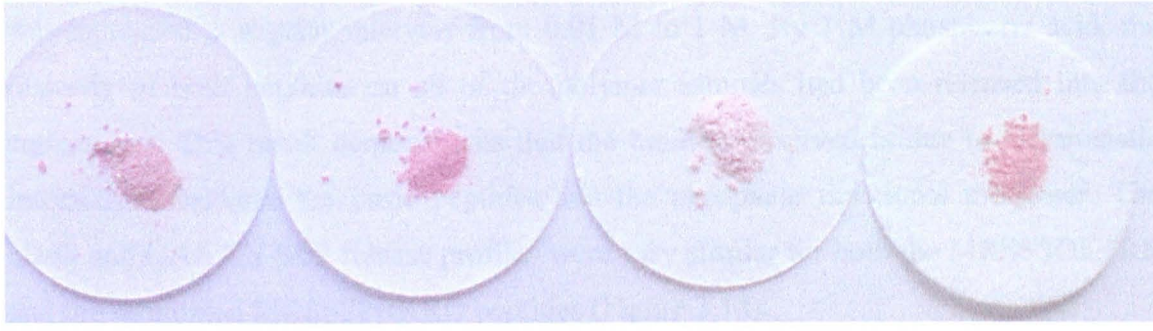

**Figure 3.13: Polymer samples with bound MRSSSDKPRR peptide at 0.05 M phosphoric acid showing colour change (L-R) DKPRR CS-MIP, Blank CS-MIP, core particles, GAA CS-MIP. DKPRR-imprinted CS-MIP remains orange, whereas the other three samples turned red/pink, which is associated with the protonated form of methyl red.**

A similar but less dramatic effect was also observed for the MRSSSPRKRD peptide study, with obvious colour changes to red/pink for the core, blank CS-MIP and GAA CS-MIP. For the MRSSSPRKRD on DKPRR CS-MIP, a colour change was observed to a darker orange. The obvious lack of colour change from orange to red for the peptide bound to DKPRR CS-MIP in the MRSSSDKPRR and MRSSSPRKRD studies demonstrates that, for these samples, protonation of the methyl red moiety was prevented. In previous experiments on the methyl red-tagged peptides in solution, it was shown that a colour change will occur as the solution becomes more acidic. It is suggested that the lack of colour change is due to the presence of the methyl red peptide in a specific binding area (cavity) in the DKPRR-imprinted particles, in which the peptide is bound to numerous functional monomer groups. This could protect the peptide from protonation and thereby prevent the colour change. For the non-specific polymers, cavities for this peptide are not present and so it is hypothesised that any bound material present is loosely bound on the surface of the particles where it is susceptible to protonation.

*Phosphoric Acid Release Study Results*

The release characteristics for the imprinted core-shell particles bound with MRSSSDKPRR and MRSSSPRKRD were assessed using a series of washes with 50% isopropyl alcohol (to prevent absorption of the peptide by hydrophobic interactions) and 50% phosphoric acid solutions at varying molarities. The molarity of phosphoric acid was increased at regular intervals from 0.01 M to 1 M. By 1 M phosphoric acid, the majority of both peptides on all of the polymer samples had been released into the supernatant. This result demonstrates that the binding observed is due to electrostatic interactions between the basic peptides and the phosphate functional monomer. The blank and GAA CS-MIP release profiles were very similar for both the MRSSSDKPRR and the scrambled MRSSSPRKRD peptides (Figure 3.14).

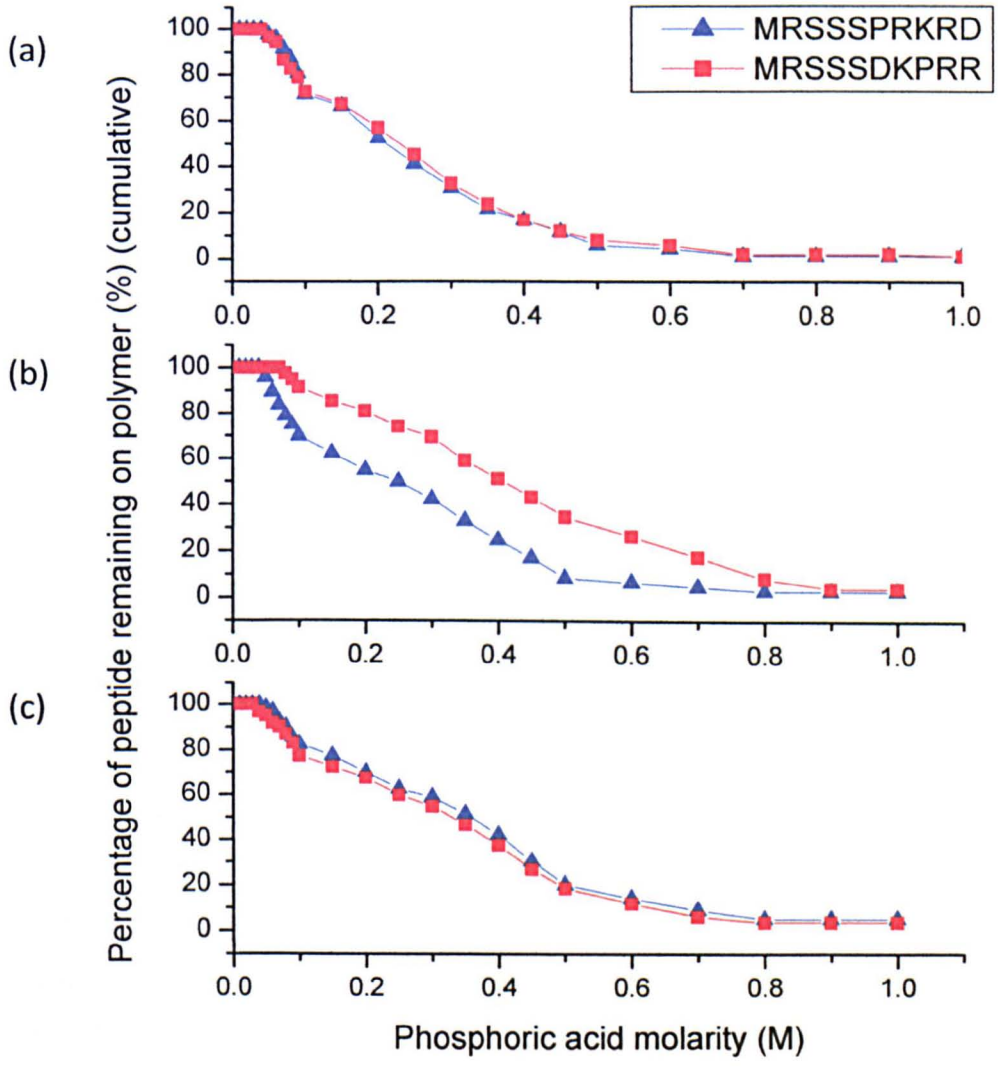


**Figure 3.14: Release profile of MRSSSDKPRR and MRSSSPRKRD from the core-shell particles in phosphoric acid/isopropyl alcohol release study. (a) Blank CS-MIP, (b) DKPRR CS-MIP, (c) GAA CS-MIP.**

For the blank CS-MIP (Figure 3.14a) the peptide was released from 0.05 M phosphoric acid in both cases. Both peptides were then steadily released from the polymer in a very similar release pattern until 0.5 M, at which point the quantity of peptide measured in the supernatant reduced until 0.7 M was reached and no further peptide was removed from the polymer. The final quantity of peptide remaining on the blank CS-MIP after all washes was 1.0% for both MRSSSPRKRD and MRSSSDKPRR peptides.

A similar result was obtained for the GAA CS-MIP, and both peptides showed very similar release patterns (Figure 3.14c). In this case the MRSSSPRKRD was released from 0.05 M phosphoric acid, and the MRSSSDKPRR was released from 0.04 M. Both peptides were then released in very similar release profiles until 0.8 M at which point no further peptide was removed. For the GAA-imprinted particles 5.3% and 3.8% of the initial peptide loading remained on the polymer after all of the washes for MRSSSPRKRD and MRSSSDKPRR respectively.

The effect of the molecular imprinting process was observed in the results for the DKPRR-imprinted particles (Figure 3.14b). For this polymer, different release profiles were observed for the methyl red-tagged DKPRR and the scrambled version, PRKRD. For MRSSSPRKRD, as for the GAA CS-MIP and the blank CS-MIP, the peptide was released from 0.05 M phosphoric acid and above. The peptide was then released steadily until 0.5 M, at which point the amount of peptide released per wash reduced until 0.8 M phosphoric acid, beyond which no further peptide was released. When considering MRSSSDKPRR, all of the peptide remained on the polymer up to 0.08 M phosphoric acid. The peptide was then released reasonably consistently until 0.9 M. After the final wash 3.1% of the MRSSSPRKRD peptide and 4.2% of the MRSSSDKPRR remained on the DKPRR-imprinted CS-MIP. The obvious differences in these release profiles, and more specifically the delay in release of the MRSSSDKPRR peptide from the DKPRR-imprinted polymer until 0.08 M phosphoric acid, suggests that the imprinting of DKPRR in the synthesis of the outer shell of the particles has led to the creation of binding regions which are selective towards DKPRR. For both of the other polymers, GAA CS-MIP and blank CS-MIP, no significant difference was observed for the two peptide sequences. The delay in the release of MRSSSDKPRR can be explained by the peptide being bound by a number of phosphate groups simultaneously, in the correct spatial arrangement for the DKPRR sequence. The

scrambled peptide sequence may also bind to the phosphate groups in these regions but may not be of the correct 3D structure to interact with all of the phosphate groups available, thus resulting in a weaker binding interaction and release of the peptide at a lower acid molarity than observed for the imprinted DKPRR sequence. The differences in release of MRSSSDKPRR and MRSSSPRKRD from the DKPRR CS-MIP is indicative of a molecular imprinting effect.

### 3.3.2 Zeta Potential Peptide Binding Study

The zeta potentials of the four particle types; core particles, blank CS-MIP, DKPRR CS-MIP and GAA CS-MIP, were analysed as it was hypothesised that the binding of the peptide to phosphate groups present in the outer shell of the polymer particles may lead to a reduction in the zeta potential of the particles, resulting in destabilisation of the latex and possibly coagulation. Two peptides were investigated, DKPRR, the basic peptide sequence from VEGF, and SSSSSSSS, an unrelated peptide sequence with no basic functionality. In order to investigate this hypothesis, the latexes were first dialysed against phosphoric acid (with sodium dodecyl sulphate (SDS)) and then deionised water (with SDS) to remove the template peptide sequences as well as any other species that may interfere with the measurement. The dialysis was carried out in the presence of SDS to ensure that the latex did not coagulate during the process. Aliquots of peptide were then added to the latexes and the zeta potential was analysed after each addition to determine the effect of peptide binding on the zeta potential.

The first three additions of DKPRR did not have a significant effect on the zeta potential of the particles, but the fourth addition led to a dramatic reduction in zeta potential for the blank-, DKPRR- and GAA-imprinted core-shell particles to -6.45 mV, -7.98 mV and -19.20 mV respectively (Figure 3.15b). The zeta potential of the core particles remained largely unaffected by the peptide additions, even up to 6 additions of DKPRR (30 μg DKPRR peptide). Due to dialysis with equal quantities of surfactant it is thought that the particles will be stabilised with comparable amounts of surfactant, and so if the observed reduction in zeta potential was due entirely to the interaction of DKPRR peptide with surfactant it is expected that a similar result would be obtained for the core particles. As this is not the case, the lack of binding of the peptide with the core particles suggests that the decrease in zeta potential observed for the core-shell particles

is a direct result of interaction of the peptide with the phosphate functionality of the outer shell.

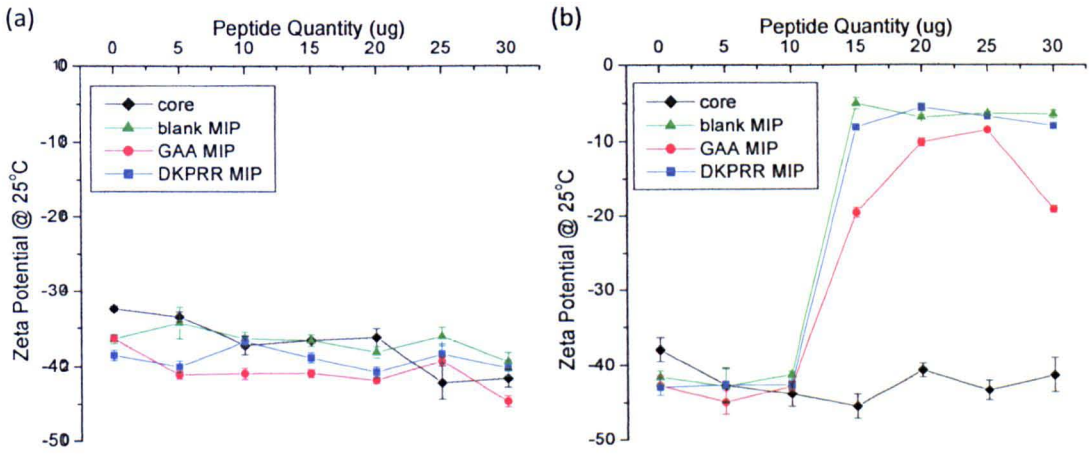


**Figure 3.15: Results of the zeta potential binding study (a) SSSSSSSS binding study (b) DKPRR binding study.**

A second zeta potential investigation was also carried out with an unrelated peptide, SSSSSSSS. The same experiment was carried out as for DKPRR peptide but in this case no reduction in zeta potential was observed for any of the particles (Figure 3.15a). In fact, the zeta potentials did not alter significantly for the entire duration of the experiment. This suggests that the binding observed through the decrease in zeta potential for core-shell particles with DKPRR was due to the functionality of the amino acids present on the DKPRR sequences, and furthermore it is anticipated that the arginine and lysine functionalities play the major role.

In polyacrylamide gel beads produced by Pang et al[166] to bind BSA, the importance of surface charge was demonstrated by zeta potential studies, as the most successful MIP formulation was shown to have a zeta potential which was of equal value but opposite charge to the BSA target molecule. In their paper, no study was shown for the zeta potential when the MIP was bound to the BSA but it does agree with the zeta potential findings in this thesis. In this thesis, the zeta potential was shown to approach zero as the basic peptide sequence, DKPRR, became bound to the core-shell particles, showing that surface charge is reduced upon binding with the positively charged peptide.

### 3.3.3 Conclusion of Peptide Binding Studies

Peptide binding to the core-shell molecularly-imprinted particles was analysed colorimetrically and by monitoring zeta potentials. Zeta potential results showed that interaction occurred between the DKPRR peptide and the functional phosphate monomer present in the outer shell of the core-shell particles, as a sharp reduction in zeta potential was observed as the peptide concentration increased for the blank-, DKPRR- and GAA-imprinted CS-MIPs. No reduction in zeta potential was observed with the core particles, confirming that the peptide interacts only with the monomer present in the outer shell. The aqueous electrophoresis studies with the peptide SSSSSSSS saw no reduction in zeta potential for any particle type. This result confirmed that the interaction between the DKPRR peptide and functional monomer is due to the basic amino acid functionality interacting with the phosphate group of the monomer. No selectivity was observed in the zeta potential study.

In the colorimetric study, binding was observed by the core-shell particles for the MRSSSDKPRR and the MRSSSPRKRD peptide types, with significantly less MRSSSSSSSSS binding to the particles. Again, this confirms the interaction between the phosphate monomer and the basic amino acid functionality. No binding selectivity was observed between the MRSSSDKPRR and MRSSSPRKRD peptides for the three types of core-shell particles. More significant differences between the core-shell particles were observed in the peptide release study, and indicated a molecular imprinting effect. Firstly, the initial addition of phosphoric acid led to a colour change of the peptide bound to the polymer from orange to red. This colour change occurred for all samples apart from MRSSSPRKRD bound to DKPRR-imprinted particles, and most significantly, MRSSSDKPRR bound to DKPRR-imprinted particles. It is suggested that this effect was due to these peptides being bound through multiple phosphate groups in imprinted cavities on the DKPRR-imprinted CS-MIP, which prevented protonation of the methyl red moiety. This result implies that a molecular imprinting effect has occurred, positioning the functional monomers in such a way as to provide specific binding sites.

This effect is further confirmed in the acid release study. For both the blank CS-MIP and the GAA CS-MIP, the MRSSSPRKRD and the MRSSSDKPRR peptides are released in a very similar pattern, suggesting no difference in binding between the two.

Conversely, for the DKPRR-imprinted CS-MIP, the MRSSSPRKRD and MRSSSDKPRR have different release profiles, with the scrambled MRSSSPRKRD peptide being released at lower acid concentrations than the MRSSSDKPRR peptide. This result also suggests that a molecular imprinting effect is occurring, as the MRSSSDKPRR peptide appears to be more strongly bound to the polymer. It is hypothesised that both MRSSSDKPRR and the MRSSSPRKRD were able to bind to the imprinted cavities present on the DKPRR polymer, but the MRSSSDKPRR polymer may be more strongly bound as the spatial arrangement of phosphate groups may lead to this peptide being bound through numerous binding regions.

No significant molecular imprinting was observed in the amount of peptide bound, but an effect was observed in the release of the peptide, as the MRSSSDKPRR peptide was more strongly bound to the DKPRR-imprinted polymer than the scrambled version. This is as might be expected when considering the similarity of the two peptides. The ability of the core-shell particles to interact with the basic peptide sequences meant that it was decided to carry out a protein binding study.

## 3.4 VEGF Binding and Release Study

The aim of the CS-MIPs was to synthesise a polymer which had been imprinted with an amino acid sequence present in VEGF and subsequently produce a material which is able to selectively bind this protein. It was also hypothesised that such an imprinted polymer would be able to bind VEGF more effectively than either blank-imprinted particles or particles imprinted with an unrelated peptide sequence (in this case GAA). The selectivity of the CS-MIPs for VEGF over different proteins has not yet been analysed, but the ability of the DKPRR-imprinted particles to bind and release VEGF in comparison to other core-shell molecularly-imprinted particles has been investigated. Consideration of the peptide binding study results meant that it was expected that all of the core-shell particles would be able to bind VEGF, and that any difference in binding was more likely to be observed on release of the protein.

The ability of the core-shell molecularly-imprinted particles to bind and subsequently release VEGF was determined using an Enzyme-Linked ImmunoSorbent Assay (ELISA). The following conditions employed were selected for an initial study and it is acknowledged that future studies with varying time scales, temperatures and doses could provide further relevant information. Future studies carried out within cell culture medium could also provide a more realistic biological environment.

To prepare the particles for analysis, 0.1 ml of emulsion (equating to 4.6 mg, 4.2 mg, 3.6 mg and 2.8 mg of core, blank CS-MIP, GAA CS-MIP and DKPRR CS-MIP respectively) was coagulated using isopropyl alcohol. The particles were then washed following the standard washing procedure previously used in the peptide binding and release study (Section 3.3). Before introduction of the VEGF, SDS removal was confirmed by conductivity analysis of the wash solutions. This was important to prevent denaturation of the protein when it came into contact with the particles. The particles were washed until no change in conductivity of the wash solution was observed. The particles were then used for the protein binding study as a damp slurry in a polypropylene eppendorf sample tube.

A solution of PBS containing 150 ng of VEGF was then added to the eppendorf tube and the particles were allowed to bind the VEGF over a 24 hour period at 4°C. After the

binding period, the supernatant solution was removed. For the release study, aliquots of PBS containing 1% bovine serum albumin (a protein stabilizer) were added to the particles, agitated and incubated at 37°C until the time point for sample collection. At each time point the sample was centrifuged and the supernatant was removed and stored at -20°C until analysis by ELISA to determine VEGF content. A fresh aliquot of 1% BSA PBS was then added to the polymer for the next time point. Time points up to 48 hours were analysed and the data was used to consider cumulative as well as instantaneous VEGF release from the CS-MIPs.

A significant result of this study is that all core-shell particles were shown to release biologically active VEGF for up to 48 hours at 37°C, as determined by ELISA. The VEGF half-life *in vivo* is reported to be less than one hour[63-66]. These results suggest that being bound electrostatically to the phosphate groups present in the core-shell particles stabilises the protein. This is in agreement with results reported by Huang et al[259], who reported that polyelectrolyte complexes were able to stabilise VEGF.

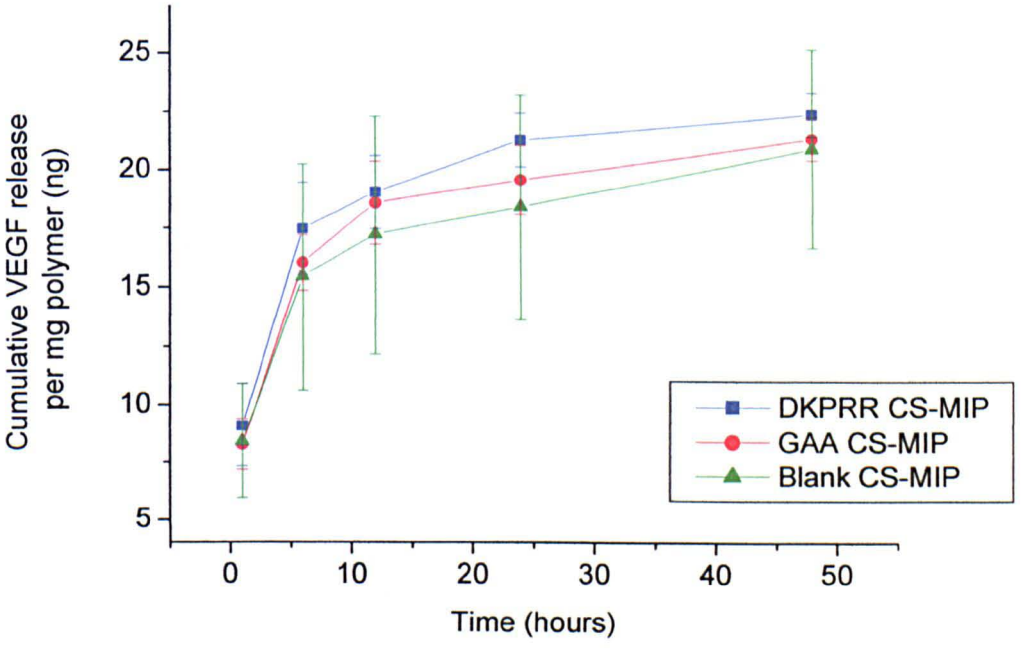


**Figure 3.16: Cumulative VEGF release per milligram of polymer over 48 hours as determined by an ELISA for human VEGF. Results shown are mean ± 95% confidence (n = 2)**

When considering the cumulative data (Figure 3.16) it is obvious that there is no significant imprinting effect on the release of VEGF over this time period. Over the 48

hour period, an average of 22.4 ng, 21.3 ng and 20.9 ng of VEGF was released per milligram of DKPRR-imprinted, GAA-imprinted and blank-imprinted CS-MIPs, respectively. The high error between the repeats in this experiment, particularly for the blank-imprinted particles at the first 2 time points, means that it is not possible to confirm whether there are any real differences between the polymers. This may be in part due to the limited number of repeats (n = 2) but also due to experimental error. It would be necessary to repeat this experiment with a higher number of repeats in order to determine whether there is any imprinting effect on the cumulative VEGF release.

The instantaneous data (Figure 3.17) reveals slightly different release patterns for the 3 polymer types. No significant difference is observed for the first 3 time points (1 hour, 6 hours and 12 hours) although the 12 hour time point is the only point at which less VEGF is released by the DKPRR-imprinted CS-MIP than both the GAA-imprinted CS-MIP and the blank-imprinted CS-MIP. Significant differences ($p < 0.05$, one-way ANOVA with post-hoc Tukey analysis) were observed at the 24 hour and 48 hour time points, at which a significantly higher quantity of VEGF was released by the DKPRR-imprinted CS-MIP than the other polymers. This suggests that sustained release of VEGF might occur for the DKPRR-imprinted CS-MIP.

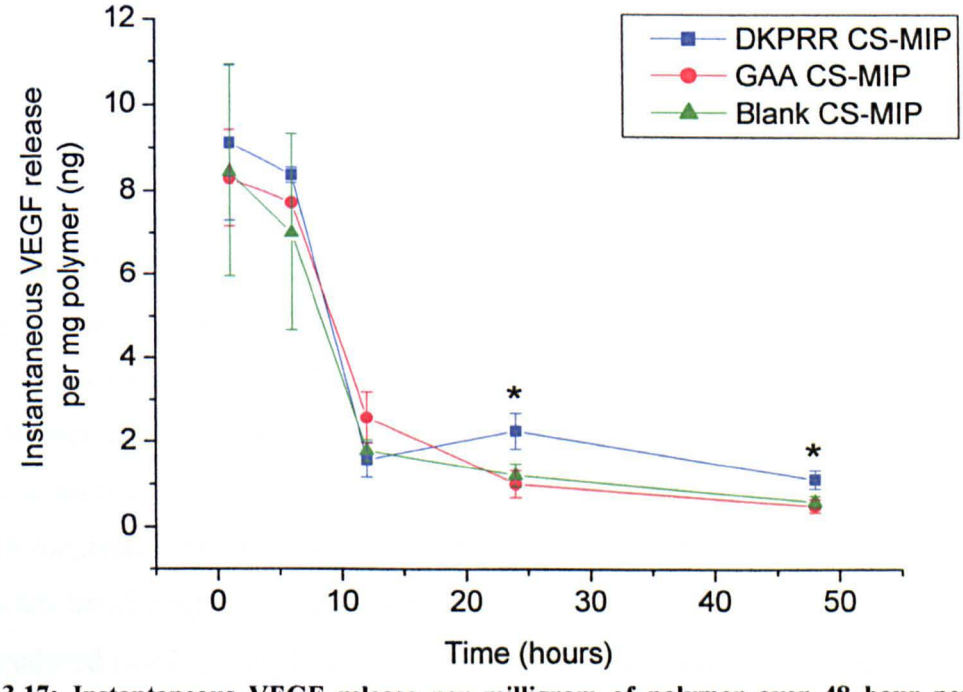


**Figure 3.17: Instantaneous VEGF release per milligram of polymer over 48 hour period a determined by an ELISA for human VEGF. Results shown are mean ± 95% confidence (n = 2). Significance was assessed using one-way ANOVA with post hoc Tukey analysis (*p < 0.05).**

## 3.5 Discussion of Results

### 3.5.1 Effect of Molecular Imprinting

The molecularly-imprinted core-shell particles were tested for their ability to bind and release both short peptide sequences and a biological protein. All core-shell particles were able to bind the two basic peptide sequences, MRSSSDKPRR and MRSSSPRKRD. It was previously discussed that the similarity in binding for the three types of core-shell particles may be due to the location of all functional monomer on the surface, thus allowing for binding of the peptide to the blank CS-MIP and the GAA CS-MIP despite the lack of selective cavities. For both the blank-imprinted CS-MIP and the GAA-imprinted CS-MIP the release profiles for both peptides were very similar. A molecular imprinting effect was observed for the DKPRR-imprinted CS-MIP, with a considerably slower release profile for the MRSSSDKPRR peptide than the scrambled MRSSSPRKRD version. This is thought to be due to the higher affinity binding of the imprinted sequence to the selective cavities in the DKPRR-imprinted CS-MIP. This was confirmed as the basic peptides, MRSSSPRKRD and particularly MRSSSDKPRR, were protected from protonation when bound to the DKPRR-imprinted CS-MIP, possibly because in this polymer the peptides were bound in an imprinted cavity to multiple phosphate groups, which prevented the structural changes which occur during protonation. It is hypothesised that protonation was possible in the blank CS-MIP and the GAA CS-MIP as in these cases the peptides are more loosely associated with the polymers and thus susceptible to protonation.

In the protein study no significant difference between the three particle types was observed in the cumulative VEGF release profile, with approximately 20 ng of VEGF per milligram of all CS-MIPs released over 48 hours. When considering the instantaneous release, a significantly higher amount of VEGF was released from the DKPRR-imprinted CS-MIP at the last two time points, 24 and 48 hours. This sustained release result may be due to an imprinting effect as the protein may remain bound to the DKPRR-imprinted polymer longer as it is bound by multiple phosphate groups. A more significant imprinting effect may be seen at later time points as no further time points were analysed in this study. This would need to be investigated in an extended study.

An interesting release study was carried out by Alvarez-Lorenzo et al[260], considering the release of norfloxacin (NRF), a low molecular weight (MW) drug, from poly(2-hydroxyethyl methacrylate) (PHEMA) hydrogels functionalised with acrylic acid. They found that at low concentrations of the drug, the imprinted hydrogels were able to take up significantly higher amounts of NRF than non-imprinted ones, but this difference was not observable at higher concentrations of NRF. They concluded that this was due to the amount of functional monomer present in the hydrogels. Imprinting at the perfect molar ratio of template to monomer should lead to high affinity binding sites, whereas with excess monomer, or in the case of the non-imprinted polymer when no template is present, the monomer can randomly distribute within the network, forming low affinity binding sites. At low NRF concentration, with only a few NRF molecules in solution, they bind exclusively to the high affinity regions but at high concentration the NRF will also bind to the low affinity binding regions, present on the non-imprinted polymer and also present on the MIP, if excess functional monomer was present during synthesis. In their case, the acrylic acid monomer was able to interact strongly with the NRF, allowing only a 1:1 template to monomer interaction to bind the NRF to the polymer. This means that at high concentration, the non-imprinted polymer may even bind more template than the MIP as it potentially contains more binding sites, albeit with less affinity for the drug. In the release study, again the most noticeable results were obtained when the drug had been bound at low concentrations. The hydrogels produced at 1:3 or 1:4 template to monomer ratio (expected to be the optimum when considering the structure of NRF) sustained release of the drug for 2-5 days, which is expected to be due to the presence of the drug in high affinity cavities.

This idea of heterogeneous binding sites due to various factors such as template to monomer stoichiometry, variability of cavity shape and flexibility of matrix, was also discussed by Umpleby et al[261]. They suggested that the heterogeneous binding sites makes the binding properties of MIPs highly concentration dependent, with low selectivity observed at high loading and high selectivity observed at low loading.

These findings are in agreement with our own conclusions in Section 3.3, that the location of the monomer on the surface of the core-shell particles due to its surfactant quality, despite the imprinting effect, means that a high amount of low affinity binding sites may be produced when the monomer is not consumed in template binding,

particularly in the case of the blank-imprinted CS-MIPs and the GAA-imprinted CS-MIPs. This is a significant observation as the functional monomer employed has a high affinity for the amine and guanidine functionality of the MRSSSDKPRR and MRSSSPRKRD peptides and therefore a 1:1 interaction can lead to binding, resulting in the lack of selectivity in the binding study. It also follows therefore, that a significant difference in release was observed for both the peptide and protein, because in this instance, the low affinity binding sites release the molecule readily, and so sustained release only occurs in the case of the imprinted polymer, where the peptide or protein is released from multiple binding points within the high affinity imprinted cavity.

### 3.5.2 Comparison of Alternative Approaches to Protein Imprinting

It is difficult to directly compare this work to reports of molecularly-imprinted proteins in the literature. In this work, the aim was to produce CS-MIPs which could bind and release bioactive VEGF over an extended period. Currently only the interaction of these particles with VEGF has been investigated. Also, in the case of most molecular imprinting literature, the work focuses primarily on the binding of the protein, whereas the work presented in this thesis has focused on the release profile of VEGF from the particles. A wealth of literature is currently available on molecular imprinting for protein binding, and it would not be possible to discuss all of the approaches utilised. Instead, the most relevant comparison to make is with similar approaches to those used in this thesis.

#### *Epitope Approach*

The epitope approach to molecular imprinting has been employed by a number of groups since the work for this thesis was begun in 2005, and has met with varying degrees of success. The majority of successful work in this area is still for the recognition of polypeptides rather than proteins, including work by Rachkov et al[190] and Titirici et al[191]. Work by Emgenbroich et al[192] has utilised the epitope approach to recognise short peptide sequences. This work aimed to recognise tyrosine phosphorylated peptides through the interaction of a phosphate group on the target molecule with a diaryl urea monomer. This relies on similar electrostatic interactions as the phosphate monomer and basic amino acids in the work discussed in this thesis. Their results show that the strong binding observed led, unsurprisingly, to MIPs with

clear selectivity for phosphorylated tyrosine over amino acids without a phosphate group, as well as being able to bind short peptide sequences containing phosphorylated tyrosine. In contrast to the results reported in this thesis, they showed that no binding is observed for the non-imprinted polymers, despite the urea monomer and phosphate target being present. It is surprising that no interaction would occur in this case. We suggest that this is due to the imprinting technique employed. Imprinting is carried out in a bulk polymerisation in the work by Emgenbroich et al[192] and so the monomer would be expected to be randomly distributed throughout the material. This may mean that in the non-imprinted polymer the urea moieties may not be accessible to the target molecule, and therefore no binding is observed, whereas the MIP would have accessible cavities after template removal. In this thesis, no significant binding difference was observed between the DKPRR CS-MIP and blank CS-MIP, possibly because the phosphate is always present on the surface in low affinity binding sites and so is always available for binding whether imprinted cavities are present or not.

A few reports have been published on the epitope approach for the binding of large proteins. Probably the most successful epitope imprinting work to date for the recognition of a protein was reported by Nishino et al[193]. Unique nonapeptide sequences of the carboxy-termini of 3 proteins; cytochrome C (Cyt C), alcohol dehydrogenase (ADH) and bovine serum albumin (BSA) were imprinted into thin MIP films by tethering the peptide to a functionalised silane surface before UV polymerising around the peptide with acrylamide, N,N-ethylenebisacrylamide and poly(ethylene glycol) 200 diacrylate. This method allowed for surface-imprinted cavities to be formed as the film was removed from the peptide substrate. Selective binding showed that each peptide imprint selectively bound only its relevant protein within detection limits, with no binding observed for the non-imprinted polymer. Also, when the BSA peptide template was altered, differing only by one amino acid, the resulting MIP bound displayed diminished affinity for BSA.

Very recently Xue et al[195] utilised a variation on the epitope approach to bind staphylococcus aureus by imprinting the staphylococcus aureus protein A (SpA), which is a protein found only on the surface of staphylococcus aureus. In this approach, polyacrylamide gel beads were used which were formed with a low crosslinker content to provide a macroporous structure for template diffusion. The results showed that the

MIP was able to bind SpA over four other proteins, whereas no absorption was observed for the non-imprinted polymer. The MIP was then shown to bind staphylococcus aureus selectively over two other types of bacteria. This is a good example of the successful application of the epitope technique, although this approach would not be compatible with the desired drug delivery application of this thesis, as there was a low elution efficiency from the beads when removing the bound target molecule, and bacterial removal required the use of acetic acid and SDS surfactant.

Brown et al[262] have imprinted lysozyme, comparing the imprinting of the whole lysozyme protein to the epitope imprinting of a 16 residue lysozyme C peptide. Only the binding process was considered, and lysozyme binding was compared with the binding of RNase A. In a non-competitive environment the MIPs behaved similarly with both materials binding approximately the same amount of lysozyme, and in both cases over five times more lysozyme bound to the MIPs than RNase A. In a competitive situation the whole protein-imprinted MIP bound four times more lysozyme than RNase A, whereas no significant difference between the two proteins was observed for the peptide-imprinted MIP. Reasons given for the lower selectivity of the peptide MIP include the fact that the smaller peptide molecules may become embedded in the polymer and therefore not be surface-accessible. Also, the use of a small peptide fragment restricts the orientation in which the protein can bind. Success for the epitope approach was reported initially by Rachkov et al[190] but the peptide imprinted in that case was 44% of the desired polypeptide. In the report by Brown et al[262] the peptide was only 12 % of the protein, which is a similar situation to the DKPRR-imprinted CS-MIP employed in this thesis. This suggests that successful epitope imprinting may require templates of a certain percentage of the overall protein.

The literature available on the epitope approach of imprinting proteins is varied, with the most success seen for the rebinding of shorter polypeptides. Some achievement has been reported with larger proteins for different formulations which offer better selectivity, but the inherent difficulties of this technique, such as the importance of orientation of the template to allow binding of the protein, may need to be overcome using techniques such as immobilised templates before this approach is truly successful for proteins. It is acknowledged that approaches by Nishino et al[193] and Xue et al[195] report favourable results for the epitope imprinting of proteins, but it seems that there

are still a lot of improvements required, and investigation into the release of bioactive protein would be necessary before this technique would produce polymers which could be used for the desired wound healing application.

***Molecularly-Imprinted Particles***

The diffusion difficulties associated with macromolecular templates mean that the majority of protein imprinting is carried out with surface imprinting techniques or mesoporous bulk polymers. Recently, the use of molecularly-imprinted particles have been popular for protein imprinting. Pang et al[166] have produced polyacrylamide gel beads via inverse-phase suspension polymerisation, with methacrylic acid as the functional monomer and bovine serum albumin as the target molecule. It was reported that the BSA-imprinted polymer was selective for BSA over a comparison protein, ovalbumin, and showed a much higher adsorption capacity than the non-imprinted beads. They report that the considerably lower absorption capacity for the non-imprinted material is due to the lack of a cavity containing multiple binding points. The functional monomer is thought to be randomly distributed throughout the gel, leading to very weak interaction and reduced BSA adsorption. In the blank-imprinted CS-MIP particles discussed in this thesis, it is also expected that the functional monomer is randomly distributed in the shell, but in this case always at the surface due to its surfactant properties. The functional monomer is a phosphate in our case, which is known to interact strongly with the basic amino acids on either peptide or protein target molecules. The lack of difference in binding observed in this project between the DKPRR-imprinted CS-MIP and the blank-imprinted CS-MIP is attributed to these points. Even in the blank-imprinted CS-MIP, the functional monomer is still accessible on the surface of the particles, and the electrostatic interaction it provides is still strong enough to tether the target molecule. Thus binding still occurs even though imprinted cavities are not present. It is therefore unsurprising that for this system the differences between the imprinted and blank-imprinted polymers are observed in the release of the compound as this will be affected by how many functional monomers are interacting with the target compound simultaneously.

Bovine serum albumin was used as a target by Tan et al[189] for core-shell particles produced by miniemulsion polymerisation. In this case the template was immobilised to the core particle via a spacer chain containing an imine bond. Formation of the shell was

then formed by polymerising around the core, producing core-shell particles with surface cavities after removing the BSA template by hydrolysis of the imine group. In batch binding studies, the MIP produced with the immobilised template bound significantly more than the non-imprinted polymer, and also bound considerably more than a MIP produced with free BSA template. In a competitive binding study of BSA and lysozyme, the free-BSA MIP and the free-BSA non-imprinted polymer showed similar non-preferential uptake of the proteins. Conversely, the immobilised BSA MIP absorbed BSA selectively, whereas the non-imprinted polymer predominantly bound lysozyme. The impressive results from these core-shell particles are attributed by the authors to the immobilisation approach, although the results also demonstrate the success of the whole protein approach to imprinting. Whether or not this method could be utilised for the desired biological application of this project would depend on whether the process is compatible for a bioactive protein. The BSA-immobilised core particle is exposed to a surfactant and prolonged synthesis at 40°C. It is not discussed by the authors whether the BSA binding sites formed bind BSA in an active conformation. To determine whether this could be an effective approach for a biological protein delivery application, it would be prudent to study the activity of the released protein.

Core-shell particles were produced by Qin et al[263] to recognise lysozyme using surface-initiated living radical polymerisation. A shell of lysozyme-imprinted copolymer of acrylamide and N,N'-methylenebisacrylamide was formed on a mesoporous chloromethylated polystyrene bead support. The imprinted beads were selective for lysozyme over four other proteins in aqueous non-competitive and competitive HPLC studies, an effect not seen for the non-imprinted bead. The retention time of lysozyme was increased on the MIP but the protein was released. This may mean that this approach could be used for a delivery application, but again no mention was made of the bioactivity of the protein after release by the MIP.

Surface-imprinted nanoparticles were produced by Tan et al[264] via miniemulsion polymerisation of methyl methacrylate and EGDMA. Varied results were reported, with a good imprinting effect for a ribonuclease A (RNase A) template, a modest effect when the template was lysozyme, and no imprinting effect was observed at all when bovine serum albumin (BSA) was imprinted. These differences were attributed to the

interaction of the protein template with surfactant used in the particle synthesis. The authors hypothesise that interaction was required between the template protein and the surfactant to partition the template at the surface of the particle, but it is important that the interaction is not enough to denature the protein. In this paper the correct balance was only achieved for the RNase A system. It was also discussed that for the successful RNase A system, only 38% of the RNase A could be removed from the particles in an entirely aqueous system. This report shows some success, but demonstrates the difficulties of imprinting proteins due to the denaturing risk during polymerisation, as well as the importance of tailoring the approach to the protein in question.

The most comparable study details core-shell particles, produced by Okutucu et al[265] to remove albumin from plasma. Albumin was the target molecule and the core-shell particles consisted of epichlorhydrin crosslinked chitosan beads and a shell of acrylamide and N,N'-methylene-bisacrylamide. Selective absorption of albumin over haemoglobin was observed in non-competitive studies, which could be repeated over a number of binding and release cycles. The selective binding observed was attributed to considerable differences in the shape of the two proteins as well as differences in charges that minimise the binding of haemoglobin. Although no comparison was made between the MIP and the non-imprinted polymer or between two similar proteins, this report shows a system which can bind bioactive polymers and release them, without them being destroyed or changing the structure, just by changing the pH.

Again, the core-shell particles produced in this thesis possess only a very modest imprinting effect in comparison to the other particulate systems discussed, but a final comparison is not possible until further selectivity studies with alternative proteins have been carried out. A number of selective particles have been discussed, but in most cases there is limited compatibility of the technique with a bioactive protein, as the release of the protein is either poor or not reported, or the technique may only be suitable for certain proteins.

### 3.5.3 Summary of Core-Shell Molecularly-Imprinted Particles

Evaluation of the core-shell particles produced in this report is difficult as currently only the target protein has been analysed for binding, but the imprinting effect observed is limited, noticeable only in release experiments. All core-shell particles were able to rebind the DKPRR sequence and also the VEGF protein, but a molecular imprinting effect was observed only for the DKPRR-imprinted CS-MIP, with delayed release of the MRSSSDKPRR peptide in comparison to the MRSSSPRKRD peptide, as well as sustained release of the VEGF protein. In order to truly determine the molecular imprinting effect it would be necessary to carry out further experiments, including binding studies with unrelated proteins, binding studies at varying concentrations of both peptide and protein, and extending the protein release study to observe the effect of sustained release over a longer time period.

Comparison of this method with other approaches to the molecular imprinting of proteins shows that the imprinting effect in this case is very modest when considering protein binding. The selective binding exhibited by other groups is not evident in this case from the experiments carried out, and the only effect of imprinting is observed upon release of the peptide and also the protein. It is evident from the literature, particularly that of Tan et al[264], that a molecular imprinting technique needs to be tailored specifically for the protein in question, the desired application and the level of specificity required. A number of approaches have been discussed by other researchers which fulfil the requirements for which they were produced, and are analysed with primary consideration for the properties required by that application. The aim of this project was primarily the binding and release of bioactive proteins from within a wound bed, which requires certain criteria either not possible with other approaches or not discussed within the reports published. For this application it was necessary to have material which could release a large proportion of the protein bound over a reasonable time frame and would allow the protein to remain biologically active. Although there are reported investigations of molecular imprinting which consider protein binding, release time and efficiency, or bioactivity of the template, to our knowledge there are very few reports currently available which consider all of these requirements.

With regard to the molecular imprinting technique, from the results of both the peptide and protein study, a slight imprinting effect was observed for the DKPRR-imprinted

CS-MIP upon release of the target molecule, but the improved properties in peptide and protein binding due to molecular imprinting are currently not considerable. Further investigations, including an extended VEGF release study and competitive and non-competitive protein binding studies with relevant proteins, would now be required. Such studies would determine whether the imprinting effect allows VEGF to be bound preferentially over other proteins, and also whether the imprinting effect allows the VEGF release to be sustained over a longer time period.

Despite the fact that no significant molecular imprinting effect was observed, there were a number of positive outcomes to this study. Core-shell particles have been produced containing surface phosphate functionality, which are capable of binding and releasing basic peptides and VEGF protein. The protein release study demonstrated that core-shell particles are able to bind and release bioactive VEGF over a 48 hour period, and possibly longer. This is a significant result as the half-life of VEGF in bolus delivery is reported to be less than one hour[63-66]. In conclusion, these core-shell particles achieve the aim of binding and releasing biologically active VEGF in a reasonable time frame. Although the imprinting effect may not be sufficient to make the time and cost of imprinting worthwhile, the use of core-shell particles containing a phosphate monomer, if found to be biocompatible, may be a suitable way to achieve protein delivery within a wound healing application.

# 4 Strategy 2: Peptide-Functionalised Hydrogels

The alternative methodology investigated utilised the VEGF-binding ability of heparin itself in order to mimic the extracellular matrix. Hydrogels were produced and then functionalised with basic peptide sequences. It was hypothesised that such basic peptide sequences would bind heparin which could in turn bind to VEGF. This approach should bind VEGF via the protein's heparin-binding region, thereby allowing VEGF to be tethered in a biologically active form (Figure 4.1).

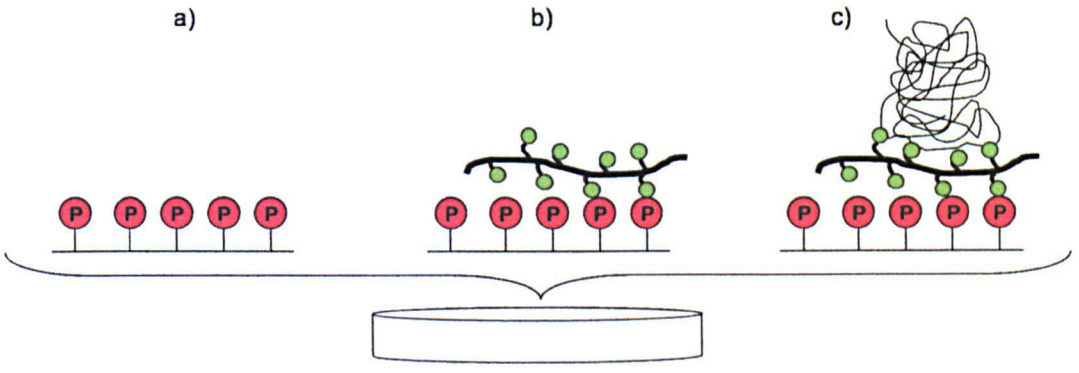


**Figure 4.1: A schematic representation of the hydrogel concept. a) A hydrogel is functionalised with basic peptide sequences, b) Heparin is bound to the hydrogel via electrostatic interactions between the peptide and sulphate moieties on the heparin, c) VEGF is bound to the hydrogel via interaction with heparin.**

For this approach it was necessary to first produce biocompatible polymers with a mechanical strength and flexibility suitable for a biological application. It was then necessary to include functionality which would allow peptide incorporation without negatively affecting the hydrogel, and an investigation into a suitable peptide and method of peptide incorporation was carried out to allow the optimum quantity of peptide to be attached to the hydrogels.

## 4.1 Determination of Methodology

### 4.1.1 Determination of Polymer Composition

Poly(N-vinylpyrrolidone) (PVP) is the water soluble homopolymer of N-vinyl-2-pyrrolidone (NVP). Initially developed by I. G. Farben during the 1930s, this material has been used extensively for a range of biomedical applications. An early use of PVP was as a blood plasma extender during World War II[266]. A large number of advantageous properties, including being water-soluble, resistant to thermal degradation and biocompatible due to its lack of toxicity, immunogenicity and antigenicity, mean that PVP has had considerable commercial success as well as prompting academic interest[267]. PVP is employed in a large number of industries including pharmaceutical, food, beverage, cosmetic, toiletry and photographic industries[266]. Major uses of PVP include contact lenses, tablet binders and as an iodine complex, commonly found under the trademark Betadine™, which is used as a topical antiseptic. PVP is also widely used in academic research as a biomaterial, including possible applications as a macromolecular drug carrier[267-269], a vitreous humour substitute[270-272] and a surface coating for biomedical applications[273].

In our research group, PVP has been investigated as a biomaterial for a number of uses including drug-conjugated PVP for pharmaceutical application[274-276], as amphiphilic diblock copolymers with poly(D,L-lactide) for micelle formation[277] and as crosslinked hydrogels for improving cell viability[278]. In a study by Smith et al[278], ethylene glycol dimethacrylate- (EGDMA) and diethylene glycol bisallylcarbonate- (DEGBAC) crosslinked NVP hydrogels were analysed to determine their ability to affect cell viability in direct and indirect contact with a range of cells. Both materials were shown to have high equilibrium water contents (EWC) and for 1% crosslinker formulations the poly(NVP-co-DEGBAC) was shown to be a considerably stronger material, making it more suitable for cell culture. Cell culture studies revealed that, whilst neither material was able to support cells cultured directly on top of the hydrogels, the polymers were biocompatible and slightly stimulatory to fibroblasts. In indirect contact the poly(NVP-co-DEGBAC) stimulated fibroblast viability more reliably than poly(NVP-co-EGDMA). Due to its superior mechanical properties and positive effect on cell culture, poly(NVP-co-DEGBAC) was chosen as the base hydrogel in this investigation.

### 4.1.2 Determination of Peptide Sequences

An important consideration for this approach was the peptide sequence to be attached to the hydrogel. It was necessary to determine a cost-effective sequence capable of interacting with heparin, which would interact adequately with the hydrogel to produce the peptide-hydrogel conjugate and which would not affect the hydrophilicity of the material. As the aim of this project is to produce a biomaterial which could be applied within the clinic, the material was designed to be as simple and as easy to produce as possible, whilst still providing the desired effect.

In order to produce a peptide-functionalised hydrogel capable of binding heparin it was thought prudent to study the interaction of heparin with proteins in nature in order to replicate the binding strategies. It is extensively reported that glycosaminoglycans bind and regulate the activities of many proteins, and a number of reviews including those by Powell et al[279] and Mulloy[280] discussed the ability of heparin and heparan sulphate sequences to bind with varying affinities to particular proteins. Mulloy[280] considered the ability of sulphated polysaccharides to bind with proteins at a number of different specificities. Firstly, non-specific binding occurs through interaction of the acidic polysaccharide with basic areas on the surface of the protein. Secondly, particular proteins are able to bind with specific substructures to the sulphated polysaccharides (for example the highly specific interaction between heparin and antithrombin, giving heparin a high specific activity as an anticoagulant through its ability to potentiate the plasma serine protease inhibitor antithrombin[280]). Finally, an intermediate reaction can occur between certain cytokines, growth factors (for example fibroblast growth factors), and morphogens with specific sulphation patterns on cell surface GAG heparan sulphate.

Research into the requirements of GAG-protein interactions has been carried out since the late 1980s. Cardin et al[281] used molecular modelling to study heparin binding in 4 proteins (human apo B, apo E, vitronectin and platelet factor 4), and found similarities between the amino acid sequences in the heparin binding domains. The basic amino acids (arginine, lysine and histidine) were present in two consensus sites with sequences XBBXBX and XBBBXXBX where B is a basic residue and X is a non-basic residue. A further sequence of XBBBXXBBBXXBBX was determined a few years later by Sobel et al[282].

Research reviewed by Hileman et al[283] shows that specific amino acid residues, as well as the spacing in between the residues, affect the strength of the interaction. Assessment of a library of 7-mer peptides by Caldwell et al[284] showed that arginine- and lysine-enriched peptides, but not histidine-enriched peptides, bound heparin and heparan sulphate with greatest affinity. Polar amino acids were also often found to be present in peptides with high heparin affinity. Asparagines and glutamine were found in heparin binding sites, presumably to provide hydrogen bonding. Fromm et al[244] used synthetic peptides to investigate the differences in binding between arginine and lysine, and found that arginine synthetic peptides bound heparin more strongly than lysine. Blocked peptides were used to prove that the differences were due only to the side chains, and the results showed that arginine was able to bind 2.5 times more strongly than lysine. Two explanations were offered for this result. Firstly stronger hydrogen bonding may occur between the guanidine and sulphate groups than the amine found on the lysine side chain. Secondly, the more diffuse (and therefore softer) guanidinium cation may interact better with the soft sulphate anion of the GAG.

From the information available on heparin-protein interactions it was decided that two basic amino acids would be expected to produce the most effective heparin binding groups, lysine and arginine. Consideration of the results of Cardin et al[281] suggests that clusters of either di- or tripeptides of basic amino acids can lead to binding with heparin. For this work tripeptides, trilysine and triarginine, were selected as it was thought that the extra length of the tripeptide over the dipeptide could act as a spacer, possibly improving the accessibility of the basic functionality for the heparin chains. A hexalysine sequence was also employed to determine whether increasing the sequence length would affect the coupling reaction.

### 4.1.3 Determination of Peptide Coupling Procedure

In order to modify a polymer with a peptide, the polymer requires a functional group to which the peptide can be attached[285]. The functional groups could either be an integral part of the material or could be incorporated through modification of the polymer or through addition of a comonomer. A number of functional groups can be employed, including carboxylic acids, amines, thiols and alcohols. Coupling reactions are carried out and generally involve the activation of the functional group, followed by bond formation between the material and the peptide. Various methods are reported for this procedure involving one or two step reactions depending on the peptide and the coupling reagents employed. The concentration of the peptide immobilised on the polymer is generally controlled by the amount of functional group incorporated into the polymer or by the amount of peptide introduced to the polymer.

For this study it was decided that acrylic acid, another water-soluble monomer, would be incorporated into the poly(NVP-co-DEGBAC) hydrogel to introduce carboxylic acid functionality. It has been shown previously by Smith[286] that poly(NVP-co-DEGBAC-co-AA) hydrogels are cytocompatible and offer the required material properties for cell culture.

The coupling procedure used in this work involves the formation of an amide bond through the reaction of an activated carboxylic acid on the polymer and a primary amine on the peptide. A standard coupling reagent for this reaction is 1-ethyl-3-(3-dimethylaminopropyl)carbodiimide (EDC)[287]. EDC coupling can be carried out in aqueous solutions, generally buffer solutions of MES[288] and PBS[289], but one drawback with EDC coupling in aqueous media is the competition of the desired reaction with hydrolysis, which will deactivate the ester to a carboxylic acid. Alternatively, depending on the polymer composition, DMF can be used as a solvent to avoid the competing hydrolysis reaction. In this case dicyclohexylcarbodiimide (DCC) can be substituted for EDC[290]. An alternative method to minimise hydrolysis whilst still allowing the reaction to take place within aqueous medium is to add N-hydroxysuccinimide (NHS)[287], forming an active ester intermediate which does not succumb so easily to hydrolysis.

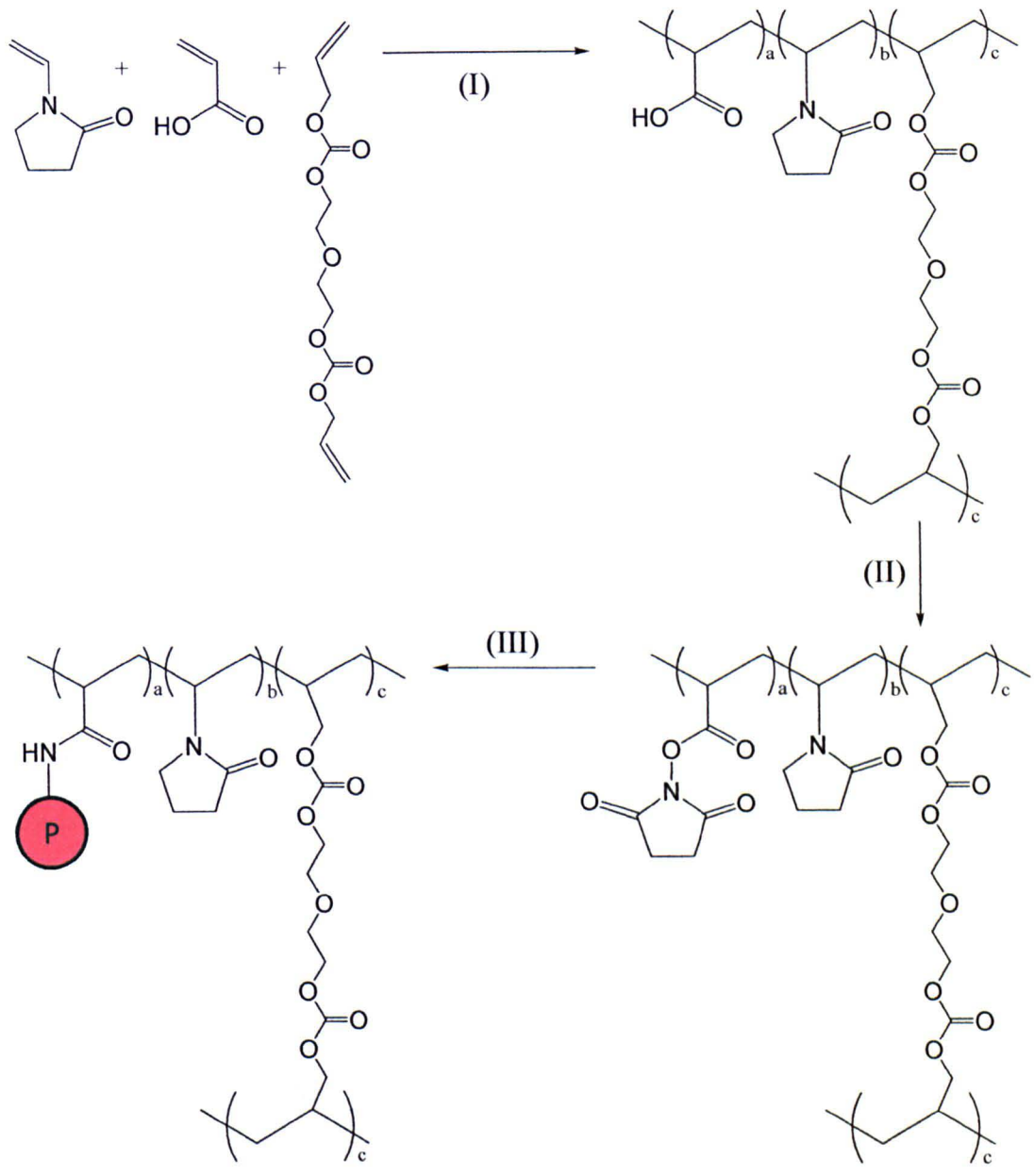


**Figure 4.2: Schematic of hydrogel synthesis and peptide functionalisation. (I) UV polymerisation of NVP, AA and DEGBAC crosslinker (II) N-hydroxysuccinimide active ester formation (III) Peptide coupling between active ester and amine from peptide to produce an amide bond (P = peptide).**

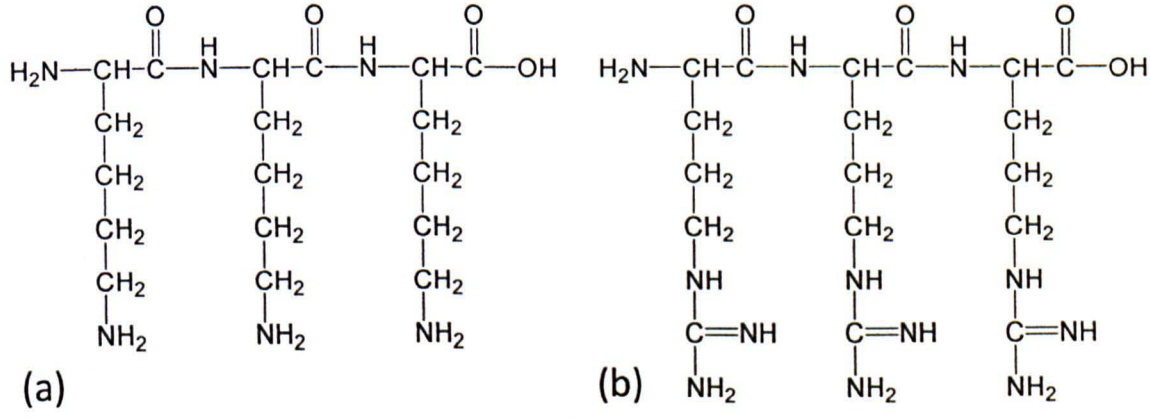


**Figure 4.3: Peptide structures (a) trilysine (b) triarginine**

## 4.2 Results of Polymer Synthesis

### 4.2.1 Thermally-Cured Poly(NVP-co-DEGBAC-co-AA) Hydrogels

Poly(NVP-co-DEGBAC-co-AA) hydrogels of 1 mm dry thickness were synthesised. The formulation utilised produced hydrogels with high equilibrium water contents. The hydrogels were produced in preformed moulds and were cured thermally with AIBN at 60°C for 24 hours. 1 wt % crosslinker was employed for a 5 wt % acrylic acid hydrogel. When 2 wt % acrylic acid hydrogels were produced with 1 % crosslinker the gels were very weak and disintegrated upon swelling in ethanol. The improved strength of the hydrogel with 5% acrylic acid may be due to intramolecular hydrogen bonding between the acrylic acid and NVP moieties. 2 wt% diethylene glycol bisallyl carbonate (DEGBAC) was required in order to produce a 2 wt % acrylic acid hydrogel with the required strength. Equilibrium water contents of the 2wt% DEGBAC polymers were determined to be 89% and 84% for the 5 wt% and 2 wt% acrylic acid formulations, respectively. Residual monomer content was determined by gas chromatography (GC) analysis of a methanol wash solution in which the hydrogel had been submerged for 24 hours. It was shown that after the wash procedure no detectable monomer remained in either of the hydrogels produced. $^{1}H$ and $^{13}C$ NMR spectra of the degraded polymers again demonstrated that no unreacted monomer remained by the absence of any vinyl peaks.

### 4.2.2 UV-Cured Poly(NVP-co-DEGBAC-co-AA) Hydrogels

UV polymerisation, an alternative to thermal curing for hydrogel synthesis, was also trialled. For this system a UV initiator was required, and 2-hydroxy-2-methylpropiophenone was selected for use in this study. Poly(NVP-co-DEGBAC-co-AA) hydrogels were produced, as for the thermally-cured hydrogels, in preformed moulds of quartz plates and with a thinner spacer (500 μm) to allow optimum penetration of UV light. Utilising UV polymerisation allows a significantly shorter reaction time of 6 minutes, during which the moulds had to be turned over every minute to allow even polymerisation on both sides of the hydrogel.

After polymerisation, the hydrogel must be removed from the mould and placed into ethanol to allow it to swell and thereby facilitate the removal of any residual monomer or other impurity. The dry hydrogels were found to be glassy and brittle materials. This

led to difficulty in removing the hydrogel from the mould. For the thicker, thermally-cured gels it was possible to synthesise gels with no solvent present, which could be relatively easily removed from the moulds. This was not the case for the UV-cured hydrogels, and in order to remove these gels without breaking the large sheets it was necessary to carry out the synthesis with 1/3 (v/v) ethanol and 2/3 (v/v) monomer mixture. The ethanol lubricated the hydrogel-mould interface and thereby allowed easier removal of the polymer.

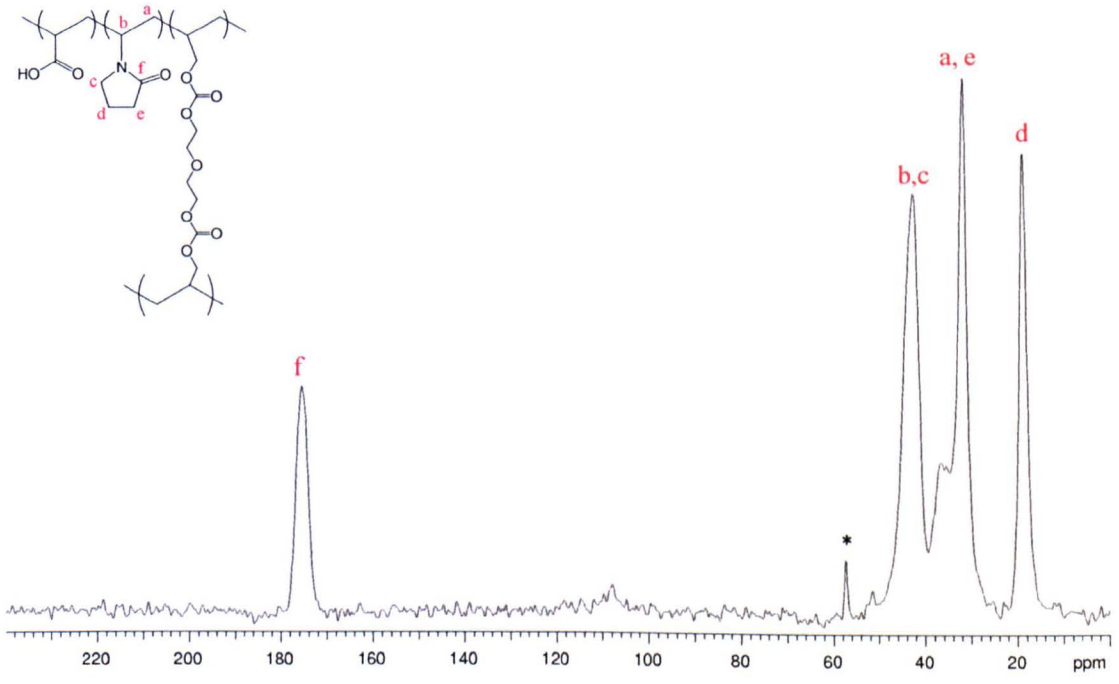


**Figure 4.4: Solid state $^{13}C$ NMR spectrum of poly(NVP-co-DEGBAC-co-AA) with 5% acrylic acid content, synthesised by UV polymerisation. Solid state NMR spectra were obtained by the Durham University Solid-State NMR Research Service using a Varian VNMRS instrument operating at 100.56 MHz for $^{13}C$. Spectral referencing is with respect to tetramethylsilane. The weak line at 108 ppm is a spinning sideband relating to the 175 ppm signal. * peak is expected to be due to residual ethanol present in the hydrogel due to the storage protocol.**

The solid state NMR spectrum shown in figure 4.4 was obtained for the UV polymerised hydrogel poly(NVP-co-DEGBAC-co-AA) with 5% acrylic acid content. This spectrum is representative of all spectra produced for the UV-polymerised hydrogels. The peaks at 176 ppm (f); 43 ppm (b, c); 32 ppm (a, e) and 19 ppm (d) are attributed to the NVP portion of the hydrogel[291, 292], which would be expected for a hydrogel with such a high NVP content. No peaks were observed in the vinyl region, suggesting that the washing steps successfully removed any unreacted monomer remaining after polymerisation. In all cases, no signals are observed for the DEGBAC,

although this may be expected at such low concentrations of crosslinker. It is also not possible to assign any individual peaks for the acrylic acid moiety. It is suggested that one signal from the acrylic acid group may overlap with the NVP residue peaks around 30-40 ppm[292]. The acid group would be expected to appear at a slightly higher chemical shift than the NVP amide peak (f) (at 176 ppm), but these peaks may have overlapped due to the linewidths of the peaks.

All of the hydrogels produced in this manner were also analysed for residual monomer by GC analysis as for the thermal hydrogels. No monomer was visible in the GC traces showing that for these hydrogels no monomer would leach from the hydrogels into the surrounding solution, a significant result when considering cytoxicity of the hydrogels.

### 4.2.3 Effect of Crosslinker and Acrylic Acid Incorporation

Hydrogels were produced with varying NVP, AA and DEGBAC concentrations to determine the effect of both the AA content and crosslinker content on the equilibrium water content (EWC) (Figure 4.5) as well as the mechanical integrity of the hydrogels in terms of ease of handling for a possible medical application.

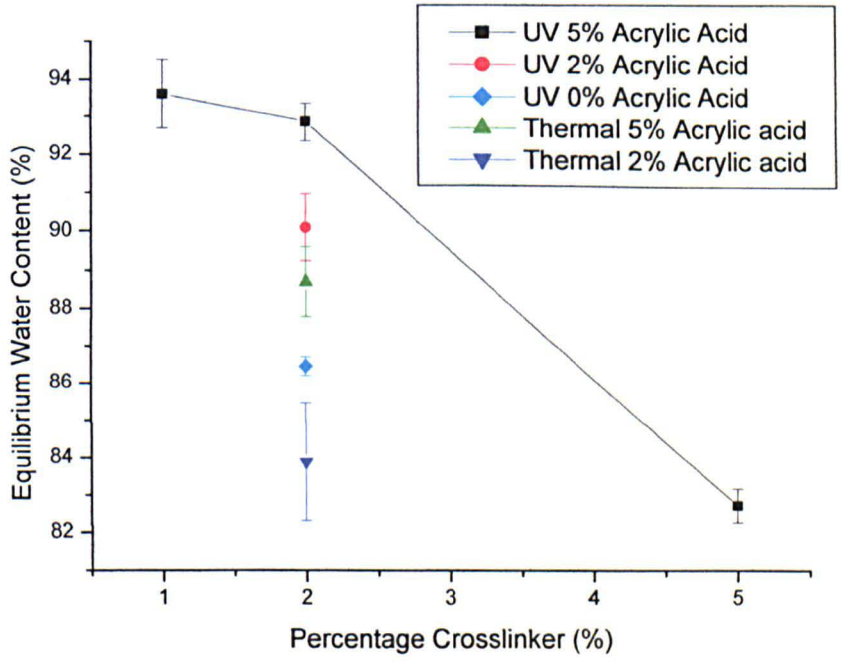


**Figure 4.5: Effect of varying the crosslinker and acrylic acid concentrations on percentage equilibrium water content (EWC) of hydrogels.**

Results for hydrogels produced by thermal polymerisation, with 2% and 5% acrylic acid at 2% DEGBAC concentration, show that increasing the amount of acrylic acid leads to an increase in equilibrium water content. For the thermal polymerisation, 5% acrylic acid incorporation and 2% acrylic acid incorporation produced hydrogels with 88.7% and 83.9% water content after equilibrium swelling. The same trend was observed for the UV-polymerised hydrogels. In this case, the equilibrium water content increased from 86.5% to 90.1% to 92.9% as the acrylic acid concentration increased from 0% to 2% and finally to 5%. This result would be expected from the thermodynamics of hydrogel swelling. The Flory Rehner analysis[293] considers hydrogels as neutral, crosslinked networks with a Gaussian distribution of polymer chains. According to this description the equilibrium water content occurs when the swelling force, due to the thermodynamic compatibility of the polymer and solvent, equals the retractive force which occurs as the network is stretched[294]. Incorporation of the highly hydrophilic acrylic acid monomer will introduce anionic charge into the hydrogels which would be expected to lead to an increase in the equilibrium water content.

It was not possible to analyse thermally-polymerised hydrogels at either 1% or 5% crosslinker as in both cases the hydrogels disintegrated upon swelling in ethanol. For the 0% and 2% acrylic acid UV hydrogels, only a crosslinker concentration of 2% enabled the polymer to remain as a sheet, as crosslinking with 1% and 5% DEGBAC produced hydrogels which disintegrated upon swelling. With 5% acrylic acid content it was possible to produce hydrogels with 1%, 2% and 5% DEGBAC. This suggests that increasing the acrylic acid content increases the strength of the hydrogel, an effect that is thought to be due to hydrogen bonding occurring between the acrylic acid and NVP moieties present on different polymer chains. Increasing the crosslinker density reduced the EWC from 93.6% for 1% DEGBAC to 92.9% for 2% DEGBAC and 82.8% for 5% DEGBAC. This is as expected, as more crosslinking would reduce the polymer chain mobility, thereby decreasing the swelling potential.

All of the hydrogels which remained intact upon swelling were brittle when dry but were reasonably flexible and easy to handle when swollen. It was thought that the mechanical properties of the hydrogels produced were suitable for a biomaterial and could be used for cell culture.

## 4.3 Results of Peptide Functionalisation

Once the hydrogels had been successfully synthesised and analysed, a number of experiments were carried out in order to determine the optimum method for coupling peptides to the polymers, trialling both EDC and DCC for the activation step and various aqueous buffers for the peptide coupling step. At this stage of the project, only the thicker, thermally-cured hydrogels had been synthesised. For this reason all of the optimisation investigations and the subsequent results for coupling peptides to hydrogels were carried out on these hydrogels. The optimised procedure determined for the thermally-cured hydrogels was then adopted for the UV-cured hydrogels without further experimentation.

### 4.3.1 Analysis of Coupling Efficiency

Due to the crosslinked nature of the hydrogels, a procedure for coupling analysis was required other than the standard NMR approach. The coupling efficiency was indirectly analysed for the majority of the polymer-peptide conjugates through the colorimetric analysis of the coupling solution post-reaction with trinitrobenzenesulphonic acid (TNBS). This assay quantifies the concentration of primary amines in solution[295]. Only primary amines are analysed in this procedure, as the reaction of secondary amines with TNBS is considerably slower and is not thought to occur within the time frame of the analysis. The TNBS molecule reacts in a 1:1 ratio with amine functionality (Figure 4.6).

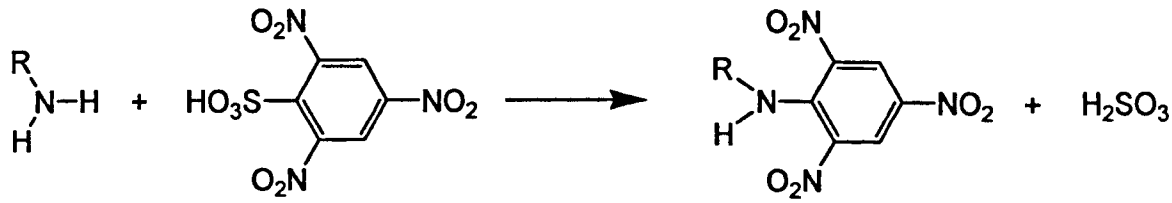


**Figure 4.6: Nucleophilic aromatic substitution reaction occurring between 2, 4, 6 –Trinitrobenzene-sulfonic acid and a primary amine group.**

The coupling efficiency was indirectly analysed by the TNBS assay by measuring the amount of amino acid or peptide remaining in an aliquot of the coupling solution and in subsequent washes (section 10.4.6). The final coupling value was then calculated by subtracting this from the initial concentration of the coupling solution. In order to confirm the accuracy of this technique, a direct measurement was carried out on a hydrogel-lysine conjugate produced. In this case the base hydrogel and the lysine-

coupled hydrogel were dissolved in 0.5 M NaOH solution, after coupling and washing for 7 days in deionised water. It is suggested that this procedure breaks down the carbonate groups in the crosslinker, producing linear polymer chains. This is confirmed by $^{1}H$ and $^{13}C$ NMR analysis which showed that the NMR spectra of the dissolved polymer hydrogels are comparable to NMR spectra produced for linear poly(NVP-co-AA). The polymer solutions produced were neutralised by the addition of 0.5 M HCl and then freeze-dried. The freeze-dried polymers were then dissolved in 0.1 M sodium tetraborate at pH 9.3, and analysed with TNBS. As expected, the hydrogel before coupling showed no response to the TNBS assay and the hydrogel after coupling gave a positive response to the presence of lysine. A comparison of the two results, obtained directly and indirectly after coupling with lysine, showed that the results were very similar. Indirectly, through analysis of the coupling solution and wash solutions, a coupling efficiency of 72.2% was determined for formulation 5. Directly, through analysis of the dissolved peptide, a coupling efficiency of 73.6% was determined. From these results it was decided that the indirect analysis of the coupling solutions was suitable for determining coupling efficiency, as well as being simpler to carry out and avoiding complications discussed in section 4.3.4, and so all subsequent results shown were determined by this method.

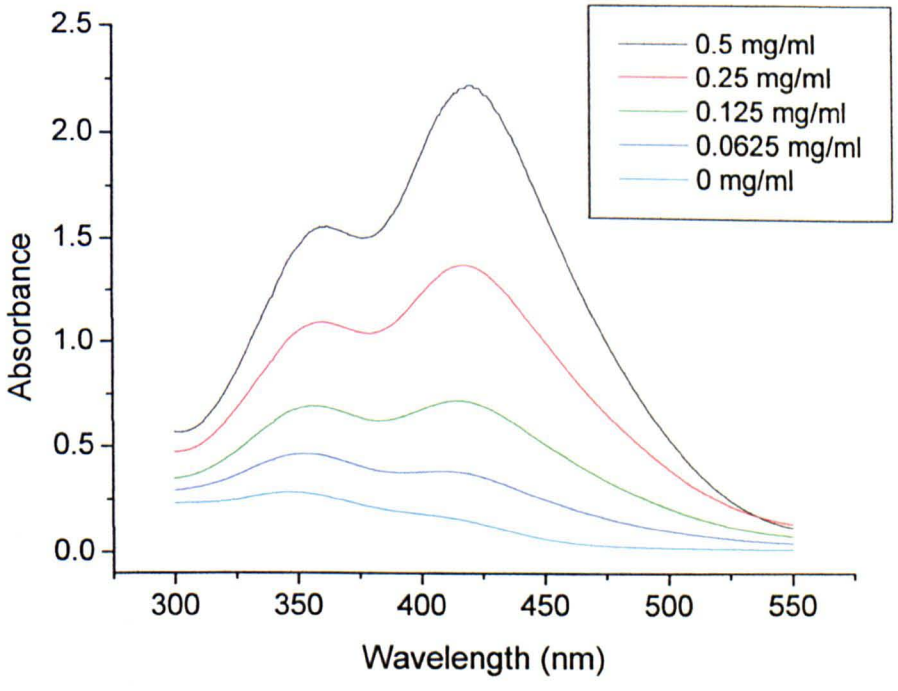


**Figure 4.7: Absorption spectra of TNBS-lysine complex**

### 4.3.2 Coupling Trials with Lysine Hydrochloride

In order to determine a successful coupling procedure for the hydrogel-peptide conjugates, experiments were first carried out with 5 wt% acrylic acid thermally-cured hydrogels and lysine hydrochloride. Lysine was substituted for the peptide sequences required, which allowed multiple experiments to be carried out which would not have been possible with synthetic peptides due to cost and time restraints. It was thought that the activity of lysine in the coupling reaction would be comparable to that of the lysine peptides. An optimised procedure for the coupling was determined from the lysine hydrochloride experiment before the synthesis of the peptide-functionalised hydrogels.

| Step | Parameter | | Formulation | | | | |
|---|---|---|---|---|---|---|---|
| | | | 1 | 2 | 3 | 4 | 5 |
| Activation Reaction | Reagent 1 | Name | EDC | EDC | EDC | EDC | DCC |
| | | Equivalent[a] | 5 | 5 | 5 | 5 | 5 |
| | Reagent 2 | Name | NHS | NHS | NHS | NHS | NHS |
| | | Equivalent[a] | 5 | 5 | 5 | 5 | 5 |
| | Solvent | | Water | Water | Water | Water | DMF |
| | Temperature (°C) | | 0 | 0 | 0 | 0 | RT |
| | Time | | 24 hours | 24 hours | 24 hours | 24 hours | 24 hours |
| Coupling Reaction | Peptide Equivalent[a] | | 2 | 2 | 2 | 2 | 2 |
| | Buffer | | Sodium acetate | Sodium acetate | PBS | PBS | PBS |
| | pH | | 5.5 | 5.5 | 8.5 | 8.5 | 8.5 |
| | Temperature | | 0 | 0 | 0 | 0 | 0 |
| | Time | | 24 hours | 72 hours | 24 hours | 72 hours | 72 hours |
| Results | Coupling Efficiency (% of theoretical coupling) | | 0 | 6.4 | 0.1 | 33.4 | 72.2 |

**Table 4.1: Parameters employed and results obtained for coupling experiments of thermally cured hydrogels (5% acrylic acid) with lysine hydrochloride. [a] Equivalent determined by theoretical acrylic acid content employed during hydrogel synthesis.**

Coupling experiments were carried out with 5 wt% acrylic acid hydrogels and lysine hydrochloride. In all cases a 2:1 molar ratio of lysine hydrochloride to acrylic acid groups was used to determine a suitable coupling procedure. Activation in both aqueous and DMF media was considered as well as coupling in different buffer systems (sodium acetate buffer at pH 5.5 and phosphate buffered saline (PBS) at pH 8.5). The effect of the length of time allowed for coupling was investigated as well as temperature effects. The different approaches trialled are detailed in Table 4.1.

For each reaction, the hydrogels produced were washed for one week in water which was changed twice daily to remove any unreacted lysine or remaining activation reagents. The coupling efficiency was analysed by TNBS assay and the water used for the washing stages was also analysed by TNBS assay to determine whether any lysine was present.

The initial approach for the modification of poly(NVP-co-DEGBAC-co-AA) hydrogels with lysine was to carry out both the activation and coupling steps in aqueous media. In aqueous environments the hydrogel is fully swollen, and it is thought that a fully swollen hydrogel would enable maximum accessibility of the activation reagents and peptide to the acrylic acid moieties present within the hydrogel. Formulations 1-4 (Table 4.1) utilised activation by EDC with NHS in water at 0°C for 24 hours. This reaction was carried out at 0°C to minimise the effect of the competing hydrolysis reaction. The activated hydrogels were then coupled to lysine under different conditions. A buffer solution of sodium acetate at pH 5.5 was investigated first in formulations 1 and 2 at 0°C for 24 hours, and 72 hours respectively. Coupling efficiencies of 0 % and 6.4 %, analysed by moles of lysine, were observed for formulations 1 and 2 respectively (Figure 4.8) and it is expected that the extremely low efficiency of this reaction is due to hydrolysis of the activated esters before reaction with lysine.

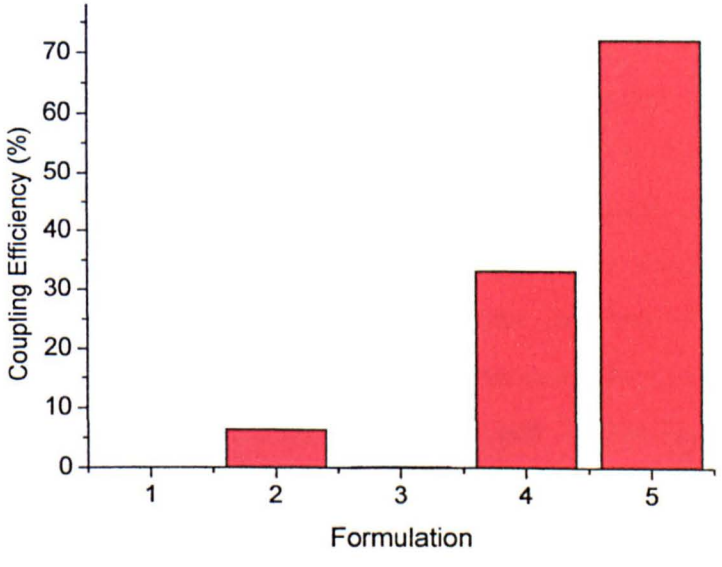


**Figure 4.8: Results of coupling experiment with lysine hydrochloride**

An alternative buffer system of 0.01 M PBS at pH 8.5 was also investigated. Activation was again carried out by EDC and NHS in water at 0°C, followed by coupling in the PBS buffer at 0°C for 24 and 72 hours for formulations 3 and 4 respectively. The use of PBS buffer at pH 8.5 led to an improvement in the coupling efficiency; 0.13% and 33.4% of the theoretical coupling possible was observed for formulations 3 and 4 respectively (Figure 4.8). From these results it is obvious that this coupling approach is more successful that the sodium acetate buffer at pH 5.5 and it was therefore used in subsequent trials. Coupling of lysine to the hydrogel in either buffer showed that after 24 hours a very low efficiency of the coupling was achieved but after 72 hours an increase in the coupling was observed. It is thought that this is, in part, due to temperature of the reaction mixture over the reaction period. In order to agitate the samples during the reaction the coupling reactions were carried out in dewars of ice on an orbital shaker. For those reactions taking place over 24 hours the solutions were maintained at 0°C for the entire reaction whereas for the 72 hour reactions the solutions remained at 0°C for the first 24 hours and then warmed up very gradually over the next 48 hours, reaching room temperature by 72 hours. It is suggested that the observed increase in coupling may occur because the optimum temperature for the reaction of lysine with the hydrogel with minimal hydrolysis competition is between 0°C and room temperature.

The maximum coupling achieved through activation with EDC and NHS was 33.4 % for formulation 4. This relatively low coupling is expected to be due to hydrolysis of the activated ester. It was therefore decided that the PBS coupling reaction would be combined with activation by DCC and NHS in DMF in order to reduce the hydrolysis reaction. The results of this trial, formulation 5, showed a greatly increased coupling efficiency at 72.2 % (Figure 4.8). This result suggests that hydrolysis limited the efficiency of this reaction in previous formulations. As formulation 5 provided significantly improved results it was decided that these conditions would be employed for subsequent reactions between the hydrogels and lysine peptides KKK and KKKKKK.

### 4.3.3 Coupling Trial with Lysine Peptides – Effect of Peptide Sequence Length

Hydrogels were modified with either trilysine or hexalysine peptide sequences using the optimised procedure determined in section 4.3.2. It was thought that this study could provide information about the effect of the length of the peptide sequence attached on the coupling reaction.

The 5 wt% and 2 wt% acrylic acid hydrogels were modified with KKK and KKKKKK peptide sequences. The peptide sequences were coupled to the polymer sheets in their crude form. Coupling efficiency was analysed indirectly by TNBS assay of the remaining peptide in the coupling solution after coupling and the washing solutions. For each different peptide, the results were determined from a calibration curve produced for that specific peptide.

The polymer-peptide conjugates were produced using the optimised procedure determined in the lysine hydrochloride trial: activation of the hydrogel with DCC and NHS in DMF followed by coupling of the peptide sequences in 0.01 M PBS buffer at pH 8.5 at 0°C for 72 hours. The results obtained are provided in table 4.2.

| Formulation | 1 | 2 | 3 | 4 |
|---|---|---|---|---|
| NVP (%) | 93 | 96 | 93 | 96 |
| Acrylic acid (%) | 5 | 2 | 5 | 2 |
| DEGBAC (%) | 2 | 2 | 2 | 2 |
| Peptide | KKK | KKK | KKKKKK | KKKKKK |
| Peptide incorporation (mg/g polymer) | 135.5 | 36.5 | 134.0 | 66.9 |
| Coupling Efficiency (%) | 48.5 | 32.6 | 25.1 | 30.6 |

**Table 4.2: Coupling conditions and results for tri- and hexa-lysine**

The results show that coupling of peptide to the hydrogels was observed in all four reactions but with varying efficiency. The highest coupling efficiencies, analysed by theoretical molar quantities of peptide reacting with acrylic acid moieties, were obtained for the polymers coupled to KKK, being 48.5% and 32.6% for 5 wt% AA polymer and 2 wt% AA polymer respectively. Lower coupling efficiencies of 25.1% and 30.6% were observed for the 5 wt% polymer and 2 wt% polymer coupled to KKKKKK. Analysis of subsequent washing steps after coupling showed that no peptide was present so it can be assumed that all peptide removed from the coupling solutions has been covalently bound to the hydrogels.

Coupling efficiencies for the KKK and KKKKKK peptides (Figure 4.9) are significantly lower than the 72.2% efficiency achieved under the same conditions for lysine (Figure 4.8). It is hypothesised that this is due to a steric effect as the single amino acid is bound with higher efficiency than the tripeptide, which is also bound more efficiently than the hexapeptide.

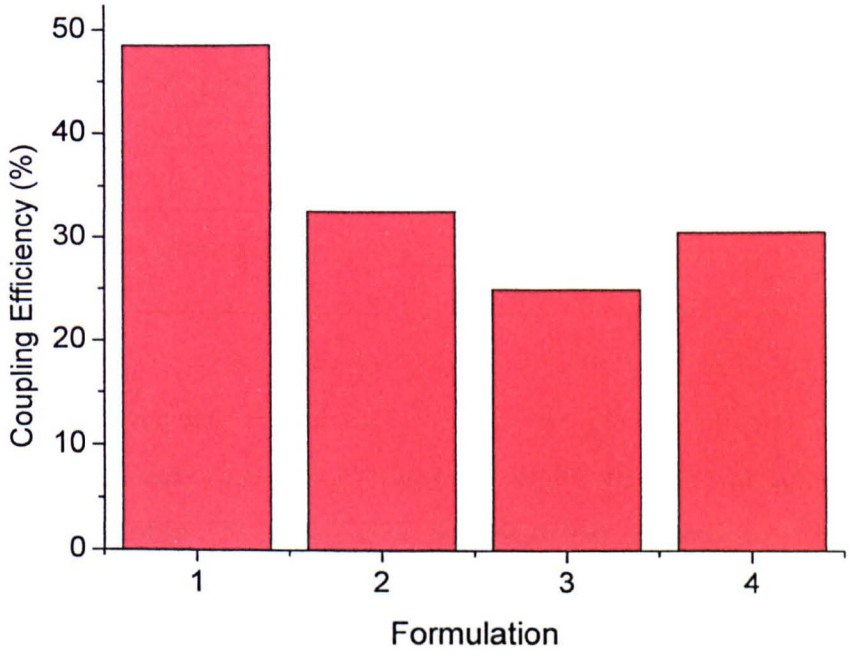


**Figure 4.9: Results of coupling trial with tri- and hexa-lysine**

Although it was not investigated further within this project, due to time and cost constraints, it is expected that a larger excess of peptide would increase coupling efficiency. Another possible improvement of this technique would be to carry out the coupling procedure in DMF as well as the activation step. Changing the activation step from water to DMF gave a significant increase in coupling efficiency and it is expected that this would also be observed in the coupling step as this would minimise the possibility of a hydrolysis side reaction.

### 4.3.4 Peptide Coupling to UV-Cured Hydrogels

Coupling of peptides to thinner UV-cured hydrogels for biological application was expected to have a number of advantages over the thicker thermally-cured hydrogels. Firstly, the thinner UV-cured gels have better mechanical properties and are easier to handle and so would be expected to be preferable for cell culture. Secondly, producing thinner functionalised hydrogels would require less monomer, peptide and reagent. This is a significant cost reduction given that it is necessary to use excess peptide. Finally, in order for coupling to occur, the peptide must diffuse through the hydrogel. For the thinner hydrogel it would be expected that the peptide could diffuse to the centre of the hydrogel more easily and so coupling may be improved.

Results from peptide coupling to thermally-cured hydrogels showed that the optimum coupling procedure involved activation of the hydrogel with DCC and NHS in DMF followed by coupling of the peptide sequences in 0.01 M PBS buffer at pH 8.5 at 0°C for 72 hours. It was also determined that trilysine coupled with a higher efficiency than hexalysine and that a higher percentage yield of coupled peptide was achieved with 5% acrylic acid hydrogel than 2% hydrogel. It was therefore decided that 5% acrylic acid UV-cured hydrogels would be coupled with two tripeptides, trilysine (KKK) and triarginine (RRR). It is the peptide-hydrogel conjugates resulting from this study that were taken forward for heparin and VEGF binding and cell culture experimentation and any further discussion of peptide-hydrogel conjugates refers to the UV-cured hydrogels produced in this manner.

The coupling efficiency and final peptide loading was determined quantitatively through indirect analysis with TNBS as described previously. Obviously, trilysine, a peptide with four amine groups which interact with TNBS, produced a significant colour change, from yellow to orange. This is observed for the peptide in solution as well as when coupled to the hydrogel, as even when bound to the hydrogel three amine groups are still available to react with TNBS. This strong colour change also allowed qualitative confirmation of the presence of lysine peptide on the polymer as shown in figure 4.10. Here it is possible to see the yellow colour of the TNBS solution in the swollen unfunctionalised polymer and the orange colour observed for the lysine-functionalised hydrogel after reaction with TNBS. The indirect approach to quantify peptide loading was also possible for the triarginine peptide as it is able to react with

TNBS via the amine-terminus of the triarginine in solution. It was not possible to qualitatively observe arginine coupling within the solid hydrogel with TNBS as this coupling uses the amine-terminus of the RRR peptide and therefore no significant colour change is observed.


**Figure 4.10: Qualitative assessment of lysine content of hydrogels by TNBS analysis. (a) acid-functionalised hydrogel (PNDA) (b) RRR-functionalised hydrogel (PNDRRR) (c) KKK-functionalised hydrogel (PNDKKK). Orange colour indicates the presence of primary amine functionality of lysine.**

In order to visualise the coupling of triarginine to the polymer an alternative colorimetric assay was undertaken. In this case the Weber modification[296] of the Sakaguchi reaction[297] for the quantitative determination of arginine was employed. Using this method, a colour change from a beige/yellow to dark red (Figure 4.11) is generated by reaction of guanidine derivatives with α-naphthol and sodium hypobromite and is stabilized with urea. Weber's modification of the Sakaguchi reaction produces a coloured complex upon interaction with arginine which undergoes initial rapid decay and therefore requires measurement exactly 20 minutes after the addition of the hypobromite reagent to ensure reproducible results[298]. Due to the importance of time in this method, it is used only qualitatively in this study as a means of confirming the presence of arginine in the hydrogel. It was decided to continue using TNBS as the quantitative assay for both peptide sequences by the indirect measurements as this method is considerably less sensitive to time.

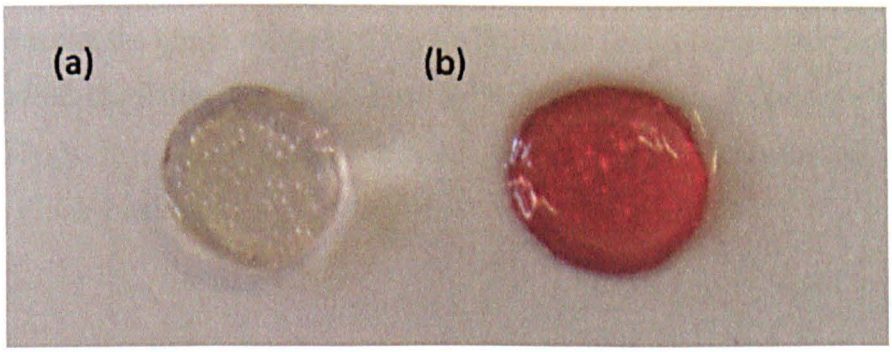


**Figure 4.11: Qualitative assessment of arginine content of hydrogels. (a) acid-functionalised hydrogel (PNDA) (b) RRR-functionalised hydrogel (PNDRRR). Red colour indicates the presence of arginine.**

For cell culture experimentation, peptide loading of the hydrogels was carried out using batches of 20 or 40 polymer discs. These were synthesised and washed before being stored in ethanol prior to use. Peptide content was analysed prior to transfer to the tissue engineering laboratory. In total five batches were utilised for cell culture with an average peptide loading shown in Table 4.3. Average coupling efficiencies of 49% for the trilysine hydrogel and 59% for the triarginine hydrogels were achieved.

| Peptide Sequence | Peptide Loading | |
|---|---|---|
| | (mg/mg hydrogel) | (Coupling efficiency (%)) |
| KKK | 0.14 ± 0.01 | 48.83 ± 3.36 |
| RRR | 0.20 ± 0.01 | 59.03 ± 1.64 |

**Table 4.3: Peptide loadings achieved for KKK- and RRR-functionalised hydrogels. Results shown are an average of 5 results ± SEM (2 d.p.)**

It was discussed previously that the poly(NVP-co-DEGBAC-co-AA) copolymer hydrogel could be dissolved by concentrated sodium hydroxide solution due to cleavage of the carbonate groups in the crosslinker producing linear polymer chains. It was observed after peptide functionalisation that hydrogels functionalised with the trilysine sequence were no longer soluble in concentrated sodium hydroxide. This was not observed for the triarginine-functionalised material which was still readily dissolved in the base. It is thought that this may be due to the lysine sequence forming crosslinks between the acid groups on the hydrogel or by reacting with the carbonate-based crosslinker[299]. The resulting crosslinks would not be expected to be affected by the sodium hydroxide and explains why the resulting hydrogels do not dissolve in an alkali solution. This may be one explanation for the lower coupling efficiency observed for the trilysine hydrogel. This effect of the lysine peptides reacting via two or more amine groups could make the direct method of the TNBS assay less accurate, but would not be expected to affect the indirect assay, and so the indirect assay was utilised for all peptide coupling analysis. It is also suggested that this lysine crosslinking may also affect the heparin and VEGF binding.

### 4.3.5 XPS and ToF-SIMS Assessment of Peptide Binding

*X-ray Photoelectron Spectroscopy (XPS)*

X-ray photoelectron spectroscopy (XPS) is a surface analysis technique commonly used to characterise biomaterials. It is able to provide information on both the elemental composition of the material and the binding environments of the elements[300], allowing understanding of the functional groups present. XPS spectra are produced when the atoms in a sample absorb X-rays and subsequently eject core and valence photoelectrons. The photoelectrons emitted have energies which are specific to each element, and furthermore, the energy of the photoelectrons emitted can also provide information about the chemical state of the element[301]. The ability of XPS to analyse both elemental composition and functionality makes this technique well suited for this project and it was therefore employed to investigate changes in the surface composition of the hydrogels upon peptide functionalisation and heparin binding. It is important to remember that XPS is an ultrahigh vacuum (UHV) technique and so requires the sample to be dry, which may affect the properties of the hydrogel. XPS is also a surface analysis technique and is therefore only able to sample material to a depth of 10 nm or less[302]. It is assumed that peptide functionalisation would occur throughout the hydrogel (this is in agreement with visual examination of colorimetrically-analysed hydrogels) and so the information provided by this surface technique for peptide functionalisation is considered qualitative.

The $C_{1s}$ profile (Figure 4.12) was utilised to analyse the effects of peptide incorporation through consideration of the overall peak shape and the different carbon environments that result in a number of overlapping peaks. Figure 4.12(a) shows the curve fit of the acid-functionalised hydrogel (PNDA). From this curve fit we can see that there are four types of binding environments distinguishable, the C-C (~285 eV), C-O/C-N (~286 eV), C=O/CNO (~288 eV) and COOH (~289 eV). In the acid-functionalised hydrogel, these peaks appear in a proportion of 50% for C-C bonds, 36% for C-O or C-N bonds, 12% for the CNO amide functionality and 2% for the acidic COOH group. The relative ratios of these peaks in the acid hydrogel, and the changes observed in these ratios upon reaction with peptide sequences, can be utilised to quantify the extent of peptide incorporation into the hydrogel.

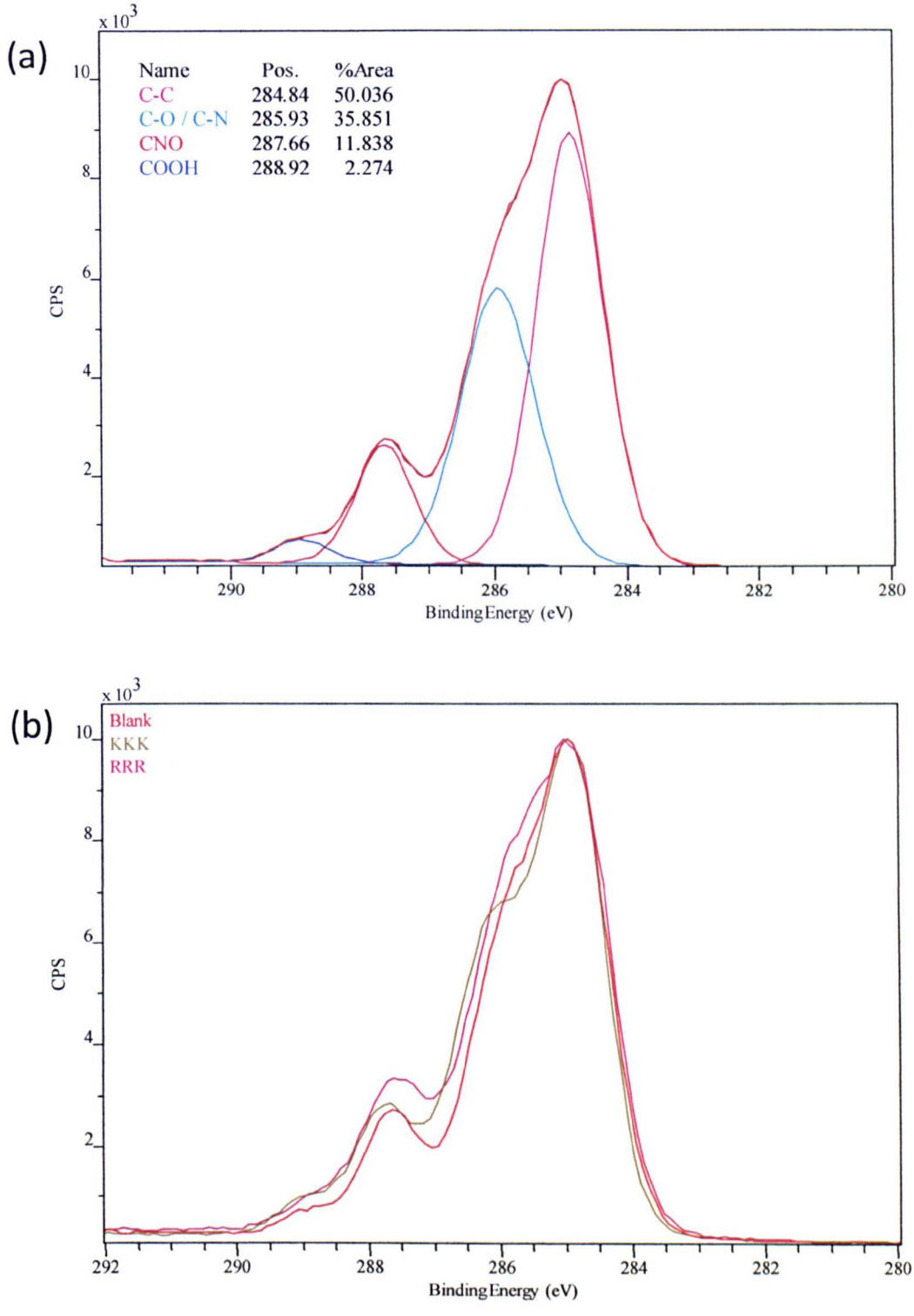


**Figure 4.12: $C_{1s}$ spectra of acrylic acid- and peptide-functionalised hydrogels. A) $C_{1s}$ spectrum of acrylic acid-functionalised hydrogel with assignment of peak areas (see colour definitions). B) Overlaid $C_{1s}$ spectra of acrylic acid- (PNDA) (--), KKK- (PNDKKK) (--) and RRR- (PNDRRR) (--) functionalised hydrogels.**

Incorporation of both trilysine (KKK) and triarginine (RRR) peptide sequences results in a reduction in the percentage of aliphatic carbon signal, from 50% to 46% and 38% for KKK and RRR respectively. The most significant change for the trilysine hydrogel (PNDKKK) is an increase from 36% to 39% in C-O or C-N bonds, which is expected to be due to C-N bonds present in the amine side chain of lysine. For the triarginine hydrogel (PNDRRR) the number of C-O/C-N bonds, again expected to be C-N bonds, increases from 36% to 45%. Such a large increase would be expected when considering the three nitrogen atoms per guanidinium group in arginine. In the triarginine hydrogel it is also possible to observe a 2% increase in amide functionality, as would be expected for the incorporation of a tripeptide.

| Hydrogel functionality | C-C | C-O/C-N | CNO | COOH |
|---|---|---|---|---|
| Acid | 50.0 | 35.9 | 11.8 | 2.3 |
| KKK | 46.5 | 38.9 | 11.2 | 3.4 |
| RRR | 38.2 | 44.9 | 14.0 | 2.9 |

**Table 4.4: Percentage of carbon environments observed for acid- and peptide-functionalised hydrogels in XPS study**

***Time of Flight Secondary Ion Mass Spectrometry (ToF-SIMS)***

Time of Flight Secondary Ion Mass Spectroscopy (ToF-SIMS) was utilised as a complementary analytical technique to identify the presence of both triarginine and trilysine on the surface of the hydrogels. ToF-SIMS is a mass spectrometry technique, able to analyse both the elemental and chemical compositions of the solid surface. This technique is highly sensitive, with a lateral resolution of approximately 50 nm, and a sampling depth of 10-20Å[303]. In principle, it has the ability to detect all elements and isotopes in the periodic table.

SIMS consists of a sputtering process[304] which involves bombarding the surface of a material with ions, which causes motion of the atoms in the sample, leading to bond cleavage. These fragments then have sufficient energy to overcome the surface binding energy and are then able to leave the material surface as neutral atoms and molecules, electrons and ions. A fraction of these sputtered fragments are ionised to produce secondary ions, the mass to charge ratio (m/z) of which can then be analysed to produce either positive or negative SIMS spectra.

The capability of SIMS to analyse the chemical composition of a material makes this technique ideal for observing surface modification (in this case with tripeptides). Consideration of the $C{\equiv}N^-$ peak in the negative ToF-SIMS spectra of the acid-, lysine- and arginine-functionalised hydrogels shows an increase in intensity of this species as the poly(NVP-co-DEGBAC-co-AA) material is functionalised with lysine and arginine. The intensity of this peak is highest in the arginine-containing hydrogel, as would be expected when considering the high nitrogen content of this amino acid.

Research by Samuel at al[305] has provided a comprehensive collection of poly(amino acid) spectra acquired with a ToF-SIMS instrument using a $Cs^+$ primary ion source. Considering these spectra and comparing to a table of features for the amino acids of interest (Table 4.5), it is possible to interpret the positive SIMS spectra produced in this study of the hydrogels, before and after peptide functionalisation, to confirm the presence of specific amino acids.

| Amino acid | Fragment | Mass |
|---|---|---|
| Lysine | $CH_4N$ | 30.03 |
| | $C_2H_6N$ | 44.05 |
| | $C_3H_6N$ | 56.05 |
| | $C_5H_{10}N$ | 84.08 |
| Arginine | $CN_3H_5$ | 59.05 |
| | $C_4H_8N$ | 70.07 |
| | $C_4H_{10}N_3$ | 100.08 |
| | $C_5H_{11}N_4$ | 127.10 |

**Table 4.5: Summary of features of peptide fragments in ToF-SIMS as reported by Samuel et al[305]**

An important consideration when analysing the SIMS spectra for these samples is the similarity in elemental content between all polymers, especially the trilysine- and triarginine-functionalised materials. In all cases, the bulk of the material is identical, and the hydrogels differ only in their functionality. For both arginine and lysine the expected fragments used to identify these peptides are based around combinations of carbon, hydrogen, nitrogen and oxygen. As the polymer also consists of carbon, hydrogen, nitrogen and oxygen, it is possible that these fragments also exist within the bulk polymer and could be produced upon sputtering or could be formed by combination of different fragments. In these cases it is not possible to distinguish the presence of a peptide from the presence of a characteristic peak, as the peak may also be present in the unfunctionalised material. Therefore, it is necessary to confirm the

presence of the peptide by the increase in intensity of the relevant fragment peaks from the acid-functionalised hydrogel relative to the peptide functionalised hydrogel.

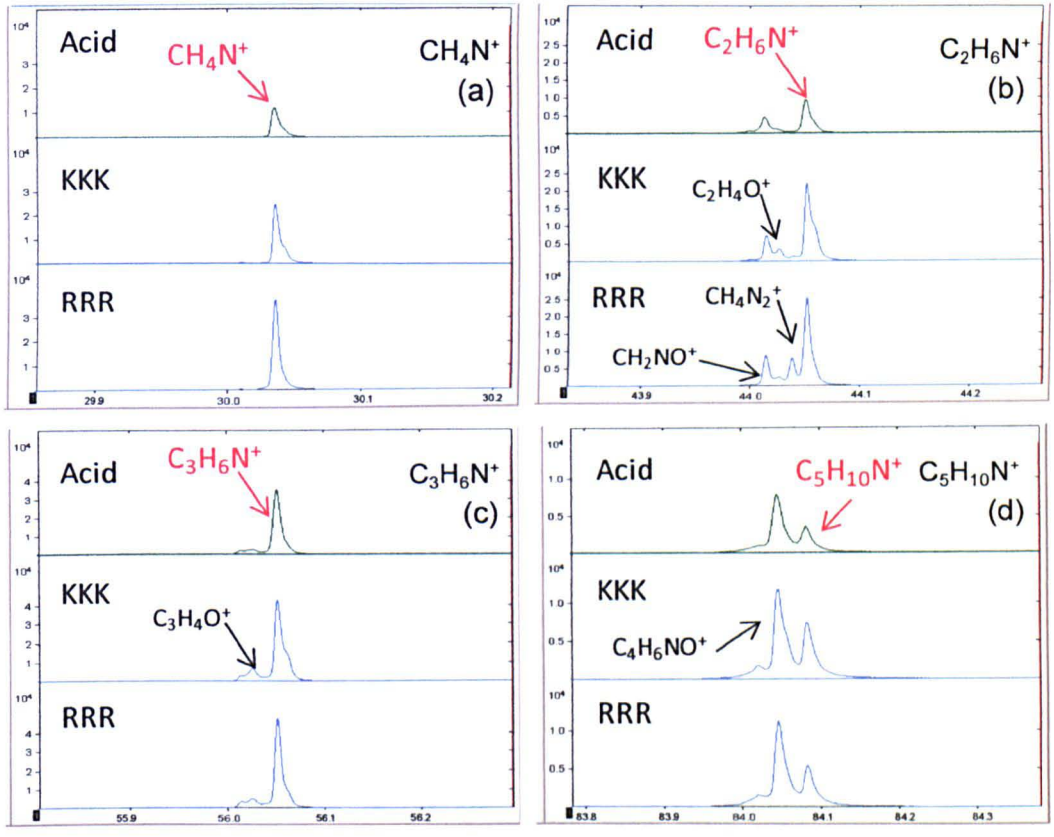


**Figure 4.13: ToF-SIMS spectra of acid-functionalised (Acid), KKK-functionalised (KKK) and RRR-functionalised (RRR) hydrogels showing mass fragments that are expected to be present in a lysine-containing material. The fragment peaks of interest are labelled in red.**

Although there are no unique peaks for lysine, fragment peaks at 30.03, 44.05, 56.05 and 84.08, for $CH_4N^+$, $C_2H_6N^+$, $C_3H_6N^+$ and $C_5H_{10}N^+$, respectively, are formed preferentially under the conditions of the SIMS experiment when lysine is present[305]. When considering these fragments it is observed there are increases in intensity for all four fragment peaks for the lysine-functionalised hydrogel in comparison to the acid-functionalised hydrogel (Figure 4.13). This is as expected and confirms the presence of lysine on the material. These peaks are also seen in the spectra of the triarginine-functionalised hydrogel, and are again at a higher intensity than those observed in the acid-functionalised material, despite no lysine being present. This is as would be expected due to the similarities between lysine and arginine and the high nitrogen content of the guanidine group.

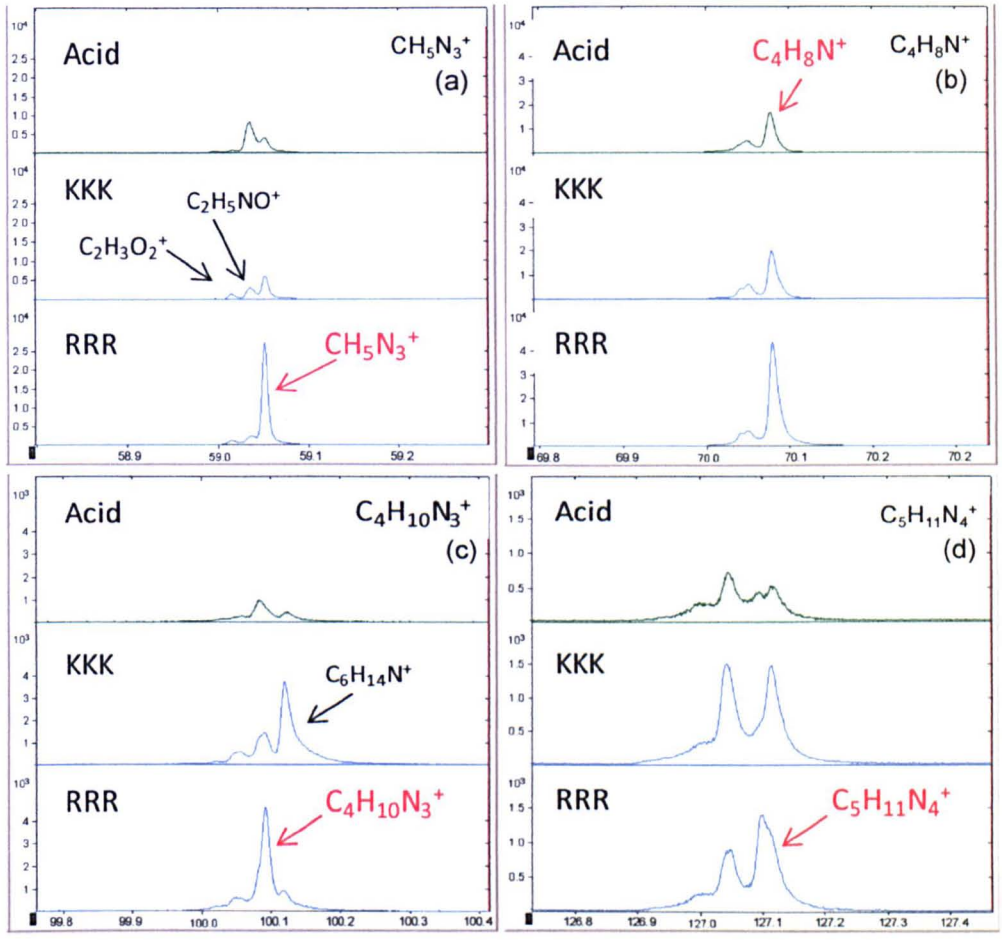


**Figure 4.14: ToF-SIMS spectra of acid-functionalised (Acid), KKK-functionalised (KKK) and RRR-functionalised (RRR) hydrogels showing mass fragments characteristic for arginine. The characteristic fragment peaks are labelled in red.**

The high nitrogen content of the arginine side chain allows for a more conclusive result for the presence of arginine. This is because a number of the characteristic fragments have a higher number of nitrogen atoms, and so are likely to be fragments that are only found in significant quantities in arginine-containing species. When considering the spectra for the acid-, trilysine- and triarginine hydrogels (Figure 4.14), the strongest signals were obtained for the arginine-containing hydrogel. This is especially noticeable for the peaks at mass 59.05 and 70.07, due to $CH_5N_3^+$ and $C_4H_8N^+$, respectively. The significant increase in intensity in these two fragments for the triarginine polymer, compared to the acid- and trilysine-functionalised hydrogel spectra, confirms the presence of arginine on the hydrogel. The spectra at masses 100.08 and 127.1, due to $C_4H_{10}N_3^+$ and $C_5H_{11}N_4^+$, respectively, also show differences in the size, shape and number of peaks in the area of interest, thereby confirming that the hydrogels have been successfully functionalised.

## 4.4 Summary of Results for Peptide-Functionalised Hydrogels

Poly(NVP-co-DEGBAC) and poly(NVP-co-DEGBAC-co-AA) hydrogels were synthesised by both thermal and UV polymerisation and analysed for residual monomer concentration, equilibrium water content and by NMR. The thinner hydrogels produced by UV polymerisation were selected for further investigation as they required less peptide for functionalisation and were easier to handle for cell culture studies.

An optimised peptide coupling procedure of activation by DCC and NHS in DMF at room temperature for 24 hours, followed by peptide coupling in PBS (pH 8.5) at 0°C for 72 hours, resulted in the synthesis of trilysine- and triarginine-functionalised poly(NVP-co-DEGBAC-co-AA) hydrogels. Peptide loadings of 0.14 g/g hydrogel and 0.20 g/g hydrogel for lysine and arginine respectively were determined by TNBS analysis. The presence of peptides was confirmed qualitatively by colorimetric analysis, XPS and ToF-SIMS.

The peptide-functionalised hydrogels were shown to contain no residual monomer and to have suitable mechanical properties and so were analysed further for heparin and VEGF binding as well as cell culture experiments.

# 5 Heparin and VEGF Binding Analysis

## 5.1 Heparin Binding Studies

Once hydrogels had been produced and coupled with peptides, the next stage of the process was to analyse the ability of the resulting material to bind heparin. The heparin chosen for this study was the sodium salt from porcine intestinal mucosa. This is a natural unfractionated heparin and supplier information (Sigma) states that the majority of the heparin chains lie in the range of 17,000 to 19,000 Da, although some chains may range from 6,000 to 30,000 Da. The heparin-binding ability of the hydrogels was analysed both quantitatively using fluorescently-tagged heparin and qualitatively by X-ray photoelectron spectroscopy (XPS). For both analytical techniques, the binding and subsequent washing steps to remove unbound heparin were carried out in PBS in an attempt to reproduce an environment similar to that which would be experienced *in vivo*. It was hypothesised that functionalising the hydrogels with peptide would increase the amount of heparin bound by the hydrogels. As discussed in section 4.1.2, Fromm et al[244] found that arginine synthetic peptides bind heparin 2.5 times more strongly than lysine, so it was expected that the RRR hydrogel would be the most successful for heparin binding.

### 5.1.1 Quantitative Fluorescent Heparin Study

The binding of heparin to the functionalised hydrogels was analysed quantitatively through a fluorescent binding study†. Heparin was tagged with fluorescein-5-thiosemicarbazide in a two step reaction. Firstly, oxidation of the uronic acid moieties of heparin were oxidised to produce an aldehyde[306], which subsequently reacted in a condensation reaction with the carbazide functionality of fluorescein-5-thiosemicarbazide to form a covalent hydrazone linkage[307] (Figure 5.1).

† This work was carried out together with a MSc student and parts of this heparin-binding data was submitted in the taught MSc report of D. Sun in 2008. However some errors in the data analysis became apparent after the submission and the data presented have been corrected for submission in this thesis.

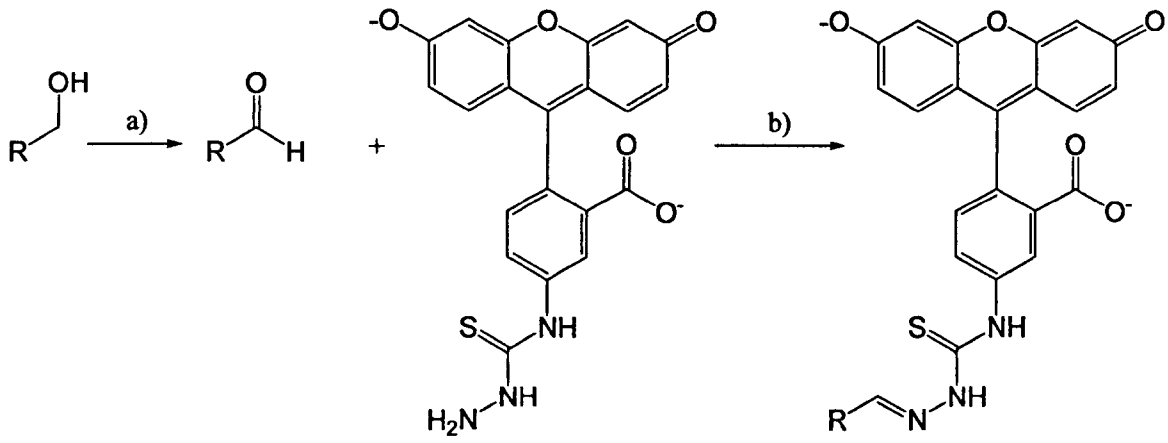


**Figure 5.1: Reaction scheme for fluorescein tagging of heparin a) oxidation of alcohol to aldehyde and b) subsequent condensation reaction between aldehyde and fluorescein-5-thiosemicarbazide[307]**

A fluorescence study was then carried out with the fluorescein-tagged heparin to quantitatively determine the heparin-binding ability of the acid-functionalised and peptide-functionalised hydrogels.

Each hydrogel was exposed to a solution of fluorescent heparin in 0.1 M sodium phosphate buffered saline at pH 7.5 and was allowed to react over 24 hours in the dark with agitation at room temperature. Each hydrogel was analysed in triplicate and all solutions for analysis were stored at 4°C in the dark until use. A number of washes were carried out to remove unbound heparin by replacing the PBS solution with fresh PBS and agitating the sample in the dark at room temperature for a set time period. The binding solutions and wash solutions were then analysed at room temperature. The binding ability of the hydrogels was then determined from these results using a calibration of fluorescein-tagged heparin at various concentrations within the required range.

Analysis of the washing solutions showed that, in all cases, no further fluorescein-tagged heparin was removed after the seventh wash. This information was then utilised when determining the heparin-binding procedure employed within the cell culture study of these materials.

The results obtained (Figure 5.2) agreed with the hypothesis that heparin would bind to basic peptide sequences and would bind most effectively with the guanidine side chain of arginine. The acid-functionalised hydrogel bound 5.2% of the heparin that it was initially exposed to, but this binding result was not very consistent, leading to a high

standard error of 3.5%. The peptide-functionalised hydrogels were shown to bind considerably more heparin, with 13.5% and 20.7% of the heparin remaining bound to the hydrogels after the wash steps for the trilysine and triarginine hydrogel respectively. These values equate to 0.030 mg, 0.077 mg and 0.117 mg of heparin binding per milligram of dry hydrogel for the acid-, KKK- and RRR-functionalised hydrogels respectively.

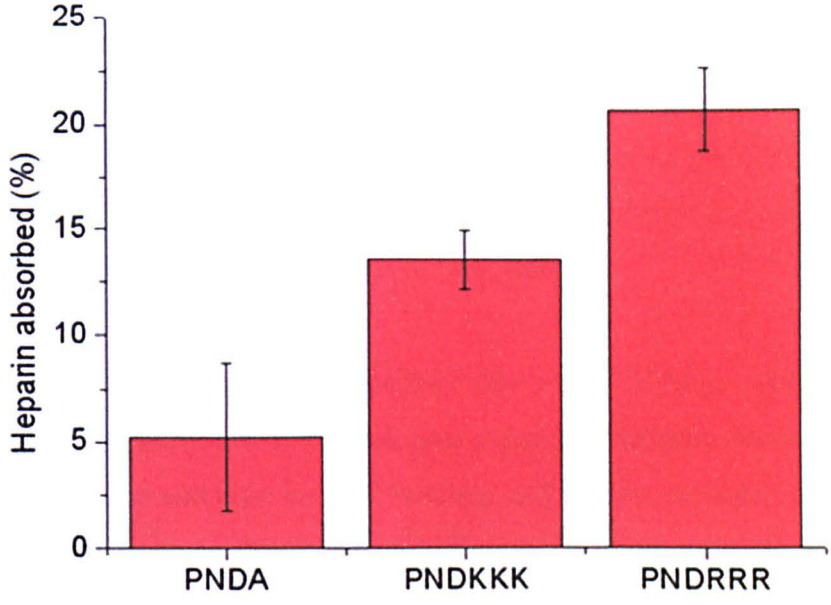


**Figure 5.2: Quantitative fluorescence study of heparin binding for acrylic acid-functionalised hydrogel, KKK-functionalised hydrogel and RRR-functionalised hydrogel. Binding data is presented as a percentage of initial heparin in solution bound to hydrogel after washing steps. Data shown is average of three results ± SEM.**

### 5.1.2 Qualitative XPS Heparin Study

X-ray photoelectron spectroscopy was employed to qualitatively confirm heparin binding to the acid- and peptide-functionalised hydrogels. In 1995, West et al[308] analysed the binding of heparin to a range of polymers to determine a method to monitor the modification of biomaterial surfaces. They showed that the presence of heparin can be confirmed by considering the oxygen, nitrogen and sulphur concentrations, as well as a change in high resolution carbon scans and the different binding states observed. Changes in $O_{1s}$ and $S_{2p}$ signals were also utilised by Steffen et al[309] to show the presence of heparin on diamond-like carbon films. More recently, Nakayama et al[310] utilised XPS spectra to analyse the $N_{1s}$ and $O_{1s}$ and the N/C and S/C elemental ratios to show heparin binding to a cationic thermoresponsive polymer. The presence of heparin was also shown through an increase in oxygen and sulphur signals as well as changes in the $C_{1s}$ peak by Meng et al[311] for polypyrrole/poly(L,L-lactide) composites, and also by Aksoy et al[312] for polyurethanes.

Three approaches have been utilised within this study. Firstly, analysis of the $S_{2p}$ spectrum, which is possible due to the sulphate content of heparin. Secondly, analysis of nitrogen content before and after heparin binding, and finally, consideration of the effect of the binding of heparin on the $C_{1s}$ spectra. Hydrogels were analysed before and after heparin binding, with both types of material undergoing washes in both PBS and water. XPS analysis was judged as only a qualitative approach to assessing the heparin binding for a number of reasons, including the surface-sensitive nature of the technique and the heterogeneity of heparin. The difficulty in determining whether heparin is absorbed evenly throughout the hydrogel and the effect that drying the hydrogel, which is necessary before XPS analysis, would have on the uniformity of heparin distribution throughout the material also meant that the results from this analysis can only be qualitative.

It was expected that the presence of heparin in the hydrogels would lead to the presence of sulphur in the XPS spectra. XPS analysis of a thick film of heparin by Robinson[313] showed heparin to contain 4.5% sulphur. Surprisingly, consideration of the spectra of acid-, lysine- and arginine-functionalised hydrogels prior to heparin binding shows that these materials contain a very low amount of sulphur. This may be due to contamination, but may also be due to background noise at such low levels and the very

large pass energy employed in this study. The presence of sulphur due to heparin was analysed by considering sulphur levels before and after heparin binding. It is obvious from the $S_{2p}$ spectra (Figure 5.3 and Table 5.1) that heparin binding with the acid-functionalised hydrogel leads to no significant change in sulphur content, suggesting that little heparin remains on this material after the washing process. A slight increase in the sulphur signal is observed for the trilysine hydrogel, showing that some heparin has been bound to this material and has remained attached throughout the washing process. A larger increase in the intensity of the $S_{2p}$ spectrum is detected after heparin binding on the triarginine hydrogel, confirming that more heparin is absorbed by the hydrogel functionalised with triarginine.

| Hydrogel | Average Sulphur Content (%) | | Average Nitrogen Content (%) | |
|---|---|---|---|---|
| | Before heparin | After heparin | Before heparin | After heparin |
| Acid-functionalised | 0.07 | 0.04 | 7.20 | 7.08 |
| KKK-functionalised | 0.03 | 0.08 | 5.90 | 4.88 |
| RRR-functionalised | 0.05 | 0.12 | 9.15 | 4.70 |

**Table 5.1: Average sulphur and nitrogen content of the hydrogels before and after heparin exposure as determined by XPS**

A change in the nitrogen content of the hydrogels was also observed upon heparin binding. Only a slight decrease in nitrogen was observed upon heparin-binding for the acid-functionalised hydrogel from 7.20% to 7.08%. A more substantial reduction in nitrogen from 5.90% to 4.88% was observed for trilysine-functionalised hydrogel and an even larger decrease from 9.15% to 4.70% was observed for the triarginine-functionalised hydrogel. This is as might be expected when considering the nitrogen content of the hydrogels and heparin. Although nitrogen is present within heparin (found to be 2% by Robinson[313]), the nitrogen content is lower within this polysaccharide than for the hydrogels, particularly the triarginine-functionalised hydrogel due to the high nitrogen content of the guanidine moiety. The decrease in nitrogen content for the trilysine- and triarginine-functionalised hydrogels therefore suggests the binding of heparin. As expected, this decrease is most significant in the triarginine-functionalised hydrogel, and is in agreement with the results of the quantitative fluorescent study and the $S_{2p}$ spectra.

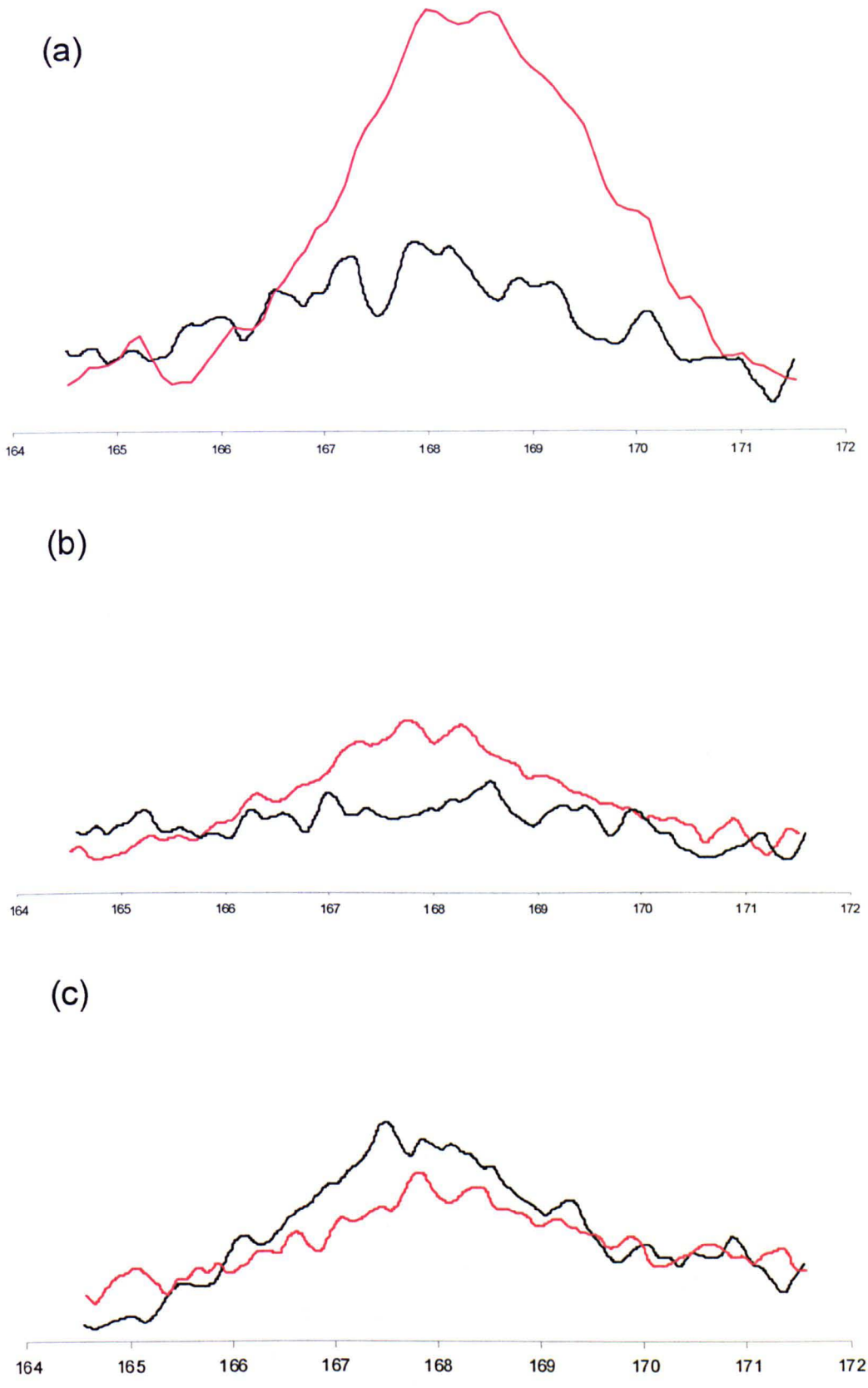


**Figure 5.3: XPS $S_{2P}$ spectra before (black) and after (red) heparin binding (a) RRR-hydrogel (b) KKK-hydrogel (c) acid-hydrogel**

In order to investigate this further, the $C_{1s}$ profiles from each of the surfaces were also analysed. The overlaid $C_{1s}$ spectra for the blank (acid-functionalised hydrogel) before and after exposure to heparin (Figure 5.5(a)) shows no significant change in ratio of carbon environments, suggesting that little or no heparin is bound in this case. Conversely, consideration of the peptide-functionalised hydrogels before and after heparin exposure (Figure 5.5(b) and Figure 5.5(c)) shows significant changes in the $C_{1s}$ spectra. In both cases, a significant decrease in the contribution from C-O/C-N bonds (~286 eV) and amide bonds (CNO, ~288 eV) is observed. This is possibly due to the surface nature of XPS. Once heparin has bound to the hydrogels this will result in the presence of heparin on the surface of the hydrogel, which is then analysed by XPS. This means that the bonds previously observed for the hydrogel may now be partially masked by the presence of heparin. The signal from the polymer bonds may therefore be reduced and signals from the heparin bonds will be seen. In the spectra produced for the hydrogels with bound heparin, the signal observed is expected to be due to heparin as well as hydrogel beneath the heparin or on the surface due to uneven coverage. After the addition of heparin to the peptide-functionalised hydrogels, all binding environments are still visible but the predominant bonds observed are now the single carbon bond as well as a significant increase in the peak shift associated with the acid (COOH, ~289 eV) bonds, as might be expected when considering the structure of a polysaccharide such as heparin (Figure 5.4). It was expected that incorporation of a polysaccharide would not result in a reduction in C-O bonds present but this was observed. It is suggested that this may occur because the C-O bonds and C-N bonds are observed at the same energy (~286 eV) and a significant reduction in C-N bonds would be expected from the high number of C-N bonds in a peptide-functionalised poly(NVP-co-DEGBAC-co-AA) hydrogel, in agreement with the decrease in nitrogen content observed upon heparin binding.

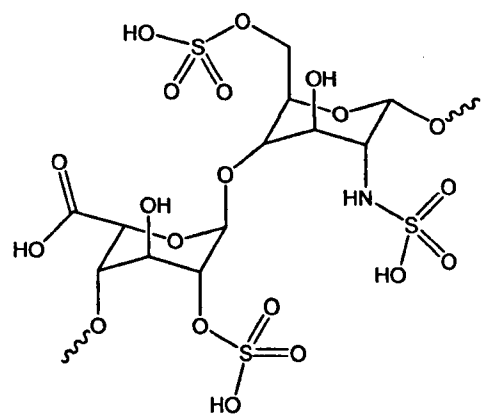


**Figure 5.4: Major repeating unit of heparin[283]**

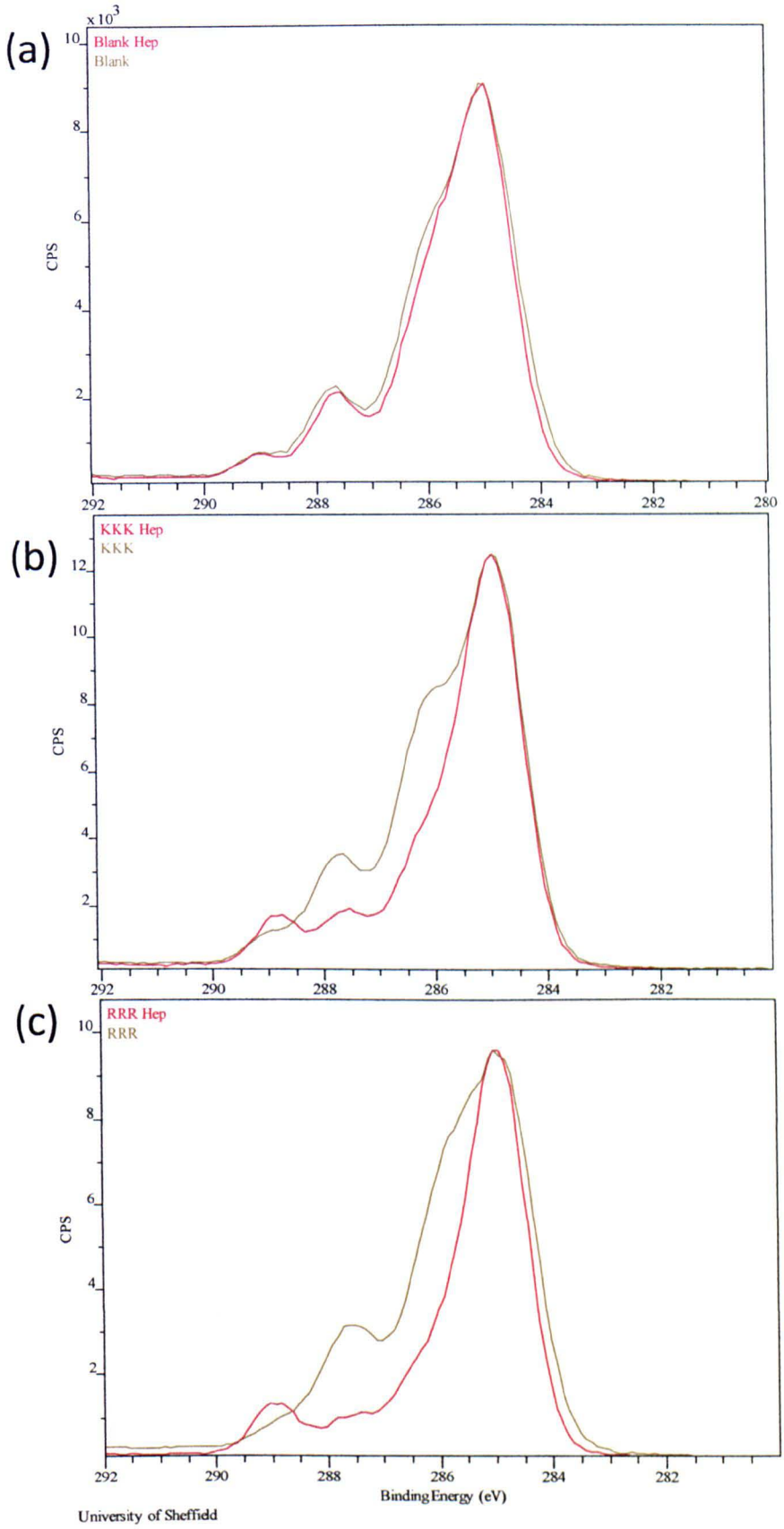


**Figure 5.5: XPS $C_{1s}$ spectra of a) acrylic acid-, b) KKK- and c) RRR-functionalised hydrogels before (--) and after (--) exposure to heparin**

### 5.1.3 Conclusion of Heparin Binding Studies

Heparin binding was analysed by a fluorescence study and XPS. Both analytical approaches were in agreement that functionalising poly(NVP-co-DEGBAC-co-AA) hydrogels with basic peptide sequences leads to an increase in heparin binding.

XPS analysis showed no change in $C_{1s}$ upon heparin binding for the acid hydrogel, and therefore no change in hydrogel composition. For both the KKK- and RRR-functionalised hydrogels a significant difference in carbon environment was observed, in particular a reduction in C-O/C-N and amide bonds and an increase in acid groups. These changes were attributed to the introduction of heparin to the hydrogel. Analysis of the $S_{2p}$ spectra showed very little heparin absorption for the acid hydrogel, slightly higher heparin absorption for the KKK hydrogel and a considerably higher heparin content for the RRR hydrogel. This is in agreement with both the XPS analysis of nitrogen content, as well as the study of fluorescently-tagged heparin which showed binding capacities of 0.030 mg, 0.077 mg and 0.117 mg of heparin per milligram of dry hydrogel for the acid, KKK and RRR hydrogels, respectively. These results agree with the hypothesis that the RRR hydrogel should bind more heparin than the KKK hydrogel. In this case the KKK hydrogel bound 66% of the heparin bound to RRR hydrogel. It is thought that the difference between the KKK and RRR hydrogels is due to the different affinities for heparin but also might be affected by the lysine-bridging observed in the KKK hydrogels (as discussed in Section 4.3.4).

These studies confirmed that the peptide-functionalised hydrogels are able to bind heparin and so were further analysed for VEGF binding and release.

## 5.2 VEGF Binding and Release Study

Analysis of the binding and release capacity of the hydrogel discs for VEGF was carried out using an Enzyme-Linked ImmunoSorbent Assay (ELISA). It was hypothesised that, due to the considerably higher heparin loading observed for the RRR-functionalised hydrogel, this hydrogel would bind the highest quantity of VEGF.

In this experiment, four types of polymer, poly(NVP-co-DEGBAC) (PND), poly(NVP-co-DEGBAC-co-AA) (PNDA), KKK-functionalised poly(NVP-co-DEGBAC-co-AA) (PNDKKK) and RRR-functionalised poly(NVP-co-DEGBAC-co-AA) (PNDRRR), were analysed in duplicate to determine how much VEGF could be bound to the material and then released over a 72 hour time period. Heparin was first bound to the hydrogel discs by soaking them in a 1 mg/ml heparin solution for 24 hours at room temperature before washing off any unbound material. VEGF binding was then carried out by placing each disc into a solution containing 100 ng VEGF in PBS in a sample vial which had been preblocked with BSA. The heparin-bound hydrogel and VEGF were allowed to bind with gentle agitation for 24 hours at 4°C. The VEGF solution was then removed from the hydrogel and stored at -20°C until analysis. Three washes were carried out at 4°C to remove unbound protein by the addition of an aliquot of PBS, which was removed each time after 30 minutes of gentle agitation. A release study at 37°C was then carried out by the addition of PBS aliquots containing 1% BSA as a protein stabiliser, mimicking the environment experienced within cell culture. The PBS aliquots containing 1% BSA were removed and replaced with fresh PBS containing 1% BSA at defined time intervals. The time intervals studied after the three washes were then 30 minutes, 1 hour, 6 hours, 12 hours, 24 hours, 48 hours and 72 hours. All aliquots were stored at -20°C until the end of the study and were then analysed by a Quantikine® Human VEGF ELISA kit.

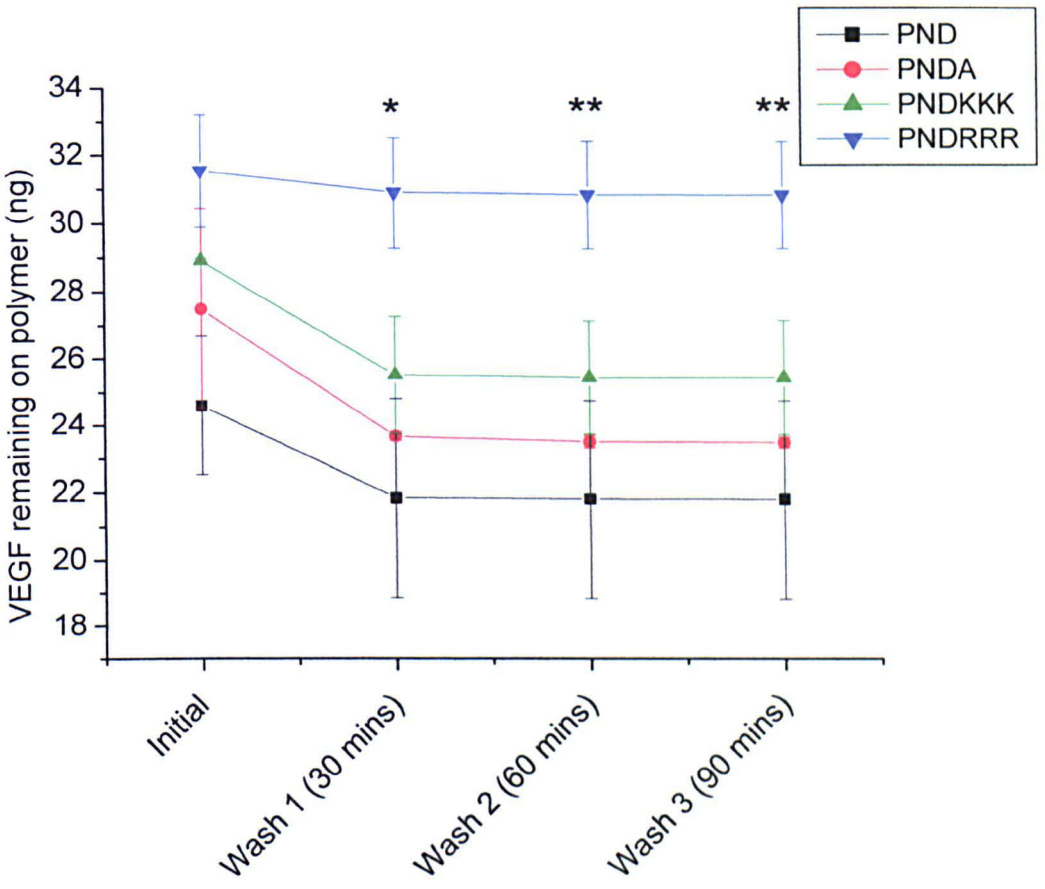


**Figure 5.6: Amount of VEGF initially adsorbed by the hydrogels and the amount of VEGF remaining attached to the hydrogel after each of the three wash steps at 4°C. Measurements expressed as mean ± 95% confidence level. (n = 2). Significance was assessed using one-way ANOVA with post-hoc Tukey analysis in comparison to non-functionalised PND hydrogel (*p < 0.05, **p < 0.01, ***p < 0.001)**

Analysis of VEGF remaining in the coupling solution, after initial exposure to the hydrogel discs, and the wash solutions (Figure 5.6) showed that, as expected, the peptide-functionalised hydrogels, particularly the triarginine-functionalised hydrogel, were able to absorb a higher quantity of the VEGF. The PND and PNDA polymers were found to absorb 24.6 ng and 27.5 ng per hydrogel disc respectively, in comparison to 28.9 ng and 31.5 ng for the PNDKKK and PNDRRR materials. These values equate to binding capacities of 21.5 ng, 24.0 ng, 25.2 ng and 27.5 ng of VEGF per milligram of dry hydrogel for PND, PNDA, PNDKKK and PNDRRR respectively. After three washes at 4°C to remove unbound material it was determined that the unfunctionalised PND had retained 21.7 ng (19.0 ng/mg dry hydrogel) of the VEGF to which it was exposed, which was slightly less than the 23.5 ng (20.5 ng/mg dry hydrogel) retained by the PNDA polymer.

It is hypothesised that the acrylic acid moieties may be able to interact with the basic amino acid groups present on the protein. 25.4 ng (22.2 ng/mg dry hydrogel) of VEGF remained on the PNDKKK hydrogel. This increase is expected due to the higher heparin content in comparison to the PNDA hydrogel. Finally, for all three washes the amount of VEGF released by the PNDRRR hydrogel was significantly less than for the other material, as determined by ANOVA analysis with post-hoc Tukey, with 30.8 ng (26.9 ng/mg dry hydrogel) of VEGF remaining attached to the PNDRRR hydrogel after the wash procedure.

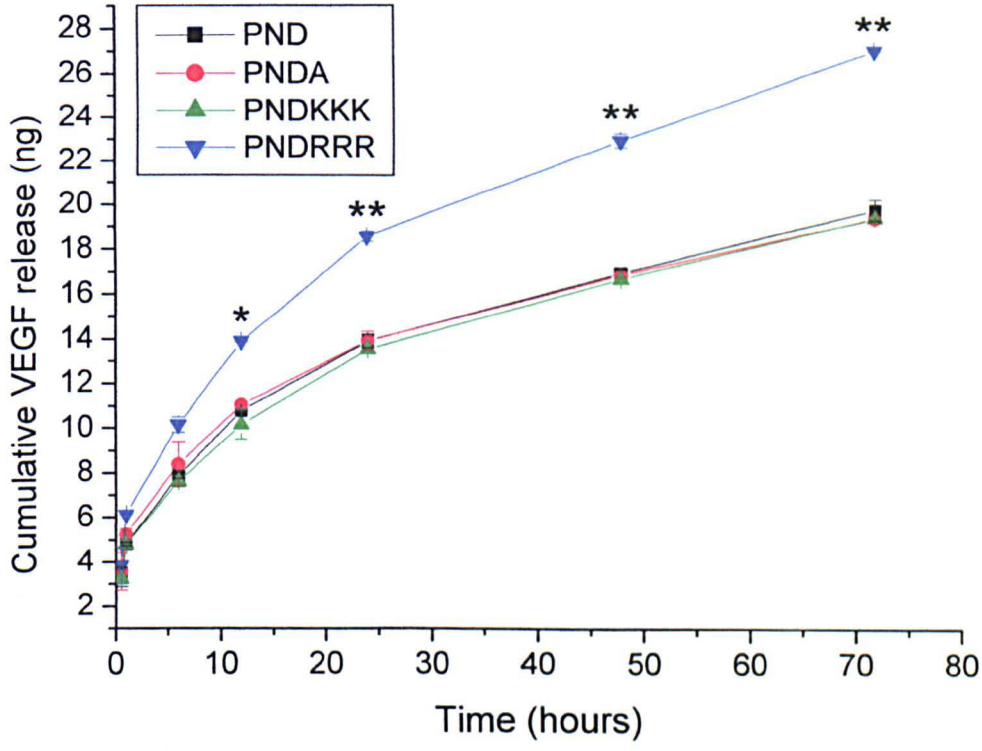


**Figure 5.7: Amount of VEGF released by the hydrogel after the wash procedure over a 72 hour time period at 37°C. Measurements expressed as mean ± 95% confidence level. (n = 2). Significance was assessed using one-way ANOVA with post-hoc Tukey analysis in comparison to non-functionalised PND hydrogel (* $p < 0.05$, ** $p < 0.01$, *** $p < 0.001$)**

Analysis of the 37°C release data (Figure 5.7) showed that for all polymers, VEGF is released over the whole time period of the study (72 hours) after the unbound VEGF had been removed in the wash steps. The VEGF release pattern is very similar for the PND, PNDA and PNDKKK hydrogels. Over this period, a total of 19.8 ng (17.3 ng/mg dry hydrogel), 19.4 ng (16.9 ng/mg dry hydrogel), and 20.1 ng (17.6 ng/mg dry hydrogel) of VEGF was released per hydrogel disc for the three polymer types

respectively, a release of 91%, 83% and 79% of the protein remaining after the wash steps for PND, PNDA and PNDKKK. At all time points analysed, the PNDRRR hydrogel was found to release more VEGF than the other polymers, with 27.0 ng (23.6 ng/mg dry hydrogel) of VEGF released per hydrogel disc in the 72 hour period, which corresponds to 88% of the protein that remained after the wash step. ANOVA with post-hoc Tukey analysis of the results revealed that this difference in release was significant after 6 hours. This result is as expected when considering the higher heparin loading of the RRR-functionalised material.

In all cases a small amount of VEGF, 1.9 ng, 4.1 ng, 5.3 ng and 3.8 ng, remained on the hydrogels after the 72 hour period for the PND, PNDA, PNDKKK and PNDRRR hydrogels respectively, equating to 1.7 ng/mg, 3.6 ng/mg, 4.6 ng/mg and 3.3 ng/mg dry hydrogel. A longer time study would be necessary to determine the time required for all VEGF to be released by the materials. It was not determined whether the heparin remains bound to the hydrogel upon VEGF release or whether the heparin is also released with the VEGF. It may therefore be useful to carry out a binding experiment, analysing both the VEGF and heparin content of the release aliquots.

The results from this study show that all of the hydrogels were able to bind and subsequently release VEGF, with the peptide-functionalised hydrogels retaining the protein most successfully, leading to an extended release. The results are in agreement with the initial hypothesis that the PNDRRR hydrogel would be able to bind and slowly release a significantly larger quantity of VEGF, which is expected to be due to the higher heparin content of the swollen hydrogel.

## 5.3 Discussion of Heparin and VEGF Binding Studies

Analysis of the PND, PNDA, PNDKKK and PNDRRR hydrogels has confirmed that when poly(NVP-co-DEGBAC-co-AA) is functionalised with basic peptide sequences an increase in heparin binding (and subsequent VEGF binding and release) is observed, in particular for the triarginine hydrogel. In all cases, around 80-90% of the bound VEGF was released over the 72 hour analysis period.

A number of research groups are also interested in the release of VEGF from biomaterials to stimulate angiogenesis, as discussed in Section 1.5. A variety of approaches have been utilised with different synthetic polymer formulations and the quantities of VEGF released are dependent on the VEGF loading employed in each study. Some of the most comparable studies are discussed below to allow comparison of these hydrogels with other materials currently being developed elsewhere.

Poly(DL-lactic acid) scaffolds produced with supercritical carbon dioxide by Kanczler et al[90] were able to release approximately 3 ng/ml of VEGF over 21 days which was able to stimulate angiogenesis. A constant release of VEGF was also achieved by Gu et al[314] by polymerising acrylated *star*-poly(ε-caprolactone-co-D,L-lactide) macromer and encapsulating VEGF, interferon-gamma (IFN-γ) and interleukin-2 (IL-2) within the elastomer matrix. A constant release was achieved over 5-8 days, but with this formulation it was observed that only 57% of the VEGF remained bioactive. A further poly (DL-lactide-co-glycolide) material was assessed by Elcin et al[315]. A burst release of 40% to 50% of the initial loading was observed, followed by slow release over 21 days with 70% -100% of the VEGF loaded being released depending on initial loading. *In vivo* studies showed that the VEGF-activated sponge was permeated with host blood vessels.

Poly(N-isopropylacrylamide) copolymer films were reported by Kavanagh et al[96] to release $VEGF_{165}$ over 7 days, with 10.75 ± 3.11 ng released after 24 hours and a total of 31.32 ± 8.5 ng released over the whole 7 day period, although this release required a high $VEGF_{165}$ solution loading concentration of 3000 ng/ml. The $VEGF_{165}$ released in this case was shown to be bioactive and increased the proliferation of human aortic endothelial cells by 18.2% over the control. Hydrogels of 2-hydroxyethyl methacrylate, NVP and poly(ethylene glycol) (400) dimethacrylate were produced and combined with poly(lactide-co-glycolide) by Norton et al[94] to release a combination of VEGF and dexamethasone. The base hydrogels, the most comparable system for this study, were shown to release between approximately 60-160 ng/ml VEGF in an initial burst in 0-3 days followed by a very slow release over 2 weeks. In total only 10% of the original VEGF loaded in this formulation was released. The release profile in this case was thought to be standard for hydrogel release and to be dependent on diffusion through the hydrogel and initial loading.

A similar burst release was observed by Patel et al[76] with gelatin microparticles, with the predominant release occurring within the first 24 hours followed by very slow release thereafter. The bioactivity of the VEGF released in this case remained over 90%, which is thought to be in part due to the association of released VEGF with gelatin fragments. The ability of alginate to stabilise VEGF was utilised by Jay et al[65] in the release of VEGF from alginate microparticles crosslinked by ionic crosslinkers. In this case release was maintained over a ten-day period, but again this release generally consisted of a high initial release followed by a slow release of low VEGF amounts over the remaining days.

Most of the above approaches show the majority of release occurring within a period of 24 hours to one week, often with a burst release in the first three days. Not all of the loaded VEGF was released in all cases and it was observed by Gu et al[314] that a decrease in bioactivity of VEGF occurred during the release procedure.

The incorporation of heparin to maintain the bioactivity of the released VEGF or bFGF was employed by various researchers. Heparin has been incorporated covalently into hydrogels by a number of groups. Yoon et al[102] detailed bFGF release from Pluronic/heparin hydrogels over 30 days. Approximately 75% of the 25 ng bFGF loaded was released from the Pluronic/heparin hydrogel with a small burst release followed by consistent release over the remaining period, in contrast to the 99% released from the Pluronic hydrogel alone. It was suggested that, for the Pluronic hydrogel, bFGF was likely to be released by diffusion, whereas the Pluronic/heparin hydrogel would specifically bind the bFGF and thus the release would also be controlled by the thermodynamic equilibrium between free bFGF and bound bFGF. A proliferation study with HUVECs showed that a higher cell viability was observed when the hydrogel contained heparin than for the Pluronic hydrogel alone, despite the Pluronic hydrogel releasing more bFGF. *In vivo* analysis showed dense capillary formation of the Pluronic/heparin hydrogel in comparison to the Pluronic hydrogel alone.

Heparin hydrogels were produced by Benoit et al[49] by modifying the heparin with methacrylate groups and copolymerising with dimethacrylated poly(ethylene glycol). Unmodified PEG gels released all bFGF bound in eight hours but release over five weeks was possible with heparin inclusion, although this release has a very large initial

release followed by low amounts of VEGF released over the remaining period. Human mesenchymal stem cells (hMSCs) were utilised to analyse these materials. The heparin-modified gels were able to promote hMSC adhesion and spreading on the hydrogels as well as proliferation. The attachment of cells to the hydrogel was dependent on the heparin dose.

Maleimide-functionalised high molecular weight heparin and thio-functionalised PEG were utilised by Nie et al[99] to produce heparin-containing hydrogels which could release up to 30% of the bound bFGF over a 6 day period. Almost no burst release was observed in this case.

Pike et al[64] produced hydrogels of hyaluronan, gelatin and small quantities of heparin. VEGF or bFGF were incorporated in the hydrogels before crosslinking. In all cases not all of the growth factor was released within the 42 day period, with release of 19% to 48% of the growth factor reported for different formulations. Heparin incorporation slowed the release of VEGF, allowing the release to last over 42 days with less than 1% heparin. In the presence of heparin, the growth factors remained active and vascularisation was sustained over 28 days.

A few groups have also considered the non-covalent incorporation of heparin. Zhang et al[316] synthesised hydrogels from a heparin-binding peptide-functionalised star PEG and low molecular weight heparin-functionalised star PEG. The release of bFGF was studied and release occurred as the hydrogel degraded. The release profile consisted of a high initial release of 25% of the bFGF in the first day and slow release thereafter up to approximately 35% of the bFGF after 10 days. Heparinised chitosan-coated calcium-induced alginate hydrogel beads were utilised by Lee et al[98] and were shown to release VEGF over 11 days with a small initial burst period.

The addition of heparin into the polymer formulations in the above studies often had the effect of prolonging growth factor release (up to six weeks) but also resulted in the *incomplete release of VEGF*, leading to the waste of expensive growth factor. It is suggested that these observations are likely to be due to the *strength of the interaction* between VEGF and heparin. When the heparin is covalently incorporated into the material, or crosslinked to a high degree, the release of VEGF would require the

disruption of the VEGF-heparin interaction. In this study the heparin is only lightly incorporated, so release could be either by disruption of the heparin-VEGF binding or the heparin-hydrogel interactions.

In those studies which compared materials containing heparin to the same materials without heparin, it was noted that all of the materials were able to bind the growth factors and it was the release profile that was affected by the presence of the polysaccharide. This was also observed in this study. All of the hydrogels were able to bind and release VEGF and for all hydrogels almost 90% of the bound VEGF was released. The release profile for the PNDRRR hydrogel during the washing procedure showed less VEGF was released than for the other hydrogels. A higher amount of heparin was bound to the hydrogel in this case and so the lower VEGF release observed initially is attributed to the VEGF being strongly bound to the heparin, rather than the weaker association to the hydrogel that is expected for the other materials, thereby retarding the VEGF release.

From the examples discussed, a considerable proportion of the literature available in this area describes release profiles with an initial burst release, followed by much slower release kinetics over the rest of the study. Generally, the majority of the release occurs within the first three days. Such results are comparable to those observed with the heparin-bound hydrogels in this study. In this case the VEGF was released relatively consistently over 72 hours and it is feasible that the small percentage of VEGF found to be remaining within the hydrogels would have also been released slowly in the days following the 72 hour period if the experiment had been extended. It would be necessary to repeat the release study for a longer period of time to confirm this hypothesis.

Fast release is observed with these hydrogels, with almost 90% of the bound VEGF released within three days. It is suggested that this is in part due to the high water content of the hydrogel, resulting in fast diffusion kinetics. Another explanation for the fast rate of release relates to how the release study was carried out. A large number of samples were taken in the 72 hour period, with five samples taken within the initial three hours. Also, as the samples for the ELISA kinetics study were taken, all of the PBS was removed and replaced with fresh PBS. This could lead to an accelerated

release assuming the release from heparin or the hydrogel is governed in part by the thermodynamic equilibrium between free VEGF and bound VEGF. Constantly replacing the PBS would create a high VEGF gradient, which could in turn cause the hydrogels to release the VEGF at a higher rate. In order to analyse this, a repeat of the release experiment would be required with only small aliquots of PBS being removed at each time point and with less frequent sampling. The different experimental methods for VEGF release studies in the examples discussed makes direct comparison difficult but it was observed from the literature available that samples were often taken less frequently (daily or less frequently) and often only a small aliquot of the solution was removed and replaced, thereby minimising the VEGF gradient.

Those groups who also studied the effect of released growth factor on bioactivity and angiogenesis showed that the released VEGF was able to induce angiogenesis. The presence of heparin was thought to maintain bioactivity during storage of the VEGF, as well as improve the angiogenic capacity by allowing the VEGF to interact with cells as a VEGF-heparin complex in those systems which allowed heparin release.

All of the hydrogels produced in this study were able to bind and release VEGF, with slower release observed for the PNDRRR hydrogel. From the literature, it can been seen that VEGF release could be tailored by heparin content and VEGF loading, as well as how quickly the surrounding environment is depleted of free VEGF. The PNDRRR hydrogel especially compares favourably in comparison to other materials detailed in the literature with a steady VEGF release of 27 ng per 5 mm diameter hydrogel over three days, and low VEGF retention on the material. In summary, the confirmation of the ability of the hydrogels to bind and release VEGF meant that these materials were suitable for cell compatibility studies and analysis of their potential as a VEGF-releasing angiogenic treatment.

# 6 Cell Compatibility of Peptide-Functionalised Hydrogels

The next stage of this project was to assess, both qualitatively and quantitatively, the effect of poly(NVP-co-DEGBAC) hydrogels, poly(NVP-co-DEGBAC-co-AA) hydrogels and peptide-functionalised poly(NVP-co-DEGBAC-co-AA) hydrogels on cells relevant to the desired wound healing application. The reasonable material properties experienced with these gels allowed them to be placed in the wells of the cell culture plates with no further support. This ease of handling allowed investigations into the effect of direct and indirect contact with the hydrogels to be carried out simultaneously. Primary human dermal fibroblast cells were investigated initially as they are suitable for generic toxicity testing; they are also a relevant cell type for skin applications. Further investigations were carried out with endothelial cells, as determining the final effect of these polymers on angiogenesis is vital for this project.

The following four polymers were analysed: poly(NVP-co-DEGBAC) (PND), poly(NVP-co-DEGBAC-co-AA) (PNDA), poly(NVP-co-DEGBAC-co-AA) functionalised with trilysine (KKK) (PNDKKK) and poly(NVP-co-DEGBAC-co-AA) functionalised with triarginine (RRR) (PNDRRR). The relevant analytical data for each polymer is provided in Table 6.1.

| Hydrogel Properties | Hydrogel Identification | | | |
|---|---|---|---|---|
| | PND | PNDA | PNDKKK | PNDRRR |
| % composition[a] | | | | |
| NVP | 98 | 93 | 93 | 93 |
| AA | 0 | 5 | 5 | 5 |
| DEGBAC | 2 | 2 | 2 | 2 |
| EWC (%)[b] | 86.5 | 92.9 | 92.9 | 92.9 |
| Peptide loading (mg/mg hydrogel)[c] | ~ | ~ | 0.14 ± 0.01 | 0.20 ± 0.01 |

**Table 6.1: Summary of properties of hydrogels analysed by cell culture. (a) calculated from original monomer composition utilised in synthesis. (b) EWC results average of 6 measurements. (c) Peptide loading determined by indirect colorimetric TNBS analysis. Result is an average of all 5 batches used in cell culture studies.**

In all cases, quantitative data on the effect of treatment on the cells was determined colorimetrically by the MTT assay[317], which is based on the purple colour of formazan formed by reduction of 3-(4,5-dimethylthiazol-2-yl)-2,5-diphenyltetrazolium bromide (MTT), as shown in Figure 6.1.

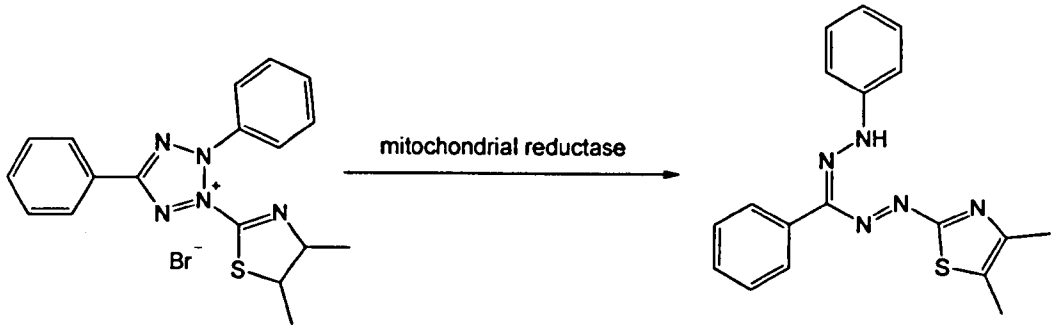


**Figure 6.1: Reduction of MTT by mitochondrial reductase enzymes[318]**

Mitochondrial reductase enzymes cause the reduction of MTT and therefore the formazan intensity is directly proportional to the activity of these enzymes. The MTT assay can therefore provide information about the number of cells present and their ability to function.

Analysis of cellular distress was visualised through the observation of cell morphology, since abnormal morphology can be an indicator of stress in a particular environment. Morphology was observed both by light microscopy and fluorescent microscopy.

One-way ANOVA with Tukey post hoc analysis was used to determine significant ($p < 0.05$) stimulation or inhibition in cell viability, as assessed colorimetrically by MTT assay within a single experiment, and the Mann Whitney U Test was utilised to assess significance ($p < 0.05$) over triplicate repeat experiments.

## 6.1 Effect of Poly(NVP-co-DEGBAC) Hydrogels with Acid and Peptide Functionalisation on Primary Human Dermal Fibroblast Cells

The fibroblasts used within this study were obtained from numerous donors and different passage numbers (passage numbers 3-9) and the hydrogel samples were from multiple batches. None of these variables were found to affect the range of results obtained.

Experiments were performed as illustrated in Figure 6.2 (all cell culture experiments and procedures are described in Chapter 10). A hydrogel disc of 5 mm swollen diameter was placed in a 48 well plate (10 mm well diameter), followed by random seeding of fibroblasts, thus allowing for cells to be cultured in both direct and indirect contact with the hydrogels simultaneously. Cells in indirect contact to the hydrogels were of interest to provide information on cytotoxicity of the biomaterials, and to determine whether the presence of the various hydrogels would have either a stimulatory or inhibitory effect on fibroblast viability. In all cases the control was cells on TCP with no hydrogel present. Cells in direct contact with the hydrogels (on top of the materials) can provide biocompatibility data, as well as determining the effect of hydrogel functionality on cell attachment.

Cells were cultured in fibroblast medium both with and without foetal calf serum (FCS) for 96 hours to determine whether the presence of serum influences the reaction of the cells to the presence of the hydrogel.

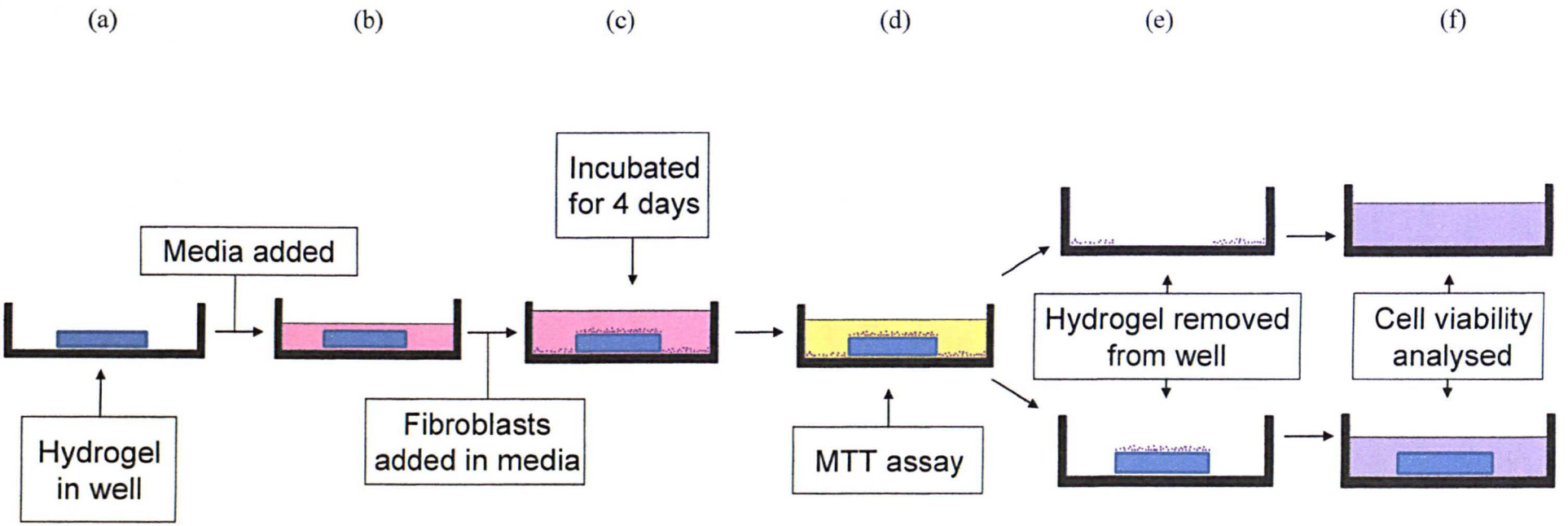


**Figure 6.2: Schematic of cytotoxicity experiments. a) hydrogel (5 mm diameter) is added to 48 well plate (10 mm diameter), b) media (with or without serum) is added to the hydrogel and incubated for 72 hours and then replaced with a further aliquot of media, c) 1 x $10^4$ cells seeded randomly into each well in a further aliquot of media and the cells were incubated for 96 hours, d) MTT assay carried out e) Hydrogel with cells on the hydrogel surface is moved to a separate well, f) Formazan is eluted from cells and cell viability is analysed colorimetrically.**

### 6.1.1 Fibroblasts Cultured in 10% FCS-Containing Medium

In the experiments carried out, the low number of cells often present on the hydrogels and the small surface area of the hydrogel meant that the cell count was often very low, leading to low precision in the MTT data, particularly for the PND and PNDA hydrogels. It is therefore important to consider the quantitative data together with the visual analysis to get a true representation of the results. However, both quantitative and qualitative analysis of the fibroblasts present on the hydrogel within serum-containing media show considerable effects of the functionalisation of the NVP-based hydrogels.

In all cases, fibroblasts were present on the tissue culture plastic (TCP) (Figure 6.3, Figure 6.5, and Figure 6.4) surrounding the hydrogel and grew to the edge of the hydrogel with a normal fibroblast morphology. These results suggest that all these materials are cell-compatible and have no cytotoxic effects. Observation of MTT-stained wells after removal of the polymer discs reveals that cells were not attached to the tissue culture plastic underneath the hydrogel in all cultures. Therefore, in order to calculate the quantitative effect of the hydrogels on cell viability in comparison to a control well, the MTT response of the control well was adjusted to give an equal TCP surface area to that available in the hydrogel-containing wells.

On tissue culture plastic a slight increase in cell viability was observed in the presence of all hydrogels in comparison to the control well (TCP) in two of the three repeat experiments but a significant increase ($p < 0.01$) was observed only in repeat 2 for the PND, PNDA and PNDKKK hydrogels. Overall, from the three repeats, it was concluded that there was no significant effect of these materials on fibroblast viability.

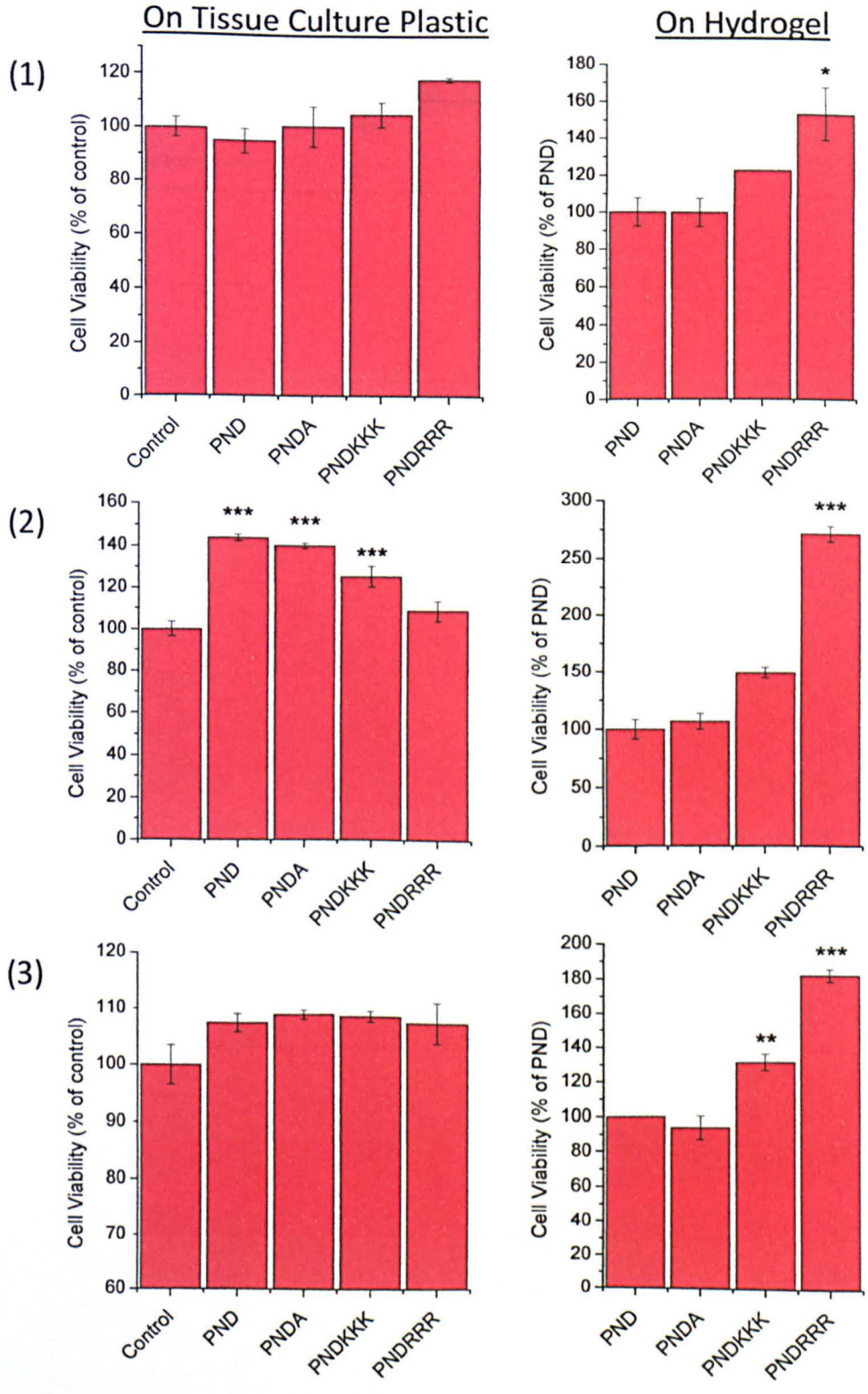


**Figure 6.3: Results of fibroblast experiment with 10% FCS DMEM medium. Results of three repeat experiments shown individually. Left column shows results of MTT assay of cells on tissue culture plastic (TCP) surrounding the hydrogel and right column shows results of MTT assay of cells present on the hydrogel. Results expressed as percentage of cell viability in comparison to control well (on TCP results) or unfunctionalised PND (on hydrogel results) ± percentage SEM. Significance was assessed using one-way ANOVA with post-hoc Tukey analysis. Significance shown is for comparison with control well (TCP) for the results on TCP, or PND (hydrogel) for the results on the hydrogels (*$p < 0.05$, **$p < 0.01$, ***$p < 0.001$).**

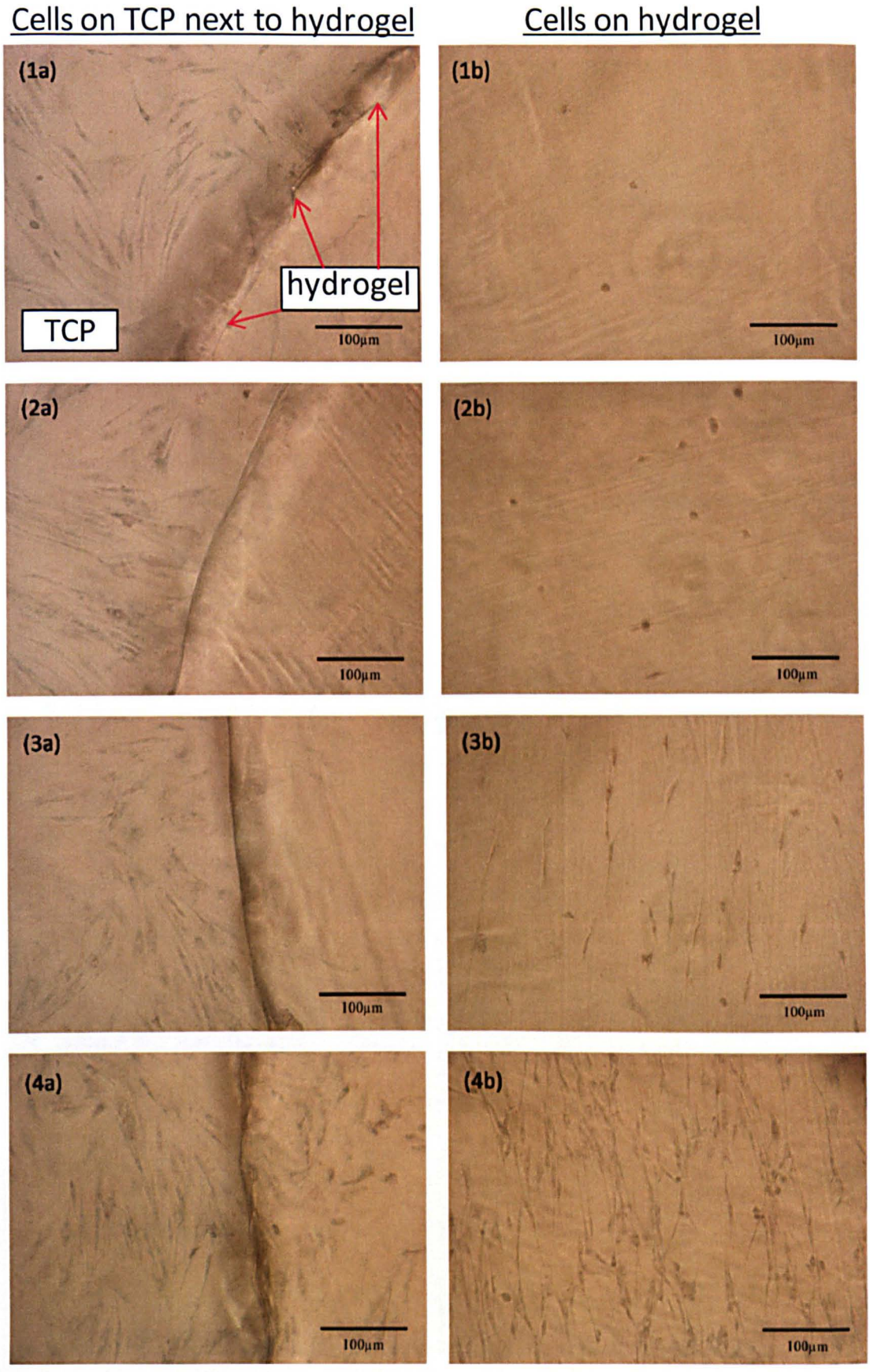


**Figure 6.4: Results of fibroblast cell culture experiment in 10% FCS DMEM medium. Fibroblast cells in direct and indirect contact with hydrogels column (a) cells on TCP adjacent to hydrogel (image shows hydrogel (on the right) and cells on TCP (labelled in image 1a)), column (b) cells on top of hydrogel. Row: (1) PND (2) PNDA (3) PNDKKK (4) PNDRRR.**

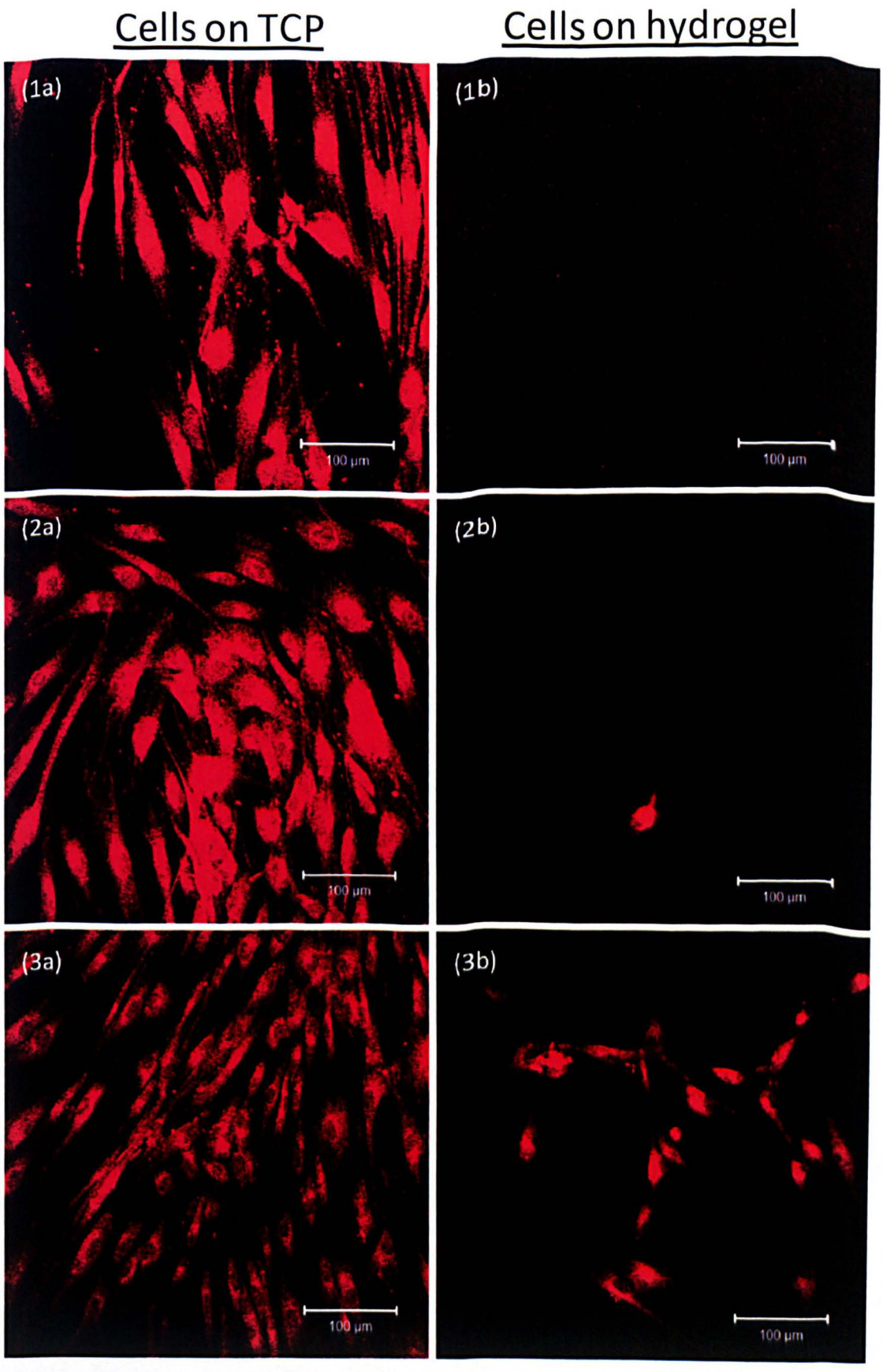


**Figure 6.5: Human dermal fibroblasts cultured in direct and indirect contact with hydrogels in medium containing 10% FCS for 96 hours. Cells were stained with CellTracker™ Red and imaged on a Zeiss LSM 510 confocal microscope (abs. 577 nm and em. 602 nm). Images in column (a): Fibroblasts on TCP in wells containing hydrogels, images in column (b): Fibroblasts on top of the hydrogels. Images in row (1): PNDA, row (2): PNDKKK, row (3): PNDRRR.**

Information regarding cell attachment to the hydrogel discs was obtained by considering the number of cells present on the surface of the polymer and their morphology. No significant quantitative difference in cell viability was observed between the PND and PNDA hydrogels. Microscopy (Figure 6.4) showed that a few more cells were consistently visible on the PNDA hydrogels than on the PND material, but cell numbers were low on both substrates. All cells present on both of these materials were viable, but upon visual inspection they were found to have an unusual morphology. The cells were often present in clumps and when individual cells were present they were of a rounded morphology, suggesting that they were stressed and not well attached to the material.

Comparison of the PND and PNDA hydrogels with the PNDKKK and PNDRRR hydrogels shows an increase in cell attachment upon peptide functionalisation. Interestingly, a difference was also observed between the PNDKKK and PNDRRR polymers, both quantitatively and qualitatively (Figure 6.3 and Figure 6.4). In all experiments a large increase in cell numbers was observed for the PNDKKK hydrogel in comparison to either the PND or PNDA hydrogel and an even larger increase in cell numbers was consistently observed on the PNDRRR hydrogels in comparison to the PNDKKK polymers. Consideration of images taken during MTT staining (Figure 6.4) shows an improvement in cell morphology as the PNDA hydrogels are functionalised with peptides. Cells present on top of the PNDKKK hydrogel appear to be less rounded than on either the PND or PNDA hydrogels, and have a more normal fibroblast morphology, suggesting that the cells are able to attach more effectively to this material and are therefore less stressed. This effect is even more obvious for the PNDRRR hydrogels, on which the cells appear to have a normal fibroblast morphology and appear relatively well attached to the hydrogel.

Images were also taken of fibroblasts stained with CellTracker$^{TM}$ Red (Figure 6.5). When this experiment was carried out no PND material was available, and therefore only PNDA, PNDKKK and PNDRRR hydrogels were analysed in this way. Again, it is possible to see that in all cases cells are visible with a normal morphology on the tissue culture plastic. The trend for cells present on the hydrogels is the same as when observed with MTT staining but it is obvious that cell numbers are considerably lower in all cases. It is postulated that the cells on the hydrogel are more loosely attached on the polymer than on the TCP and therefore a number of the cells detach during the

washing procedure. It is possible to see that the cells present on the RRR hydrogel have conventional fibroblast morphology and appear to remain reasonably well attached. The observation that a significant proportion of cells attached to the hydrogels detach easily upon washing is a positive observation for the required application as hydrogels to which cells adhere only loosely would allow easier removal from a wound after use.

### 6.1.2 Fibroblasts Cultured in Serum-Free Medium

The experiment described previously was also carried out within a serum-free environment to determine the effect of the serum on the cell compatibility study.

As observed in serum-containing medium, no cytotoxicity effect was observed for cells present on TCP in PND, PNDA and PNDKKK hydrogel-containing wells, as cells were present with a normal morphology adjacent to the polymer (Figure 6.6, Figure 6.7 and Figure 6.8). For PND and PNDA hydrogels a slight stimulatory effect was observed in two of three repeats, although a significant effect ($p < 0.01$) was only observed in one of the three repeats. No significant effect was observed for the PNDKKK hydrogel. Overall, for these three materials, no significant effect ($p > 0.05$) was observed when analysed by the Mann Whitney U test.

A very different effect was observed for the PNDRRR hydrogel. In this case, cells on the TCP were either clumped together or they had a rounded morphology, and a considerable proportion of the cells present on the TCP surrounded the hydrogel closely (Figure 6.7). This inhibitory effect, observed qualitatively and also quantitatively through MTT analysis (Figure 6.6), was seen for all repeats and was significant ($p < 0.001$) in two of the three repeats. It is suggested that in the serum-free medium this is due to amino acid absorption by the hydrogel (further discussed in Section 6.3).

Very few cells were observed on the hydrogel discs in all cases. A slight increase in the number of cells present on the polymer was observed for the KKK hydrogel, although this was not found to be statistically relevant. On all materials the cells were present with a rounded, stressed morphology.

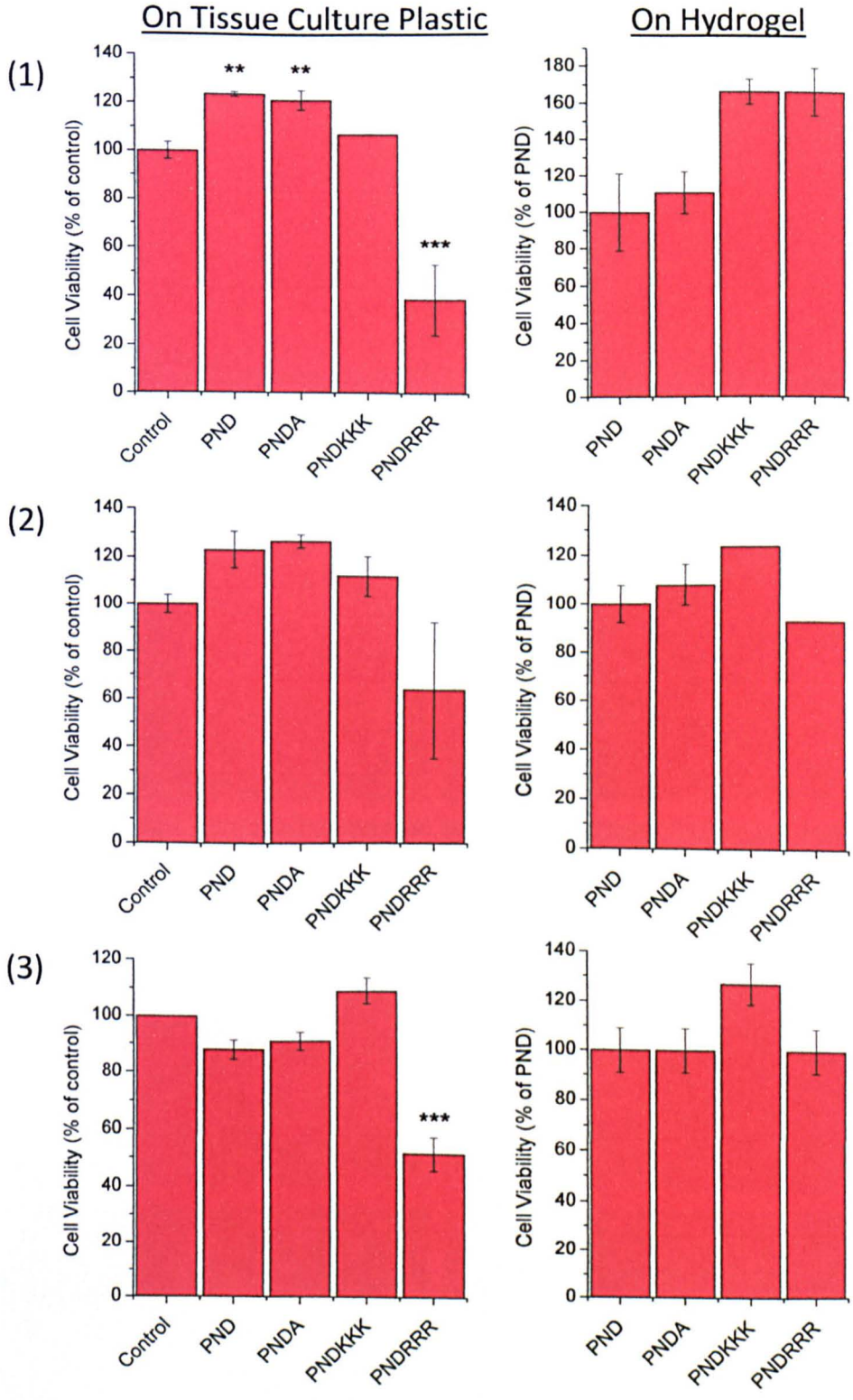


**Figure 6.6: Results of fibroblast experiment with serum-free DMEM medium. Results of three repeat experiments shown individually. Left column shows results of MTT assay of cells on tissue culture plastic (TCP) surrounding the hydrogel and right column shows results of MTT assay of cells present on the hydrogel. Results expressed as percentage of cell viability in comparison to control well (on TCP results) or unfunctionalised PND (on hydrogel results) ± percentage SEM. Significance was assessed using one-way ANOVA with post-hoc Tukey analysis. Significance shown is for comparison with control well (on TCP results) or PND (on hydrogel results) (*$p < 0.05$, **$p < 0.01$, ***$p < 0.001$).**

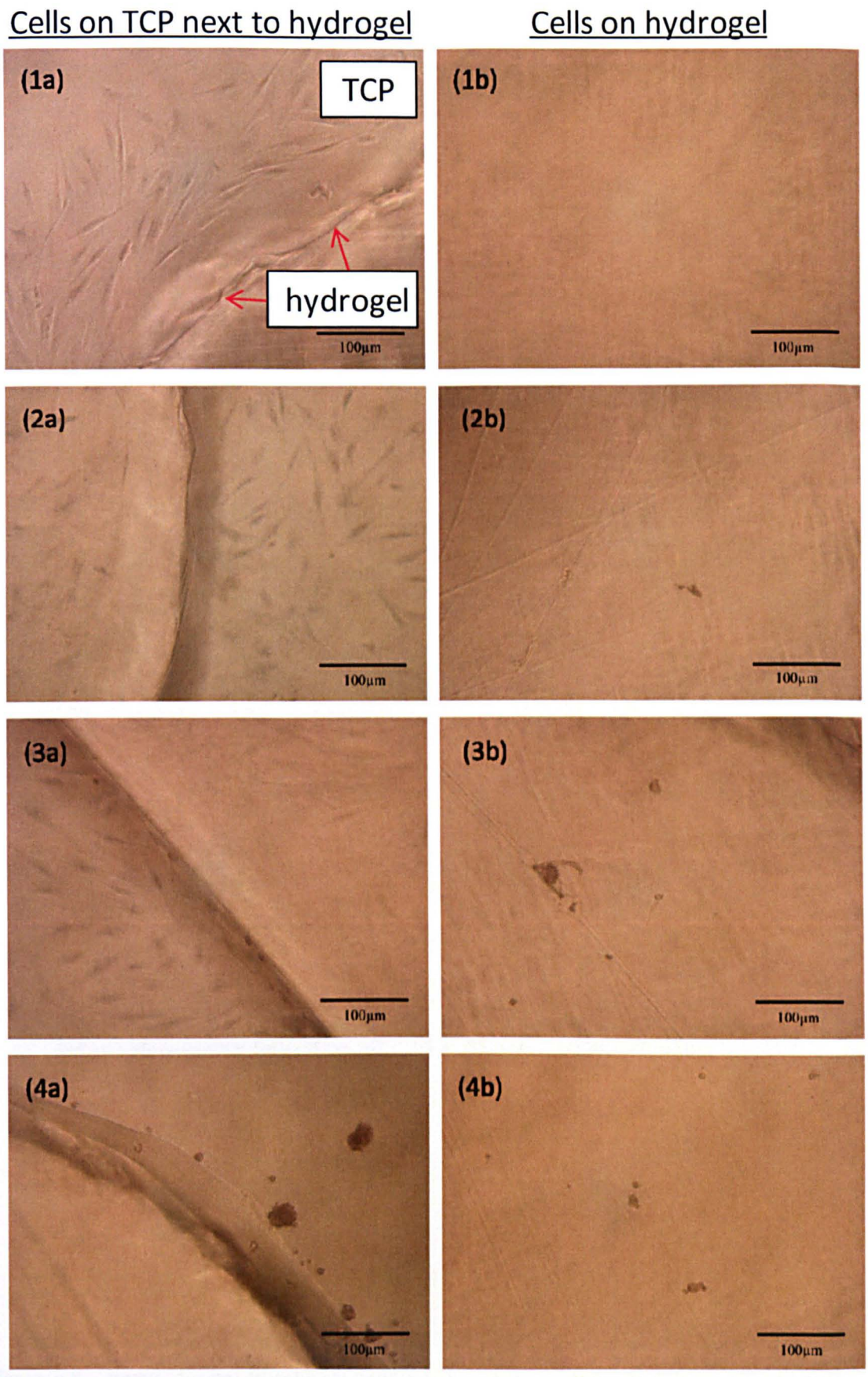


**Figure 6.7: Results of fibroblast cell culture in serum-free DMEM medium. Fibroblast cells in direct and indirect contact with hydrogels. Images in column (a) cells on TCP adjacent to hydrogel (image shows hydrogel and cells on TCP (labelled in image 1a)), column (b) cells on top of hydrogel. Row (1) PND (2) PNDA (3) PNDKKK (4) PNDRRR**

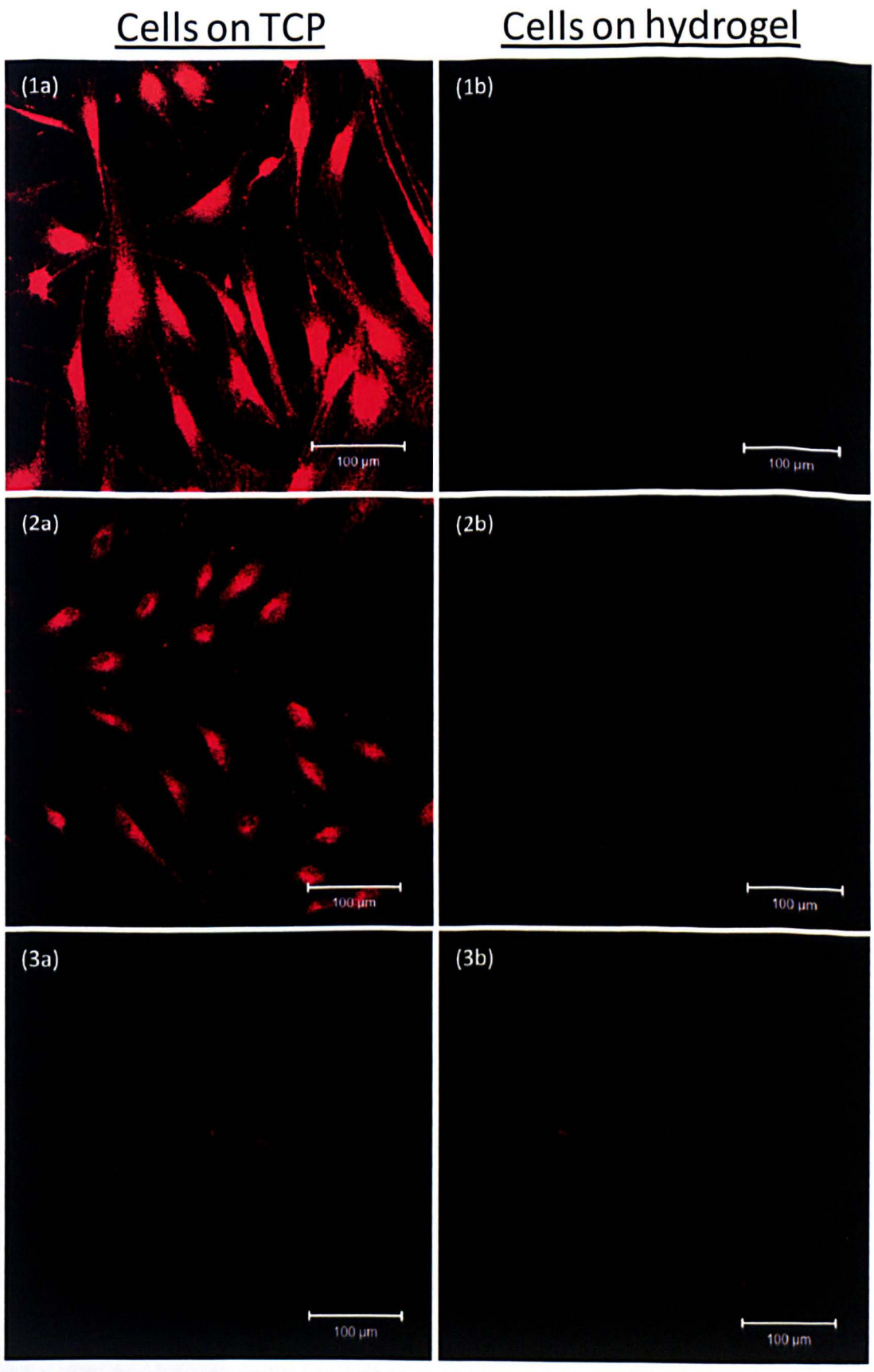


**Figure 6.8: Human dermal fibroblasts cultured in direct and indirect contact with hydrogels in medium without FCS for 96 hours. Cells were stained with CellTracker™ Red and imaged on a Zeiss LSM 510 confocal microscope (abs. 577 nm and em. 602 nm). Images in column (a) cells on TCP adjacent to hydrogel, column (b) cells on top of hydrogel. Row (1) PNDA (2) PNDKKK (3) PNDRRR.**

## 6.2 Effect of Poly(NVP-co-DEGBAC) Hydrogels with Acid and Peptide Functionalisation on Human Dermal Microvascular Endothelial Cells

In this experiment, normal human dermal microvascular endothelial cells from Promocell® were used to determine the effect of the hydrogels on endothelial cells, the cells which form the walls of blood vessels. Dermal microvascular endothelial cells were selected as this cell type is closely related to the required application. Cells were used between passage numbers 4 and 8. FACS analysis of the endothelial cells used in all cell culture studies was kindly carried out by Dr. Emilia Krajewska and showed strong expression of CD31, a marker specific for this cell type.

Experiments were performed as described in Figure 6.2 to enable determination of cytotoxicity of the hydrogels. This experiment was carried out over 96 hours with growth factor-supplemented endothelial cell growth medium with 5% serum, which was replaced with fresh medium every 24 hours. This was necessary to ensure that a suitable number of cells remained viable until MTT analysis as endothelial cells are very sensitive to the protein content of the growth medium. For this cell type, the 96 hour experiment was carried out only in serum-containing medium, as it was not possible to maintain a suitably high content of viable cells for this time period in a serum-starved environment.

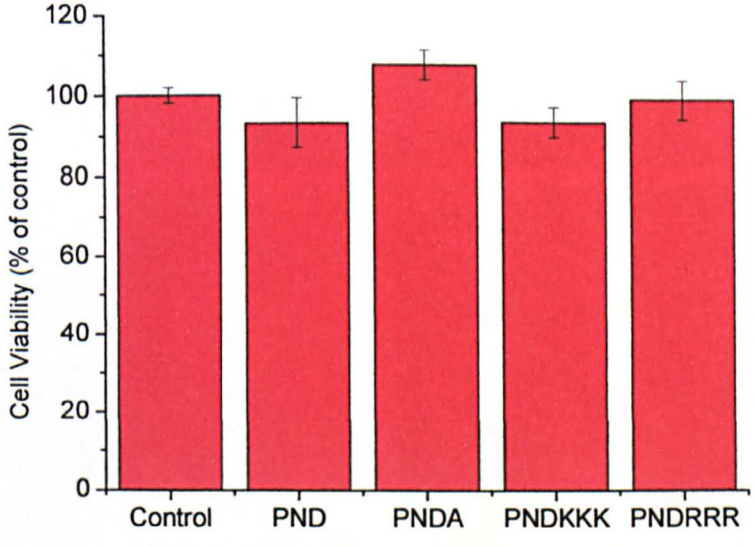


**Figure 6.9: Effect of the presence of hydrogels on the viability of HDMEC on tissue culture plastic (TCP) when cultured for 96 hours within endothelial cell growth medium with 5% foetal calf serum. Results shown are the percentage means ± SEM of 3 experiments (3 replicates per experiment)**

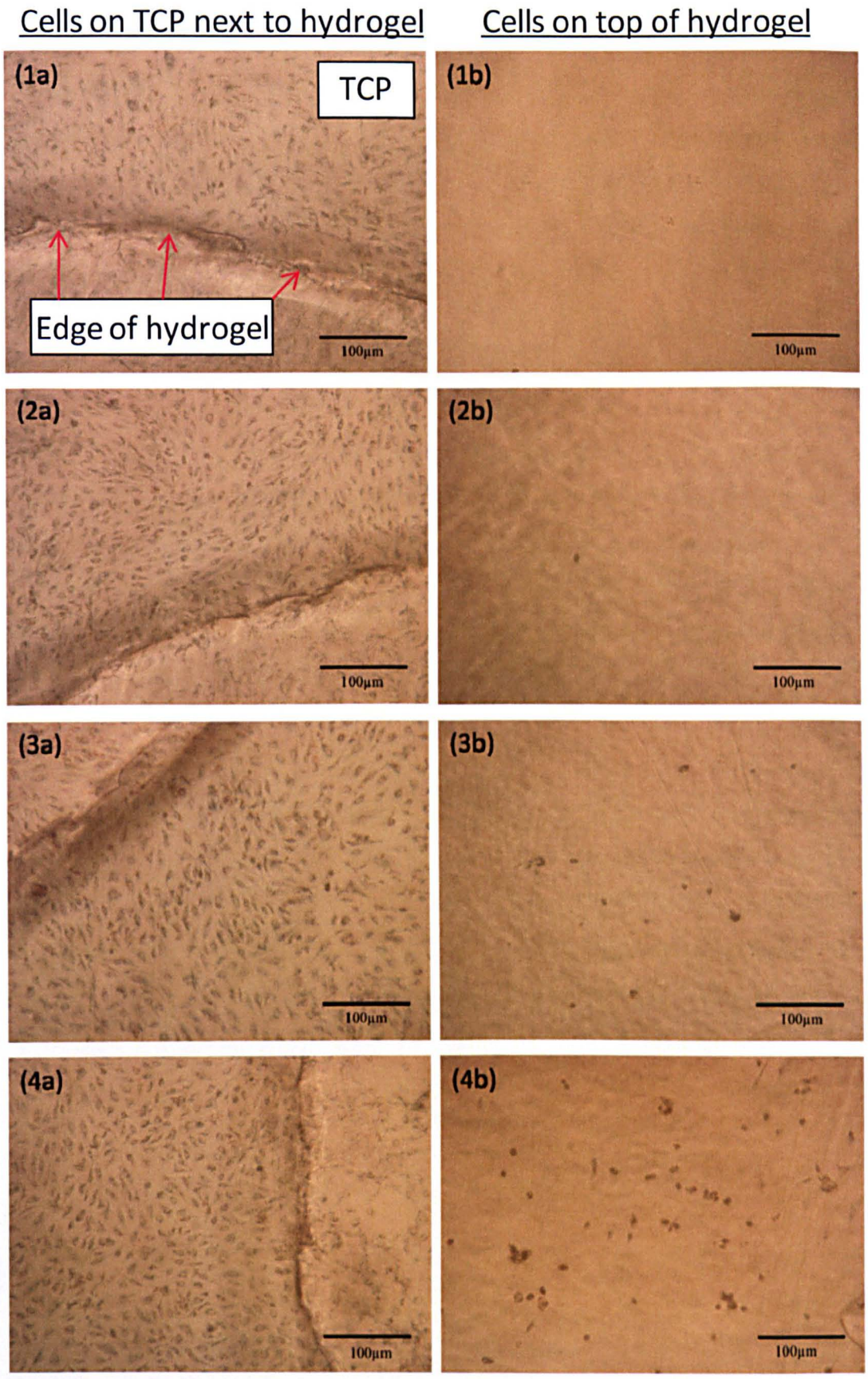


**Figure 6.10: Results of 4 day endothelial cell culture experiment in endothelial cell growth medium with 5% FCS. Endothelial cells shown after MTT staining in direct and indirect contact with hydrogels. Images in column (a) cells on TCP adjacent to hydrogel (image shows hydrogel and cells on TCP (labelled in image 1a)), column (b) cells on top of hydrogel. Row (1) PND (2) PNDA (3) PNDKKK (4) PNDRRR**

None of the four hydrogels, PND, PNDA, PNDKKK and PNDRRR, had any cytotoxic effect on HDMECs (one-way ANOVA with post-hoc Tukey analysis) (Figure 6.9). As seen in the fibroblast data, cells were not attached to the TCP underneath the hydrogel but were present over the rest of the available TCP right up to the edges of the hydrogel. The cells had a normal "cobblestone" appearance associated with this cell type in growth medium (Figure 6.10). The results show that the cells were not unduly stressed in this environment. These indirect contact results agree with those obtained for fibroblasts in serum-containing medium, and indicate that these materials are suitable biomaterials for the desired application and therefore suitable for further investigations.

The ability of cells to attach to these materials and proliferate on them was analysed qualitatively only for the endothelial cells, as so few cells attached to the polymer and the MTT response was too low to provide a quantitative signal. The images in Figure 6.10 are endothelial cells after MTT staining, as the flat morphology of the HDMECs prevented clear images being taken without staining. The images provided are representative of the three repeat experiments undertaken.

The morphology of the cells that did attach to the hydrogels is rounded, and occasionally clumps of cells are visible, suggesting that these cells are only loosely attached to these materials. Visually, it is easy to see that almost no endothelial cell attachment occurs with the PND and PNDA materials. As the material was functionalised with KKK peptide (PNDKKK) a few cells remained attached to the material after four days. Functionalising the material with RRR (PNDRRR) resulted in a few more cells remaining attached to the polymer after the four-day experiment.

## 6.3 Conclusion of Cell Compatibility Study

Experiments were carried out to determine the cytotoxicity of the PND hydrogel, PNDA hydrogel and peptide-functionalised PNDA hydrogels. The results from both the fibroblast and endothelial cell studies revealed that the materials are cell compatible and the base polymer of poly(NVP-co-DEGBAC) is a suitable biomaterial for this work. Previous work on poly(NVP-co-DEGBAC) by Smith et al[278] showed this polymer to be cytocompatible but a poor substrate for cell attachment.

In the serum-containing experiments for fibroblast and endothelial cells, no significant effect on the cells in indirect contact with the materials was observed upon introduction of any of the hydrogels. Overall for the serum-free fibroblast experiment a similar result is observed for PND, PNDA and PNDKKK, with no overall influence on cell viability. Interestingly a significant decrease in cell viability was observed for the fibroblast cells in indirect contact with the PNDRRR hydrogels in serum-free medium. It is hypothesised that in this case the superior affinity of the RRR group for certain components of the medium, primarily amino acids, has led to adsorption of these substances, resulting in a surrounding medium that is deficient in key components and therefore cannot sustain the cell viability observed in the control well. It is not thought that this would cause difficulties in a biological application as the environment experienced *in vivo* is more likely to resemble the conditions of the serum-containing medium in which no inhibition was observed.

When considering the cells in direct contact with the hydrogels, i.e. those cells present on the top of the hydrogel, a substantial effect was observed as the hydrogels were functionalised. For the base poly(NVP-co-DEGBAC) hydrogels it was observed that it is difficult to grow cells in direct contact with the swollen hydrogel (confirming earlier work from this lab[278]) . The few cells that did attach appeared to be stressed and poorly attached. One reason for the lack of cell adhesion to this material could be the extremely high water content experienced with this formulation. Analysis of amphiphilic networks by Haigh et al[319] showed that the EWC had a significant effect on cell attachment with a decrease in cell coverage observed as the EWC was increased beyond 29%. In these non-functionalised hydrogels, a combination of the high EWC and lack of protein binding sites would minimise the ability of the hydrogels to absorb

proteins. This would be expected to lead to minimal cell attachment, as cells do not adhere directly to biomaterial surfaces, but in fact bind through adhesion proteins (including fibronectin, laminin and vitronectin) which in turn adsorb onto the biomaterial, as demonstrated by Nuttelman et al[320] through fibronectin-functionalised poly(vinyl alcohol) hydrogels. The requirement for the ECM cell adhesion proteins was also shown by Hynd et al[321] who observed directed cell growth on hydrogels with bound ECM proteins. It is thought that protein adsorption to the poly(NVP-co-DEGBAC) material is negligible, resulting in the low cell adhesion observed for both cell types.

Following this hypothesis it was expected that incorporation of charge in the form of carboxylic acid groups would lead to cell attachment. However, this was not the case, and no significant differences were observed between poly(NVP-co-DEGBAC) (PND) and poly(NVP-co-DEGBAC-co-AA) (PNDA). This result is in agreement with previous work by Sun et al[322], analysing polymethacrylate networks as cell culture substrates, who showed that the incorporation of carboxylic acid groups into their materials allowed some attachment of human dermal fibroblasts but the cells did not spread well and were poorly attached to the hydrogels in serum-containing medium. In contrast to this result they also showed that incorporation of charge via amines (basic functionality) was able to increase cell coverage of the materials, but that this effect was significantly influenced by the length of the carbon chain between the amine groups. A chain of a minimum of three carbons between the amine groups was required to produce materials which were as effective for cell culture as TCP. Epithelialisation of these materials by primary amine functionalisation was shown in a later publication[323] when corneal epithelial cells were co-cultured with stromal cells.

Functionalisation with the basic peptide sequences, KKK and RRR, as expected, led to an increase in cell adhesion, resulting in both an increase in the number of cells attaching to the materials and an improvement in the cell morphology, especially for the fibroblast cells in 10% FCS, for which the change in morphology is more easily recognised. This result was anticipated as the peptide sequences firstly offered protein adhesion points through the basic side chain groups for cell adhesion proteins, and secondly the amino acids selected were of the required carbon chain length as discussed by Sun et al[322]. These results are in agreement with a number of other pieces of work

currently in the literature. Recent work by Kim et al[324] showed that higher charge density on HEMA by copolymerisation with 2-(methacryl)-(oxy)ethyl trimethyl ammonium chloride (MAETAC) promoted greater cell attachment, thought to be due to either absorption of adhesion proteins or through charge-charge interactions between the cell and the hydrogel surface. A study on the same polymers by Haxhinasto et al[325] had also shown that incorporation of acidic moieties could increase cell attachment but that the effect was dependent on the base polymer. It is thought that the increase seen by peptide incorporation in this study is predominantly due to the adsorption of cell adhesion proteins from serum, as this effect was not observed in the serum-free fibroblast experiment.

Interestingly, the increase observed in both cell number and cell morphology is most significant for cells in direct contact with the PNDRRR hydrogel, with a considerable difference being observed between the PNDKKK and PNDRRR materials. For the fibroblast study (10% FCS), the PNDRRR hydrogel was able to sustain almost a fully confluent sheet of cells, and the presence of the cells on the hydrogel in the CellTracker™ experiment confirmed that the cells were more strongly attached, although a significant number of the attached cells could still be easily removed upon washing. The difference between the PNDRRR and PNDKKK hydrogels could be due to the slightly higher peptide loading achieved with the PNDRRR peptide, but the improvement in morphology suggests that it is more likely to be due to differences in affinity for the cell adhesion proteins. As discussed previously, arginine is more basic than lysine due to the guanidinium group and so would be expected to bind more strongly to the proteins required for cell adhesion, thereby leading to the significant increase in cell adhesion observed for RRR-functionalised poly(NVP-co-DEGBAC-co-AA) (PNDRRR).

The results obtained show that all of these materials are non-cytotoxic and differ markedly in their cell attachment capabilities. The materials were determined to be suitable for further cell culture experimentation and possible biological applications.

# 7 Assessment of VEGF- and Heparin-Bound Peptide-Functionalised Hydrogels as a Pro-Angiogenic Treatment

As previously discussed, angiogenesis is currently a topic of great interest, predominantly due to the role of this process in tumour development. A large number of angiogenesis models have therefore been developed in order to study both the fundamental biological processes and to enable the development of pro- or anti-angiogenic treatments. It is acknowledged that analysis of pro- or anti-angiogenic agents would be most accurate *in vivo* as such assays are able to provide realistic extracellular environments as well as allowing the effect of non-endothelial cells to be determined.

There are a large number of different *in vivo* assays including implantation of sponges or Matrigel[326], the widely used chick chorioallantoic membrane assay[327], the corneal assay[328], chamber assays[329] and the zebrafish assay[330]. There are also a number of difficulties associated with *in vivo* studies[331, 332], primarily due to the high variability of possible results but also due to difficulties in quantification, the length of time required for experimentation and the complex nature of the experiments. A popular alternative to *in vivo* assays are organ culture assays in which angiogenesis is assessed in either whole or partial organ culture. The types of assays available include the rat or mouse aortic ring[333], the embryoid body assay[334] and the mouse metatarsal assay[335], all of which enable the number and length of microvessel outgrowths from the primary explants to be measured. This approach has the advantage of providing a more realistic environment with other cell types as well as being simpler than *in vivo* assays. However, as with *in vivo* assays, they can be difficult to quantify and can suffer from high variability.

*In vitro* cell culture approaches to the analysis of angiogenesis also have their pros and cons[331, 332]. *In vitro* studies have the advantages of being fast, relatively easy to carry out, readily quantifiable and reproducible. The disadvantages are obvious. The experiments are carried out in an artificial environment in which the cells may behave differently to how they would behave *in vivo*[336], and it is not possible to account for the complex interactions that occur *in vivo*. There are a number of ways to analyse angiogenesis *in vitro*; consideration of matrix degradation, endothelial cell proliferation, migration (which is possible due to the fact that endothelial cells can move towards a

gradient of angiogenesis-inducing factors), or the ability of the cells to form tubules in response to exogenous agents[337].

The opposing advantages and disadvantages for *in vivo* and *in vitro* studies mean that ultimately a combination of the two approaches may be necessary to provide a detailed insight into the effect of a particular treatment agent on angiogenesis. The logical first approach however, due to the advantages previously noted, when studying a new pro- or anti-angiogenic treatment is the simpler *in vitro* analysis.

In this study, two approaches were used to analyse the effect of the VEGF- and heparin-bound hydrogels on human dermal microvascular endothelial cells (HDMECs), a proliferation assay and a tubular assay. The proliferation assay, in this case performed with MTT, has the advantages of being easy to perform and very easy to quantify. This assay indicates the viability of the endothelial cells in the presence of the treatment but no information is provided regarding the ability of the cells to form tubes. To complement this study, a tubular formation assay with growth-factor reduced Matrigel was also carried out on HDMECs.

## 7.1 Effect of VEGF and Heparin on HDMEC Proliferation

Prior to analysis of the effect of VEGF- and heparin-bound hydrogels on endothelial cell culture, the effect of free heparin and VEGF on endothelial cell proliferation both individually and combined was analysed in two experiments. In the first experiment, varying concentrations of VEGF and heparin were individually added to endothelial cells, which had been pre-seeded 24 hours before experimentation and starved in 2% serum medium overnight, to determine the most effective concentrations of each to stimulate endothelial cell proliferation. In the second experiment, the most successful VEGF and heparin concentrations determined previously were applied to the cells both individually and combined to determine whether there was a cumulative effect of the growth factor and polysaccharide combined.

### 7.1.1 Vascular Endothelial Growth Factor Dosing

It was necessary to determine the concentration of VEGF which elicits a stimulatory effect on endothelial cells. This was determined by treating normal human dermal microvascular endothelial cells with varying concentrations of VEGF and analysing the results by MTT assay after three days. $VEGF_{165}$ was utilised and was present within endothelial cell growth medium with 2% FCS and no other growth factor additions.

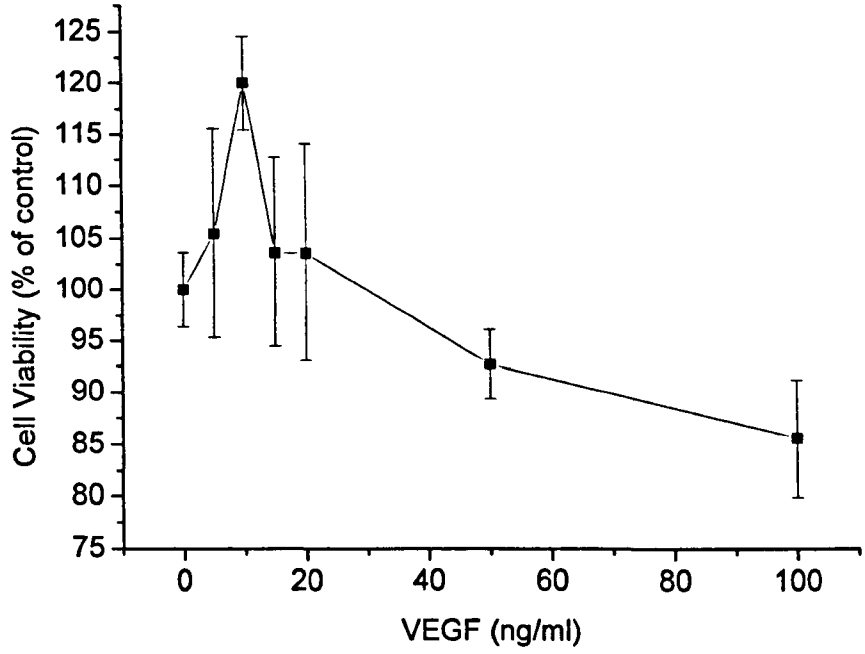


**Figure 7.1: Effect of increasing concentration of $VEGF_{165}$ on the proliferation of endothelial cells over three days in serum-starved endothelial cell growth medium. Data expressed as percentage cell viability compared to cells with no VEGF present (TCP control) ± percentage SEM (N = 1 experiment, three replicates).**

There is an obvious effect of VEGF on the endothelial cells in this experiment although a number of repeat experiments would be required to determine the statistical relevance of these results. Consideration of these results (Figure 7.1) shows that a concentration of 10 ng/ml is the most effective, leading to a 20% increase in cell viability in comparison to a TCP control. Slight increases in viability were also observed for concentrations of 5 ng/ml, 15 ng/ml and 20 ng/ml VEGF in this study. By 50 ng/ml VEGF the cell viability had reduced to below that of the TCP control and the viability reduced further to 85% with the addition of 100 ng/ml VEGF. From these results it was decided that, for further studies, the most successful VEGF concentration of 10 ng/ml would be employed. This result is in agreement with the optimum $VEGF_{165}$ dose of 10 ng/ml for human umbilical vein-derived endothelial cells determined by Cohen et al[45].

### 7.1.2 Heparin Dosing

In order to determine the effect of heparin on endothelial cell proliferation, a similar experiment was carried out as for VEGF (7.1.1) with varying heparin concentrations.

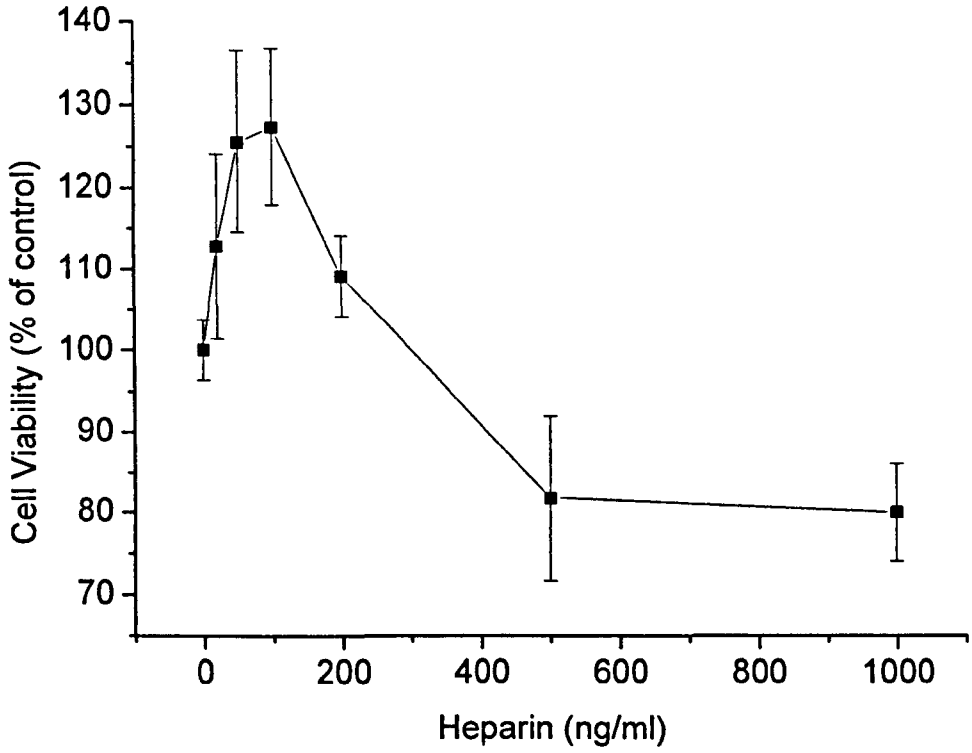


**Figure 7.2: Effect of increasing concentration of heparin on the proliferation of endothelial cells over three days in serum-starved endothelial cell growth medium. Data expressed as percentage cell viability compared to cells with no heparin present (TCP control) ± percentage SEM (N = 1 experiment, three replicates).**

The dose response curve for heparin (Figure 7.2) shows that this polysaccharide does have an effect on normal HDMECs cultured *in vitro*. This study was carried out once only and further repeats would be required to determine the significance of this data. It is clear that heparin doses between 20 ng/ml and 200 ng/ml have a stimulatory effect on endothelial cell proliferation, with a peak between 50 ng/ml and 100 ng/ml. Again, as for VEGF, a higher dose of heparin results in an inhibitory effect, in this case doses of 500 ng/ml and 1000 ng/ml lead to cell viabilities of 82% and 80% of the cell viability observed for TCP alone. From this study it was determined that the most effective dose of heparin is around 50 ng/ml to 100 ng/ml and so it was these concentrations which were studied further.

### 7.1.3 Combined VEGF and Heparin Dosing

An investigation was carried out to determine whether a combination of VEGF and heparin would stimulate cell viability to a greater extent than each individual component. The concentrations previously determined in 7.1.1 and 7.1.2 were utilised in an experiment as described for the compounds individually.

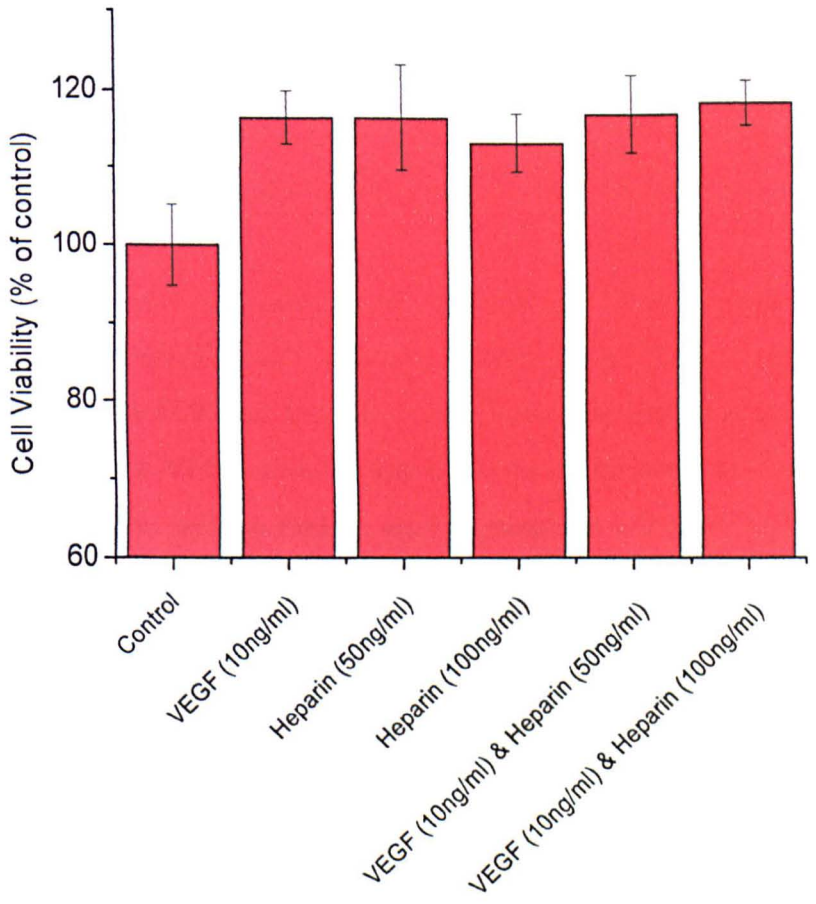


**Figure 7.3: Effect of combination of VEGF and heparin on the proliferation of endothelial cells over three days in serum-starved endothelial cell growth medium. Data expressed as percentage cell viability compared to cells with no VEGF or heparin present (TCP control) ± percentage SEM (N = 3, three replicates).**

As in the individual experiments, the addition of VEGF and heparin alone to the endothelial cell growth medium (2% FCS) led to an increase in cell viability in comparison to endothelial cell growth medium alone. No increase was observed when VEGF was combined with heparin (Figure 7.3), although a stimulatory effect was still observed, demonstrating that the combination of VEGF and heparin did not have a negative effect.

It was expected that a combination of VEGF and heparin could result in a synergistic effect, as both components stimulate endothelial cell proliferation individually. A similar study by Yamashita et al[338], employing bFGF instead of VEGF, on pulmonary artery endothelial cells showed that cell proliferation was increased by the addition of the growth factor (analysed up to 3 ng/ml) and by the addition of heparin with an optimum concentration of 100 ng/ml, followed by an inhibitory effect above 1000 ng/ml. These results were in agreement with the findings of this study. In contrast to this study, they found that a combination of bFGF and heparin lead to a further increase in cell viability with an optimum heparin concentration of 100 ng/ml, followed by a significant decrease in viability at 1000 ng/ml heparin and above.

A study by Weatherford et al[339] analysed the effect of VEGF and heparin in a fibrin glue on human aortic endothelial cell (HAEC) proliferation. It was reported that the combined addition of VEGF and heparin to the fibrin glue improved stimulation of the HAEC in comparison to VEGF alone at day 1, but no difference was observed by day 3. It was suggested by the authors that an early synergistic effect of VEGF and heparin occurs that plateaus at a level equal to VEGF alone by day 3. It is possible that this is also the case in this study as the cell viability was analysed at day 3 only, so any synergistic effect occurring at other time points would not have been seen. It would therefore be necessary to repeat this study with analysis at a number of time points to either confirm or refute this hypothesis.

These results confirm VEGF and heparin to be slightly stimulatory to endothelial cell viability over three days. Hence whether VEGF is released from the hydrogel alone or bound to the heparin one might expect stimulation of cell viability, and so in either event the release of VEGF from a hydrogel may still have the desired effect.

## 7.2 Effect of VEGF- and Heparin-Bound Peptide-Functionalised Hydrogels on HDMEC Proliferation

It has already been discussed in this thesis that VEGF has a significant effect on HDMEC proliferation (Figure 7.1) and that the hydrogels produced bind and release VEGF, especially the PNDRRR hydrogel. A study was then carried out to determine the effect of VEGF released by the hydrogels on HDMECs (Figure 7.4). This study was carried out simultaneously in both endothelial cell growth medium containing 5% serum, and in "starved" endothelial cell growth medium containing only 2% serum. For the experiment carried out in starved medium the endothelial cells were serum-starved overnight in 2% serum prior to the experiment. Starved medium containing only 1% serum was initially trialled but a very low cell viability was observed after the required experimental time period, and so 2% serum medium was selected. Both serum and serum-starved environments were investigated to determine whether the hydrogels may have more effect in one of these environments. Investigations into the four hydrogel types (PND, PNDA, PNDKKK and PNDRRR), as hydrogel alone, heparin-bound and VEGF- and heparin-bound, were carried out in a combined experiment.

For this investigation the hydrogels were prepared as described previously and were washed in sterile PBS before use in cell culture. Firstly, heparin was bound to the hydrogels by soaking the hydrogels in a 1 mg/ml heparin solution (PBS) for 24 hours at room temperature with gentle agitation. The hydrogels were then washed in sterile PBS seven times to remove unbound polysaccharide. To then bind VEGF, the heparin-bound hydrogels were soaked in a 200 ng/ml VEGF solution (PBS) at 4°C for 24 hours with gentle agitation, followed by three PBS washes to remove any unbound protein.

The hydrogels, alone, heparin-bound and VEGF- and heparin-bound, were then placed in a 48 well plate and allowed to equilibrate in the appropriate medium for 2 hours. The cells were then seeded into the well (10,000 cells per well), allowing the cells to attach to either the hydrogels or the tissue culture plastic surrounding the hydrogels. The medium was replaced on both the serum and serum-starved experiments daily. This was necessary for the serum-starved experiment to give a quantifiable cell viability and was also carried out in the 5% serum experiment to ensure that the results were comparable. An MTT assay was carried out after three days.

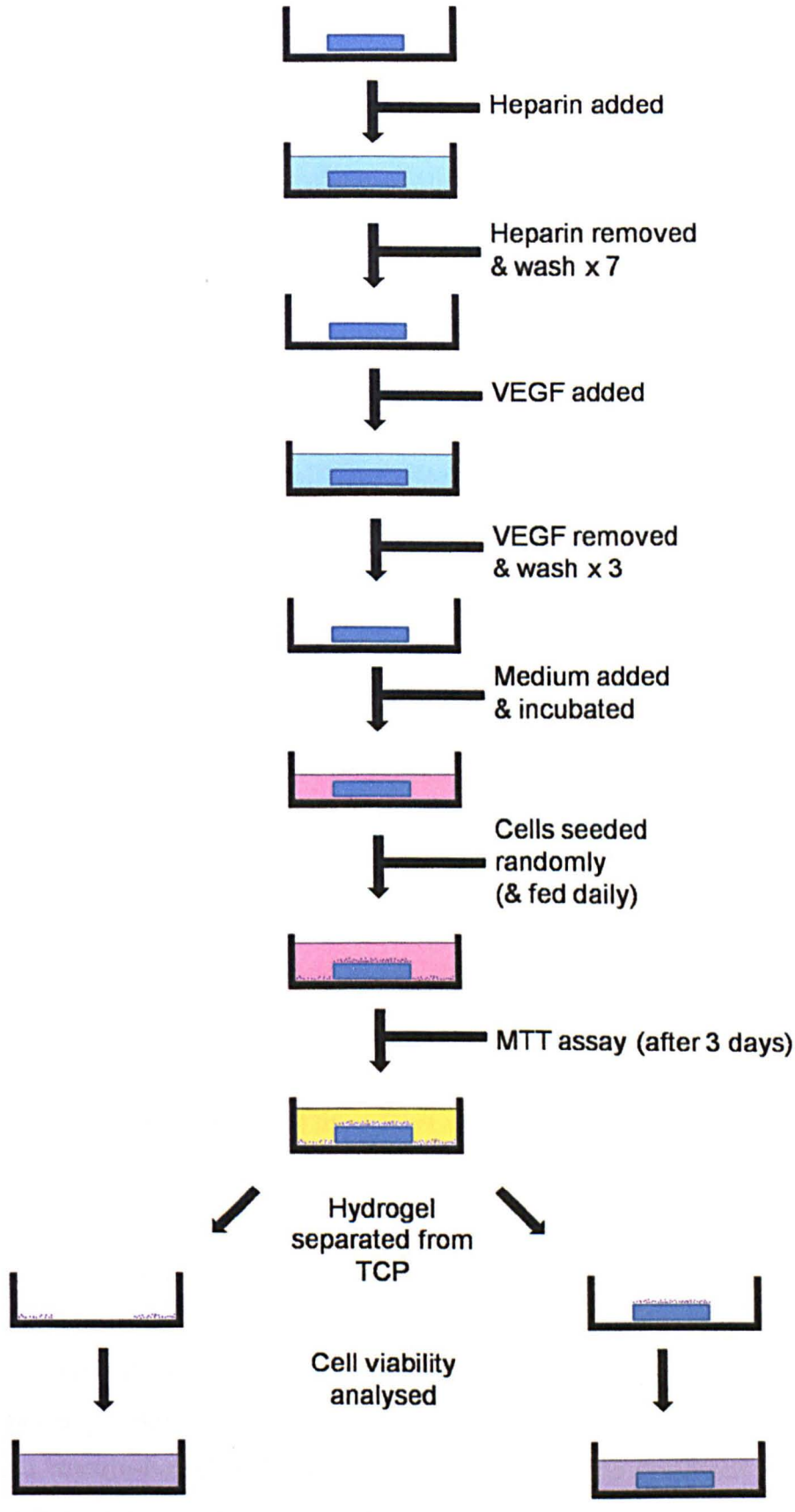


**Figure 7.4: Schematic of experiment to determine effect of VEGF released from hydrogel on endothelial cell proliferation. Experiment carried out in both serum medium (5% FCS) and serum-starved medium (2% FCS).**

### 7.2.1 Effect of VEGF- and Heparin-Bound Hydrogels (5% Serum Medium)

This experiment was carried out in triplicate in medium with 5% serum and the results for the quantitative MTT assay of cells in indirect contact with the hydrogels are shown in Figure 7.5. Significance within each experiment was determined by one-way ANOVA with Tukey post-hoc analysis (Family error rate = 5). In all cases, the morphology of the cells present on the TCP in indirect contact with the hydrogels was standard for endothelial cells, i.e. they appeared to resemble cobblestones.

When considering these results (Figure 7.5), for repeats 1 and 2, no significant effect was observed due to the presence of the PND hydrogel, either alone, heparin-bound or VEGF- and heparin-bound. A significant effect ($p < 0.05$) was observed for repeat 3 between the control and the PND hydrogel. However, overall these three experiments show no significant effect when the cells were in the presence of any of the PND hydrogels, even though the ELISA results discussed in Section 5.2 show that over the three-day period 19.8 ng VEGF would be released into the medium for the VEGF- and heparin-bound PND hydrogel. A similar result was found for the PNDA hydrogel. Although a significant increase in cell viability from the TCP control was observed in one of the repeats for the heparin-bound PNDA hydrogel ($p < 0.05$) and in one of the repeats for the VEGF- and heparin-bound PNDA hydrogel ($p < 0.05$), no overall effect of the PNDA hydrogels was observed. This VEGF- and heparin-bound hydrogel was also shown by ELISA to release VEGF over a three-day period.

In contrast, the presence of the PNDKKK hydrogels led to an increase in cell viability in two of the three experiments, but the only result that achieved significance ($p < 0.05$) was observed for the heparin-bound hydrogel in comparison to the TCP control in repeat 2. No overall trend was shown for the PNDKKK hydrogels in this study. In all cases in the PNDRRR hydrogel study, the heparin-bound hydrogel and the VEGF- and heparin-bound hydrogel were shown to lead to a higher viability of cells in indirect contact with the polymers than the control and PNDRRR-hydrogel alone. This increase was significant ($p < 0.01$) in two of the three experiments. The increase observed for the VEGF- and heparin-bound hydrogel was as expected, as the PNDRRR hydrogel was shown to release more VEGF (27 ng) over the 72 hour period than the other hydrogels. Interestingly, in all three experiments the heparin-bound PNDRRR hydrogel produced a larger increase in proliferation than the VEGF- and heparin-bound PNDRRR hydrogel.

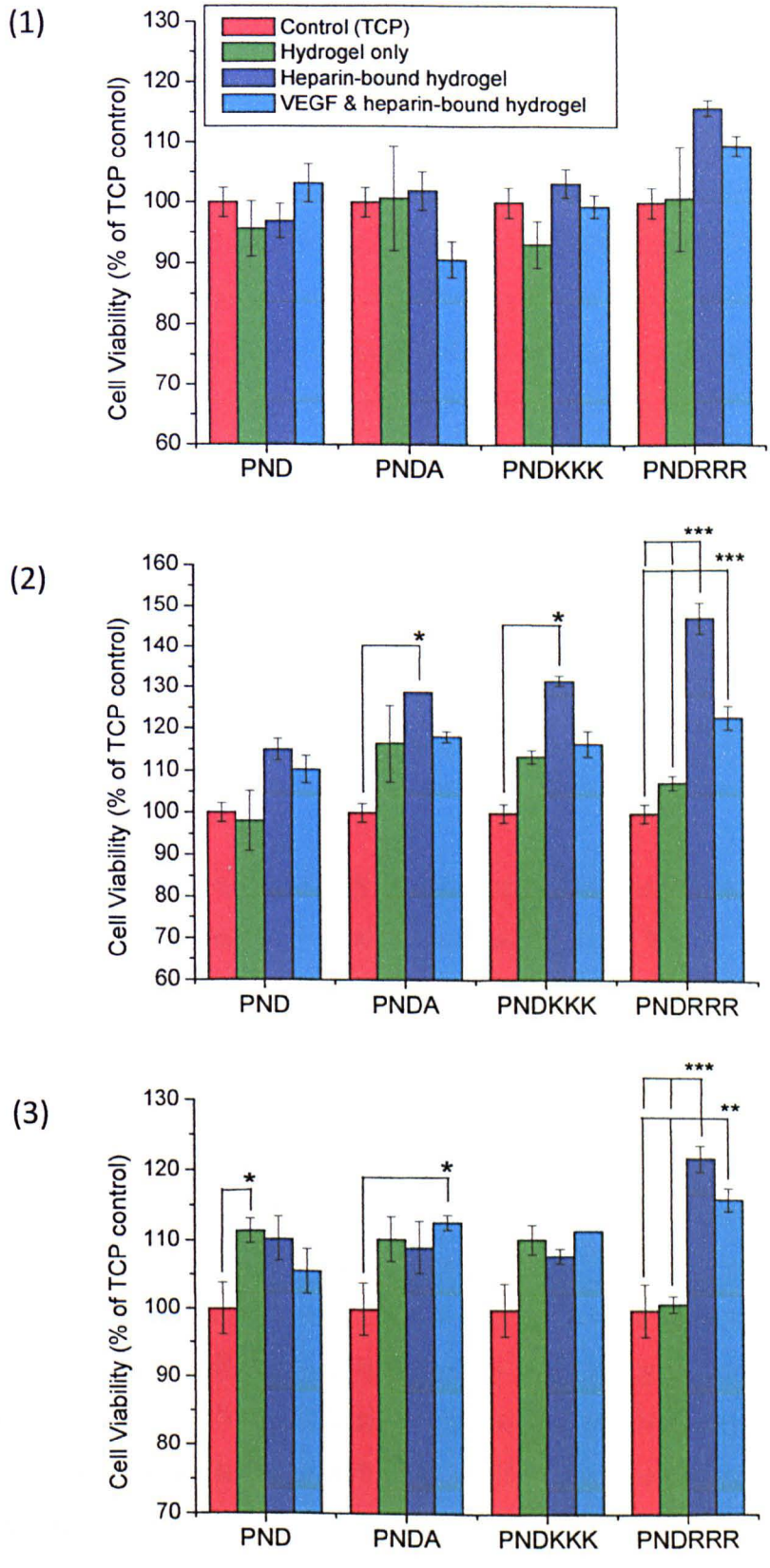


**Figure 7.5: Effect of VEGF- and heparin-bound hydrogels on endothelial cells in indirect contact, cultured in serum-containing medium (5% FCS) for three days. Results of three repeat experiments shown individually. Data expressed as mean percentage of TCP control (shown in red) ± percentage SEM (3 replicates per experiment). Significance assessed using one-way ANOVA with post-hoc Tukey analysis (*$p < 0.05$, **$p < 0.01$, ***$p < 0.001$).**

The Mann Whitney U Test was used to analyse the combined results of the three repeats, and showed that only the heparin-bound PNDRRR material gave a significant cell viability increase from the control and PNDRRR-hydrogel alone ($p < 0.01$). The heparin-bound PNDRRR hydrogel leading to a significant increase in cell viability over the three repeats as opposed to the VEGF- and heparin-bound PNDRRR hydrogel was an unexpected result. One hypothesis to explain this is that the heparin-bound PNDRRR hydrogel would be able to bind a number of proteins present in the serum in the medium as opposed to only containing VEGF. This combination of proteins may have had more of a significant effect on the proliferation of the endothelial cells than VEGF alone. In this experiment the medium was replaced daily, and so the heparin-bound PNDRRR hydrogel may have been able to store the required components of the medium and release them over the course of the experiment, thus leading to an increase in cell viability. Also any effects of VEGF may have been masked by the presence of a high quantity of proteins in the foetal calf serum, thus not leading to any significant increase in cell proliferation. This however is speculation and was not investigated further in this study.

This experiment also allowed analysis of the cell attachment capabilities of the hydrogels either alone, bound with heparin or bound with VEGF and heparin. As discussed in Chapter 6, the number of cells present on the polymer after three days was so low that these could be visualised using MTT assay but not quantified.

The MTT assay images (Figure 7.6), taken after three days in culture, show that there was no real difference in the number of cells attached to any of the polymers when alone, heparin-bound or VEGF- and heparin-bound. No cells were present on any of the PND polymers in all three repeats, and there were very few cells on any of the PNDA materials. An increase in cell number occurred as the hydrogels were functionalised with the trilysine peptide (PNDKKK), although the cell number was still low and no effect was seen when either heparin or VEGF and heparin were bound. As in the four day experiment (Figure 6.10), a considerably higher number of cells were present on the PNDRRR hydrogel in all three cases in all three repeats. From these results it was concluded that no significant effect was observed for the number of cells attaching to the polymers when either heparin alone or VEGF and heparin were bound to the hydrogels.

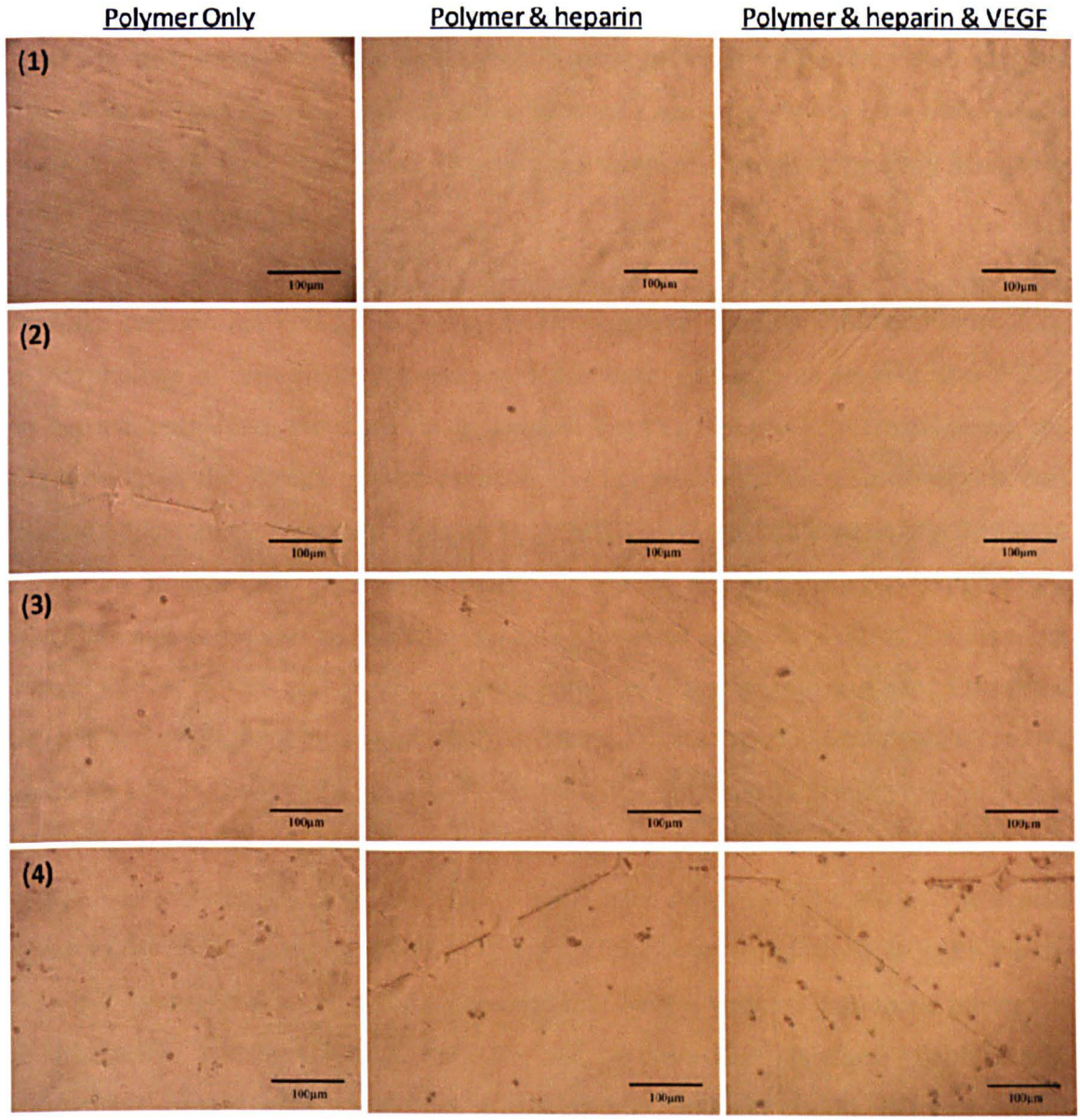


**Figure 7.6: Results of endothelial cell culture experiment in 5% FCS endothelial cell growth factor medium with hydrogels alone (column 1), heparin-bound hydrogels (column 2) and VEGF- and heparin-bound hydrogels (column 3). Endothelial cells shown are those on top of the hydrogels after three days, stained with MTT. Row (1) PND (2) PNDA (3) PNDKKK (4) PNDRRR**

In all of the MTT images (Figure 7.6) for cells attached to the hydrogels, the cells appear rounded, stressed and not well attached to the material. However, visual analysis of the cells showed that, for the PNDRRR hydrogels only, this is not how they appear prior to the MTT assay, suggesting that in these cases their appearance may be due to the MTT staining procedure.

When the cells on the PNDRRR hydrogels are observed without staining (Figure 7.7), the morphology of the cells present on top of the hydrogels vary as heparin, and VEGF and heparin combined, are added to hydrogels. For the PNDRRR hydrogel alone, the cells present on the surface appear rounded and not well attached. Conversely, a very different appearance is observed when the PNDRRR hydrogel has heparin attached to it. In this case, a large proportion of the cells have a long, thin and stretched morphology, often shown to be emanating out from a small cluster of cells. This effect is even more obvious for the VEGF- and heparin-bound hydrogels, where a large number of stretched cells are observed, the majority of which originate from a small cluster of cells. In this case, with VEGF present, the stretched cells are often shown to be joining two groups of cells. These stretched cells are present on both the heparin-bound and VEGF- and heparin-bound hydrogels from days 1 to 3 in all three repeats of this study. These cells appear to be more strongly attached to the hydrogels in comparison to cells on the PNDRRR hydrogel alone. The cells also appear to be less stressed than those present on the PNDRRR hydrogel alone, and do not possess the standard "cobblestone" morphology usually observed within a proliferation study in endothelial cell growth medium on tissue culture plastic.

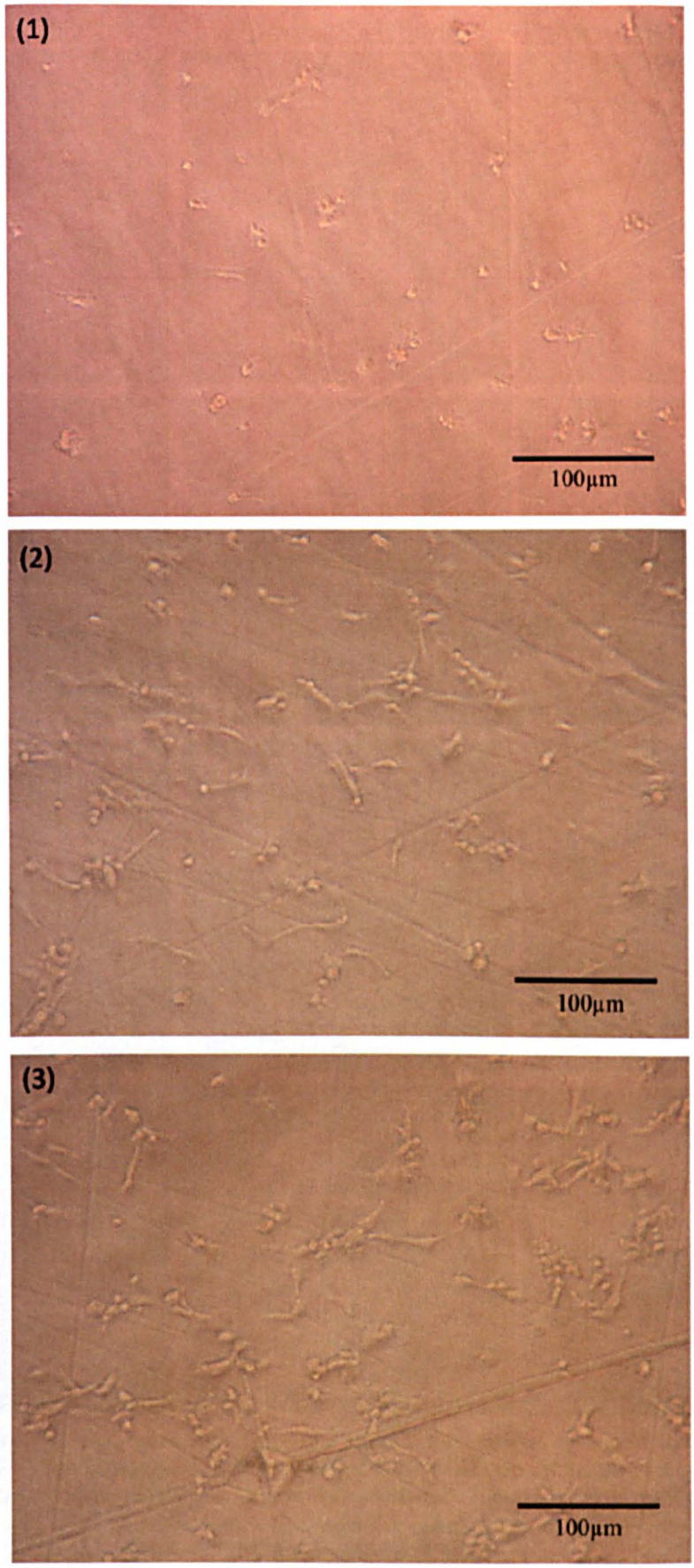


**Figure 7.7: Endothelial cells on top of RRR-functionalised hydrogels (PNDRRR) with no staining after 24 hours in 5% serum medium. (1) PNDRRR hydrogel alone (2) Heparin-bound PNDRRR hydrogel (3) VEGF- and heparin-bound PNDRRR hydrogel.**

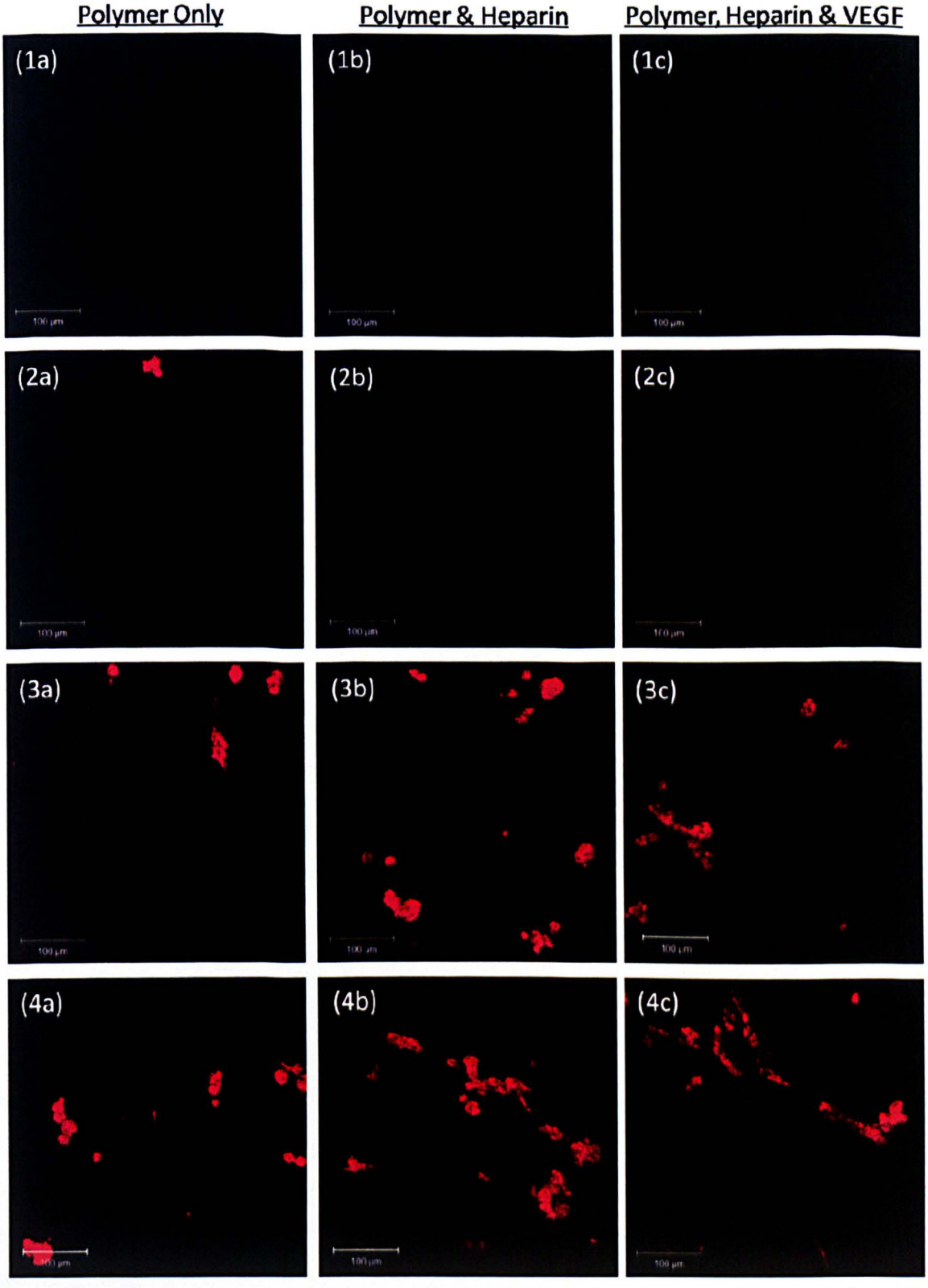


**Figure 7.8: Human dermal microvascular endothelial cells cultured on top of hydrogels in media containing 5% FCS for 72 hours. Cells were stained with CellTracker™ Red and imaged on a Zeiss LSM 510 confocal microscope (abs. 577 nm and em. 602 nm). Images (a) cells on top of the hydrogel alone, (b) cells on top of heparin-bound hydrogel (c) cells on top of VEGF- and heparin-bound hydrogel. Row (1) PND (2) PNDA (3) PNDKKK (4) PNDRRR.**

In order to confirm the change in morphology observed upon binding heparin and VEGF to the polymers, images were taken of cells stained with CellTracker™ Red (Figure 7.8). The cells were stained prior to the experiment to minimise stress to the cells attached to the polymer during the experiment. In all cases the cells in indirect contact were found to be present on the TCP with standard morphology (Figure 7.9 is representative of all wells analysed). It was noted that lower strength signals were consistently observed for endothelial cells compared to fibroblasts.

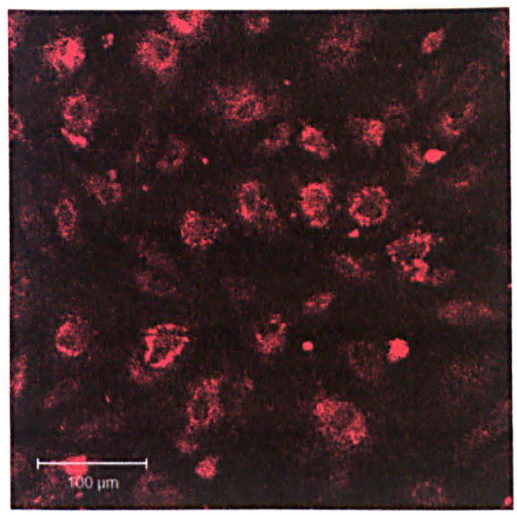


**Figure 7.9: Human dermal microvascular endothelial cells cultured in indirect contact with RRR-hydrogel (PNDRRR) in 5% FCS medium for 72 hours. Cells were stained with CellTracker Red and imaged on a Zeiss LSM 510 confocal microscope (abs. 577 nm and em. 602 nm).**

When looking at cell attachment, for the PND hydrogels, the results were the same as observed by MTT, with no cells present on the polymers. A very low number of cells were also observed for the PNDA hydrogels in all three cases. For the PNDKKK hydrogels a number of cells were observed on the surface of all three hydrogels after the washing procedure for CellTracker™ Red, showing that these cells were reasonably well attached, although a number of less well attached cells were detached during these washing steps. Again, no significant difference was observed for the PNDKKK hydrogel alone, heparin-bound, or VEGF- and heparin-bound. A number of cells were washed off during the CellTracker™ Red procedure on the PNDRRR hydrogels, showing these cells are still relatively loosely attached, but cells were present on the PNDRRR hydrogel alone, as well as on the heparin-bound and VEGF- and heparin-bound PNDRRR hydrogels. The cells remaining attached to the PNDRRR hydrogel alone appear rounded, whereas the images of the heparin-bound and VEGF- and heparin-bound hydrogels show stretched cells joining small clusters of cells together, confirming the visual analysis prior to staining.

### 7.2.2 Effect of VEGF- and Heparin-Bound Hydrogels (Serum-Starved Medium)

In the serum-starved experiment (Figure 7.10), there were no significant differences or obvious trends observed for either the PND polymers or the PNDA polymers.

However, for the trilysine-functionalised materials (PNDKKK), the heparin-bound and VEGF- and heparin-bound hydrogels were consistently shown to increase cell viability in this study, with the VEGF- and heparin-bound hydrogel giving the largest increase, which was found to be significant ($p < 0.05$) in two repeats. A similar result, an increase in cell viability for the heparin-bound hydrogel and the VEGF- and heparin-bound hydrogel, was obtained for the PNDRRR polymers, and in all cases the increase observed was always larger than that observed for the trilysine material. The VEGF- and heparin-bound PNDRRR polymer consistently led to a considerably larger increase than the heparin-bound PNDRRR material, and the improvement in cell viability for the VEGF- and heparin-bound PNDRRR hydrogel in comparison to the TCP control and PNDRRR hydrogel alone was shown by a one-way ANOVA with post-hoc Tukey analysis to be significant ($p < 0.01$) in all repeats.

In contrast to the study in serum-containing medium, this study showed the VEGF- and heparin-bound PNDRRR hydrogel to have the most significant effect on endothelial cell proliferation rather than the heparin-bound PNDRRR hydrogel as found in 5% serum medium. This is as would be expected as the PNDRRR hydrogel was shown to release a higher quantity of VEGF over the 72 hour study period than any of the other hydrogels. It is expected that this is due to the fact that this study was carried out in a serum-starved environment, and so unlike the serum-containing experiment, the heparin-bound hydrogel was unable to bind as much protein from the medium to release over the experiment and thereby affect the proliferation of the endothelial cells. The lack of protein in the medium meant that the VEGF released from the VEGF- and heparin-bound PNDRRR hydrogel could have a more significant effect on the endothelial cells than in 5% serum medium. The effect of serum reduction from 5% to 2% on cells on TCP can be seen in Figure 7.11. The ELISA study carried out showed that VEGF was released over the whole of the 72 hour period and therefore would have been able to have a significant effect on the cells, despite the medium being replaced daily.

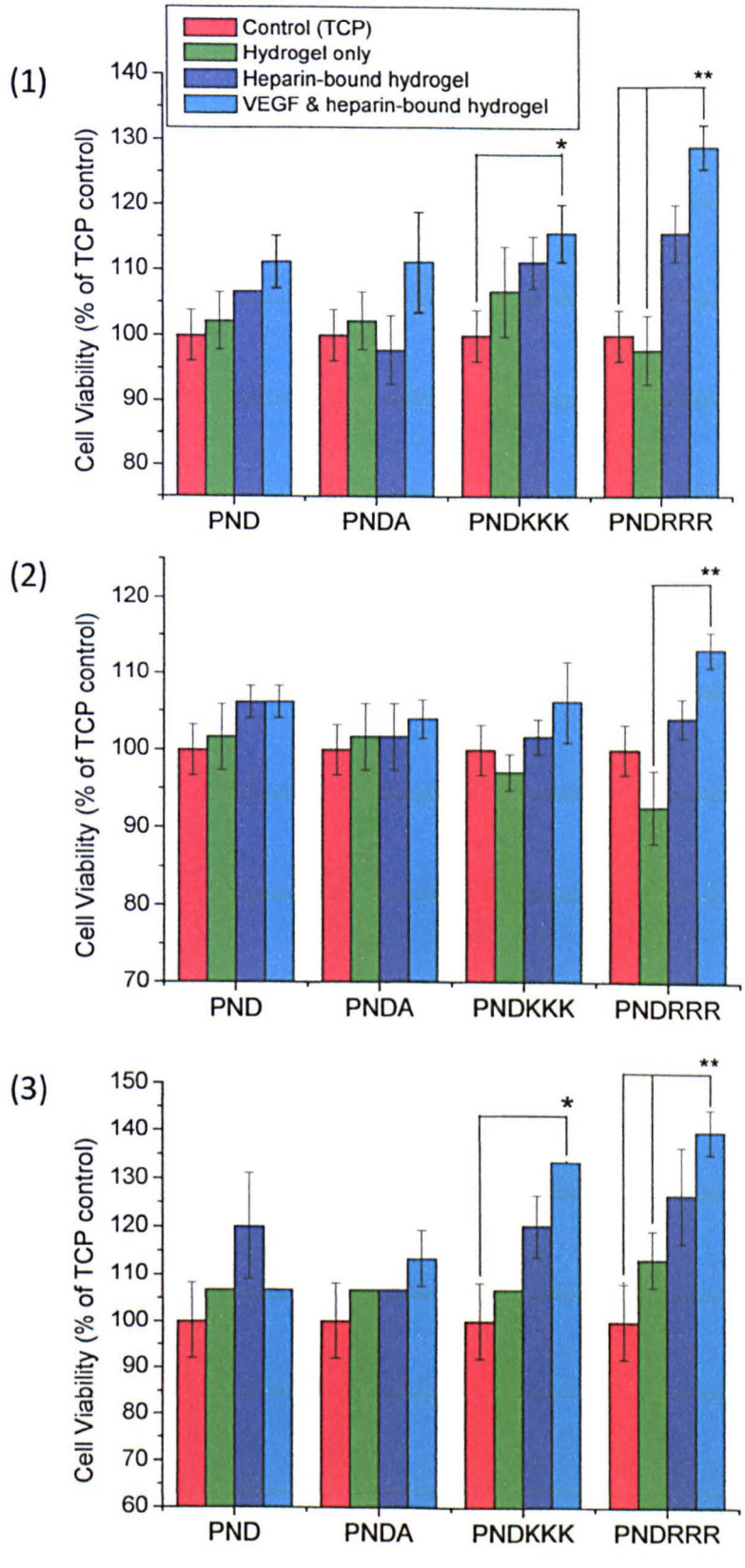


**Figure 7.10: Effect of VEGF- and heparin-bound hydrogels on endothelial cells in indirect contact, cultured in serum-starved medium (2% FCS) for three days. Results of three repeat experiments shown individually. Data expressed as mean percentage of TCP control (shown in red) ± percentage SEM (3 replicates per experiment). Significance assessed using one-way ANOVA with post-hoc Tukey analysis (*$p < 0.05$, **$p < 0.01$, ***$p < 0.001$).**

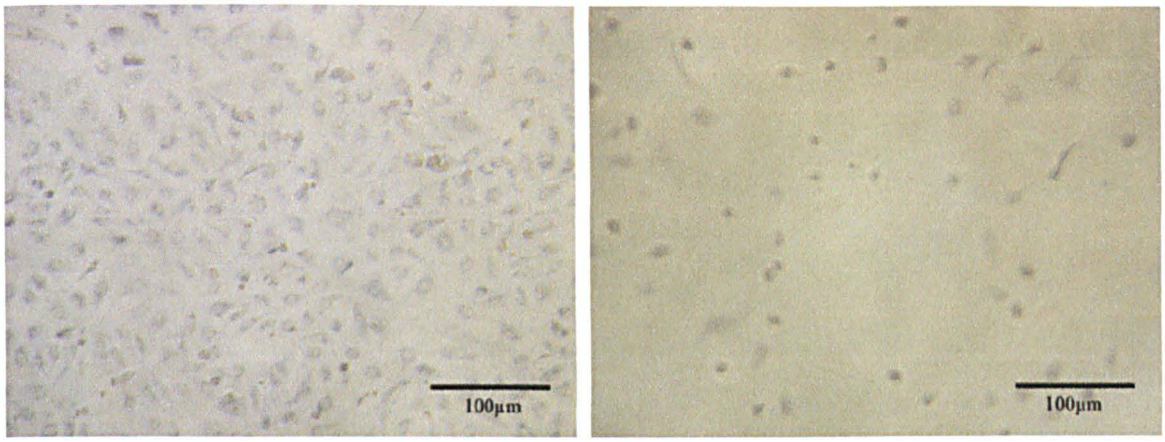


**Figure 7.11: Endothelial cells cultured for three days in 5% serum (left) and 2% serum (right) endothelial cell growth medium. Cells shown are cells present on TCP, stained with MTT.**

Quantitative analysis of cell attachment in serum-starved medium (Figure 7.12) shows a similar trend to that observed in serum-containing medium, although the overall number of cells observed is considerably lower. This suggests that the attachment observed in the serum-containing medium is dependent on the proteins present in the foetal calf serum.

No cells are present on any of the PND polymers, and a very low number of cells are observed on the PNDA and PNDKKK materials for the hydrogels alone, with heparin and with VEGF and heparin. For the PNDRRR hydrogel, a low number of cells attached to the polymer alone in all three repeats. The number of cells did increase upon heparin binding and VEGF binding, although the number of cells was still low in comparison to the serum-containing medium.

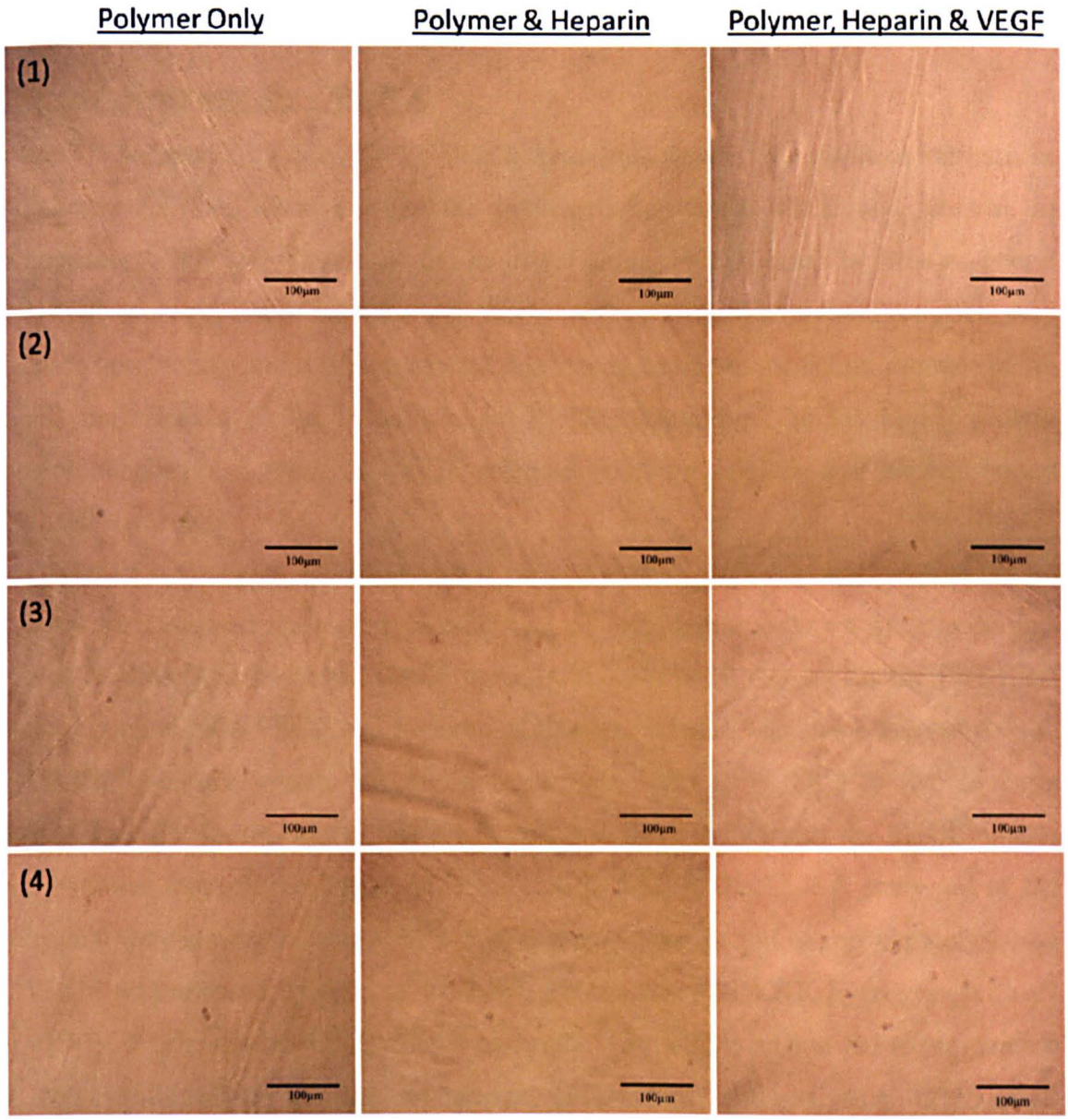


**Figure 7.12: Results of endothelial cell culture experiment in 2% FCS "serum-starved" endothelial cell growth factor medium with hydrogels alone (column 1), heparin-bound hydrogels (column 2) and VEGF- and heparin-bound hydrogels (column 3). Endothelial cells shown are those on top of the hydrogels after three days, stained with MTT. Row (1) PND (2) PNDA (3) PNDKKK (4) PNDRRR**

## 7.3 Discussion of Proliferation Data

### *Cells in Indirect Contact – On TCP*

In the 5% serum study, only the PNDRRR hydrogels showed a consistent increase in endothelial cell proliferation when the hydrogels contained VEGF and heparin, in comparison to the TCP control or the hydrogel alone. In this case, the heparin-bound PNDRRR hydrogel led to the most significant increase in proliferation. This effect was discussed previously and it was suggested that it may be due to the serum proteins being bound and released by the heparin-bound PNDRRR hydrogel, or the higher protein content masking the effect of VEGF released from the VEGF- and heparin-bound PNDRRR hydrogel.

The results discussed show that proliferation of endothelial cells on TCP in serum-starved medium was increased significantly ($p < 0.01$) in all repeats for the PNDRRR hydrogel bound with VEGF and heparin. A smaller increase was also observed for the PNDKKK hydrogel, which was found to be significant ($p < 0.05$) in two of three repeats. In order to understand this result it is necessary to consider the VEGF release data obtained through the VEGF ELISA (Section 5.2). In the ELISA study, all of the hydrogels were shown to release VEGF over the 72 hour period. Approximately 20 ng of VEGF was released by each of the PND, PNDA and PNDKKK hydrogels, with 27 ng of VEGF released by the PNDRRR hydrogel. The VEGF release led to an increase in cell proliferation for the triarginine (PNDRRR) and trilysine (PNDKKK) functionalised materials but no significant increase was observed for the PND and PNDA materials, despite the 20 ng of VEGF released by each polymer.

It is possible that the significant increase in endothelial cell proliferation observed for the VEGF- and heparin-bound PNDRRR hydrogel was simply due to the increased VEGF concentration in the medium in comparison to the control and also the other hydrogels, but it is hypothesised that there may also be other factors involved. The feasibility of the involvement of other factors is also suggested when considering the results for the VEGF- and heparin-bound PNDKKK hydrogel. In this case an increase in proliferation was observed in comparison to the control, which was found to be significant in two of three repeats. This increase was observed for PNDKKK but no increase was observed for the PND or PNDA materials, despite equal quantities of

VEGF being released by each of these hydrogels, as determined by an ELISA. These results therefore suggest that the observed improvement in endothelial cell proliferation may be due to both the amount of VEGF released, and also to how VEGF is bound to, and released by, the polymer.

In Chapter 5, a quantitative heparin-binding study was carried out, complemented by an XPS study. These experiments showed that 0.117 mg of heparin was bound per milligram of PNDRRR polymer, 0.077 mg of heparin was bound per milligram of PNDKKK polymer and 0.030 mg of heparin was bound per milligram of PNDA polymer, although in this case the measurement error was high. From these results it is suggested that the method of VEGF binding would differ for each hydrogel. The high quantity of heparin bound by the PNDRRR polymer would suggest that a large amount of the VEGF bound to this hydrogel would be bound through the heparin present. It is expected that this would be similar for the PNDKKK hydrogel, although the lower heparin content may have led to the lower VEGF content. A low amount of heparin was found to be present on the PNDA hydrogels, thus suggesting that, in this case, the VEGF present may have been bound directly to the polymer, possibly through hydrogen bonding with the acid functionality. Although no analysis has been carried out on the heparin content for the PND hydrogel, it is expected to have a low heparin content and so it is likely that the VEGF in this hydrogel would also be bound directly to the hydrogel via non-covalent interactions.

Through consideration of heparin and VEGF binding studies, as well as cell culture results, it is thought that increases in cell proliferation coincide with the likelihood that VEGF is bound via heparin to the hydrogel. It is therefore hypothesised that the presence of heparin plays an important role in the ability of these hydrogels to stimulate endothelial cell proliferation. The exact method for this would need to be investigated further, but it is known that in the ECM, heparin and heparan sulphate are thought to influence growth factors in a number of different ways. The heparin utilised in this study may also be having a similar effect on VEGF in the following ways.

*Protection and Maintenance of Bioactivity*

One significant effect of this method of VEGF delivery may be due to the stability of the protein. The half-life of this protein *in vivo* is very short, with free VEGF being

degraded in less than one hour after a bolus injection[63-66]. Endothelial cell-derived heparan sulphate was shown by Saksela et al[340] to protect bFGF from proteolytic degradation. Soluble bFGF was shown to be readily degraded by plasmin, whereas when the growth factor was bound to heparan sulphate it was protected from degradation. This protection was not seen after treatment of the heparan sulphate with heparinase. The protein may also be degraded by physical factors *in vitro* and it is suggested that this may be reduced if the growth factor is bound to heparin. In a study by Gosporarowicz et al[341], heparin was shown to have a significant protective effect for basic and acidic FGF. Heparin was able to prevent a decline in potency upon storage of FGF at -80°C as well as in acidic conditions and with short heat exposure. Brandner et al[342] reported that heparin binding to VEGF stabilised the protein in a number of tests, and thereby concluded that GAG binding *in vivo* may stabilise the active conformation of this growth factor. The role of the polysaccharide is also in agreement with results from Huang et al[259], who produced VEGF-loaded nanoparticles with self-assembled polyelectrolyte complexes. It was noted that in this study binding with a polyelectrolyte was shown to stabilise VEGF and release bioactive protein in a sustained manner.

*Storage and Release*

The ability of heparin to bind growth factors means that in biology it is expected that heparin, in heparan sulphate form or as a heparan sulphate proteoglycan, is able to act as a growth factor reservoir. Studies on FGF have shown that basic fibroblast growth factor-heparan sulphate complexes can be released from such a reservoir by proteolysis of the proteoglycan[343], as well as the release of basic FGF by partial degradation of the heparan sulphate by heparanase[344]. Salbach et al[345] report from an *in vivo* study of hepatocyte growth factor (HGF) (a heparin-binding growth factor) in humans that the administration of heparin resulted in a strong and rapid increase in HGF serum levels. It was suggested that HGF is dissociated from the cellular surface and the ECM into circulation by the heparin.

*Growth Factor-Heparin Complex*

In 1991, Yayon et al[346] showed that the high affinity binding of bFGF to its receptor requires prior low-affinity binding to free heparin or heparan sulphate. Thus heparin plays an important role in the interaction of this growth factor with its receptor. It was suggested by the authors that this may be due to a conformational change in basic FGF

upon heparin binding to enable the FGF to bind with the receptor. Heparin related species also play an important role in the binding of VEGF to its receptor. The binding of $VEGF_{165}$ to vascular endothelial cells is strongly modulated by cell surface associated heparin-like molecules, and can also be modulated by the addition of exogenous heparin[44]. The most significant effect of heparin was observed for unfractionated heparin or heparin fragments longer than 22 sugar units[47]. The therapeutic effect of the VEGF-GAG interaction on VEGF potency has been demonstrated by the use of synthetic GAG mimetics. Carboxymethylbenzylamine dextrans inhibit $VEGF_{165}$ activity by interfering with heparin binding to $VEGF_{165}$ and $VEGF_{165}$-KDR receptor complexes[347], whereas a carboxymethyl dextran sulphate was shown to potentiate $VEGF_{165}$-induced proliferation and migration of HUVEC[348].

*Conclusion*

The results in both serum and serum-starved media show that the PNDRRR hydrogel in particular is able to bind heparin, which can in turn bind heparin-binding proteins, including VEGF. The subsequent release of VEGF and the effect on cell culture was most successfully demonstrated in the serum-starved environment, in which the presence of the VEGF- and heparin-bound PNDRRR hydrogel led to a statistically significant increase in endothelial cell proliferation over three days.

***Cells in Direct Contact – On Hydrogel Surface***

During both the 5% serum and the serum-starved study, there are more cells present on the PNDRRR hydrogel than the other hydrogel types. In the serum-starved experiment, a slight increase in cell number on the PNDRRR hydrogel was qualitatively observed as VEGF and heparin were present in the hydrogel, although this effect was not observed in the 5% serum experiment. In all cases the cells were thought to be relatively weakly bound to the hydrogel, as the majority of cells were removed during any washing procedure. This is a positive observation for the intended application, as it would be desirable to remove the hydrogel after treatment in a wound healing application without also removing the healing tissue.

In the 5% serum experiment, the cells on the VEGF- and heparin-bound PNDRRR materials have a stretched morphology not observed for the PNDRRR hydrogel alone. Endothelial cells are anchorage-dependent cells which adhere to extracellular matrix proteins or a substrate at focal adhesion points[349], which consist of a complex network of ECM, membrane and cytoplasmic components [350]. These anchorage sites play a critical role in maintaining the shape of the cell and differentiation, as well as in proliferation and migration[351]. When adhering to biomaterials, cell-material binding could be either non-receptor-mediated cell adhesion via weak non-covalent bonds directly to the material, or receptor-mediated and signal transmitting cell adhesion mediated by ECM molecules[352]. In the latter case, anchorage-dependent cells bind specific amino acid sequences of those molecules through integrin receptors. It is discussed by Oezyuerek et al[353] that GAGs provide specific cell adhesion ligands, and that cell surface receptors, including selectins, bind to sulphated GAG ligands on cell surfaces, in the ECM or on artificial materials.

It is expected that the poor cell adhesion observed for the hydrogel without heparin is due to weak interactions directly between the materials and the cells. The heparin-bound hydrogels allow specific cell adhesion either directly to the heparin, or to ECM proteins which have been tethered to the hydrogel via the sulphated heparin, thus allowing adhesion of endothelial cells which appear to be well attached due to the stretched morphology. These results are in agreement with those for glycol-block copolymers reported very recently by Oezyuerek et al[353].

It is observed that a number of the endothelial cells present on the VEGF- and heparin-bound PNDRRR hydrogels in 5% serum have a stretched morphology, and are stretching between groups of cells, resembling the morphology of cells on Matrigel at the very beginning of tube formation. It was reported by Kubota et al[354] that endothelial cells are able to rapidly differentiate on a basement membrane-like matrix. Within this study it is possible that the presence of heparin on the hydrogels may allow accumulation of ECM molecules, either present within the medium or synthesised and deposited by the cells themselves, and thereby begin to more closely resemble an ECM-coated surface. It is feasible that this environment may then be able to begin to stimulate morphological differentiation of endothelial cells into tube-like structures.

## 7.4 Effect of VEGF- and Heparin-Bound Hydrogels on Angiogenesis – Tubule Formation Assay

As the ability of the hydrogels to stimulate endothelial cell proliferation has been demonstrated, it was decided to analyse the most effective hydrogel, the triarginine-functionalised polymer, for its ability to induce endothelial cell functions specific to angiogenesis. Angiogenesis requires a number of endothelial cell functions, including matrix degradation, migration and tubule formation, a process also referred to as morphogenesis and differentiation.

*In vitro* assays stimulating capillary-like tube formation usually involve culturing endothelial cells on matrices consisting of fibrin, collagen or Matrigel[355, 356]. Although there are problems with this procedure, namely whether lumen formation occurs[354], and that other cell types can also form networks[357], this tube-forming assay is a very popular *in vitro* assay for analysing pro- and anti-angiogenic treatments.

In this case Matrigel was employed as the matrix. Matrigel is a mixture of basement membrane and extracellular proteins which have been derived from the mouse Engelbreth-Holm-Swarm sarcoma. It was shown by Kubota et al[354] that human umbilical vein endothelial cells seeded at certain densities are able to attach to Matrigel and rapidly form tubes which can be maintained for between 12 and 24 hours. Standard Matrigel is very rich in angiogenic growth factors and therefore it can be difficult to observe the effect of any pro-angiogenic treatment, as network formation occurs readily with no extra treatment. An alternative, growth factor (GF)-reduced Matrigel, is now available with markedly lower concentrations of the stimulatory growth factors, thereby reducing the problem of the treatment effect being masked by the standard Matrigel response. In this case a pro-angiogenic treatment is being studied and so GF-reduced Matrigel was employed.

Initially an experiment was carried out to determine the effect of soluble VEGF and heparin alone and VEGF and heparin combined on endothelial network formation on growth factor-reduced Matrigel. This was followed by an experiment to analyse the effect of the most successful polymer, the VEGF- and heparin-bound PNDRRR hydrogel, on tube formation.

### 7.4.1 Effect of Soluble Heparin and VEGF on Tube Formation

Prior to analysis of the effect of VEGF- and heparin-bound PNDRRR hydrogel on tube formation, the effect of heparin and VEGF on endothelial cell tube formation was determined both individually and combined. For this experiment, a layer of Matrigel was laid in a 48 well plate and incubated at 37°C for 1 hour to allow the Matrigel to set. Endothelial cells, which had been previously starved overnight in 1% serum medium, were then seeded in a small volume of serum-starved medium (1% serum) and allowed to attach before the addition of the treatment medium. The 48 well plate was then incubated at 37°C for six hours before imaging of the wells by light microscopy.

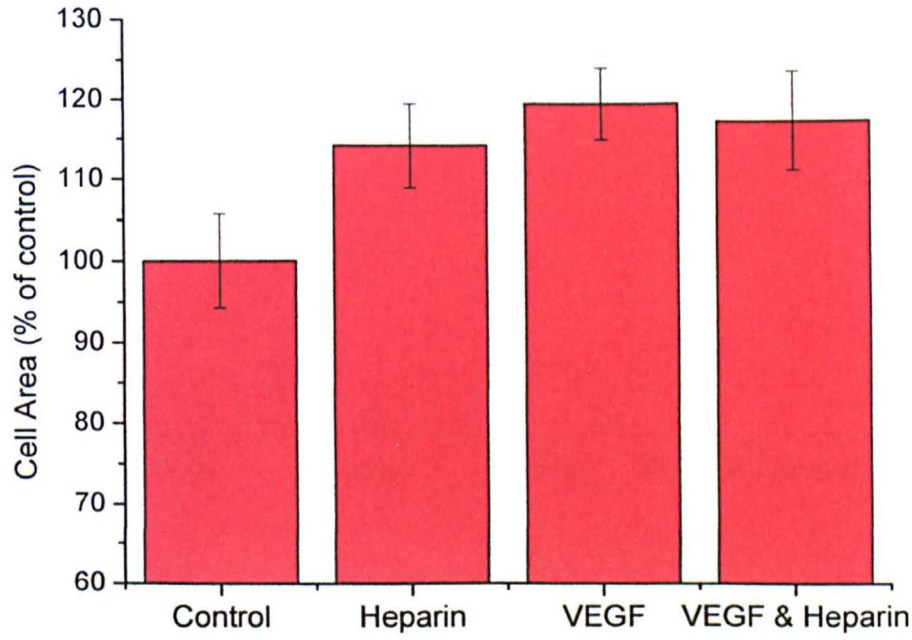


**Figure 7.13: Effect of heparin, VEGF and VEGF and heparin combined on cell area within a tubule formation assay. Data expressed as mean percentage of Matrigel control ± percentage SEM (three experiments with three replicates per experiment).**

The effect of VEGF, heparin and the two combined was measured by two methods, firstly by analysis of the cell area, and secondly by analysis of the length of tubes formed. Scion image (Frederick, MA) was employed to analyse these experiments. Cell area was determined by quantifying the area occupied by cells in each image. Average tube length was calculated by manually selecting and measuring ten tubes at random

from each image. In each case, a number of images were analysed for each environment.

When considering the effect on cell area (Figure 7.13), the addition of VEGF, heparin or the two combined led to an increase in cell area, although no significant statistical difference was observed overall.

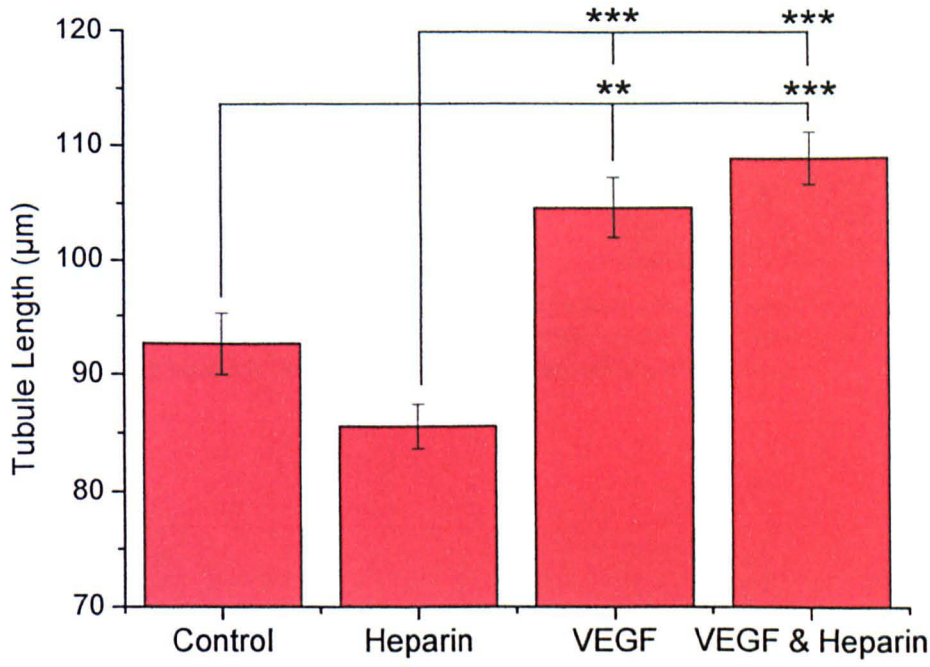


**Figure 7.14: Effect of heparin, VEGF and VEGF and heparin combined on tubule length within a tubule formation assay. Data expressed as mean percentage of Matrigel control ± percentage SEM (three experiments with three replicates per experiment). Significance assessed using one-way ANOVA with post-hoc Tukey analysis (*p < 0.05, **p < 0.01, ***p < 0.001).**

Tube length (Figure 7.14 & Figure 7.15) however was found to differ from the control upon addition of the growth factor and polysaccharide. The control well containing Matrigel only, with no further addition, was found to have an average tube length of 93 µm. This average tube length decreased slightly to 86 µm upon the addition of heparin, although variation in the results meant that no significant difference between the two was observed. Tube length increased to 105 µm upon the addition of VEGF and 109 µm for VEGF and heparin combined, which in both cases was a significant increase from the Matrigel control.

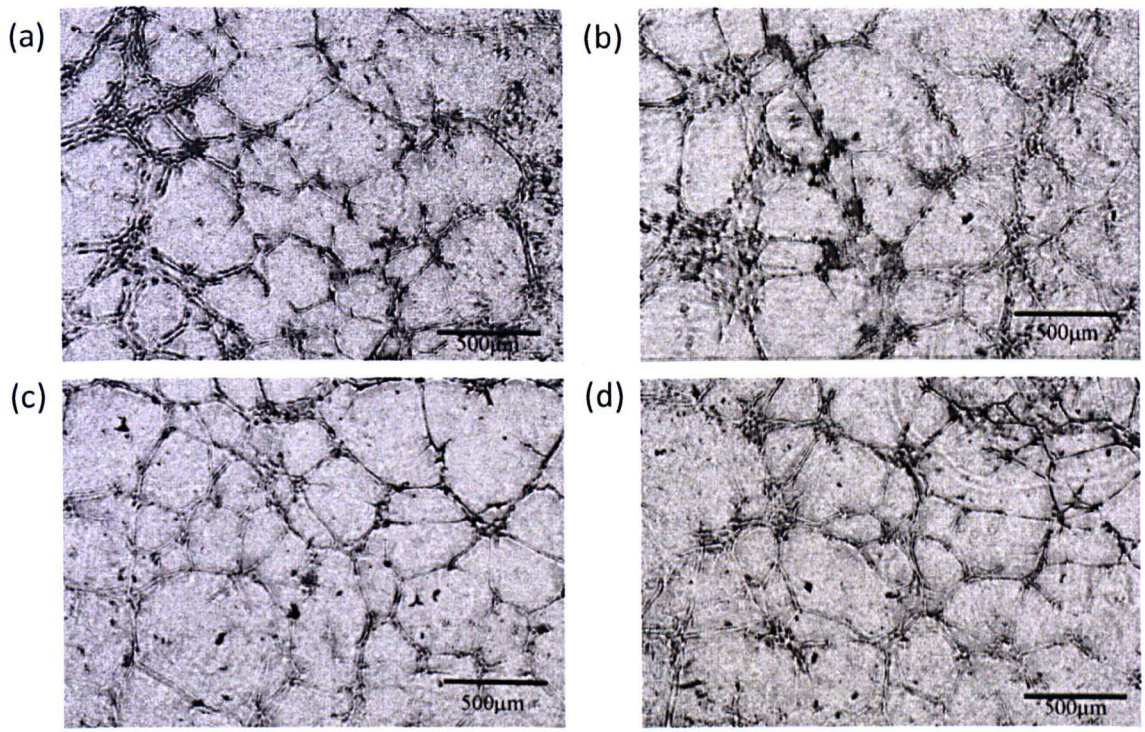


**Figure 7.15: Images of endothelial cells on Matrigel taken after six hours in serum-starved medium (1% serum) (a) control well (medium with no supplement) (b) heparin-containing medium (c) VEGF-containing medium (d) VEGF- & heparin-containing medium.**

### 7.4.2 Effect of VEGF- and Heparin-Bound RRR Hydrogel on Tube Formation

The final investigation in this study was to determine the effect of the VEGF- and heparin-bound PNDRRR hydrogel on two other aspects of angiogenesis, migration and tube formation.

Cell migration can be either random or directional. Directional endothelial cell migration occurs through three major mechanisms: haptotaxis, the migration towards a gradient of immobilised ligands; mechanotaxis, migration due to mechanical forces; and chemotaxis, migration towards a gradient of chemoattractive stimulus[20]. Analysis of endothelial cell migration is generally carried out by a wound healing assay[358] or by a variation of the method developed by Boyden[359], commonly referred to as the Boyden chamber. It is well known that soluble VEGF is able to induce endothelial cell migration in a concentration-dependent manner, but this process is a balance of many growth factors and integrin-stimulated signals, and therefore different cells and different conditions may lead to varying results[360]. Mastyugin et al[361] demonstrated human umbilical vein endothelial cell migration due to VEGF, and showed that migration was inhibited by the known VEGFR tyrosine kinase inhibitors PTK787 and AAL993. Shamloo et al[362] reported that HUVECs chemotax towards VEGF from 18-32 ng/ml VEGF and that the steepness of the VEGF gradient was shown to influence directional migration, whereas Barkefors et al[363] found that migration of endothelial cells occurred at stable gradients of 0-50 ng/ml over a distance of 400 μm.

The effect of chemotaxis on endothelial cells has also been observed for surface-density gradients. HUVEC attachment is affected by a RGDS peptide gradient on PEG hydrogels[364], and bovine aortic endothelial cells (BAECs) migrated on a surface-bound fibronectin gradient[365]. Liu et al[366] showed migration on material with immobilised VEGF and fibronectin. Gradients of both proteins stimulated directional migration and an increased effect was observed for the two combined in a 24-hour cell culture experiment. It has also been reported that endothelial cells guide outgrowing capillaries in response to the gradients of VEGF in retinal angiogenesis[367].

Angiogenic factors spatially affect the direction of tube formation during angiogenesis. This is well demonstrated by organ culture assays and *in vivo* assays. Popular methods

include the subcutaneous implantation of a polymeric material containing an angiogenic factor followed by analysis of the vessel growth into the plug of material[326], and the chick chorioallantoic membrane (CAM) assay[327], in which angiogenic factors can be placed on the CAM through a window in the eggshell. The angiogenic stimulator will then typically cause a radial rearrangement of blood vessels towards the implant and an increase of vessels around it. VEGF-induced angiogenesis in the CAM assay *in vivo*, as well as inhibition by anti-angiogenic factors, was nicely demonstrated by Benndorf et al[368].

It was hypothesised that VEGF released from the PNDRRR hydrogel would produce a VEGF gradient, and therefore may cause cell migration and spatially influence tube formation in an angiogenesis assay. A method to analyse both migration and tube formation simultaneously, whilst maintaining the simplicity of an *in vitro* experiment and minimising the effect of external factors, was designed to compare the effect of the VEGF- and heparin-bound PNDRRR hydrogel and the PNDRRR hydrogel alone (Figure 7.16). For this investigation the hydrogels were prepared as described previously in Chapter 4, and VEGF and heparin were bound as previously described in Section 7.2. After the final PBS wash the hydrogels were placed in 1 ml of serum-starved medium (1% serum) and allowed to equilibrate. Meanwhile, a layer of Matrigel was allowed to set in the wells of a 48 well plate before careful addition of one disc of hydrogel to each, avoiding disruption of the Matrigel layer. The cells, starved overnight prior to the experiment in 1% serum medium, were then randomly seeded into the well. The 48 well plate was then incubated at 37°C for six hours before the cells were imaged by light microscopy.

The addition of a polymer disc covering one quarter of the area of a well meant that it was not possible to analyse the tube formation in the standard quantitative method. Instead, the effect of the polymer plus heparin and VEGF was compared qualitatively to the polymer alone and a control Matrigel well. Within each experiment, three repeats of each environment were carried out and the entire experiment was carried out in triplicate.

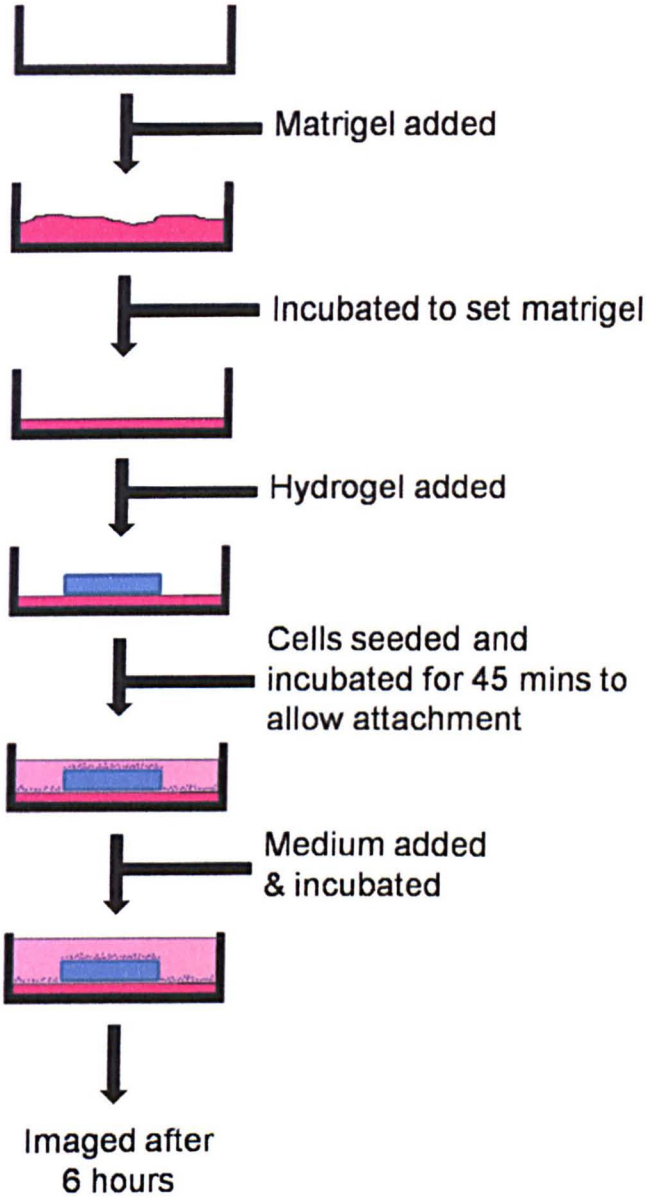


**Figure 7.16: Schematic of experiment to determine effect of VEGF released from hydrogel on endothelial cell differentiation. Studies were carried out in serum-starved medium (1% FCS) on growth-factor reduced Matrigel.**

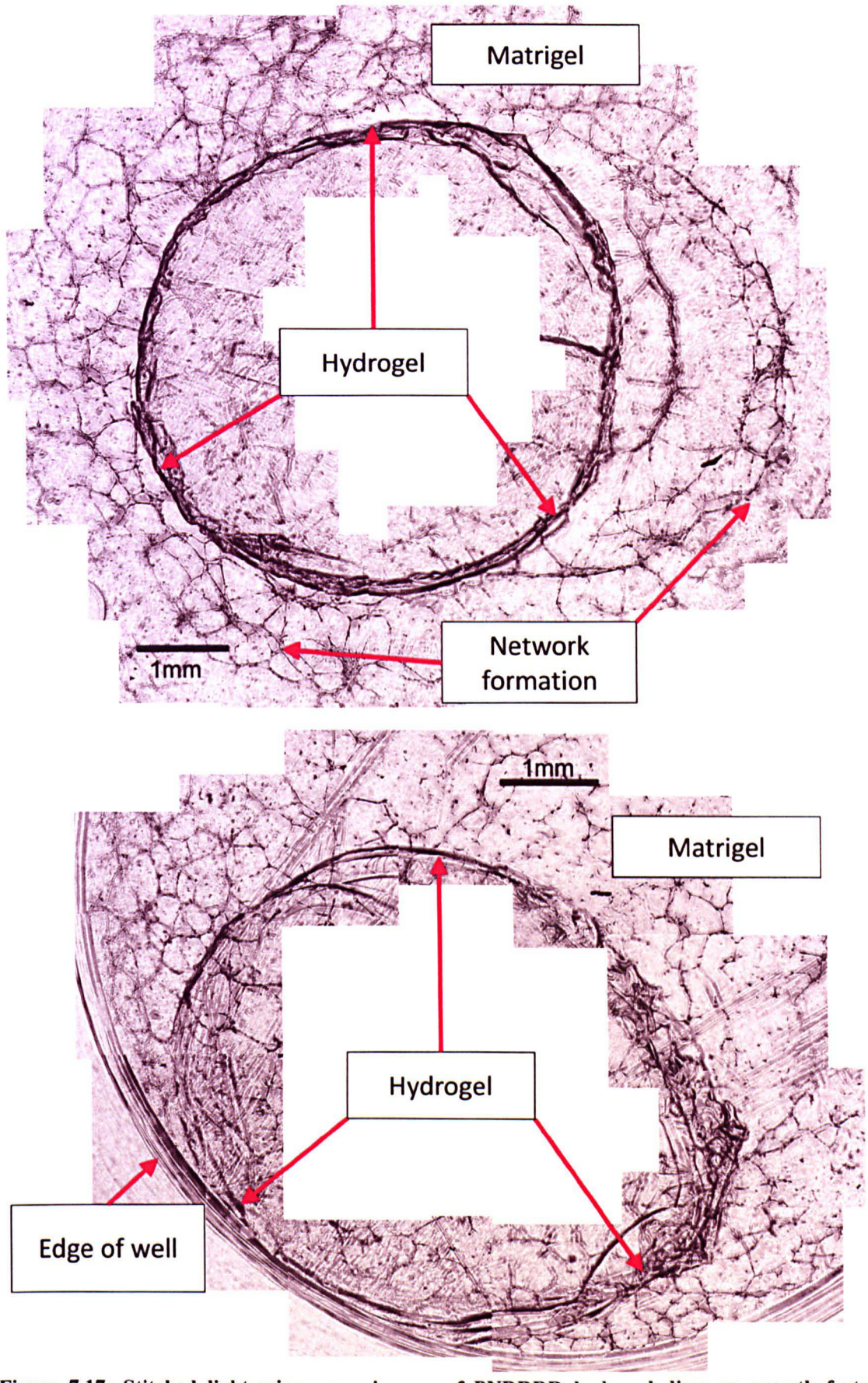


**Figure 7.17: Stitched light microscopy images of PNDRRR hydrogel discs on growth factor-reduced Matrigel. Top image: VEGF- and heparin-bound PNDRRR hydrogel. Bottom image: PNDRRR hydrogel alone (near to well edge). Images show networks of endothelial cells forming around the VEGF- and heparin-bound PNDRRR hydrogel where disc has been shifted slightly to the left.**

Previously it was shown that culture of endothelial cells on Matrigel alone leads to the formation of an EC network with tubes forming in random directions (Figure 7.15). The images in Figure 7.17 show PNDRRR hydrogel alone (bottom image) and VEGF- and heparin-bound PNDRRR hydrogel (top image) in wells coated with GF-reduced Matrigel. In both cases, the hydrogel itself is visible in the centre of the image (labelled to show the edge of the hydrogel) with endothelial cells present on the Matrigel surrounding it. Culture of endothelial cells on GF-reduced Matrigel in the presence of VEGF- and heparin-loaded PNDRRR hydrogel led to a significant spatial arrangement of the EC network, such that the EC network formed radially around the hydrogel (Figure 7.17 (top)). In this image, the hydrogel has shifted slightly to the left, revealing the tube formation that had occurred. For this VEGF- and heparin-bound PNDRRR hydrogel, a higher presence of endothelial cells was also observed directly surrounding the material than in other areas of the well. This effect was clearly observable after six hours of culture for all nine repeats carried out. Such an effect was not observed for the control PNDRRR hydrogel with no VEGF and heparin present, with random tube formation observed throughout the well in this case (Figure 7.17 (bottom)). These results suggest that VEGF is released by the VEGF- and heparin-bound PNDRRR hydrogel in such a way as to produce a VEGF gradient, thus resulting in EC migration towards the source. It is also shown that tube formation is spatially affected by VEGF release. Tube formation is observed radially around the VEGF- and heparin-bound PNDRRR polymer, but not in direct contact with the hydrogel. This is a positive result for a potential wound healing application, as it is hypothesised that the material could be removed without seriously damaging the healing tissue or new capillary network.

A similar spatial effect was previously reported by Tufro[369] for mouse glomerular endothelial cell response to avascular metanephric kidneys from rat embryos and VEGF-coated agarose beads to confirm that VEGF directs angiogenesis. In this case, EC networks were previously formed for 24 hours on collagen I gel before addition of either the kidney or the VEGF-loaded beads. Co-culture with the kidney induced spatial rearrangement of the EC network, with cells directed towards the explant. The effect was observable within 48 hours, at which time a network extending 1373 ± 44.6 μm radially surrounded each explant. The presence of anti-VEGF neutralising antibodies minimised migration. A similar spatial rearrangement was also observed for VEGF-coated Affi-Gel blue agarose beads in the same study.

## 7.5 Discussion of Angiogenesis Assay Results

Endothelial cell proliferation studies of VEGF- and heparin-bound hydrogels revealed that the most significant stimulatory effect was achieved with the PNDRRR hydrogel. This material was therefore selected for further analysis as an angiogenesis stimulator.

In this final study of VEGF- and heparin-bound PNDRRR hydrogels, a simple *in vitro* cell culture study on GF-reduced Matrigel was used to determine the effect of the VEGF- and heparin-bound hydrogel on migration and tube formation. The PNDRRR hydrogel alone had little effect on tube formation. The tubes present were randomly distributed and networks present did not extend above a few tubes. On the other hand, the VEGF- and heparin-bound PNDRRR hydrogel had a significant spatial effect on tube formation, with a relatively well-formed network of tubes present radially around the hydrogel in all repeats. Visual comparison of the two wells also shows increased tube numbers in the well with the VEGF- and heparin-bound PNDRRR hydrogel.

Comparison of these results with other growth factor releasing materials is complicated due to the different *in vitro* and *in vivo* assays employed to analyse angiogenesis. Also, although the bioactivity of VEGF and proliferation of endothelial cells was often analysed in comparable growth factor delivery systems, only a small number of the growth factor delivery systems discussed in Section 5.3 provide information on the effect of the delivery system on angiogenesis. The chick chorioallantoic membrane assay was utilised by Kanczler et al[90] to show that increased numbers of blood vessels surrounded their VEGF-encapsulated poly(D,L-lactic acid) scaffolds compared to control scaffolds *in vivo*. Yoon et al[102] implanted bFGF-loaded Pluronic/heparin hydrogels into subcutaneous pockets in the dorsal side of male SD rats and showed that the tissue layer formed on the surface of these hydrogels contained more dense capillaries than the Pluronic hydrogel control. This observation was confirmed by histology of the tissues. Steffens et al[103] employed both of these techniques followed by capillary counting or analysis of haemoglobin content to confirm that the presence of both VEGF and heparin in collagen matrices led to an increased angiogenic potential. Interestingly, an increased angiogenic potential was observed for the heparinised matrix alone as well as the VEGF-loaded heparinised matrix, although a higher increase in angiogenesis was observed in the presence of both VEGF and heparin.

Pike et al[64] produced hyaluronan hydrogels containing gelatin and heparin as well as VEGF or bFGF which were implanted into the ear pinnas of Balb/c mice. The results showed that the vascularisation observed could be sustained for up to 28 days with the presence of heparin. Another report from the Peattie group[84] also showed that the presence of heparin in hyaluronan-based hydrogels could sustain release of growth factors over a period of weeks. In an *in vivo* mouse model, heparin-containing hydrogels loaded with both VEGF and angiopoietin-1 led to the development of more mature microvessel networks than when the hydrogels lacked heparin or one of the growth factors. This result is in agreement with those discussed by Richardson et al[89] who analysed angiogenic potential by implanting their poly(lactide-co-glycolide) scaffolds into the subcutaneous tissue of Lewis rats. No increase in blood vessel density was observed for bolus delivery of VEGF and/or PDGF, but delivery of the growth factors from the scaffolds had a significant effect. Histology revealed that release of VEGF led to increased blood vessel density but the blood vessels remained immature, whereas PDGF release led to blood vessel maturation. Combined release of the two growth factors led to the formation of mature blood vessels. Despite the variety of assays available to analyse angiogenesis, all of the approaches discussed are in agreement with the results presented here, namely that the release of VEGF from a biomaterial can positively affect the process of angiogenesis.

In conclusion, the RRR-functionalised hydrogel (PNDRRR) has been shown to be a promising biomaterial for VEGF delivery in a wound healing application. This heparin-binding biocompatible material has been shown to non-covalently bind and release biologically active VEGF over a 72 hour period, significantly increasing endothelial cell proliferation. The presence of VEGF and heparin bound to the hydrogel also led to significant increase in cell attachment. An *in vitro* study has shown that the VEGF- and heparin-bound PNDRRR hydrogel has a positive spatial effect on the formation of tube structures on GF-reduced Matrigel. These results suggest that these hydrogels could be suitable as wound healing materials by acting as a VEGF reservoir and thereby stimulating EC proliferation and tube formation adjacent to the material. Further experimentation to examine the angiogenic potential of this hydrogel *in vivo* would now be justified.

# 8 Conclusion

The aim of this work was to develop a material capable of binding and releasing bioactive VEGF (an angiogenic stimulator) for a wound healing application. The materials were designed to operate as VEGF-reservoirs, binding endogenous VEGF within a wound environment, maintaining VEGF concentrations within a localised area and thus aiding the process of angiogenesis and subsequent wound healing. The biomaterial was required to act as a "heparin-mimic", interacting non-covalently with the basic heparin-binding regions present on the VEGF protein. Two biomaterials were investigated to determine their potential for use in this application; core-shell molecularly-imprinted particles and heparin-bound peptide-functionalised poly(NVP-co-DEGBAC-co-AA) hydrogels.

***Core-Shell Molecularly-Imprinted Particles***

CS-MIPs were developed initially, using the methodology previously employed by Carter et al[157, 159, 160]. The epitope imprinting approach[190] was employed in order to overcome difficulties associated with the imprinting of biomacromolecules, and DKPRR was selected as the template molecule. A low temperature initiator system of potassium persulphate and ascorbic acid was investigated, allowing the synthesis of core and core-shell particles but affording only a 1.9% incorporation of the functional monomer (OPHP). In order to increase OPHP incorporation a number of alternative initiator systems were trialled, with the most successful system found to be initiation by potassium persulphate at 70°C, resulting in 11.7% of the OPHP employed being incorporated into the outer shells. This system was optimised to produce stable latexes of core particles and core-shell particles.

This system was then employed to produce a series of MIPs; one imprinted with DKPRR, a pentapeptide sequence present at the carboxy-terminus of $VEGF_{165}$; one imprinted with GAA, an unrelated peptide sequence; and a blank version, produced without the presence of the template. A colorimetric peptide binding study showed that binding occurred between the surface phosphate functionality of the core-shell particles and the basic amino acids, confirmed by a zeta potential binding study which showed a considerable decrease in surface charge for all core-shell particles as they interacted with the DKPRR peptide but not with the SSSSSSSS peptide. A slight influence of

molecular imprinting was observed during the colorimetric peptide release study as a higher acid concentration was required to remove MRSSSDKPRR from the DKPRR CS-MIP than was required for MRSSSPRKRD, a scrambled version of the peptide. For the GAA CS-MIP and the blank CS-MIP the release of the two peptides was very similar in each case and resembled the release of MRSSSPRKRD from the DKPRR CS-MIP. The delayed release of MRSSSDKPRR is attributed to the binding of the DKPRR group to molecularly-imprinted cavities, resulting in multiple interactions between the polymer and the peptide. A study of VEGF binding and release for the three core-shell particle types revealed that over a 48 hour period 22.4 ng, 21.3 ng and 20.9 ng of bioactive $VEGF_{165}$ was released per milligram of the DKPRR-, GAA- and blank-imprinted CS-MIPs respectively.

From the studies carried out to date, no significant effect of molecular imprinting was observed in binding or release of the protein, suggesting that the molecular imprinting process may not offer any advantages for this application. Nevertheless, synthetic core-shell particles with surface phosphate functionality have been developed which are capable of binding and releasing $VEGF_{165}$ over a 48 hour period whilst maintaining the bioactivity of this protein, thereby showing the potential of core-shell particles with phosphate functionality for heparin-binding protein delivery applications.

***Heparin-Bound Peptide-Functionalised Hydrogels***

The second approach investigated involved a heparin-bound peptide-functionalised hydrogel for interaction with VEGF. Poly(NVP-co-DEGBAC) polymers were employed as the base hydrogel as this material had already been employed in our research group[286]. Consideration of heparin-protein interactions led to the selection of triarginine and trilysine as heparin-binding peptides. Poly(NVP-co-DEGBAC-co-AA) hydrogels were designed to couple the peptides via an amide bond between the acrylic acid residues and the amine functionality of the peptide. An optimised two-step coupling procedure was determined for thermally-initiated hydrogels, involving an activation step with DCC and NHS in DMF at room temperature for 24 hours and a coupling step with two equivalents of peptide in PBS (pH 8.5) at 0°C for 72 hours. The highest peptide loadings were achieved using this system with tripeptide sequences and 5% acrylic acid hydrogels.

These optimised conditions were employed in the coupling of UV-initiated hydrogels to trilysine (0.14 mg/mg hydrogel) and triarginine (0.2 mg/mg hydrogel), which were employed in all further investigations, as these hydrogels required less peptide and offered superior mechanical properties than the thermally-initiated hydrogels. The ability of these materials to bind heparin was confirmed via XPS and a fluorescent heparin study; they were shown to bind 0.077 mg and 0.117 mg of heparin per milligram of dry hydrogel for the PNDKKK and PNDRRR hydrogels respectively. An ELISA study of the heparin-bound hydrogels revealed that these materials were able to bind VEGF, resulting in a release of 20.1 ng and 27.0 ng of biologically active VEGF per PNDKKK hydrogel and PNDRRR hydrogel disc respectively over a 72 hour period, in comparison to 19.8 ng and 19.4 ng for the PND and PNDA hydrogels. The higher VEGF release from the PNDRRR hydrogel was attributed to the higher incorporation of heparin in the hydrogel. A low retention of VEGF on all hydrogels was observed after the study, suggesting this material is suitable for a delivery system.

Cell compatibility studies on PND, PNDA, PNDKKK and PNDRRR revealed that all materials are cytocompatible. When considering fibroblasts and HDMECs in indirect contact with the hydrogels, no significant effect was observed due to the presence of the hydrogels in FCS-containing medium. In the fibroblast serum-starved experiment, a decrease in viability (significant ($p < 0.001$) in two of three repeats) was observed in the presence of PNDRRR, which is attributed to absorption of vital media components by this hydrogel. Interestingly, a significant increase in the number of cells in direct contact with the hydrogels (on top) was observed for both cell types as the hydrogels were functionalised with peptides, with the most significant effect being observed for the PNDRRR hydrogel.

In a study of HDMEC proliferation in indirect contact with the hydrogels in 5% serum medium, an increase in cell proliferation was observed in the presence of both the heparin-bound and the VEGF- and heparin-bound PNDRRR hydrogels. Overall, in 5% serum medium, only the heparin-bound PNDRRR hydrogel was shown to lead to a significant increase in HDMEC proliferation, which is expected to be due to masking of the VEGF effect of the VEGF- and heparin-bound PNDRRR hydrogel by the serum in the medium. The presence of VEGF- and heparin-bound PNDRRR hydrogels in a serum-starved environment led to a significant increase in proliferation in all repeats,

and a smaller increase was also observed for the VEGF- and heparin-bound PNDKKK hydrogels in two of the three repeats. These results are expected to be due to both the VEGF and heparin loadings for these hydrogels, as the presence of heparin is thought to increase the effect of VEGF on endothelial cells through a number of mechanisms. The PNDRRR hydrogel was shown to bind the most heparin and VEGF and was therefore able to have the most significant effect on the endothelial cells. Interestingly, cells observed on top of the heparin-bound and VEGF- and heparin-bound PNDRRR hydrogels had a stretched morphology not observed for the PNDRRR hydrogel alone. This could be due to improved cell adhesion in the presence of heparin, or possibly due to the heparin-bound hydrogels more closely resembling the ECM. Thus they should be more suitable for differentiation of the endothelial cells into tube-like structures.

An *in vitro* experiment was carried out with growth-factor reduced Matrigel in the presence of the PNDRRR hydrogel alone and VEGF- and heparin-bound PNDRRR hydrogel to determine the effect of these materials on endothelial cell migration and tube formation. In the presence of the PNDRRR hydrogel alone tube formation occurred randomly throughout the well, as was observed for Matrigel alone. The presence of the VEGF- and heparin-bound PNDRRR led to the formation of a radial endothelial cell network around the hydrogel, with a higher concentration of cells surrounding the polymer than in other areas of the well, suggesting that a VEGF gradient is formed upon release of the protein from the hydrogel, causing endothelial cell migration towards the source. The radial tube formation surrounding the hydrogel suggests that the orientation of the tubes was also affected by directional VEGF release.

This work clearly shows the potential of these hydrogels, particularly the PNDRRR hydrogel, to meet the initial aim of this project. Triarginine- and trilysine-functionalised poly(NVP-co-DEGBAC-co-AA) hydrogels were synthesised and were able to bind and release biologically-active $VEGF_{165}$ over a 72 hour period. These materials were shown to be cytocompatible and increased cell attachment was observed in comparison to the poly(NVP-co-DEGBAC) and poly(NVP-co-DEGBAC-co-AA) hydrogels. Most importantly, the triarginine-functionalised hydrogels were shown to have potential as stimulators of angiogenesis, as the VEGF- and heparin-bound PNDRRR hydrogels were able to significantly increase HDMEC proliferation, and lead to endothelial cell migration and directional tube formation *in vitro*.

***Summary***

Both systems investigated resulted in polymers able to bind and release similar quantities of $VEGF_{165}$, whilst maintaining the biological activity of the protein, with an average of 22.4 ng of $VEGF_{165}$ released per milligram of the DKPRR CS-MIP (over 48 hours) and 27.0 ng released per triarginine-functionalised hydrogel disc (over 72 hours). It is expected that these materials would similarly be able to bind and release other heparin-binding proteins.

These two materials offer different approaches to achieve the project aim, and as such each method has different advantages and disadvantages. The core-shell particles are able to bind VEGF in a one-step system as the phosphate functionality required is present within the material. This functionality was shown to bind the protein with the appropriate strength to be able to release it over a 48 hour period in a biologically-active form. It is suggested that this synthetic approach would enable simple control of protein binding by varying the phosphate concentration on the particle surface, offering a versatile system. It is acknowledged that such particles could not be used directly in a wound environment, possibly even being of a size to have implications of phagocytosis, and would therefore require coating on, or encapsulating within, a secondary material. The triarginine-functionalised poly(NVP-co-DEGBAC-co-AA) hydrogels were also able to bind and release bioactive $VEGF_{165}$. This cytocompatible material has the required mechanical properties without necessitating a secondary material support. This system would require a two-step process in order to be utilised in a wound healing application as it first needs to interact with heparin before binding VEGF. The use of heparin as an intermediate binding system also means that it may be difficult to control protein binding amounts and the release kinetics by material design. However, this system has the advantage of enabling protein binding in a more natural environment, thus possibly allowing growth factor release in response to biological factors.

To conclude, two systems have been developed that are capable of binding and releasing bioactive VEGF. In addition, triarginine-functionalised hydrogels were shown to be both cytocompatible and able to increase HDMEC viability and influence angiogenesis *in vitro*. In both cases, the results discussed demonstrate the potential of these materials for further development towards the final aim of an angiogenesis-stimulating material for a wound healing application.

# 9 Future Work

There are number of areas where further work could be carried out to improve the understanding of the results presented and to further develop the materials produced.

Further peptide and protein binding studies, including a competitive protein binding study, would complete the molecular imprinting aspect of the CS-MIP work for academic interest, even though the molecular imprinting technique would not be suggested for further development of the core-shell particles. It is also suggested that more comprehensive VEGF binding and release studies be carried out to determine the release kinetics over a longer time period. Control of the binding capacity of phosphate-functionalised core-shell particles could also be investigated by varying the concentration of phosphate monomer in the synthesis of the outer shell, or by the use of alternative phosphate monomers. For further development of the core-shell particles, the cytocompatibility of these materials needs to be determined and, upon a positive outcome, the possibility of incorporating the core-shell particles into a secondary material to achieve suitable material properties could be investigated. If the core-shell particles were found to be cytocompatible and it was possible to incorporate them into secondary materials, it would then be necessary to determine the effect of these particles on angiogenesis *in vitro* and *in vivo*.

With respect to the heparin-bound hydrogels, it is suggested that future work should focus on the development of the most successful material, the triarginine-functionalised poly(NVP-co-DEGBAC-co-AA) hydrogel. It would be interesting to investigate whether VEGF alone or heparin-bound VEGF is released from the hydrogel in order to further understand the effect of this system on angiogenesis. This may be possible by a labelled-heparin study or through XPS analysis of the hydrogels after VEGF release. In order to determine the true potential of this material for the application it would also be prudent to carry out further angiogenesis studies. The use of the chick chorioallantoic membrane angiogenesis assay could be the next logical step.

# 10 Materials and Methods

## 10.1 Peptide Synthesis

### 10.1.1 Materials

All resins for solid phase peptide synthesis were purchased from Novabiochem with the first amino acid attached, Fmoc-Arg(Pbf)-Wang resin (100-200 mesh), Fmoc-Lys(Boc)-Wang resin (100-200 mesh), Fmoc-Asp(OtBu)-Wang resin and Fmoc-Ser(tBu)-Wang resin, and were used as supplied. All amino acids were purchased from Novabiochem as N-α-Fmoc protected amino acids with side chain protection when appropriate and used without further purification. Fmoc-Arg(Pbf)-OH, Fmoc-Asp(OtBu)-OH, Fmoc-Lys(Boc)-OH, Fmoc-Ser(tBu)-OH, and Fmoc-Pro-OH were used as supplied. Methyl Red (ACS reagent, Sigma Aldrich) was used as supplied. Coupling reagents 2-mercaptobenzothiazol (2-MBT, 97%, Aldrich), 2-(1H-benzotriazole-1-yl) -1,1,3,3-tetramethyluronium hexafluorophosphate (HBTU, Novabiochem), 1-hyroxybenzotriazole hydrate (HOBt, 99.8% dry weight, >20% water, Alfa Aesar), *N,N*-diisopropylethylamine (DIPEA, 99%, reagent grade, Aldrich) and cleavage reagents, piperidine (99%, Aldrich) trifluoroacetic acid (TFA, 99%, Reagent Plus, Aldrich), phenol (≥99%, ACS reagent, Aldrich) and triisopropylsilane (TIPS, ≥98%, purum, Fluka), were also used as supplied. Solvents were used as supplied; acetonitrile (HPLC grade, Far UV, Fisher) dichloromethane (DCM, HPLC grade, Fisher), diethyl ether (anhydrous, laboratory reagent grade, Fisher), *N,N*-dimethylformamide (DMF, laboratory reagent grade, Fisher) and methanol (HPLC grade, Fisher). Deionised water was used throughout.

### 10.1.2 Equipment

Peptide synthesis was carried out on a Chemspeed Technologies PSW1100 automatic synthesizer. Analytical HPLC-MS was performed on a Waters 2690 Separations Module with Micromass Platform MCZ with a Prosphere HP C18 column (300 Å, 5 μm, length = 150 mm, ID = 4.6 mm). Preparative HPLC was carried out on a Polymer Laboratories LC1150 module with a Prosphere HP C18 column (300 Å, 10 μm, length = 100 mm, ID = 22 mm). NMR spectra were obtained on a DRX 500 MHz spectrometer using $D_2O$ throughout.

### 10.1.3 Solid Phase Peptide Synthesis (SPPS) Protocol

The synthesis was carried out in DMF under an argon environment on an automated peptide synthesiser which was programmed individually for each synthesis.

| Reagent | Molarity of Solution (M) | Required Amount (fold excess) HBTU |
|---|---|---|
| Amino acid | 0.5 | 5 |
| Coupling reagent (HBTU) | 0.5 | 5 |
| HOBt | 0.5 in coupling reagent | 5 |
| DIPEA | Neat | 10 |

**Table 10.1: Relative reagent quantities employed in solid phase peptide synthesis**

#### *General Synthetic Procedure*

The resin with first amino acid attached (≤ 500 mg) was placed into the reaction vials in the automatic peptide synthesis robot. The resin was swollen in 5 ml DMF overnight under an argon atmosphere and 350 rpm vortex and then washed six times with 5 ml DMF. Deprotection of the first α-amino group was carried out by the addition of 5 ml of 20% piperidine in DMF which was reacted for 5 minutes whilst vortexing at 350 rpm before being removed. This was repeated twice in order to achieve optimum coupling. The resin was then washed six times with 5 ml DMF. Chain elongation of the peptide sequence with subsequent amino acids was carried out using standard HBTU protocols. 5 equivalents of the amino acid (0.5 M), 5 equivalents of HBTU (0.5 M), 5 equivalents of HOBt (0.5 M in HBTU) and 10 equivalents of DIPEA were added to the washed resin. The coupling reaction was allowed to continue for 1 hour under argon and vortex of 350 rpm before being removed from the reaction vessel. This coupling procedure was repeated once. The resin was then washed with 5 ml DMF six times. The above procedure of triple deprotection and double coupling was then repeated for the remaining amino acids in the required sequence. Once the final amino acid had been added the resin was washed six times with 5 ml DMF, six times with 5 ml DCM and finally six times with 5 ml methanol before being dried for storage.

### 10.1.4 Peptide Cleavage

The terminal Fmoc protecting group was removed, followed by removal of the resin and side-chain protecting group through treatment with trifluoroacetic acid (TFA) in the presence of various scavengers. A general procedure for peptide cleavage is described and the specific cleavage solutions for each peptide sequence is provided in table 10.2.

***Removal of Fmoc Protection***

The peptide sequence on the resin was swollen in DMF (10 ml per gram of resin) overnight and then dried gently under vacuum. The swollen resin was deprotected in 5 ml of 20% piperidine in DMF solution for 5 minutes. This was repeated three times. The resin was then washed three times each with DMF, DCM and finally with methanol to remove all traces of DMF. The peptide sequence on the resin was then placed in a vacuum oven for one day to ensure it was completely free of solvents.

***Removal of Side-Chain Protecting Groups and Solid Support***

Peptides were cleaved from the resin using a TFA cleavage cocktail (10 ml per gram of resin) for two hours. The resin was washed with 1 x cleavage cocktail and 3 x TFA. The TFA was stripped off by rotary evaporation and the peptide was afforded by the addition of diethyl ether into the reaction vessel and subsequent trituration. The diethyl ether was decanted off and replaced five times, each time being triturated, to remove the remaining TFA and scavengers. Finally, the diethyl ether was removed by rotary evaporation and a small amount of an acetonitrile/water mixture was added to the flask to dissolve the peptide. The peptide was then freeze-dried and stored at -8°C.

| Peptide | Cleavage Cocktail |
|---|---|
| DKPRR | TFA, $H_2O$, Phenol, TIPS (88:5:5:2) |
| KKK | TFA, $H_2O$ (95:5) |
| KKKKKK | TFA, $H_2O$ (95:5) |
| RRR | TFA, $H_2O$, Phenol, TIPS (88:5:5:2) |
| SSSSSSSS | TFA, $H_2O$, Phenol, TIPS (88:5:5:2) |
| MRSSSDKPRR | TFA, $H_2O$, Phenol, TIPS (88:5:5:2) |
| MRSSSPRKRD | TFA, $H_2O$, Phenol, TIPS (88:5:5:2) |
| MRSSSSSSSS | TFA, $H_2O$, Phenol, TIPS (88:5:5:2) |

**Table 10.2: Cleavage solutions for specific peptide sequences**

## 10.1.5 Peptide Analysis

$^{13}C$ analysis: On numerous occasions the number of peaks does not equal the number of carbon environments. This is attributed to coincident signals due to high similarities between a number of the carbon environments. In cases where not enough peptide was synthesised to produce NMR spectra, only HPLC-MS data is provided.

***Trilysine (KKK)***

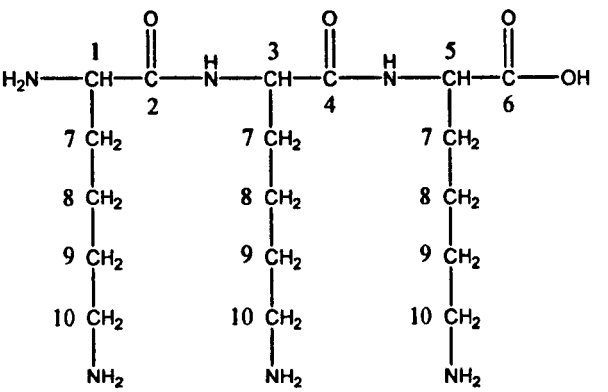

$^1H$ NMR ($D_2O$, 500 MHz): $\delta_H$ (ppm) = 1.34 (m, 6H, C<u>H</u>$_2$ *(8)*), 1.54-1.83 (m, 12H, C<u>H</u>$_2$ *(7,9)*), 2.87 (m, 6H, C<u>H</u>$_2$ *(10)*), 3.90 (t, 1H, C<u>H</u> *(1)*), 4.15-4.24 (m, 2H, C<u>H</u> *(3,5)*). $^{13}C$ NMR (JMOD, 250 MHz) $\delta_C$ (ppm) = 21.16, 21.94, 22.17 (3C, <u>C</u> *(8)*), 26.32, 26.40 (3C, <u>C</u> *(7)*), 29.96, 30.49, 30.56 (3C, <u>C</u> *(9)*), 39.07, 39.24 (3C, <u>C</u> *(10)*), 52.82, 53.03, 53.83 (3C, <u>C</u> *(1,3,5)*), 169.63, 173.41, 175.56 (3C, <u>C</u> *(2,4,6)*). HPLC-MS $ES^+$: elution time 11.45 minutes (5% ACN (0.1% TFA): 95% $H_2O$ (0.1% TFA) isocratic gradient over 30 minutes, Alltech Prosphere HP C18 column 150 x 4.6 mm). Mass peaks (ToF MS ES+); 404 $MH^+$. 100 % purity by integration of peaks generated by detector at 215 nm before preparative HPLC so no further purification was undertaken.

***Hexalysine (KKKKKK)***

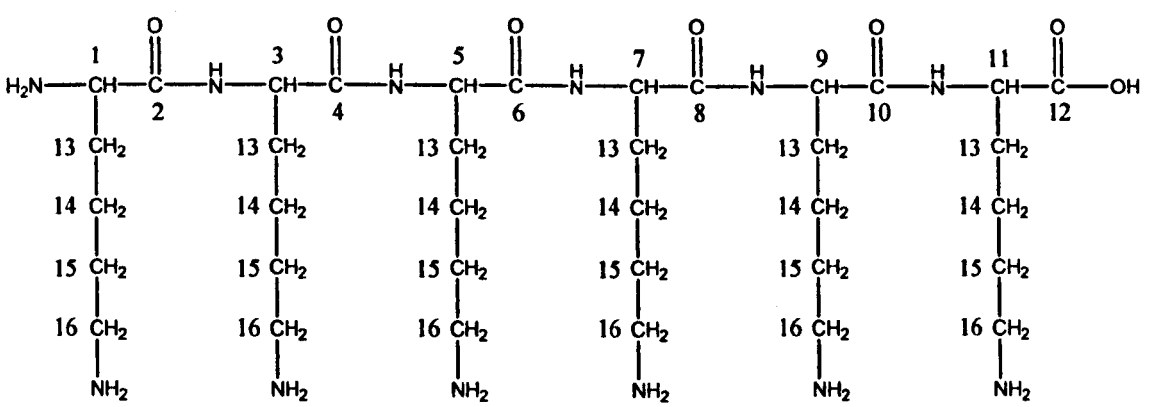

$^1$H NMR ($D_2O$, 500 MHz): $\delta_H$ (ppm) = 1.38-1.45 (m, 12H, C<u>H</u>$_2$ *(14)*), 1.59-1.88 (m, 24H, C<u>H</u>$_2$ *(13,15)*), 2.91-2.95 (m, 12H, C<u>H</u>$_2$ *(16)*), 3.94-3.98 (t, 1H, C<u>H</u> *(1)*), 4.20-4.28 (m, 5H, C<u>H</u> *(3,5,7,9,11)*). $^{13}$C NMR (JMOD, 125 MHz) $\delta_C$ (ppm) = 21.27, 21.91, 22.04, 22.08, 22.12 (6C, <u>C</u> *(14)*), 26.25, 26.32, 26.35 (6C, <u>C</u> *(13)*), 29.83, 30.45, 30.59, 30.66 (6C, <u>C</u> *(15)*), 38.96, 39.13 (6C, <u>C</u> *(16)*), 52.75, 52.82, 53.42, 53.48, 53.52, 53.63 (6C, <u>C</u> *(1,3,5,7,9,11)*), 169.66, 173.31, 173.44, 173.59, 175.38 (6C, <u>C</u> *(2,4,6,8,10,12)*). HPLC-MS ES$^+$: elution time 15.87 minutes (5% ACN (0.1% TFA): 95% $H_2O$ (0.1% TFA) isocratic gradient over 30 minutes, Alltech Prosphere HP C18 column 150 x 4.6 mm). Mass peaks; 788 (MH+). 95.41% purity by integration of peaks generated by detector at 215 nm of crude peptide and therefore no further purification was carried out.

***<u>Aspartic Acid-Lysine-Proline-Arginine-Arginine (DKPRR)</u>***

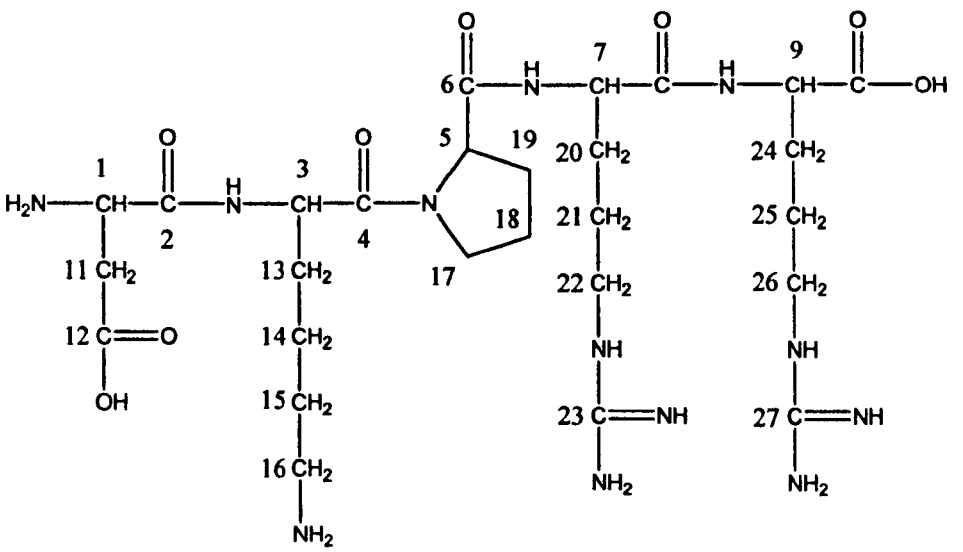

$^1$H NMR ($D_2O$, 500 MHz): $\delta_H$ (ppm) = 1.42 (m, 2H, C<u>H</u>$_2$*(14)*), 1.54-2.29 (m, 16H, C<u>H</u>$_2$ *(13, 15, 18, 19, 20, 21, 24, 25)*), 2.86-3.00 (m, 4H, C<u>H</u>$_2$ *(11, 16)*), 3.15 (m, 4H, C<u>H</u>$_2$ *(22, 26)*), 3.57 & 3.77 (double multiplet, 2H, C<u>H</u>$_2$ *(17)*), 4.23 (t, 1H) & 4.28-4.37 (m, 3H) & 4.59 (m, 1H) ((R)HN-C<u>H</u>(R)-CO(R) *(1, 3, 5, 7, 9)*). HPLC-MS ES$^+$: elution time 46.80 minutes (3% ACN (0.1% TFA): 97% $H_2O$ (0.1% TFA) isocratic gradient over 50 minutes, Alltech Prosphere HP C18 column 150 x 4.6 mm) Mass peaks; 671 (MH$^+$), 411, 336 (2+ ion), 279. 94.81% purity by integration of peaks generated by detector at 215 nm before preparative HPLC, 98.62% purity after purification.

***Triarginine (RRR)***

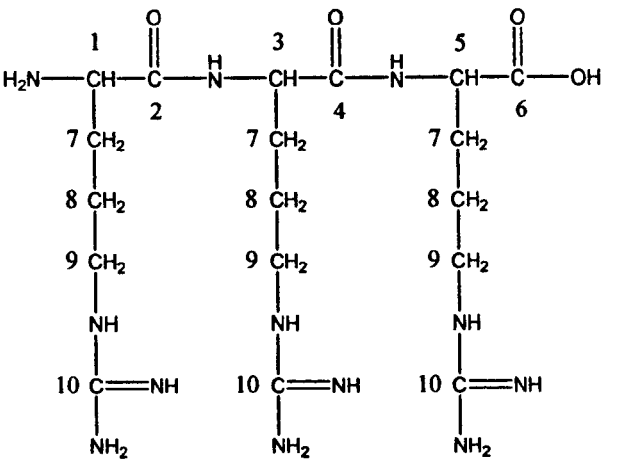

$^{1}$H NMR ($D_2O$, 500 MHz): $\delta_H$ (ppm) = 1.53-1.56 (m, 6H, C<u>H</u>$_2$ *(8)*), 1.66-1.93 (m, 6H, C<u>H</u>$_2$ *(7)*), 3.07-3.11 (m, 6H, C<u>H</u>$_2$ *(9)*), 3.98 (t, 1H, C<u>H</u> *(1)*), 4.20-4.25 (M, 2H, C<u>H</u>$_2$ *(3,5)*). $^{13}$C NMR (JMOD, 250 MHz) $\delta_C$ (ppm) = 23.44, 24.34, 24.56, (3C, <u>C</u> *(8)*), 27.78, 28.10 (3C, <u>C</u> *(7)*) 40.45, 40.58 (3C, <u>C</u> *(9)*), 52.58, 52.79, 53.84 (3C, <u>C</u> *(1,3,5)*), 156.88 (3C, <u>C</u> *(10)*), 169.63, 173.36, 175.37 (3C, <u>C</u> *(2,4,6)*). HPLC-MS ES$^+$: elution time 9.40 minutes (5% ACN (0.1% TFA): 95% $H_2O$ (0.1% TFA) isocratic gradient over 30 minutes, Alltech Prosphere HP C18 column 150 x 4.6 mm). Mass peaks; 591, 487 ($MH^+$), 313 M (RR fragment). 68% purity by integration of peaks generated by detector at 215 nm before preparative HPLC (32% RR). It was not possible to successfully separate the tripeptide (RRR) from the dipeptide (RR) with the required yield, so this peptide was utilised as a mixture of the tri- and dipeptides.

***Octaserine (SSSSSSSS)***

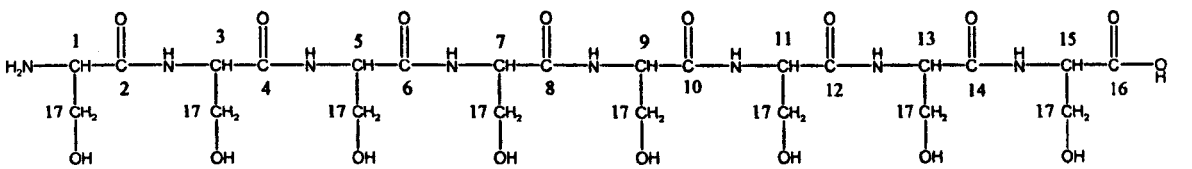

HPLC-MS ES$^+$: elution time 9.55 minutes (25% ACN (0.1% TFA): 75% $H_2O$ (0.1% TFA) isocratic gradient over 30 minutes, Alltech Prosphere HP C18 column 150 x 4.6 mm). Mass peaks (ToF MS ES-); 811, 713 ($M^-$). 20.39% purity by integration of peaks generated by detector at 215 nm before preparative HPLC, 86.58% purity after purification.

***Methyl Red-Tagged DKPRR (MRSSSDKPRR)***

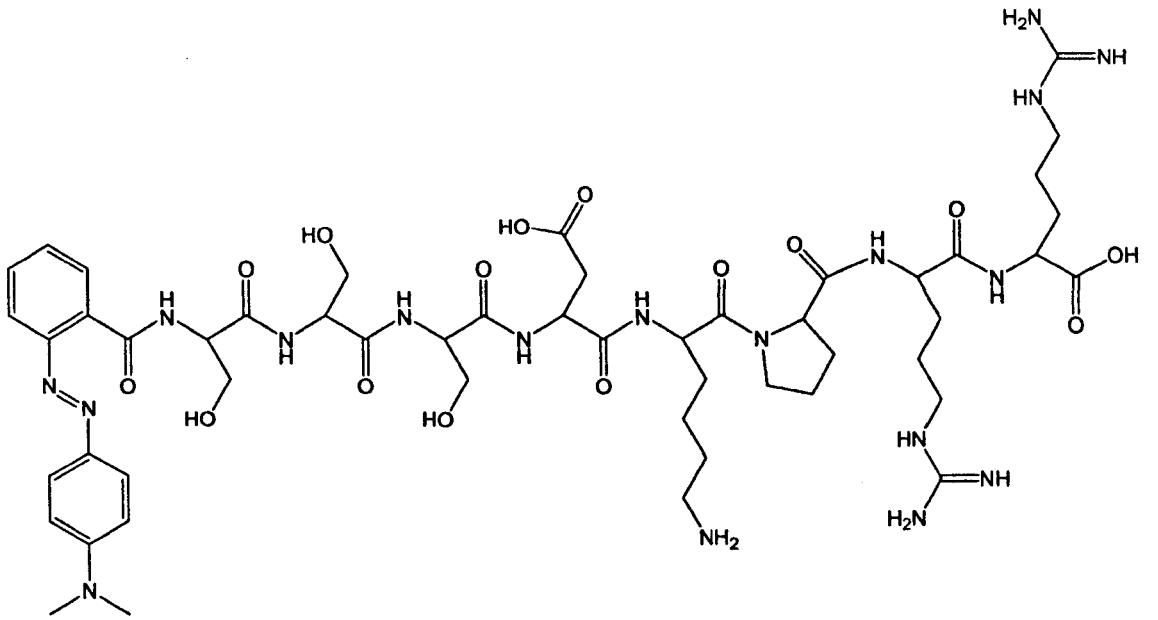

HPLC-MS $ES^+$: elution time 24.97 minutes (25% ACN (0.1% TFA): 75% $H_2O$ (0.1% TFA) isocratic gradient over 30 minutes, Alltech Prosphere HP C18 column 150 x 4.6 mm). Mass peaks (ToF MS ES+); 1183 ($MH^+$); 592 (2+ ion); 252 (methyl red fragment, $C_{15}H_{14}N_3O$). 30.23% purity by integration of peaks generated by detector at 215 nm before preparative HPLC, 93.03% purity after purification.

***Methyl Red-Tagged Octaserine Peptide (MRSSSSSSSS)***

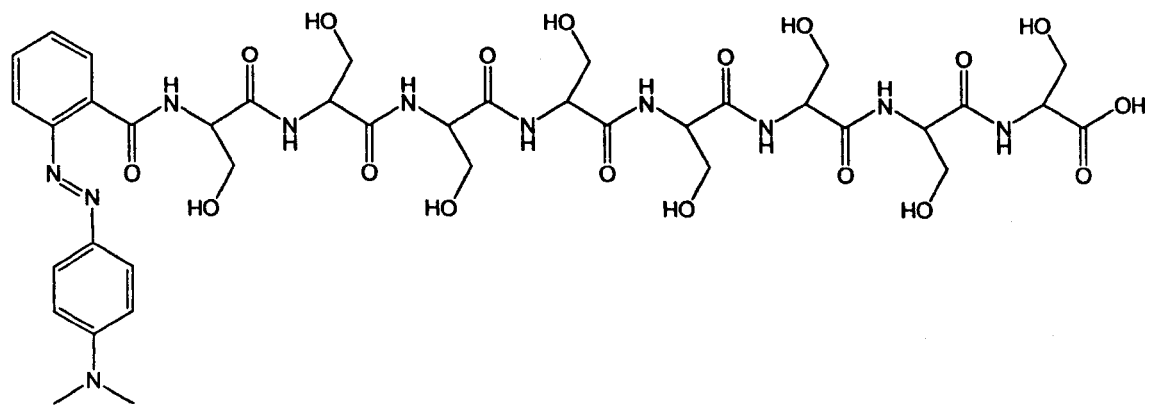

HPLC-MS $ES^+$: elution time 21.51 minutes (25% ACN (0.1% TFA): 75% $H_2O$ (0.1% TFA) isocratic gradient over 30 minutes, Alltech Prosphere HP C18 column 150 x 4.6 mm). Mass peaks (ToF MS ES-); 964 ($M^-(-H^+)$. 30.36% purity by integration of peaks generated by detector at 215 nm before preparative HPLC, 94.60% purity after purification.

***Methyl Red-Tagged PRKRD Scrambled Peptide (MRSSSPRKRD)***

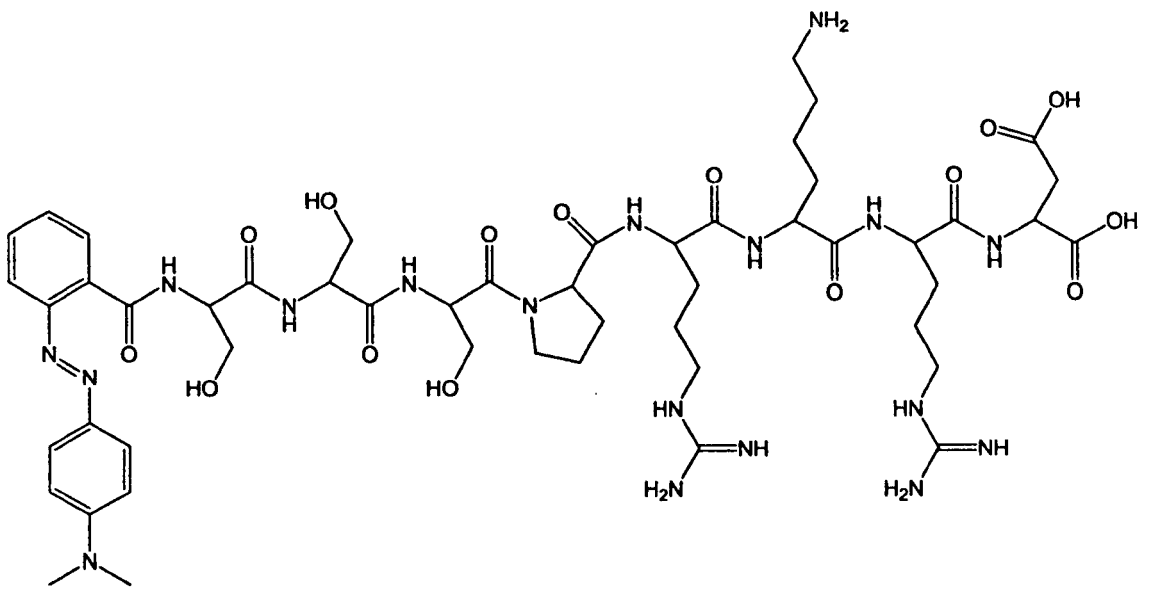

HPLC-MS $ES^+$: elution time 26.88 minutes (25% ACN (0.1% TFA): 75% $H_2O$ (0.1% TFA) isocratic gradient over 30 minutes, Alltech Prosphere HP C18 column 150 x 4.6 mm). Mass peaks (ToF MS ES+); 1184 ($MH^+$); 592 (2+ ion); 546; 252 (methyl red fragment, $C_{15}H_{14}N_3O$). 32.67% purity by integration of peaks generated by detector at 215 nm before preparative HPLC, 92.53% purity after purification.

## 10.2 Monomer Synthesis

### 10.2.1 Materials

Oleyl alcohol (85%, Aldrich) and phenyl dichlorophosphate (95+%, Aldrich) were used as supplied. Deionised water was used throughout, and chloroform (HPLC grade, Fisher), dichloromethane (DCM, HPLC grade, Fisher) and diethyl ether (anhydrous, laboratory reagent grade, Fisher) were used as supplied. Silica Gel 60 (230-400 Mesh, Merck) was used for silica chromatography purification. Thin layer chromatography (TLC) was carried out using Merck Silica Gel 60 $F_{254}$ (aluminium sheet) plates developed with para-anisaldehyde and potassium permanganate solutions and viewed under UV light.

### 10.2.2 Instrumentation

$^{1}H$, $^{13}C$ and $^{31}P$ NMR spectra were obtained on a Bruker AC 250 MHz and AMX2-400 MHz spectrometer using deuterated chloroform throughout.

### 10.2.3 Synthesis of Oleyl Phenyl Hydrogen Phosphate

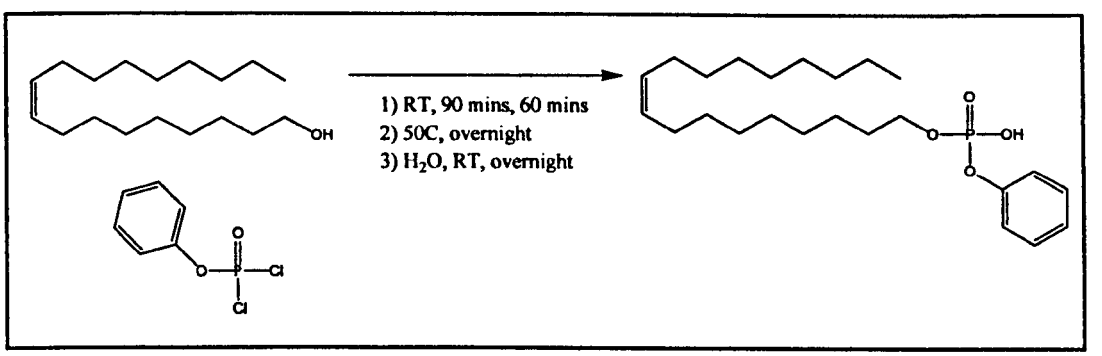


Oleyl alcohol (65.5 g, 0.24 mol) was added dropwise to stirring phenyl dichlorophosphate (50.0 g, 0.24 mol) over 90 minutes at room temperature and the resulting solution was then stirred for a further 60 minutes. The temperature was then increased to 50°C and stirring was continued for a further 16 hours. The resultant reaction mixture was then added dropwise to 300 ml of rapidly stirring ice-cold water and the organics were extracted into diethyl ether (3 x 100 ml) after 60 minutes. Anhydrous sodium sulphate was used to dry the combined organic extracts, which were

then filtered and rotary evaporated to produce a viscous yellow oil. Purification was carried out by flash column chromatography on silica using 100% DCM to 2-10% methanol/98-90% DCM to give a straw-coloured oil as the final product of 8.39 g (8.24%) (Rf = 0.26 on silica, 37:2:1 $CH_2Cl_2$/MeOH/AcOH). 1H NMR ($CDCl_3$, 250 MHz) δH (ppm): 0.87 (t, 3H, $C\underline{H}_3$), 1.26 (m, br, 22H, -$C\underline{H}_2$-), 1.62 (m, br, 2H, -$C\underline{H}_2CH_2$-OP), 2.00 (m, br, 4H, -$C\underline{H}_2CH$=), 4.05 (dt, 2H, -$C\underline{H}_2$OP, JPH = 6.71, JHH = 6.71), 5.38 (m, br, 2H, -$C\underline{H}$=$C\underline{H}$-), 7.10-7.32 (m, 5H, -$C_6\underline{H}_5$-), 8.88 (s, 1H, O$\underline{H}$). 31P NMR (CDCl3, 162MHz) δP (ppm): -4.0228. 13C NMR ($CDCl_3$, 100MHz) δC (ppm): 14.55 (-$\underline{C}H_3$), 23.11-33.04 ((R)C-$\underline{C}H_2$-C(R), 14C), 68.98 (-$\underline{C}H_2$-OP-), 120.56, 125.42, 130.02, 130.19, 130.38 (-$CH_2$-$\underline{C}H$=$\underline{C}H$-$CH_2$- and -$\underline{C}_6H_5$-, 7C), 151.00 (O-$\underline{C}$ (aromatic)). $^{13}C$ spectrum provided below (Figure 10.1). Exact $^{13}C$ peak assignments were not possible in all cases as this spectrum was complicated by $^{31}P$ splitting. Elemental analysis: $C_{24}H_{41}O_4P$ Found (calc) (%): C 68.14 (67.90) H 10.43 (9.73).

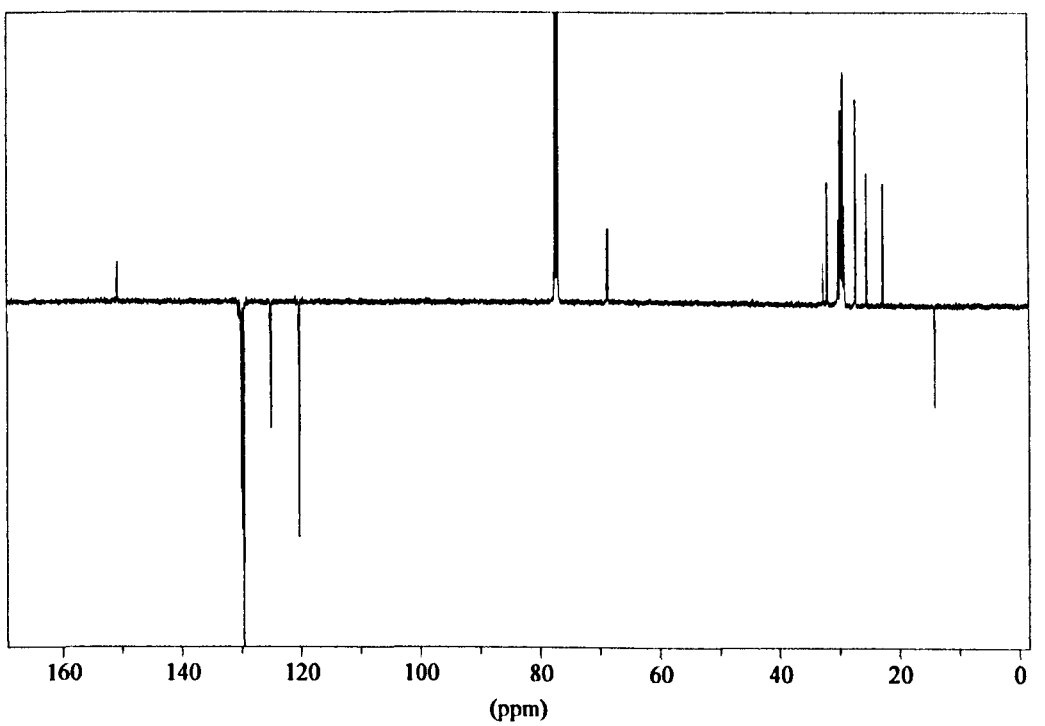


**Figure 10.1: $^{13}C$ NMR spectrum of oleyl phenyl hydrogen phosphate**

## 10.3 Core-Shell Particle Synthesis and Characterisation

### 10.3.1 Materials

Styrene (99%, Aldrich), divinylbenzene (DVB, 80%, mixture of isomers, Aldrich) and ethylene glycol dimethacrylate (EGDMA, 98%, Aldrich) were purified by washing with 10% aqueous sodium hydroxide solution three times, then deionised water three times, drying over magnesium sulphate and distillation under reduced pressure. Monomers were stored in the freezer until use. The surfactant, sodium dodecyl sulphate (SDS, BDH), 2-(N-morpholino)ethanesulfonic acid (MES hydrate, Aldrich) and initiators and associated oxidising agents, potassium persulphate (99+%, ACS reagent, Aldrich), ammonium persulphate (98%, Aldrich), 4,4'-azobis(4-cyanopentanoic acid) (≥98%, Fluka), N,N,N',N'-tetramethylethylenediamine (≥ 98%, purum, Fluka), L-ascorbic acid (99+%, ACS reagent, Aldrich) and hydrogen peroxide (laboratory reagent grade, Fisher) were used as supplied. The solvents; acetone (laboratory reagent grade, Fisher), methanol (HPLC grade, Fisher) and isopropyl alcohol (HPLC grade, Fisher) were used as supplied and deionised water was used throughout. H-Gly-β-Ala-β-Ala peptide (GAA, BACHEM) was used as supplied and all other peptides were synthesised as described in 10.1. Quantikine® Human VEGF ELISA Kit was supplied by R&D Systems and was used as provided.

### 10.3.2 Instrumentation

Centrifugation was carried out using a Fisons MSE Chilspin centrifuge and MSE Micro Centaur centrifuge. Centrifugation cartridges (Vivaspin 20, poly(ether sulfone), MWCO 100,000, 20 ml and Vivaspin 500, poly(ether sulfone), MWCO 30,000, 500 µl) were from Sartorius (Surrey, U.K.)). Slide-A-Lyzer® Dialysis Cassettes (Extra Strength) 10,000 MWCO, 0.5-3 ml capacity, were obtained from Pierce. Particle size and zeta potential analysis were carried out on a Brookhaven Instruments Corporation ZetaPALS Zeta Potential Analyser with the 90Plus/BI-MAS Multi Angle Particle Sizing Option. UV analysis was carried out on a Dynex Technologies MRXII UV-Vis Plate Reader or a HITACHI U-2010 Spectrophotometer. ICP-AES analysis was carried out on a Spectro Ciros ICP emission spectrometer (Radial and Axial) by N. Bramall at the University of Sheffield Centre for Analytical Sciences. TEM images and EDS analysis were carried out by Dr. H. Bagshaw from the University of Sheffield Sorby Centre for Electron

Microscopy on a FEI Tecnai G2 Biotwin "Spirit" 120 kV Transmission Electron Microscope, running at an accelerating voltage of 80 kV with spot size 3, and EDS analysis was carried out on a Link eXL system with "menus" software, running at 120 kV accelerating voltage.

### 10.3.3 Optimisation of Synthetic Procedure for Core Particles

A general formulation for synthesis of poly(styrene-co-divinylbenzene) core particles was determined to allow initiation by the redox system of potassium persulphate and ascorbic acid. The monomer composition, reaction temperature and surfactant quantity were varied to determine the optimum procedure and details of the various formulations are provided in Table 10.3. A table of the varied parameters is provided below and the optimised synthetic procedure for this initiator system is described.

| Sample | Styrene (g) | DVB (g) | Molar Ratio | SDS (g) | Temp (°C) | Potassium Persulphate (g) | Ascorbic acid (g) | Molar Ratio |
|---|---|---|---|---|---|---|---|---|
| 1 | 4.64 | 5.82 | 1:1 | 1.00 | RT | 0.105 | 0.068 | 1:1 |
| 2 | 8.36 | 1.16 | 9:1 | 1.00 | RT | 0.105 | 0.068 | 1:1 |
| 3 | 8.36 | 1.16 | 9:1 | 0.50 | 30 | 0.105 | 0.068 | 1:1 |
| 4 | 8.36 | 1.16 | 9:1 | 2.00 | 30 | 0.105 | 0.068 | 1:1 |
| 5 | 8.36 | 1.16 | 9:1 | 1.00 | 30 | 0.105 | 0.068 | 1:1 |
| 6 | 8.36 | 1.16 | 9:1 | 1.00 | 30 | 0.209 | 0.068 | 2:1 |
| 7 | 4.50 | 0.50 | 11:1 | 1.00 | 30 | 0.209 | 0.068 | 2:1 |

**Table 10.3: Latex formulations for poly(styrene-co-divinylbenzene)**

***Optimised Synthesis of Poly(styrene-co-divinylbenzene) Core Particles for Redox Initiation with Potassium Persulphate and Ascorbic Acid***

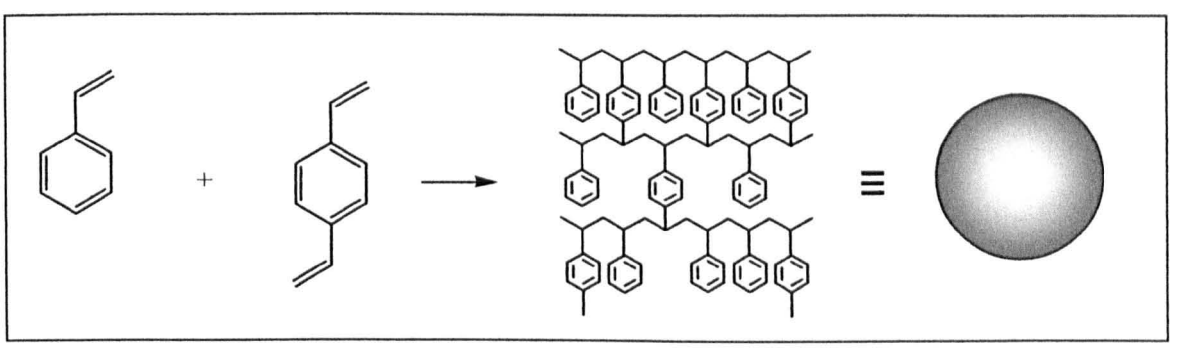

A 50 mM solution of MES buffer in deionised water was produced by dissolving MES buffer (0.533 g, 2.73 mmol) in 45 ml deionised $H_2O$. This solution was purged with nitrogen for 15 minutes and SDS surfactant (1 g, 3.47 mmol) was added and stirred until dissolved. The solution with surfactant was sonicated for 10 minutes and then adjusted to pH 6 through dropwise addition of 0.5 M NaOH solution. Polymerisation was conducted in a 100 ml jacketed glass flange reaction vessel with a five necked lid equipped with paddle stirrer, nitrogen inlet, reflux condenser, temperature probe and pressure equalised dropping funnel. The buffer solution was introduced to the reaction vessel which was heated and previously purged with nitrogen. The buffer solution was stirred at 400 rpm and brought to 30°C. Styrene (4.50 g, 43.21 mmol) and DVB (0.50 g, 3.84 mmol) were combined, purged with $N_2$ for 5 minutes and added dropwise to the solution via an addition funnel over a 30 minute period. Potassium persulphate (0.209 g, 0.774 mmol) and ascorbic acid (0.068 g, 0.387 mmol) were dissolved in 5 ml $H_2O$ and this initiator solution was then purged with nitrogen for 5 minutes before being added to the stirring monomer suspension in a one-shot initiation. Emulsion polymerisation was carried out overnight.

### 10.3.4 Synthesis of Poly(OPHP-co-EGDMA) Outer Shell (Core-Shell Particle)

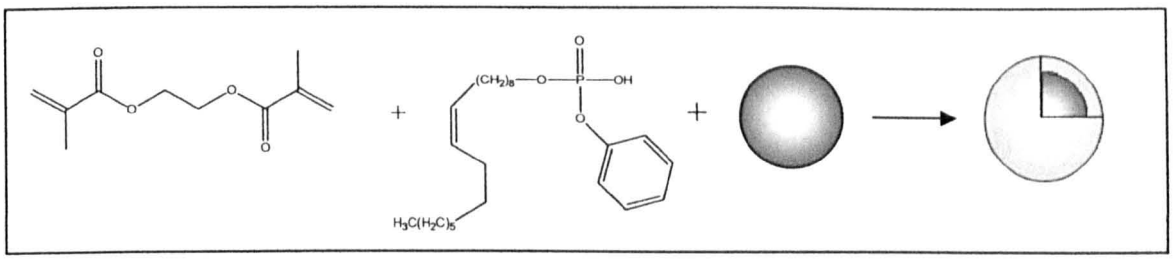


EGDMA (0.226 g, 1.14 mmol) and oleyl phenyl hydrogen phosphate (0.204 g, 0.482 mmol) were suspended in 13.5 ml of deionised water and added dropwise to the stirring emulsion of core particles over 15 minutes. The monomer was allowed to equilibrate around the core particles for one hour. The initiator solution was produced by dissolving potassium persulphate (0.209 g, 0.774 mmol) and ascorbic acid (0.068 g, 0.387 mmol) in 5 ml $H_2O$ and then the solution was purged for 5 minutes with nitrogen. This solution was added to the latex in one shot. The emulsion was reacted at 30°C overnight.

### 10.3.5 Study of Initiator Systems for Core and Core-Shell Particle Synthesis

The procedures detailed previously for the synthesis of the core and the core-shell particles were repeated with various initiator conditions. The procedures described in 10.3.3 and 10.3.4 were only altered by the reaction temperature and initiation step, the conditions and procedures for which are detailed in table 10.4.

| Initiator System | Temp (°C) |
|---|---|
| Potassium persulphate & ascorbic acid | 30 |
| Hydrogen peroxide & ascorbic acid | 35 |
| Ammonium persulphate & N,N,N',N' tetramethyl-ethylenediamine | 30 |
| 4,4'-azobis(4-cyanovaleric acid) | 60 |
| Potassium persulphate | 70 |

**Table 10.4: Initiator systems trialled for core-shell particle synthesis**

#### *Redox Initiation by Potassium Persulphate and Ascorbic Acid*

The synthetic procedure was carried out in a reactor heated to 30°C. The initiator solution was produced by dissolving potassium persulphate (0.209 g, 0.774 mmol) and ascorbic acid (0.068 g, 0.387 mmol) in 5 ml $H_2O$ and purging with nitrogen for 5 minutes before adding to the reactor in a one-shot initiation.

#### *Redox Initiation by Hydrogen Peroxide and Ascorbic Acid*

The synthetic procedures were carried out in a reactor at room temperature. The initiator solution was produced by dissolving ascorbic acid (3.7 mg, 0.021 mmol) in 5 ml of deionised water. 0.122 ml of hydrogen peroxide solution (30% w/v solution) (0.037 g, 1.09 mmol) was combined with the ascorbic acid solution, the solution was purged with $N_2$ for 5 minutes and then added to the reactor in one shot. The reaction mixture was heated to 35°C and reacted overnight.

#### *Redox Initiation by Ammonium Persulphate and N,N,N',N'-Tetramethyl-ethylenediamine (TEMED)*

The synthetic procedures were carried out in a reactor at 30°C. The initiator solution was produced by combining ammonium persulphate (0.269 g, 1.18 mmol) and TEMED (0.269 ml, 2.31 mmol) in 5 ml of deionised water. This solution was purged with $N_2$ for 5 minutes and added to the reaction mixture in one shot.

***Thermal Initiation by 4,4'-Azobis(4-cyanovaleric acid)***

The synthetic procedures were carried out in a reactor at 60°C. Initiation was afforded by the addition of 4,4'azobis(4-cyanovaleric acid) (0.33 g, 1.18 mmol) directly into the reaction mixture.

***Thermal Initiation by Potassium Persulphate***

The synthetic procedures were carried out in a reactor at 70°C. The reaction was initiated by the one shot addition of potassium persulphate (0.32 g, 1.18 mmol) in 7.5 ml deionised $H_2O$, prepurged with $N_2$ for 5 minutes.

### 10.3.6 Synthesis of Core-Shell Particles by Starve-Fed Monomer Addition

The core particles were synthesised as described in section 10.3.3 through thermal initiation by potassium persulphate at 70°C (detailed in section 10.3.5). Potassium persulphate (0.32 g, 1.18 mmol) in 7.5 ml deionised $H_2O$ was added into a stirring emulsion of core particles at 70°C. Immediately after initiation the monomers, oleyl phenyl hydrogen phosphate (0.204 g, 0.482 mmol) and EGDMA (0.226 g, 1.14 mmol), were combined and added dropwise to the emulsion suspended in 30 ml of deionised $H_2O$ at 0.2 ml/min via a peristaltic pump. The reaction was continued for 24 hrs.

### 10.3.7 Final Synthetic Procedure for Core and Core-Shell Particles

***Core Particles***

A 50 mM solution of MES buffer in deionised water was produced by dissolving MES buffer (0.533 g, 2.73 mmol) in 45 ml deionised $H_2O$. This solution was purged with nitrogen for 15 minutes and SDS surfactant (1 g, 3.47 mmol) was added and stirred until dissolved. The solution with surfactant was sonicated for 10 minutes and then adjusted to pH 6 through dropwise addition of 0.5 M NaOH solution. Polymerisation was conducted in a 100 ml jacketed glass flange reaction vessel with a five necked lid equipped with paddle stirrer, nitrogen inlet, reflux condenser, temperature probe and pressure equalised dropping funnel. The buffer solution was introduced to the reaction vessel. The buffer solution was stirred at 400 rpm and brought to 30°C. Styrene (4.50 g, 43.21 mmol) and DVB (0.50 g, 3.84 mmol) were combined, purged with $N_2$ for 5 minutes and added dropwise to the solution via an addition funnel over a 30 minute

period. The initiator solution was produced by dissolving potassium persulphate (0.16 g, 0.59 mmol) in 7.5 ml $H_2O$ and then purging the solution for 5 minutes with nitrogen before adding to the stirring monomer suspension in a one-shot initiation. Emulsion polymerisation was carried out at 70°C overnight.

***Core-Shell Particles***

EGDMA (0.226 g, 1.14 mmol) and oleyl phenyl hydrogen phosphate (0.204 g, 0.482 mmol) were suspended in 13.5 ml of deionised water and added dropwise to the stirring emulsion of core particles at 70°C over 15 minutes. The monomer was allowed to equilibrate around the core particles for one hour. The initiator solution was produced by dissolving potassium persulphate (0.16 g, 0.59 mmol) in 7.5 ml $H_2O$ and then purging the solution for 5 minutes with nitrogen. The second stage of polymerisation was then initiated by the addition of this solution to the stirring latex in one shot. The emulsion was allowed to react at 70°C overnight.

### 10.3.8 Synthesis of Molecularly-Imprinted Core-Shell Particles

Core particles were synthesised as described in section 10.3.7. EGDMA (0.045 g, 0.228 mmol) and oleyl phenyl hydrogen phosphate (0.041 g, 0.096 mmol) were suspended in 2.7 ml of deionised water and added dropwise to the stirring emulsion of core particles (10 ml) over 15 minutes. The monomer was allowed to equilibrate around the core particles for one hour. The template compound (0.096 mmol, 1 eq.) was added in 2 ml of 50 mM MES buffer at pH 6 and stirring was continued for an hour. The initiator solution was produced by dissolving potassium persulphate (0.032 g, 0.118 mmol) in 1.5 ml $H_2O$ and then purging the solution for 5 minutes with nitrogen. The second stage of polymerisation was initiated via the addition of this solution to the stirring latex in one shot. The emulsion was allowed to react at 70°C overnight. Blank-imprinted particles were prepared by repeating the procedure in the absence of a template.

| Polymer | Template | Quantity (mg) | Equivalent (peptide:functional monomer) |
|---|---|---|---|
| DKPRR CS-MIP | DKPRR | 64.7 | 1:1 |
| GAA CS-MIP | GAA | 20.9 | 1:1 |
| Blank CS-MIP | None | 0 | - |

**Table 10.5: Template quantities employed in molecular imprinting of core-shell emulsion particles**

### 10.3.9 Analysis

***Solid Content Analysis***

An aliquot of emulsion of core or core-shell particles and 3 ml of acetone were pipetted into a centrifuge tube and agitated to allow precipitation of the whole sample. The sample was then centrifuged at 3000 rpm for 5 minutes before removing the supernatant. This process was repeated three times. The acetone was again decanted off, replaced with deionised water and centrifuged for 5 minutes at 3000 rpm. This was repeated twice more with deionised water and finally three times with methanol before the solvent was decanted off and the solid was allowed to dry to a constant mass.

$$\text{Solid content} = W_p / \text{mass of latex}$$

Where $W_p$ = mass of dried polymer

***Particle Size Analysis***

To prepare the samples, five drops of a particular latex were added to 20 ml of a 1 mmol KCl solution. This solution was then sonicated for 20 seconds, filtered through a 0.45 μm aqueous filter and added to a cuvette for measurement at 25°C. Ten analysis runs were carried out in triplicate for each sample.

***Zeta Potential Analysis***

Samples were prepared for zeta potential analysis by the addition of five drops of a particular latex into 20 ml of a 1 mmol KCl solution. This solution was pipetted into a zeta potential cuvette for analysis, ensuring no air bubbles were present at the electrode surface. The zeta potentials were analysed at 25°C in five analysis cycles, each consisting of ten repeat runs.

***TEM and EDS Studies***

A 2 ml aliquot of the core or CS-MIP emulsion was injected into a Slide-A-Lyzer® cassette. The emulsions were then dialysed against 1 M phosphoric acid, with the addition of 2.5% sodium dodecyl sulphate to prevent coagulation, over three days with the solution changed twice daily. Finally, the emulsions were dialysed against 2.5% sodium dodecyl sulphate/distilled water for three days, again with twice daily solution changes. Materials were prepared for EDS by evaporating the colloidal suspensions

onto 600 mesh, 3 mm diameter copper grids coated with a carbon film. Materials were prepared for TEM by adsorbing a drop of emulsion onto a carbon-coated grid and leaving for 1 minute. The grid was then blotted, washed in a drop of distilled water and blotted again. The grid was washed once more in a drop of uranyl formate, blotted and then negatively stained by holding the grid in a drop of uranyl formate for 20 seconds before blotting.

***Inductively Coupled Plasma Atomic Emission Spectroscopy***

Latexes produced during the initiator trial as well as latex produced by starve-fed monomer addition and all molecularly-imprinted particles were analysed for total oleyl phenyl hydrogen phosphate content by Inductively Coupled Plasma Atomic Emission Spectrometry (ICP-AES).

*Preparation of Solid Resins for Inductively Coupled Plasma Atomic Emission Spectroscopy (ICP-AES)*

An emulsion sample (2 ml) was added to a 20 ml centrifugation cartridge (MWCO 100,000) followed by the dropwise addition of isopropyl alcohol (1.1 ml) to induce coagulation. The centrifuge cartridge was agitated gently until the solids had precipitated out. The sample was allowed to stand for 10 minutes to allow complete precipitation and was then centrifuged at 4500 rpm at room temperature using a benchtop centrifuge with swing-bucket rotor for 30 minutes. The damp solids remaining were washed with 7:3 IPA/$H_2O$ (5 ml) and the suspension was then agitated and centrifuged at 4500 rpm for 30 minutes. This procedure was carried out six times. The solids were then washed with deionised water (5 ml) (or 1 M $H_3PO_4$ for elution of template on CS-MIP), gently agitated to produce a suspension and then centrifuged at 4500 rpm for 5 minutes. This washing step was also repeated six times. The final washing step was washing the solids with methanol (5 ml), followed by agitation and centrifuging at 4500 rpm for 5 minutes. This step was also repeated six times. The polymer was then dried to a constant mass in a vacuum oven at 60°C for 48 hours. The polymer was then refluxed in concentrated nitric acid (5 ml) at 160°C for 4 hours followed by perchloric acid at 200°C for 30 minutes and the resulting solution was then analysed for phosphorous content by ICP-AES.

### 10.3.10 Colorimetric Peptide Binding Study

***Preparation of Polymer***

An aliquot of emulsion (0.1 ml) was pipetted into a 30,000 MWCO Vivaspin centrifugal concentrator, followed by isopropyl alcohol (0.5 ml) to coagulate the latex. The sample was agitated on an orbital shaker plate at 150 rpm for 10 minutes before being centrifuged at 10,000 rpm for 10 minutes. The coagulated polymer was then washed with a 7:3 IPA/$H_2O$ solution, agitated for 10 minutes on an orbital shaker plate at 150 rpm and then removed by centrifugation for 10 minutes at 10,000 rpm. This wash step was carried out six times with 7:3 IPA/$H_2O$, six times with 1 M $H_3PO_4$ (solvent removed by centrifuging for 5 minutes at 5,000 rpm), six times with $H_2O$, six times with methanol and finally six times with $H_2O$. The polymer slurry was used damp.

***Peptide Binding Study***

0.5 ml of peptide solution (30 μg/ml, MRSSSDKPRR, MRSSSPRKRD or MRSSSSSSSS) was added to the polymer slurry and the resulting suspension was agitated on an orbital shaker plate at 200 rpm for 30 minutes. The supernatant was removed after centrifugation for 20 minutes at 10,000 rpm. The peptide was then removed from the polymer with solutions of IPA/$H_2O$ with IPA percentages of 5, 10, 20, 30, 35, 40, 45, 50, 60, 70, 80, 90 and 100. In all cases the solution was removed after 30 minutes by centrifugation for 20 minutes at 10,000 rpm. All peptide solutions were analysed by UV in quartz cuvettes with a 1 mm path length at 470 nm.

***Peptide Release Study***

The remaining methyl red-tagged peptide was removed by sequential washes with 50% phosphoric acid solutions and 50% IPA. The acid/IPA solutions were added to the polymer slurry, the suspension was agitated and then left on an orbital shaker plate at 200 rpm for 30 minutes. The liquid was removed by centrifugation for 20 minutes at 10,000 rpm. The peptide was then washed off the polymer with solutions of acid/IPA with phosphoric acid molarities of 0.01 M, 0.02 M, 0.03 M, 0.04 M, 0.05 M, 0.06 M, 0.07 M, 0.08 M, 0.09 M, 0.1 M, 0.15 M, 0.2 M, 0.25 M, 0.3 M, 0.35 M, 0.4 M, 0.45 M, 0.5 M, 0.6 M, 0.7 M, 0.8 M, 0.9 M and 1 M. In all cases the solution was removed by centrifugation for 20 minutes at 10,000 rpm. All peptide solutions were then analysed by UV spectrometry in quartz cuvettes with a 1 mm path length at 510 nm.

### 10.3.11 Zeta Potential Peptide Binding Study

A 2 ml aliquot of the core or CS-MIP emulsion was injected into a Slide-A-Lyzer® cassette. The emulsions were then dialysed against 1 M phosphoric acid, with the addition of 2.5% sodium dodecyl sulphate to prevent coagulation, over three days with twice daily solvent changes. Finally, the emulsions were dialysed against 2.5% sodium dodecyl sulphate/distilled water for three days with solvent changed twice daily. 0.1 ml of emulsion was added to 2 ml of 1 mmol KCl and was agitated to produce a homogeneous latex. The zeta potentials were analysed at 25°C in five analysis cycles, each consisting of ten repeat runs. 10 µl of DKPRR or SSSSSSSS peptide solution (0.5 mg/ml) was added to each emulsion and agitated before measuring the pH of the solution and the zeta potential. In total, six aliquots of each peptide were added and analysed for pH and zeta potential.

### 10.3.12 Enzyme-Linked ImmunoSorbent Assay (ELISA) of VEGF Binding (MIP)

Three polymer types were analysed in duplicate for this study; DKPRR-imprinted, GAA-imprinted and blank-imprinted core-shell particles. The polymers (0.1 ml emulsion) were coagulated with 0.5 ml isopropyl alcohol and were then washed as described in Section 10.3.10. A conductivity meter was utilised to analyse the final wash solutions to confirm SDS removal. VEGF solutions (150 ng in 0.5 ml PBS) were then added to the polymer in a polypropylene tube. The solutions were agitated and then allowed to interact for 24 hours at 4°C. The suspensions were then centrifuged at 13,000 rpm for 20 minutes and the supernatant was removed and stored at -20°C until an ELISA study was carried out.

0.5 ml of fresh 1% BSA PBS solution was added to the polymer samples, then agitated and placed in an incubator at 37°C for the release study. At defined time points (1 hr, 6 hrs, 12 hrs, 24 hrs and 48 hrs) the protein solution was removed and replaced with 0.5 ml fresh 1% BSA PBS solution. The protein solutions retrieved were stored at -20°C in polypropylene tubes until analysis with an ELISA kit. The BSA was utilised to stabilise the VEGF during the release study and storage period. Each experimental condition was carried out and analysed in duplicate.

#### *ELISA Procedure*

The ELISA was carried out as described by the manufacturer. 50 µl of assay diluents was added to a 96 well plate coated with a mouse monoclonal antibody for VEGF. 200 µl of either the standard, control or sample was added to each well and the plate was agitated gently at room temperature for 2 hours. Each well was washed six times with wash buffer (400 µl) and any remaining wash buffer was removed by blotting on clean paper towels. VEGF conjugate (200 µl) was added to each well, followed by gentle agitation for 2 hours at room temperature. Each well was washed a further six times. Substrate solution (200 µl), consisting of equal quantities of stabilised hydrogen peroxide and stabilised tetramethylbenzidine, was added to each well and was agitated gently at room temperature for 20 minutes whilst being protected from the light. Sulphuric acid (2 M, 50 µl) was added to the wells to stop the reaction and the optical density was measured within 30 minutes at 450 nm on a UV-Vis plate reader.

## 10.4 Hydrogel Synthesis, Functionalisation and Characterisation

### 10.4.1 Materials

The monomers N-vinyl-2-pyrrolidone (NVP, ≥99%, Aldrich) and acrylic acid (99%, Aldrich) were purified by distillation at reduced pressure and were stored at 4°C until use. The crosslinker, diethylene glycol-bisallyl carbonate (DEGBAC, 94%, Pfalz & Bauer Inc.) and the initiators, 2,2'-azobisisobutyronitrile (AIBN, 97%, BDH) and 2-hydroxy-2-methylpropiophenone (HMPP, 97%, Aldrich) and were used as supplied. The coupling reagents 1-ethyl -3-(3-dimethylaminopropyl)-carbodiimide (EDC, Aldrich), N,N'-dicyclohexyl-carbodiimide (DCC, 99%, Aldrich), N-hydroxy-succinimide (98%, Aldrich), sodium acetate (anhydrous, May and Baker), sodium dihydrogen phosphate dehydrate (Fluka) and disodium hydrogen phosphate dehydrate (Fluka) were used as supplied. The coupling analysis reagents 2,4,6-trinitrobenzenesulphonic acid solution (5% w/v solution, Sigma), 1-napthol (97%, Fisons), urea (≥ 98%, Sigma) and bromine (Aldrich) were used as supplied. Heparin (Sodium salt, Grade 1-A, from porcine intestinal mucosa, Sigma), fluorescein-5-thiosemicarbazide (fluorescence grade, Fluka) and methylene blue (certified by the BSC, Sigma Aldrich) were used as supplied. The solvents; ethanol (absolute, laboratory reagent grade, Fisher), diethyl ether (anhydrous, laboratory reagent grade, Fisher) *N,N*-dimethylformamide (laboratory reagent grade, Fisher) were used as supplied, and deionised water was used throughout. A Quantikine® Human VEGF ELISA Kit was supplied by R&D Systems and was used as supplied.

### 10.4.2 Instrumentation

$^{1}H$ and $^{13}C$ spectra were obtained on a Bruker AC 250 MHz and AMX2-400 MHz spectrometer using deuterated water throughout. Gas chromatography was carried out on a Perkin Elmer Instruments Autosystem XL Gas chromatograph with autosampler and FID detector. UV analysis was carried out on a Dynex Technologies MRXII UV-Vis Plate Reader or a HITACHI U-2010 Spectrophotometer. Fluorescence spectroscopy was carried out on a Luminescence Spectrometer LS50B (Perkin-Elmer Ltd). Slide-A-Lyzer® Dialysis Cassettes (Extra Strength) 3,500 MWCO, 0.5-3 ml capacity were obtained from Pierce. XPS and SIMS analysis was carried out by Dr. T. Whittle at the Kroto Institute, University of Sheffield. X-ray photoelectron spectra were acquired on a

Kratos Axis Ultra X-ray photoelectron spectrometer (Kratos Ltd, Manchester). All samples were run as insulators, requiring use of the electron flood gun. The flood gun was operated at a filament current of 1.8 A and charge balance of 3.4 V. The X-ray source was a monochromated Al source operated with an X-ray emission current of 10 mA and an anode high throughput (acceleration voltage) of 15 kV. Survey scans were acquired with a pass energy of 160 eV and a step size of 1.0 eV, whilst high resolution $C_{1s}$ were collected at a pass energy of 20 eV and a step size of 0.1 eV. Secondary Ion Mass Spectrometry data were acquired on an Ion-ToF V mass spectrometer (Ion-ToF, Munster, Germany), equipped with a bismuth liquid metal primary ion beam with an energy of 25 keV. Samples were all run as insulators. Positive and negative ion spectra were recorded from a fresh 150 μm x 150 μm analysis area using the $Bi_3^{++}$ cluster ion source. The primary ion beam current was adjusted to be less than 0.22 pA at 100 μs cycle time.

### 10.4.3 Synthesis of Diethylene Glycol Bisallyl Carbonate (DEGBAC)-Crosslinked Poly(NVP-co-AA) Hydrogels

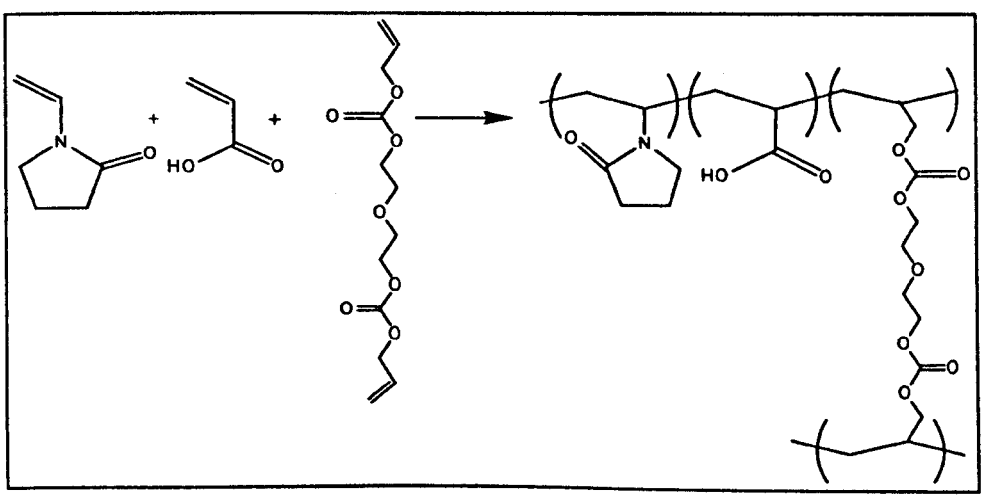

***Thermal Polymerisation: Poly(NVP-co-DEGBAC-co-AA) Hydrogels***

Into a 100 ml beaker were weighed NVP, DEGBAC, acrylic acid and AIBN (0.1 g, 0.6 mmol). Nitrogen was bubbled through the stirring reaction mixture for 30 minutes to degas and homogenise the solution. The solution was injected into a pre-made mould of dimensions 7.5 x 7.5 $cm^2$ and thickness of 1 mm, consisting of glass plates and a PTFE gasket. The mould was then placed horizontally into an oven at 60°C to react for 24 hours. The hydrogel produced was removed from the mould and placed in ethanol on an

orbital shaker plate at 100 rpm. The ethanol was changed daily for one week before final storage in ethanol.

| Polymer | NVP | | | DEGBAC | | | Acrylic acid | | |
|---|---|---|---|---|---|---|---|---|---|
| | Mass (g) | % | mmol | Mass (g) | % | mmol | Mass (g) | % | Mmol |
| 1 | 9.3 | 93 | 83.7 | 0.2 | 2 | 0.7 | 0.5 | 5 | 6.9 |
| 2 | 9.6 | 96 | 86.4 | 0.2 | 2 | 0.7 | 0.2 | 2 | 2.8 |

**Table 10.6: Formulations for thermally-cured hydrogels**

***UV Polymerisation: Poly(NVP-co-DEGBAC-co-AA) Hydrogels***

NVP, DEGBAC, acrylic acid and 2-hydroxy-2-methylpropiophenone (0.1 g, 0.6 mmol) were weighed into a 100 ml beaker. Ethanol was added to give a 33% ethanol solution (v/v). Nitrogen was bubbled through the stirring reaction mixture for 30 minutes in the dark to degas and homogenise the solution. The solution was injected into a pre-made mould of dimensions 7.5 x 7.5 $cm^2$ and a thickness of 500 μm, consisting of two quartz plates and a PTFE gasket. The mould was then placed horizontally into a UV oven and allowed to react for 6 minutes, 1 minute on each side alternately. The hydrogel produced was removed from the mould and placed in ethanol on an orbital shaker plate at 100 rpm. The ethanol was changed daily for one week before final storage in ethanol.

| Polymer | NVP | | | DEGBAC | | | Acrylic acid | | |
|---|---|---|---|---|---|---|---|---|---|
| | Mass (g) | % | Mmol | Mass (g) | % | mmol | Mass (g) | % | Mmol |
| 1 | 9.7 | 97 | 87.3 | 0.1 | 1 | 0.4 | 0.2 | 2 | 2.8 |
| 2 | 9.4 | 94 | 84.6 | 0.1 | 1 | 0.4 | 0.5 | 5 | 6.9 |
| 3 | 9.8 | 98 | 88.2 | 0.2 | 2 | 0.7 | 0 | 0 | 0 |
| 4 | 9.6 | 96 | 86.4 | 0.2 | 2 | 0.7 | 0.2 | 2 | 2.8 |
| 5 | 9.3 | 93 | 83.7 | 0.2 | 2 | 0.7 | 0.5 | 5 | 6.9 |
| 6 | 9.3 | 93 | 83.7 | 0.5 | 5 | 1.8 | 0.2 | 2 | 2.8 |
| 7 | 9.0 | 90 | 81.0 | 0.5 | 5 | 1.8 | 0.5 | 5 | 6.9 |

**Table 10.7: Formulations for UV-cured hydrogels**

### 10.4.4 Hydrogel Analysis

***Equilibrium Water Content (EWC)***

The equilibrium water content of the hydrogels was analysed by cutting a circular disc from a sheet of hydrogel swollen in water. Any excess water was removed gently by a paper towel and the swollen weight of the polymer was recorded. The polymer was then placed in a vacuum oven at 50°C over a 48 hour period. The weight of the polymer disc was then recorded every two hours until the weight remained constant.

$$\text{EWC}\,(\%) = ((W_w - W_d)/W_w) \times 100$$

Where $W_w$ = wet weight and $W_d$ = dry weight

***Residual Monomer Analysis by Gas Chromatography***

1 $cm^2$ of hydrogel was weighed and placed in 2 ml of methanol for 24 hours on an orbital shaker plate in sealed glass bottles. The solvent was then analysed by GC under the conditions described in Table 10.8. The residual monomer content was calculated by comparison to calibration curves for the relevant monomers.

| Gas Chromatography Operating Parameters | |
|---|---|
| GC Instrument | Perkin Elmer Autosystem XL |
| Column | Phenomenex, ZB-5 (5% Phenyl Polysiloxane) |
| Column Dimensions | L = 30 m x ID = 25 nm x DF = 25 μm |
| Oven Temperature | Initial = 60°C, increasing 10°C/min to 260°C |
| Carrier Gas and flow | Helium, 0.8 ml/min |
| Split Flow Rate | 50.0 ml/min |
| Injection source and mode | Autosampler, Split with a ratio of 61.5/1 |
| Injection temperature and volume | 250°C, 0.5 ml |
| Detector | FID at 250°C |
| Sampling rate | 6.25 pts/s |

**Table 10.8: Gas chromatography operating parameters for residual monomer analysis**

## 10.4.5 Synthesis of Peptide-Hydrogel Conjugates

### *Determination of Reaction Conditions*

In order to determine a successful procedure for the synthesis of a polymer-peptide conjugate a number of coupling reactions were trialled for the synthesis of a poly(NVP-co-DEGBAC-co-AA)-lysine conjugate through a two-step reaction involving activation of the acid functionality followed by coupling of the activated group and lysine. The coupling procedures trialled are detailed in Table 10.9 and a general procedure is provided.

| | | Trial No. | | | | |
|---|---|---|---|---|---|---|
| | | 1 | 2 | 3 | 4 | 5 |
| Activation | Reagent 1 (compound, equivalent) | EDC (5) | EDC (5) | EDC (5) | EDC (5) | DCC (5) |
| | Reagent 2 (compound, equivalent) | NHS (5) | NHS (5) | NHS (5) | NHS (5) | NHS (5) |
| | Solvent | Water | Water | Water | Water | DMF |
| | Temp. (°C) | 0 | 0 | 0 | 0 | RT |
| | Time (hr) | 24 | 24 | 24 | 24 | 24 |
| Peptide Coupling | Peptide Equivalent | 2 | 2 | 2 | 2 | 2 |
| | pH | 5.5 | 5.5 | 8.5 | 8.5 | 8.5 |
| | Buffer | Sodium acetate | Sodium acetate | PBS (0.01M) | PBS (0.01M) | PBS (0.01M) |
| | Temp. (°C) | 0 | 0 | 0 | 0 | 0 |
| | Time (hr) | 24 | 72 | 24 | 72 | 72 |

**Table 10.9: Experimental parameters for coupling trials of lysine to acid-functionalised hydrogels. Equivalent values calculated from molar acrylic acid quantities.**

### *General Procedure*

The poly(NVP-co-DEGBAC-co-AA) hydrogel was removed from the sterile ethanol solution and placed in 10 ml of the solvent utilised in the activation reaction step. The solvent was replaced after 1 hour and this was repeated three times. The hydrogel was placed into the activation solution (10 ml, 5 eq. reagents 1 and 2) and the reaction vessel was placed on an orbital shaker at 350 rpm for 24 hours either at room temperature or in a dewar with ice at 0°C under nitrogen. The hydrogel was removed from the activation solution and placed into 10 ml of the solvent utilised in the activation step for one hour to remove the remaining activation reagents. The solution was replaced three times and the hydrogel was then placed into the coupling solution (10 ml, 2 eq. lysine or lysine

peptide). The reaction vessel was placed in a dewar of ice under nitrogen at 0°C on an orbital shaker for 24 or 72 hours. Once the coupling reaction was complete the polymer-peptide conjugate hydrogel was placed in 10 ml water to remove any non-covalently bound peptide and to hydrolyse any activated acid groups remaining. The water was changed twice daily for one week before the hydrogel was finally placed in absolute ethanol for storage until use.

***Finalised Coupling Procedure for Peptide-Conjugated Hydrogel Synthesis***

20 discs of UV-cured poly(NVP-co-DEGBAC-co-AA) hydrogel (5 mm swollen diameter, 2 wt% DEGBAC, 5 wt% acrylic acid) was removed from the sterile ethanol solution and placed in anhydrous DMF (4 ml) under nitrogen and allowed to equilibrate for 1 hour. The DMF was replaced twice under nitrogen to ensure that the polymer was equilibrated within the solvent. The DMF was replaced under nitrogen with activation solution (NHS & DCC in 10 ml DMF, 5 eq.) and the reaction vessel was placed on an orbital shaker at 350 rpm for 24 hours at room temperature. The activation solution was removed under nitrogen and replaced with 5 ml of DMF with agitation for 1 hour to remove the remaining activation reagents. The DMF was replaced twice before removal of DMF and addition of the coupling solution (10 ml) containing the peptides (KKK or RRR, 2 eq.) in 0.01 M PBS (pH 8.5). The reaction vessel was placed in a dewar of ice at 0°C on an orbital shaker for 72 hours. Once the coupling reaction was complete, the peptide-conjugated hydrogels were placed in 10 ml water to remove any non-covalently bound peptide and to hydrolyse any activated acid groups remaining. The water was changed once a day for one week before the hydrogels were finally placed in absolute ethanol for storage until use.

These peptide-functionalised hydrogels were equilibrated in the relevant medium and analysed directly by solid state NMR, XPS and ToF-SIMS. The hydrogels were used directly for heparin and VEGF binding and cell culture.

### 10.4.6 Analysis of Coupling Efficiency

The coupling efficiency was analysed quantitatively by a colorimetric assay for primary amines with 2,4,6-trinitrobenzenesulphonic acid (TNBS). The coupling efficiency was analysed both indirectly through analysis of peptide concentration remaining in the coupling solution after coupling, and directly through the analysis of the concentration of the peptide on the hydrogel after the washing steps. Coupling efficiency was determined through a calibration curve produced for each individual peptide sequence. A fresh calibration was carried out for each analysis. Qualitative coupling analysis for arginine presence was carried out by the Weber modification[296] of the Sakaguchi process[297].

#### *Preparation of Poly(NVP-co-DEGBAC-co-AA) Hydrogels for Direct Analysis*

A piece of hydrogel was placed in 5 ml of aqueous NaOH (0.5 M) on an orbital shaker at 350 rpm for one hour until dissolved. Hydrochloric acid (0.5 M) was added to the solution until neutral pH was reached, as measured by a pH meter. The water was then removed by freeze-drying before analysis. The freeze-dried polymer obtained was then analysed to determine coupling efficiency.

#### *Colorimetric TNBS Analysis of Coupling Efficiency*

Analyte solution (coupling solution before and after the coupling reaction, wash solution or degraded hydrogel in sodium tetraborate solution) was combined with sodium tetraborate (0.10 M, pH 9.3) and 0.1 ml of aqueous TNBS solution (0.03 M) (Table 10.10). This solution was agitated to ensure complete mixing and allowed to stand for 30 minutes at room temperature. Absorbance was read on a UV/Vis spectrophotometer at 420 nm (Molar extinction coefficient for TNBS-lysine conjugate, $\varepsilon = 9787 \pm 590$ $Lmol^{-1}cm^{-1}$ at 420 nm).

| Analyte | Amount of analyte | Volume of sodium tetraborate (ml) | Volume of TNBS solution (ml) |
|---|---|---|---|
| Coupling solution | 0.25 ml | 1.65 | 0.1 |
| Washing solution | 1 ml | 0.9 | 0.1 |
| Dissolved polymer | 2 mg | 1.9 | 0.1 |

**Table 10.10: Volumes employed in colorimetric TNBS analysis of peptide coupling efficiency**

***Colorimetric Arginine Determination – Weber Modification of Sakaguchi Reaction***[296]

Reagents:

(A) 10% KOH aqueous solution

(B) 0.1% 1-napthol in 50% ethanol

(C) 5% urea

(D) 0.64 ml bromine in 100 ml of 5% KOH (prepared daily)

One piece of hydrogel was added to 1 ml of A and 1 ml of B and allowed to stand for 3 minutes. Then 1 ml of C was added with mixing, followed by the addition of 2 ml of D with continuous shaking. The solution was allowed to stand for 5 minutes before qualitative analysis was undertaken.

### 10.4.7 Fluorescent Heparin Binding Study

#### *Synthesis of Fluorescently-Tagged Heparin*

Heparin (50 mg) was dissolved in 2 ml of a 0.1 M phosphate buffered saline solution (0.1 M sodium phosphate, 0.15 M sodium chloride, pH 7.5). 250 mM sodium iodate solution (0.2 ml in 0.1 M phosphate buffered saline solution) was added to the heparin solution whilst being protected from light and was allowed to react for 2.5 hours. The heparin solution was placed into a pre-wetted Slide-a-Lyzer® dialysis cassette and dialysed against 1500 ml deionised water in the dark for 1 hour. The heparin solution was then dialysed against 1500 ml 0.1 M phosphate buffered saline at pH 7.5 for 16 hours, stirring and in the dark at room temperature. The oxidised heparin solution was removed from the cassette, added to fluorescein-5-thiosemicarbazide (FTSC) in DMF (0.4 ml, 150 mM) and reacted for 2.5 hours at room temperature in the dark. The heparin solution was placed into a pre-wetted Slide-a-Lyzer® dialysis cassette and dialysed against 1500 ml deionised water in the dark for 1 hour. The heparin solution was then dialysed against 1500 ml 0.1 M phosphate buffered saline at pH 7.5 for 16 hours, stirring and in the dark at room temperature. The dialysis solution was replaced until no more dye leeched from the Slide-a-Lyzer® cassette.

#### *Quantification of Heparin Solution Concentration*

A calibration curve for methylene blue with heparin in deionised water was produced by the analysis of solutions of constant methylene blue concentration (0.04 mM, 1 ml) and increasing heparin concentrations (0 μg/ml – 100 μg/ml). The absorption of these solutions was analysed at 630 nm on a U-2010 spectrophotometer. Triplicate readings of polysaccharide-FTSC solution (1 μl of solution/ml methylene blue solution) were taken at 630 nm and the concentration of the heparin-FTSC was derived from the calibration curve produced.

#### *Quantification of Fluorescein-5-Thiosemicarbazide (FTSC) Loading*

A standard calibration curve for FTSC in deionised water was produced at 492 nm on a U-2010 spectrophotometer. Triplicate readings of the polysaccharide-FTSC solution were analysed at 492 nm and the concentration of fluorescein in the solution was determined from the calibration curve.

***Steady-State Binding Study***

*Calibration*

A calibration of fluorescent heparin was carried out, from 0 mg/ml to 0.01 mg/ml, in 0.1 M PBS at pH 7.5 at room temperature on the same day as the experiment.

*Sample Preparation for Steady State Binding Study*

Poly(NVP-co-DEGBAC-co-AA) and KKK- and RRR-functionalised poly(NVP-co-DEGBAC-co-AA) hydrogels were analysed for heparin binding. A known mass of swollen hydrogel was equilibrated in 0.1 M phosphate buffered saline at pH 7.5 at room temperature for 1 hour before being placed in a fluorescent heparin solution (0.7 mg/ml, 0.25 ml) and allowed to react at room temperature in the dark on an orbital shaker plate at 150 rpm for 24 hours. The hydrogel was removed from the coupling solution and placed into 0.25 ml of 0.1 M phosphate buffered saline at pH 7.5 for 1 hour. The 0.1 M PBS solution was replaced hourly for 3 hours and subsequently replaced daily for a further three days.

*Analysis*

Analysis was carried out on a Luminescence Spectrometer LS50B (Perkin-Elmer Ltd) with excitation at 490 nm, emission at 500-600 nm. The slits were 2.5-2.5 nm for the excitation and emission source and 10 accumulation scans were carried out for each spectrum. Analysis of the coupling solution was carried out by diluting 20 µl of heparin solution in 4 ml of 0.1 M PBS and analysing this solution in a quartz cuvette. Analysis of PBS wash solutions was carried out by diluting 0.25 ml of wash solution in 2 ml PBS before analysis in a quartz cuvette. The amount of fluorescein tagged-heparin washed from the hydrogel was determined using the calibration curve produced prior to the experiment.

**10.4.8 XPS Heparin Binding Study**

***Preparation of Heparin-Bound Hydrogels for XPS Analysis***

Poly(NVP-co-DEGBAC-co-AA) and KKK- and RRR-functionalised poly(NVP-co-DEGBAC-co-AA) hydrogels were analysed in duplicate by XPS for heparin binding. For samples of hydrogel after exposure to heparin, hydrogel discs (5 mm swollen diameter) were equilibrated in 0.1 M phosphate buffered saline (pH 7.5) at room

temperature for 1 hour before being placed in a 1 mg/ml heparin solution (1 ml) and allowed to react at room temperature on an orbital shaker plate at 150 rpm for 24 hours. The hydrogels were removed from the coupling solution and placed into 1 ml 0.1 M phosphate buffered saline (pH 7.5) for 1 hour. The PBS solution was replaced hourly for 3 hours and subsequently replaced daily for a further three days. The samples were then washed five times in water before being air-dried for 24 hours ready for XPS analysis. For samples of hydrogel without exposure to heparin, the above procedure was repeated without the presence of heparin. The samples produced were air-dried before being submitted for XPS and SIMS analysis by Dr. T. Whittle, University of Sheffield.

### 10.4.9 Enzyme-Linked ImmunoSorbent Assay of VEGF Binding (Hydrogels)

***Sample Preparation***

Four polymer types were analysed in duplicate for this study, PND, PNDA, PNDKKK and PNDRRR. For each sample a hydrogel disc (5 mm swollen diameter) was placed into a sample tube and was submerged in 1 ml of a 1 mg/ml heparin solution in PBS. The hydrogel was then left to bind in this solution for 24 hours at room temperature on an orbital shaker at 150 rpm. The hydrogel was washed seven times with fresh PBS. Soda glass sample tubes were blocked from protein absorption by the addition of a 3% BSA solution in PBS which was agitated at room temperature on an orbital shaker at 150 rpm for 4 hours. The solution was removed and the tubes were rinsed three times with fresh PBS. The heparin-bound hydrogels were transferred to pre-blocked sample tubes and 200 ng/ml VEGF in PBS (0.5 ml) was added. The hydrogel was allowed to interact with the VEGF for 24 hours at 4°C on an orbital shaker at 150 rpm. The hydrogel discs were then washed by being submerged in fresh PBS solution at 4°C for 30 minutes. This was carried out three times.

A release study was then carried out by submerging the hydrogel in 0.5 ml of 1% BSA PBS solution and allowing release to occur at 37°C. At defined time points (30 mins, 1 hr, 6 hrs, 12 hrs, 24 hrs, 48 hrs and 72 hrs) the protein solution was removed and was replaced with 0.5 ml fresh 1% BSA PBS solution. The protein solutions retrieved were stored at -20°C in polypropylene tubes until analysis with an ELISA kit as described in Section 10.3.12. BSA was utilised to stabilise the VEGF during the release study and storage period. Each experimental condition was carried out and analysed in duplicate.

## 10.5 Cell Culture

### 10.5.1 Materials

Hydrogel discs (5 mm swollen diameter) were produced as described in Section 10.4 and were washed five times in sterile PBS and stored at 4°C before use in cell culture. Dulbeccos' Modified Eagles Medium (DMEM) was obtained from Sigma, UK or Biowest Biosera. Foetal calf serum was obtained from Biowest Biosera. L-glutamine, penicillin-streptomycin, trypsin-ethylenediaminetetraacetic acid (EDTA) (0.05% w/v trypsin/0.02% w/v EDTA) and 0.4% w/v Trypan blue were obtained from Sigma, UK. Phosphate buffered saline tablets (Dulbeccos' A) were obtained from Oxoid, UK and CellTracker™ Red CMTPX (C34552) was obtained from Molecular Probes™. Endothelial Cell Growth Medium MV 2 and supplements, and endothelial cell detach kit (containing HepesBSS, trypsin/EDTA solution and trypsin neutralising solution) were obtained from Promocell GMBH. Trypsin 0.1% w/v was obtained from Difco, UK. 3-(4,5-dimethylthiazol-2-yl)-2,5-diphenyltetrazolium bromide (MTT) and 2-ethoxyethanol (Cellusolve) were obtained from Sigma, UK.

Skin for fibroblast cell isolation was obtained from patients undergoing routine breast reductions and abdominoplastics at the Northern General Hospital, Sheffield. Full informed consent was given by all patients for skin to be used for research through a protocol approved by the Ethical Committee of the Northern General Hospital Trust, Sheffield, UK. Human Dermal Microvascular Endothelial Cells (HDMECs) were obtained as proliferating cells (C-12260) from PromoCell, U.K.

### 10.5.2 Equipment

Cell counts were performed using a modified Neubauer haemocytometer from Weber Scientific International, UK. Plasticware for cell culture was purchased from Costar, UK. All sterile reagents and cells were handled in class II laminar flow hoods. Cell culture was performed at 37°C, 5% $CO_2$, 95% humidity, in Sanyo $CO_2$ incubators. Light microscopy of cell cultures was performed using an Olympus CK40-F200 light and phase contrast microscope. Still photographs were taken using a Nikon Coolpix 990 digital camera. MTT assays were performed at 540 nm using a Dynatech MR5000 plate reader with a reference wavelength of 630 nm. Confocal images were taken using a Zeiss LSM 510 Confocal Microscope (abs. 577 nm, em. 602 nm).

### 10.5.3 Standard Solutions

*Trypsin Solution*

"Difco Trypsin" 0.1% w/v was prepared by adding 0.5 g of Difco Trypsin powder, 0.5 g D-glucose and 0.5 ml phenol red to 500 ml PBS. This was adjusted to pH 7.45 using 2 M NaOH using a pH meter. This was filter sterilised and aliquots stored at -20°C until needed.

*Phosphate Buffered Saline (PBS)*

Phosphate buffered saline was prepared by adding 1 PBS tablet per 100 ml of distilled water. This solution was autoclaved at 115°C for 15 minutes and left to cool before use.

*Trypan Blue*

Trypan blue solution was made from a 1:1 mixture of 0.4% trypan blue and PBS.

*Serum-Supplemented Fibroblast Culture Medium*

DMEM high glucose (4500 mg/l glucose) supplemented with 10% v/v foetal calf serum (FCS), 2 mM l-glutamine, 0.625 μg/ml amphotercin B, 100 IU/ml penicillin and 100 μg/ml streptomycin. The supplements were mixed at room temperature in a class II laminar flow hood to a total volume of 500 ml. The resultant medium was stored at 4°C for a maximum of six weeks prior to use. Medium was warmed to 37°C before use.

*Serum-Free Fibroblast Culture Medium*

DMEM high glucose (4500 mg/l glucose) supplemented with $2x10^{-3}$ M l-glutamine, 0.625 μg/ml amphotercin B, 100 IU/ml penicillin and 100 μg/ml streptomycin. The supplements were mixed at room temperature in a class II laminar flow hood to a total volume of 500 ml. The resultant medium was stored at 4°C for a maximum of six weeks prior to use. Medium was warmed to 37°C before use.

*Supplemented Endothelial Cell Growth Medium (MV2)*

Endothelial cell growth medium (MV2) (Promocell GMBH), with added supplements of 0.05 ml/ml foetal calf serum, 5 ng/ml EGF, 0.5 ng/ml VEGF, 10 ng/ml bFGF, 20 ng/ml IGF-1, 0.2 μg/ml hydrocortisone, 1 μg/ml ascorbic acid. The supplements were added at room temperature in a class II laminar flow hood. The resultant medium was

stored at 4°C for a maximum of six weeks prior to use. Medium was warmed to 37°C before use.

*Endothelial Cell Growth Medium (MV2) (5% Serum Medium)*

Endothelial cell growth medium (MV2) (Promocell GMBH), with 5% foetal calf serum (0.05 ml/ml). The FCS was added at room temperature in a class II laminar flow hood. The resultant medium was stored at 4°C for a maximum of six weeks prior to use. Medium was warmed to 37°C before use.

*Serum-Starved Endothelial Cell Growth Medium (MV2)*

Endothelial cell growth medium (MV2) (Promocell GMBH), with added 1% or 2% foetal calf serum (0.01 ml/ml or 0.02 ml/ml). The FCS was added at room temperature in a class II laminar flow hood. The resultant medium was stored at 4°C for a maximum of six weeks prior to use. Medium was warmed to 37°C before use.

### 10.5.4 Cell Counts and Viability Assessment

***Cell Viability Determination by Trypan Blue***

Trypan blue was used for cell counts and viability assessments. Cells were suspended in a known volume of cell culture medium and 20 µl of this cell suspension was combined with 20 µl of trypan blue stock solution. Non-viable cells appear blue, allowing viable cells to be counted using a Neubauer haemocytometer and a concentration of viable cells to be calculated.

***Cell Viability Assay – MTT***

MTT solution was produced by dissolving MTT in sterile PBS to a final concentration of 0.5 mg/ml. The medium was removed from the sample wells and the samples were washed gently with PBS. 0.5 ml MTT solution was added to each well. The plates were incubated with MTT solution for 40 minutes at 37°C, 5% $CO_2$ in a humidified atmosphere. The MTT solution was removed from the wells and then polymer was also removed from the wells and placed into individual wells. 0.3 ml of Cellusolve was then added to each well and was left for a few moments to allow the formazan product to elute from the cells. 0.1 ml of the Cellusolve solution was then placed in a 96 well plate in duplicate and the optical density was read at 540 nm.

## 10.5.5 Cell Culture

### *Fibroblast Sub-Culture*

Cells were cultured in T75 flasks and incubated at 37°C, 5% $CO_2$ in a humidified atmosphere. The medium was changed every three to four days until the cells were 80% confluent. Once the fibroblasts were confluent, the medium was removed and the cell layer was washed three times with 10 ml sterile PBS solution. 2 ml trypsin/EDTA solution was added to the fibroblasts, which were then incubated at 37°C for 5 minutes. Fibroblasts were encouraged to detach by gentle tapping and phase contrast microscopy was used to confirm cell detachment. 10 ml of serum-supplemented medium was added to the flask to neutralise the trypsin. The resulting cell suspension was centrifuged at 1000 rpm for 5 minutes to produce a cell pellet. The supernatant medium was removed from the cell pellet and the cells were resuspended in 1 ml of medium to allow a cell count to be performed. The fibroblasts were then used between passages three and nine.

### *Endothelial Cell Sub-Culture*

Cells were cultured in T25 flasks and incubated at 37°C, 5% $CO_2$ in a humidified atmosphere. The medium was changed every two to three days until the cells were 80% confluent. Once the endothelial cells were confluent, the medium was removed and the cell layer was washed with 5 ml HepesBSS solution. 2.5 ml trypsin/EDTA solution was added to the endothelial cells, which were allowed to detach at room temperature for 5 minutes. Endothelial cells were encouraged to detach by gentle tapping, and phase contrast microscopy was used to confirm cell detachment. 2.5 ml of trypsin neutralising solution (TNS) was added to the flask to neutralise the trypsin. The resulting cell suspension was centrifuged at 1400 rpm for 5 minutes to produce a cell pellet. The supernatant medium was removed from the cell pellet and the cells were resuspended in 1 ml of medium to allow a cell count to be performed. The endothelial cells were then used between passages four and eight.

### 10.5.6 Fibroblast Experiments

***Fibroblast Polymer Compatibility Study***

1 sample of each hydrogel (5 mm swollen diameter) was placed into a well in a 48 well plate. 0.5 ml of serum-free fibroblast culture medium was added to each well and the polymers were incubated for 72 hours. The medium was removed and 0.25 ml of either serum-free or serum-supplemented fibroblast culture medium was added to each well. Fibroblasts were then seeded at 10,000 cells per well in 0.25 ml of medium. Cells were cultured in direct contact with hydrogel samples for four days before an MTT assay was carried out and the hydrogels were moved to separate wells to analyse cell viability. Each polymer was analysed in triplicate in three repeat experiments.

***Fibroblast CellTracker™ Red Staining***

1 sample of each hydrogel (5 mm swollen diameter) was placed into a well in a 48 well plate. 0.5 ml of serum-free fibroblast culture medium was added to each well and the polymers were incubated for 72 hours. The medium was removed and 0.25 ml of either serum-free or serum-supplemented fibroblast culture medium was added to each well. Fibroblasts were then seeded at 10,000 cells per well in 0.25 ml of medium. Cells were cultured in direct contact with hydrogel samples for four days. The medium was removed and each well was washed twice with PBS. 50 μg of CellTracker™ Red was dissolved in 20 μl DMSO and added to serum-free medium (5 ml). 0.3 ml of this solution was added to each well and the cells were then incubated for 40 minutes. The medium was removed, the wells were washed three times with PBS and 0.5 ml of serum medium was added to each well before incubating again for 30 minutes. Finally, the medium was removed, each well was washed three times with PBS and 0.5 ml PBS was added. The cells were imaged on an inverted confocal microscope (abs. 577 nm, em. 602 nm) at room temperature.

### 10.5.7 Endothelial Cell Experiments

***Endothelial Cell Polymer Compatibility Study***

One sample of each hydrogel (5 mm swollen diameter) was placed into a well in a 48 well plate. 0.5 ml of endothelial cell growth medium without supplements was added to each well and the polymers were incubated for 72 hours. The medium was removed and 0.75 ml of endothelial cell growth medium with supplements was added to each well. HDMECs were then seeded at 10,000 cells per well in 0.25 ml of medium. Cells were cultured in direct contact with hydrogel samples for four days, with a daily change of medium, before the hydrogels were moved to separate wells and an MTT assay was carried out. Each polymer was analysed in triplicate in three repeat experiments.

***Endothelial Cell Heparin and VEGF Dosing Experiment***

HDMECs were seeded at a density of 8,000 cells per well in a 96 well plate and allowed to attach to the tissue culture plastic for 5 hours in 0.2 ml fully-supplemented medium. The cells were then starved overnight in 2% serum endothelial cell growth medium (MV2). The starving medium was replaced with 0.2 ml of 2% serum medium containing the relevant quantities of VEGF and/or heparin and was incubated for 72 hours before analysis by MTT assay. Each environment was carried out in triplicate within the experiment.

***Endothelial Cell Proliferation with Hydrogel Alone, Heparin-Bound Hydrogel and VEGF- and Heparin-Bound Hydrogel (5% Serum Medium)***

Hydrogel discs (5 mm swollen diameter) were equilibrated in sterile PBS before use in this experiment. To produce heparin-bound hydrogels, the hydrogel discs were placed in 1 mg/ml heparin solutions (PBS) and agitated on a shaker plate at room temperature for 24 hours. The hydrogels were then washed in sterile PBS seven times before storage at 4°C. VEGF- and heparin-bound hydrogels were produced by placing heparin-bound hydrogels in 0.5 ml of a 200 ng/ml VEGF solution (PBS) in a cold room at 4°C. The hydrogels were agitated in this solution for 24 hours at 4°C. The hydrogels were then washed three times in sterile PBS. The hydrogels were then placed into cold 48 well plates and 0.75 ml of 5% serum medium was added to each well. The 48 well plate was placed in an incubator for 2 hours. HDMECs were then seeded at a density of 10,000 cells per well in 0.25 ml of 5% serum medium. The medium was replaced daily and an

MTT assay was carried out after 64 hours. Each polymer type was analysed in triplicate in three repeat experiments.

***Endothelial Cell with Hydrogel Alone, Heparin-Bound Hydrogel and VEGF- and Heparin-Bound Hydrogel (Serum-Starved Medium)***

Hydrogel discs (5 mm swollen diameter) were equilibrated in sterile PBS before use in this experiment. To produce heparin-bound hydrogels, the hydrogel discs were placed in 1 mg/ml heparin solutions (PBS) and agitated on a shaker plate at room temperature for 24 hours. The hydrogels were then washed in sterile PBS seven times before storage at 4°C. VEGF- and heparin-bound hydrogels were produced by placing heparin-bound hydrogels in 0.5 ml of a 200 ng/ml VEGF solution (PBS) in a cold room at 4°C. The hydrogels were agitated in this solution for 24 hours at 4°C and then washed three times in sterile PBS. The hydrogels were placed into cold 48 well plates and 0.75 ml of 2% serum medium with no further supplements was added to each well. The 48 well plate was placed in the incubator for 2 hours. HDMECs had previously been starved overnight in 2% serum medium and were then seeded at a density of 10,000 cells per well in 0.25 ml of medium. The medium was replaced daily and an MTT assay was carried out after 64 hours. Each polymer type was analysed in triplicate in three repeat experiments.

***Endothelial CellTracker™ Red Experiment***

50 µg of CellTracker™ Red was dissolved in 20 µl DMSO and added to warm PBS (5 ml). This CellTracker™ Red solution was then added to one confluent T25 flask of HDMECs and the cells were then incubated for 40 minutes at 37°C. The CellTracker™ Red solution was then removed and the cells were washed three times with PBS before 5 ml of fully supplemented endothelial cell medium was added. The CellTracker™ Red-stained HDMECs were then used in experiments as described above. After the experiments, the cells were washed three times with warmed PBS before imaging the cells in PBS on an inverted confocal microscope (abs. 577 nm, em. 602 nm) at room temperature.

***Tubule Formation Assay – Effect of Soluble VEGF and Heparin***

In order to assess the ability of HDMECs to proliferate and differentiate, the tubular network formation assay was used. Microtiter 48 well plates were coated with 68 µl/well of growth factor-reduced Matrigel and placed in an incubator at 37°C to set for

1 hour. HDMECs were serum starved overnight (1% FCS) before the experiment, trypsinised and washed. 16,000 cells were then seeded per well in starving medium (0.1 ml, 1% FCS) and left to attach for 45 min. The medium was then discarded and replaced with 1 ml of treatment medium containing starving medium (1% FCS) either alone or with VEGF (10 ng/ml), heparin (50 ng/ml) or a combination of VEGF (10 ng/ml) and heparin (50 ng/ml). The endothelial cells were incubated at 37°C and migrated and formed tubules on this matrix within six hours of plating. Tubule formation was monitored at six hours by light microscopy. Each treatment group was performed in triplicate and three independent experiments were performed and analysed using the image analysis package, Scion Image (Frederick, MA).

***Tubule Formation Assay – Effect of VEGF- and Heparin-Bound RRR Hydrogel***

The effect of VEGF- and heparin-bound RRR hydrogels on endothelial cell tube formation on growth factor-reduced Matrigel was analysed *in vitro.*

VEGF- and heparin-bound hydrogel discs were produced by placing the hydrogels in heparin solutions (1 mg/ml) and agitated on a shaker plate at room temperature for 24 hours. The hydrogels were then washed in sterile PBS 7 times before storage at 4°C. VEGF- and heparin-bound hydrogels were produced by placing heparin-bound hydrogels in 0.5 ml of a 200 ng/ml VEGF solution (PBS) in a cold room at 4°C. The hydrogels were agitated in this solution for 24 hours at 4°C. The hydrogels were washed three times in sterile PBS and equilibrated in 1 ml 1% serum medium for 15 minutes.

Microtiter 48-well plates were coated with 68 µl/well of growth factor-reduced Matrigel and placed in an incubator at 37°C to set for 1 hour. One VEGF- and heparin-bound PNDRRR hydrogel disc or PNDRRR hydrogel disc alone was placed into each well and was incubated at 37°C for 30 minutes. 16,000 cells (pre-starved in 1% serum medium overnight) were then seeded per well in starving medium (0.1 ml, 1% FCS) and left to attach for 45 minutes at 37°C. Further starving medium (0.9 ml, 1% FCS) was added to each well before incubation at 37°C. HDMECs on this matrix migrated and formed tubules within six hours of plating. Tubule formation was monitored at six hours by light microscopy. Each treatment group was performed in triplicate and three independent experiments were performed and analysed using the image analysis package, Scion Image (Frederick, MA).

# 11 References


1. Graham-Brown, R. A. C.; Burns, T., *Dermatology, Ed. 9* **2007,** Wiley-Blackwell, 1-9.
2. Powell, J., Skin Physiology. *Surgery* **2006,** 24, (1), 1-4.
3. Marieb, E. N.; Hoehn, K., *Human Anatomy and Physiology, Ed. 7* **2007,** Pearson Education, 152-163.
4. Sloane, E., *Anatomy and Physiology: An Easy Learner* **1994,** Boston Jones & Bartlett Publishers Inc., 84-86.
5. Boateng, J. S.; Matthews, K. H.; Stevens, H. N. E.; Eccleston, G. M., Wound Healing Dressings and Drug Delivery Systems: A Review. *Journal of Pharmaceutical Sciences* **2008,** 97, (8), 2893-2923.
6. Benbow, M., Healing and wound classification. *Journal of Community Nursing* **2007,** 21, (9), 26-32.
7. Whitney, J., Overview: Acute and Chronic Wounds. *Nursing Clinics of North America* **2005,** 40, 191-205.
8. Martin, P., Wound Healing - Aiming for Perfect Skin. *Science* **1997,** 276, 75-81.
9. Strodtbeck, F., Physiology of Wound Healing. *Newborn and Infant Nursing Reviews* **2001,** 1, (1), 43-52.
10. Russell, L., Understanding physiology of wound healing and how dressings help. *British Journal of Nursing* **2000,** 9, (1), 10-20.
11. Witte, M. B.; Barbul, A., General Principles of Wound Healing. *Surgical Clinics of North America* **1997,** 77, (3), 509-528.
12. Fonder, M. A.; Lazarus, G. S.; Cowan, D. A., Treating the chronic wound: A practical approach to the care of nonhealing wounds and wound care dressings. *Journal of the American Academy of Dermatology* **2008,** 58, (2), 185-206.
13. Klagsbrun, M.; D'Amore, P., Vascular endothelial growth factor and its receptors. *Cytokine & Growth Factor Reviews* **1996,** 7, (3), 259-270.
14. Folkman, J., Angiogenesis in cancer, vascular, rheumatoid and other disease. *Nature Medicine* **1995,** 1, (1), 27-31.
15. Arnold, F.; West, D. C., Angiogenesis in wound healing. *Pharmacology and therapeutics* **1991,** 52, (3), 407-422.
16. Carmeliet, P., Mechanisms of angiogenesis and arteriogenesis. *Nature Medicine* **2000,** 6, (3), 389-395.
17. Dvorak, H. F.; Brown, L. F.; Detmar, M.; Dvorak, A. M., Vascular Permeability Factor/Vascular Endothelial Growth Factor, Microvascular Hyperpermeability and Angiogenesis. *American Journal of Pathology* **1995,** 146, (5), 1029-1040.
18. Dvorak, H. F., VPF/VEGF and the Angiogenic Response. *Seminars in Perinatology* **2000,** 24, (1), 75-78.
19. Roy, R.; Zhang, B.; Moses, M. A., Making the cut: Protease-mediated regulation of angiogenesis. *Experimental Cell Research* **2006,** 312, 608-622.
20. Lamalice, L.; Le Boeuf, F.; Huot, J., Endothelial Cell Migration During Angiogenesis. *Circulation Research* **2007,** 100, 782-794.
21. Hoeben, A.; Landuyt, B.; Highley, M. S.; Wildiers, H.; Van Oosterom, A. T.; De Bruijn, E., Vascular Endothelial Growth Factor and Angiogenesis. *Pharmacological Reviews* **2004,** 56, (4), 549-580.
22. Darland, D. C.; D'Amore, P. A., Blood vessel maturation: vascular development comes of age. *The Journal of Clinical Investigations* **1999,** 103, (2), 157-158.
23. Ferrara, N.; Henzel, W. J., Pituitary Follicular Cells Secrete A Novel Heparin-Binding Growth Factor Specific For Vascular Endothelial Cells. *Biochemical and Biophysical Research Communications* **1989,** 161, (2), 851-858.
24. Senger, D. R.; Galli, S. J.; Dvorak, A. M.; Perruzzi, C. A.; Harvey, V. S.; Dvorak, H. F., Tumor Cells Secrete a Vascular Permeability Factor That Promotes Accumulation of Ascites Fluid. *Science* **1983,** 219, 983-985.
25. Ferrara, N.; Davis-Smyth, T., The biology of vascular endothelial growth factor. *Endocrine Reviews* **1997,** 18, (1), 4-25.

26. Ferrara, N.; Gerber, H.-P.; LeCouter, J., The biology of VEGF and its receptors. *Nature Medicine* **2003,** 9, (6), 669-676.
27. Yamazaki, Y.; Morita, T., Molecular and functional diversity of vascular endothelial growth factors. *Molecular Diversity* **2006,** 10, 515-527.
28. Robinson, C. J.; Stringer, S. E., The splice variants of vascular endothelial growth factor (VEGF) and their receptors. *Journal of Cell Science* **2001,** 114, (5), 853-865.
29. Kim, K. J.; Li, B.; Winer, J.; Armanini, M.; Gillett, N.; Phillips, H. S.; Ferrara, N., Inhibition of vascular endothelial growth factor-induced angiogenesis suppresses tumour growth in vivo. *Nature* **1993,** 362, 841-844.
30. Otrock, Z. K.; Makarem, J. A.; Shamseddine, A. I., Vascular endothelial growth factor family of ligands and receptors: Review. *Blood Cells, Molecules, and Diseases* **2007,** 38, 258-268.
31. Muller, Y. A.; Christinger, H. W.; Keyt, B. A.; De Vos, A. M., The crystal structure of vascular endothelial growth factor (VEGF) refined to 1.93A resolution: multiple copy flexibility and receptor binding. *Structure* **1997,** 5, (10), 1325-1338.
32. Sun, P. D., The cysteine-knot growth factor superfamily. *Annual Review of Biophysics and Biomolecular Structure* **1995,** 24, 269-291.
33. Vincenti, V.; Cassano, C.; Rocchi, M.; Persico, M. G., Assignment of the Vascular Endothelial Growth Factor Gene to Human Chromosome 6p21.3. *Circulation* **1996,** 93, 1493-1495.
34. Muller, Y. A.; Li, B.; Christinger, H. W.; Wells, J. A.; Cunningham, B. C.; de Vos, A. M., Vascular endothelial growth factor: crystal structure and functional mapping of the kinase domain receptor binding site. *Proceedings of the National Academy of Sciences of the United States of America* **1997,** 94, (14), 7192-7197.
35. Fairbrother, W. J.; Champe, M. A.; Christinger, H. W.; Keyt, B. A.; Starovasnik, M. A., Solution structure of the heparin-binding domain of vascular endothelial growth factor. *Structure* **1998,** 6, (5), 637-648.
36. Stauffer, M. E.; Skelton, N. J.; Fairbrother, W. J., Refinement of the solution structure of the heparin-binding domain of vascular endothelial growth factor using residual dipolar couplings. *Journal of Biomolecular NMR* **2002,** 23, (1), 57-61.
37. Vries, C. D.; Escobedo, J. A.; Ueno, H.; Houck, K.; Ferrara, N.; Williams, L. T., The fms-like Tyrosine Kinase, A Receptor for Vascular Endothelial Growth Factor
*Science* **1992,** 255, (5047), 989-991.
38. Terman, B. I.; Dougher-Vermazen, M.; Carrion, M. E.; Dimitrov, D.; Armellino, D. C.; Gospodarowicz, D.; Boehlen, P., Identification of the KDR tyrosine kinase as a receptor for vascular endothelial cell growth factor. *Biochemical and Biophysical Research Communications* **1992,** 187, (3), 1579-1586.
39. Vives, R. R.; Pye, D. A.; Salmivirta, M.; Hopwood, J. J.; Lindahl, U.; Gallagher, J. T., Sequence analysis of heparan sulphate and heparin oligosaccharides. *Biochemistry Journal* **1999,** 339, 767-773.
40. Sasisekharan, R.; Venkataraman, G., Heparin and heparan sulfate: biosynthesis, structure and function. *Current Opinion in Chemical Biology* **2000,** 4, 626-631.
41. Capila, I.; Linhardt, R. J., Heparin-Protein Interactions. *Angewandte Chemie International Edition* **2002,** 41, 390-412.
42. Park, J. E.; Keller, G. A.; Ferrara, N., The vascular endothelial growth factor (VEGF) isoforms: Differential deposition into the subepithelial extracellular matrix and bioactivity of extracellular matrix-bound VEGF. *Molecular Biology of the Cell* **1993,** 4, (12), 1317-1326.
43. Houck, K. A.; Leung, D. W.; Rowland, A. M.; Winer, J.; Ferrara, N., Dual Regulation of Vascular Endothelial Growth Factor Bioavailability by Genetic and Proteolytic Mechanisms. *The Journal of Biological Chemistry* **1992,** 267, (36), 26031-26037.
44. Gitay-Goren, H.; Soker, S.; Vlodavsky, I.; Neufeld, G., The Binding of Vascular Endothelial Growth Factor to Its Receptors Is Dependant on Cell Surface-associated Heparin-like Molecules. *The Journal of Biological Chemistry* **1992,** 267, (9), 6093-6098.
45. Cohen, T.; Gitay-Goren, H.; Sharon, R.; Shibuyai, M.; Halaban, R.; Levi, B.-Z.; Neufeld, G., $VEGF_{121}$, a Vascular Endothelial Growth Factor (VEGF) Isoform Lacking Heparin

Binding Ability, Requires Cell-surface Heparan Sulfates for Efficient Binding to the VEGF Receptors of Human Melanoma Cells. *The Journal of Biological Chemistry* **1995,** 270, (19), 11322-11326.
46. Tessler, S.; Rockwell, P.; Hicklin, D.; Cohen, T.; Levi, B.-Z.; Witte, L.; Lemischka, I. R.; Neufeld, G., Heparin Modulates the Interaction of VEGF165 with Soluble and Cell Associated flk-1 Receptors. *The Journal of Biological Chemistry* **1994,** 269, (29), 12456-12461.
47. Soker, S.; Goldstaub, D.; Svahn, C. M.; Vlodavsky, I.; Levi, B.-Z.; Neufeld, G., Variations in the size and sulfation of heparin modulate the effect of heparin on the binding of $VEGF_{165}$ to its receptors. *Biochemical and Biophysical Research Communications* **1994,** 203, (2), 1339-1347.
48. Keyt, B. A.; Berleau, L. T.; Nguyen, H. V.; Chen, H.; Heinsohn, H.; Vandlen, R.; Ferrara, N., The carboxyl-terminal domain (111-165) of vascular endothelial growth factor is critical for its mitogenic potency. *Journal of Biological Chemistry* **1996,** 271, (13), 7788-95.
49. Benoit, D. S. W., Heparin functionalized PEG gels that modulate protein adsorption for hMSC adhesion and differentiation. *Acta Biomaterialia* **2005,** 1, 461-470.
50. Lee, H.; Chung, H. J.; Park, T. G., Perspectives On: Local and Sustained Delivery of Angiogenic Growth Factors. *Journal of Bioactive and Compatible Polymers* **2007,** 22, 89-114.
51. Zisch, A. H.; Lutolf, M. P.; Hubbell, J. A., Biopolymeric delivery matrices for angiogenic growth factors. *Cardiovascular Pathology* **2003,** 12, 295-310.
52. Ferrara, N.; Alitalo, K., Clinical applications of angiogenic growth factors and their inhibitors. *Nature Medicine* **1999,** 5, (12), 1359-1364.
53. Wieghaus, K. A.; Capitosti, S. M.; Anderson, C. R.; Price, R. J.; Blackman, B. R.; Brown, M. L.; Botchwey, E. A., Small molecule inducers of angiogenesis for tissue engineering. *Tissue Engineering* **2006,** 12, (7), 1903-1913.
54. Baumgartner, I.; Pieczek, A.; Manor, O.; Blair, R.; Kearney, M.; Walsh, K.; Isner, J. M., Constitutive Expression of phVEGF165 After Intramuscular Gene Transfer Promotes Collateral Vessel Development in Patients with Critical Limb Ischemia. *Circulation* **1998,** 97, 1114-1123.
55. Henry, T. D.; Krishna, R.-S.; Isner, J. M.; Kereiakes, D. J.; Giordano, F. J.; Simons, M.; Losordo, D. W.; Hendel, R. C.; Bonow, R. O.; Eppler, S. M.; Zioncheck, T. F.; Holmgren, E. B.; McCluskey, E. R., Intracoronary administration of recombinant human vascular endothelial growth factor to patients with coronary artery disease. *The American Heart Journal* **2001,** 142, (5), 872-880.
56. Hopkins, S. P.; Bulgrin, J. P.; Sims, R. L.; Bowman, B.; Donovan, D. L., Controlled delivery of vascular endothelial growth factor promotes neovascularization and maintains limb function in a rabbit model of ischemia. *Journal of Vascular Surgery* **1998,** 27, (5), 886-895.
57. Kipshidze, N.; Chekanov, V.; Chawla, P.; Shankar, L. R.; Gosset, J. B.; Kumar, K.; Hammen, D.; Gordon, J.; Keelan, M. H., Angiogenesis in a Patient with Ischemic Limb. *Texas Heart Institute Journal* **2000,** 27, 196-200.
58. Laham, R. J.; Sellke, F. W.; Edelman, E. R.; Pearlman, J. D.; Ware, J. A.; Brown, D. L.; Gold, J. P.; Simons, M., Local Perivascular Delivery of Basic Fibroblast Growth Factor in Patients Undergoing Coronary Bypass Surgery: Results of a Phase 1 Randomized, Double-Blind, Placebo-Controlled Trial. *Circulation* **1999,** 100, (1865-1871).
59. Schumacher, B.; Pecher, P.; Von Specht, B. U.; Stegmann, T., Induction of Neoangiogenesis in Ischemic Myocardium by Human Growth Factors: First Clinical Results of a New Treatment of Coronary Heart Disease. *Circulation* **1998,** 1998, (97), 645-650.
60. Sun, Q.; Chen, R. R.; Shen, Y.; Mooney, D. J.; Rajagopalan, S.; Grossman, P. M., Sustained Vascular Endothelial Growth Factor Delivery Enhances Angiogenesis and Perfusion in ISchemic Hind Limb. *Pharmaceutical Research* **2005,** 22, (7), 1110-1116.
61. Takeshita, S.; Zheng, L. P.; Brogi, E.; Kearney, M.; Pu, L.-Q.; Bunting, S.; Ferrara, N.; Symes, J. F.; Isner, J. M., Therapeutic Angiogenesis. A Single Intraarterial Bolus of Vascular Endothelial Growth Factor Augments Revascularization in a Rabbit Ischemic Hind Limb Model. *Journal of Clinical Investigations* **1994,** 93, 662-670.

62. Epstein, S. E.; Fuchs, S.; Zhou, Y. F.; Baffour, R.; Kornowski, R., Therapeutic interventions for enhancing collateral development by administration of growth factors: basic principles, early results and potential hazards. *Cardiovascular Research* **2001,** 49, 532-542.
63. Eppler, S. M.; Combs, D. L.; Henry, T. D.; Lopez, J. J.; Ellis, S. G.; Yi, J.-H.; Annex, B. H.; McCluskey, E. R.; Zioncheck, T. F., A target-mediated model to describe the pharmacokinetics and hemodynamic effects of recombinant human vascular endothelial growth factor in humans. *Clinical Pharmacology & Therapeutics* **2002,** 72, (1), 20-32.
64. Pike, D. B.; Cai, S.; Pomraning, K. R.; Firpo, M. A.; Fisher, R. J.; Shu, X. Z.; Prestwich, G. D.; Peattie, R. A., Heparin-regulated release of growth factors in vitro and angiogenic response in vivo to implanted hyaluronan hydrogels containing VEGF and bFGF. *Biomaterials* **2006,** 27, 5242-5251.
65. Jay, S. M.; Saltzman, W. M., Controlled delivery of VEGF via modulation of alginate microparticle ionic crosslinking. *Journal of controlled release* **2009,** 134, (1), 26-34.
66. Lazarous, D. F.; Shou, M.; Scheinowitz, M.; Hodge, E.; Thirumurti, V.; Kitsiou, A. N.; Stiber, J. A.; Lobo, A. D.; Hunsberger, S.; Guetta, E.; Epstein, S. E.; Unger, E. F., Comparative Effects of Basic Fibroblast Growth Factor and Vascular Endothelial Growth Factor on Coronary Collateral Development and the Arterial Response to Injury *Circulation* **1996,** 94, (5), 1074-1082.
67. Andreadis, S. T.; Geer, D. J., Biomimetic approaches to protein and gene delivery for tissue regeneration. *TRENDS in Biotechnology* **2006,** 24, (7), 331-337.
68. Fischbach, C.; Mooney, D. J., Polymers for pro- and anti-angiogenic therapy. *Biomaterials* **2007,** 28, 2069-2076.
69. Watanabe, E.; Smith, D. M.; Sun, J.; Smart, F. W.; Delcarpio, J. B.; Roberts, T. B.; Van Meter Jr., C. H.; Claycomb, W. C., Effect of basic fibroblast growth factor on angiogenesis in the infarcted porcine heart. *Basic Research in Cardiology* **1998,** 93, 30-37.
70. Berscht, C. P.; Nies, B.; Liebendoerfer, A.; Kreuter, J., Incorporation of basic fibroblast growth factor into methylpyrrolidinone chitosan fleeces and determination of the in vitro release characteristics. *Biomaterials* **1994,** 15, (8), 593-600.
71. Ehrbar, M.; Zeisberger, S. M.; Raeber, G. P.; Hubbell, J. A.; Schnell, C.; Zisch, A. H., The role of actively released fibrin-conjugated VEGF for VEGF receptor 2 gene activation and the enhancement of angiogenesis. *Biomaterials* **2008,** 29, 1720-1729.
72. Wong, C.; Inman, E.; Spaethe, R.; Helgerson, S., Fibrin-based biomaterials to deliver human growth factors. *Journal of Thrombosis and Haemostasis* **2003,** 89, 573-582.
73. Koch, S.; Yao, C.; Grieb, G.; Prevel, P.; Noah, E. M.; Steffens, G. C. M., Enhancing angiogenesis in collagen matrices by covalent incorporation of VEGF. *Journal of Materials Science* **2006,** 17, 735-741.
74. Kanematsu, A.; Yamamoto, S.; Ozeki, M.; Noguchi, T.; Kanatani, I.; Ogawa, O.; Tabata, Y., Collagenous matrices as release carriers of exogenous growth factors. *Biomaterials* **2004,** 25, 4513-4520.
75. Tabata, Y.; Miyao, M.; Ozeki, M.; Ikada, Y., Controlled release of vascular endothelial growth factor by use of collagen hydrogels. *Journal of Biomaterials Science, Polymer Edition* **2000,** 11, (9), 915-930.
76. Patel, Z., S.; Ueda, H.; Yamamoto, M.; Tabata, Y.; Mikos, A. G., In Vitro and In Vivo Release of Vascular Endothelial Growth Factor from Gelatin Microparticles and Biodegradable Composite Scaffolds. *Pharmaceutical Research* **2008,** 25, (10), 2370-2378.
77. Sakakibara, Y.; Tambara, K.; Sakaguchi, G.; Lu, F.; Yamamoto, M.; Nishimura, K.; Tabata, Y.; Komeda, M., Towards surgical angiogenesis using slow-released basic fibroblast growth factor. *European Journal of Cardio-thoracic Surgery* **2003,** 24, 105-112.
78. Hosaka, A.; Koyama, H.; Kushibiki, T.; Tabata, Y.; Nishiyama, N.; Miyata, T.; Shigematsu, H.; Takato, T.; Nagawa, H., Gelatin hydrogel microspheres enable pinpoint delivery of basic fibroblast growth factor for the development of functional collateral vessels. *Circulation* **2004,** 110, 3322-3328.
79. Draget, K. I.; Skjak-Braek, G.; Smidsrod, O., Alginate Based New Materials. *International Journal of Biological Macromolecules* **1997,** 21, 47-55.

80. Peters, M. C.; C., I. B.; Rowley, J. A.; Mooney, D. J., Release from alginate enhances the biological activity of vascular endothelial growth factor. *Journal of Biomaterials Science Polymer Edition* **1998,** 9, (12), 1267-1278.
81. Gu, F.; Amsden, B.; Neufeld, R., Sustained delivery of vascular endothelial growth factor with alginate beads. *Journal of Controlled Release* **2004,** 96, 463-472.
82. Elcin, Y. M.; Dixit, V.; Gitnick, G., Extensive in vivo angiogenesis following controlled release of human vascular endothelial cell growth factor: implications for tissue engineering and wound healing. *Artificial Organs* **2001,** 25, (7), 558-565.
83. Hosack, L. W.; Firpo, M. A.; Scott, A. J.; Prestwich, G. D.; Peattie, R. A., Microvascular maturity elicited in tissue treated with cytokine-loaded hyaluronan-based hydrogels. *Biomaterials* **2008,** 29, 2336-2347.
84. Riley, C. M.; Fuegy, P. W.; Firpo, M. A.; Shu, X. Z.; Prestwich, G. D.; Peattie, R. A., Stimulation of in vivo angiogenesis using dual growth factor-loaded crosslinked glycosaminoglycan hydrogels. *Biomaterials* **2006,** 27, 5935-5943.
85. Peattie, R. A.; Nayate, A. P.; Firpo, M. A.; Shelby, J.; Fisher, R. J.; Prestwich, G. D., Stimulation of an in vivo angiogenesis by cytokine-loaded hyaluronic acid hydrogel implants. *Biomaterials* **2004,** 25, 2789-2798.
86. Peattie, R. A.; Rieke, E. R.; Hewett, E. M.; Fisher, R. J.; Shu, X. Z.; Prestwich, G. D., Dual growth factor-induced angiogenesis in vivo using hyaluronan hydrogel implants. *Biomaterials* **2006,** 27, 1868-1875.
87. Sheridan, M. H.; Shea, L. D.; Peters, M. C.; Mooney, D. J., Bioabsorbable polymer scaffolds for tissue engineering capable of sustained growth factor delivery. *Journal of controlled release* **2000,** 64, 91-102.
88. King, T. W.; Patrick Jr., C. W., Development and in vitro characterization of vascular endothelial growth factor (VEGF)-loaded poly (DL-lactic-co-glycolic acid)/poly(ethylene glycol) microspheres using a solid encapsulation/single emulsion/solvent extraction technique. *Journal of Biomedical Materials Research* **2000,** 51, 383-390.
89. Richardson, T. P.; Peters, M. C.; Ennett, A., B.; Mooney, D. J., Polymeric system for dual growth factor delivery. *Nature Biotechnology* **2001,** 19, 1029-1034.
90. Kanczler, J. M.; Barry, J.; Ginty, P.; Howdle, S. M.; Shakesheff, K. M.; Oreffo, R. O. C., Supercritical carbon dioxide generated vascular endothelial growth factor encapsulated poly(DL-lactic acid) scaffolds induce angiogenesis in vitro. *Biochemical and Biophysical Research Communications* **2007,** 352, 135-141.
91. Cleland, J. L.; Duenas, E. T.; Park, A.; Daugherty, A.; Kahn, J.; Kowalski, J.; Cuthbertson, A., Development of poly-(D,L-lactide-coglycolide) microsphere formulations containing recombinant human vascular endothelial growth factor to promote local angiogenesis. *Journal of Controlled Release* **2001,** 72, 13-24.
92. Park, T. G., Degradation of poly(lactic-co-glycolic acid) microspheres: effect of copolymer composition. *Biomaterials* **1995,** 16, 1123-1130.
93. Hiemstra, C.; Zhong, Z.; van Steenbergen, M. J.; Hennink, W. E.; Feijen, J., Release of model proteins and basic fibroblast growth factor from in situ forming degradable dextran hydrogels. *Journal of controlled release* **2007,** 122, 71-78.
94. Norton, L. W.; Tegnell, E.; Toporek, S. S.; Reichert, W. M., In vitro characterization of vascular endothelial growth factor and dexamethasone releasing hydrogels for implantable probe coatings. *Biomaterials* **2005,** 26, 3285-3297.
95. Zisch, A. H.; Lutolf, M. P.; Ehrbar, M.; Raeber, G. P.; Rizzi, S. C.; Davies, N.; Schmoekel, H.; Bezuidenhout, D.; Djonov, V.; Zilla, P.; Hubbell, J. A., Cell-demanded release of VEGF from synthetic, biointeractive cell-ingrowth matrices for vascularized tissue growth. *The FASEB Journal* **2003.**
96. Kavanagh, C. A.; Gorelova, T. A.; Selezneva, I. I.; Rochev, Y. A.; Dawson, K. A.; Gallagher, W. M.; Gorelove, A. V.; Keenan, A. K., Poly(N-isopropylacrylamide) copolymer films as vehicles for the sustained delivery of proteins to vascular endothelial cells. *Journal of Biomedical Materials Research - Part A* **2005,** 72, (1), 25-35.

97. Ehrbar, M.; Schoenmakers, R.; Christen, E. H.; Fussenegger, M.; Weber, W., Drug-sensing hydrogels for the inducible release of biopharmaceuticals. *Nature Materials* **2008,** 7, 800-804.
98. Lee, K. W.; Yoon, J. J.; Lee, J. H.; Kim, S. Y.; Jung, H. J.; Kim, S. J.; Joh, J. W.; Lee, H. H.; Lee, D. S.; Lee, S. K., Sustained Release of Vascular Endothelial Growth Factor From Calcium-Induced Alginate Hydrogels Reinforced by Heparin and Chitosan. *Transplantation Proceedings* **2004,** 36, 2464-2465.
99. Nie, T.; Baldwin, A.; Yamaguchi, N.; Kiick, K. L., Production of heparin-functionalized hydrogels for the development of responsive and controlled growth factor delivery systems. *Journal of Controlled Release* **2007,** 122, 287-296.
100. Sakiyama, S. E.; Hubbell, J. A., Development of fibrin derivatives for controlled release of heparin-binding growth factors. *Journal of controlled release* **2000,** 65, 389-402.
101. Nillesen, S. T. M.; Geutjes, P. J.; Wismans, R.; Schalkwijk, J.; Daamen, W. F.; Van Kuppevelt, T. H., Increased angiogenesis and blood vessel maturation in acellular collagen-heparin scaffolds containing both FGF2 and VEGF. *Biomaterials* **2007,** 28, 1123-1131.
102. Yoon, J. J.; Chung, H. J.; Park, T. G., Photo-crosslinkable and biodegradable Pluronic/heparin hydrogels for local and sustained delivery of angiogenic growth factor. *Journal of Biomedical Materials Research: Part A* **2007,** 83, (3), 597-605.
103. Steffens, G. C. M.; Yao, C.; Prevel, P.; Markowicz, M.; Schenck, P.; Noah, E. M.; Pallua, N., Modulation of Angiogenic Potential of Collagen Matrices by Covalent Incorporation of Heparin and Loading with Vascular Endothelial Growth Factor. *Tissue Engineering* **2004,** 10, (9/10), 1502-1509.
104. Jeon, O.; Kang, S.-W.; Lim, H.-W.; Chung, J. H.; Kim, B.-S., Long-term and zero-order release of basic fibroblast growth factor from heparin-conjugated poly(L-lactide-co-glycolide) nanospheres and fibrin gel. *Biomaterials* **2006,** 27, 1598-1607.
105. Wulff, G.; Sarhan, A., Use of polymers with enzyme-analogous structures for the resolution of racemates. *Angewandte Chemie, International Edition in English* **1972,** 11, (4), 341.
106. Ansell, R. J., Molecularly imprinted polymers in pseudoimmunoassay. *Journal of Chromatography, B: Analytical Technologies in the Biomedical and Life Sciences* **2004,** 804, (1), 151-165.
107. Ansell, R. J., Molecularly imprinted polymers for the enantioseparation of chiral drugs. *Advanced Drug Delivery Reviews* **2005,** 57, (12), 1809-1835.
108. Hillberg, A. L.; Brain, K. R.; Allender, C. J., Molecular imprinted polymer sensors: Implications for therapeutics. *Advanced Drug Delivery Reviews* **2005,** 57, (12), 1875-1889.
109. Kandimalla, V. B.; Ju, H., Molecular imprinting: a dynamic technique for diverse applications in analytical chemistry. *Analytical and Bioanalytical Chemistry* **2004,** 380, (4), 587-605.
110. Nilsson, J.; Spegel, P.; Nilsson, S., Molecularly imprinted polymer formats for capillary electrochromatography. *Journal of Chromatography, B: Analytical Technologies in the Biomedical and Life Sciences* **2004,** 804, (1), 3-12.
111. Owens, P. K.; Karlsson, L.; Lutz, E. S. M.; Andersson, L. I., Molecular imprinting for bio- and pharmaceutical analysis. *TrAC, Trends in Analytical Chemistry* **1999,** 18, (3), 146-154.
112. Piletsky, S. A.; Subrahmanyam, S.; Turner, A. P. F., Application of molecularly imprinted polymers in sensors for the environment and biotechnology. *Sensor Review* **2001,** 21, (4), 292-296.
113. Takeuchi, T.; Haginaka, J., Separation and sensing based on molecular recognition using molecularly imprinted polymers. *Journal of Chromatography, B: Biomedical Sciences and Applications* **1999,** 728, (1), 1-20.
114. Ulbricht, M., Membrane separations using molecularly imprinted polymers. *Journal of Chromatography, B: Analytical Technologies in the Biomedical and Life Sciences* **2004,** 804, (1), 113-125.
115. Alvarez-Lorenzo, C.; Concheiro, A., Molecularly imprinted polymers for drug delivery. *Journal of Chromatography, B: Analytical Technologies in the Biomedical and Life Sciences* **2004,** 804, (1), 231-245.

116. Haupt, K., Imprinted polymers-tailor-made mimics of antibodies and receptors. *Chemical Communications* **2003**, (2), 171-178.
117. Mayes, A. G.; Whitcombe, M. J., Synthetic strategies for the generation of molecularly imprinted organic polymers. *Advanced Drug Delivery Reviews* **2005**, 57, 1742-1778.
118. Mosbach, K., Molecular imprinting. *Trends in Biochemical Sciences* **1994**, 19, (1), 9-14.
119. Wulff, G., Molecular imprinting in crosslinked materials with the aid of molecular templates - a way towards artificial antibodies. *Angewandte Chemie, International Edition in English* **1995**, 34, (17), 1812-32.
120. Ye, L.; Mosbach, K., The technique of molecular imprinting - principle, state of the art, and future aspects. *Journal of Inclusion Phenomena and Macrocyclic Chemistry* **2001**, 41, (1-4), 107-113.
121. Whitcombe, M. J.; Vulfson, E. N., Imprinted Polymers. *Advanced Materials* **2001**, 13, (7), 467-478.
122. Spivak, D. A., Optimization, evaluation, and characterization of molecularly imprinted polymers. *Advanced Drug Delivery Reviews* **2005**, 57, (12), 1779-1794.
123. Komiyama, M.; Takeuchi, T.; Mukawa, T.; Asanuma, H., *Molecular Imprinting - From Fundamentals to Applications* **2003**, Wiley-VCH Verlag GmbH & Co.
124. Arshady, R.; Mosbach, K., Synthesis of substrate-selective polymers by host-guest polymerisation. *Macromolecular Chemistry* **1981**, 182, 687.
125. Vlatakis, G.; Andersson, L. I.; Mueller, R.; Mosbach, K., Drug assay using antibody mimics made by molecular imprinting. *Nature* **1993**, 361, (6413), 645-647.
126. Whitcombe, M. J.; Rodriguez, M. E.; Villar, P.; Vulfson, E. N., A New Method for the Introduction of Recognition Site Functionality into Polymers Prepared by Molecular Imprinting: Synthesis and Characterization of Polymeric Receptors for Cholesterol. *Journal of the American Chemical Society* **1995**, 117, (27), 7105-11.
127. Klein, J. U.; Whitcombe, M. J.; Mulholland, F.; Vulfson, E. N., Template-mediated synthesis of a polymeric receptor specific to amino acid sequences. *Angewandte Chemie, International Edition* **1999**, 38, (13/14), 2057-2060.
128. Yilmaz, E.; Haupt, K.; Mosbach, K., The Use of Immobilised Templates - A New Approach in Molecular Imprinting. *Angewandte Chemie, International Edition* **2000**, 39, (12), 2115-2118.
129. Ramstroem, O.; Ansell, R. J., Molecular imprinting technology: Challenges and prospects for the future. *Chirality* **1998**, 10, 195-209.
130. Bossi, A.; Bonini, F.; Turner, A. P. F.; Piletsky, S. A., Molecularly imprinted polymers for the recognition of proteins: The state of the art. *Biosensors and Bioelectronics* **2007**, 22, 1131-1137.
131. Bergmann, N. M.; Peppas, N. A., Molecularly imprinted polymers with specific recognition for macromolecules and proteins. *Progress in Polymer Science* **2008**, 33, 271-288.
132. Turner, N. W.; Jeans, C. W.; Brain, K. R.; Allender, C. J.; Hlady, V.; Britt, D. W., From 3D to 2D: A review of the molecular imprinting of proteins. *Biotechnology Progress* **2006**, 22, 1474-1489.
133. Hillberg, A. L.; Tabrizian, M., Biomolecule imprinting: Developments in mimicking dynamic natural recognition systems. *ITBM-RBM* **2008**, 29, 89-104.
134. Takeuchi, T.; Hishiya, T., Molecular imprinting of proteins emerging as a tool for protein recognition. *Organic and Biomolecular Chemistry* **2008**, 6, 2459-2467.
135. Janiak, D. S.; Kofinas, P., Molecular imprinting of peptides and proteins in aqueous media. *Analytical and Bioanalytical Chemistry* **2007**, 389, 399-404.
136. Hilt, J. Z.; Byrne, M. E., Configurational biomimesis in drug delivery: molecular imprinting of biologically significant molecules. *Advanced Drug Delivery Reviews* **2004**, 56, 1599-1620.
137. Hansen, D. E., Recent developments in the molecular imprinting of proteins. *Biomaterials* **2007**, 28, 4178-4191.
138. Flam, F., Molecular Imprints Make a Mark. *Science* **1994**, 263, 1221-1222.

139. Nicholls, I. A., Thermodynamic considerations for the design of molecularly imprinted polymers with ligand recognition sites. *Chemistry Letters* **1995**, (11), 1035-6.
140. Ge, Y.; Turner, A. P. F., Too large to fit? Recent developments in macromolecular imprinting. *Trends in Biotechnology* **2008**, 26, (4), 218-224.
141. Nicholls, I. A.; Ramstroem, O.; Mosbach, K., Insights into the role of the hydrogen bond and hydrophobic effect on recognition in molecularly imprinted polymer synthetic peptide receptor mimics. *Journal of Chromatography, A* **1995**, 691, (1-2), 349-53.
142. Yu, C.; Mosbach, K., Molecular Imprinting Utilizing an Amide Functional Group for Hydrogen Bonding Leading to Highly Efficient Polymers. *Journal of Organic Chemistry* **1997**, 62, (12), 4057-4064.
143. Mathew, J.; Buchardt, O., Molecular Imprinting Approach for the Recognition of Adenine in Aqueous Medium and Hydrolysis of Adenosine 5'-Triphosphate. *Bioconjugate Chemistry* **1995**, 6, (5), 524-8.
144. Piletsky, S. A.; Matuschewski, H.; Schedler, U.; Wilpert, A.; Piletska, E. V.; Thiele, T. A.; Ulbricht, M., Surface Functionalization of Porous Polypropylene Membranes with Molecularly Imprinted Polymers by Photograft Copolymerization in Water. *Macromolecules* **2000**, 33, (8), 3092-3098.
145. Sellergren, B., Imprinted dispersion polymers: a new class of easily accessible affinity stationary phases. *Journal of Chromatography A* **1994**, 673, 133-141.
146. Piletska, E. V.; Romero-Guerra, M.; Guerreiro, A. R.; Karim, K.; Turner, A. P. F.; Piletsky, S. A., Adaptation of the molecular imprinted polymers towards polar environment. *Analytica Chimica Acta* **2005**, 542, (1), 47-51.
147. Asanuma, H.; Akiyama, T.; Kajiya, K.; Hishiya, T.; Komiyama, M., Molecular imprinting of cyclodextrin in water for the recognition of nanometer-scaled guests. *Analytica Chimica Acta* **2001**, 435, 25-33.
148. Matsumoto, J.; Ijiro, K.; Shimomura, M., Molecular Recognition and Photopolymerization of Nucleobase Monolayer Containing Diacetylene Group at the Air-Water Interface. *Chemistry Letters* **2000**, 11, 1280-1281.
149. Diaz-Garcia, M. E.; Laino, R. B., Molecular imprinting in sol-gel materials: recent developments and applications. *Microchimica Acta* **2005**, 149, 19-36.
150. Vaihinger, D.; Landfester, K.; Kraeuter, I.; Brunner, H.; Tovar, G. E. M., Molecularly Imprinted Polymer Nanospheres as Synthetic Affinity Receptor Obtained by Miniemulsion Polymerisation. *Macromolecular Chemistry and Physics* **2002**, 203, 1965-1973.
151. Lehmann, M.; Dettling, M.; Brunner, H.; Tovar, G. E. M., Affinity parameters of amino acid derivative binding to molecularly imprinted nanospheres consisting of poly[(ethylene glycol dimethacrylate)-co-(methacrylic acid)]. *Journal of Chromatography, B: Analytical Technologies in the Biomedical and Life Sciences* **2004**, 808, (1), 43-50.
152. Weber, A.; Dettling, M.; Brunner, H.; Tovar, G. E. M., Isothermal Titration Calorimetry of Molecularly Imprinted Polymer Nanospheres. *Macromolecular Rapid Communications* **2002**, 23, 824-828.
153. Lehmann, M.; Brunner, H.; Tovar, G. E. M., Selective separations and hydrodynamic studies: a new approach using molecularly imprinted nanosphere composite membranes. *Desalination* **2002**, 149, (1-3), 315-321.
154. Perez, N.; Whitcombe, M. J.; Vulfson, E. N., Surface Imprinting of Cholesterol on Submicrometer Core-Shell Emulsion Particles. *Macromolecules* **2001**, 34, (4), 830-836.
155. Perez-Moral, N.; Mayes Andrew, G., Noncovalent imprinting in the shell of core-shell nanoparticles. *Langmuir : ACS journal of surfaces and colloids* **2004**, 20, (9), 3775-9.
156. Perez-Moral, N.; Mayes, A. G., Molecularly Imprinted Multi-Layer Core-Shell Nanoparticles - A surface Grafting Approach. *Macromolecular Rapid Communications* **2007**, 28, (22), 2170-2175.
157. Carter, S. R.; Rimmer, S., Molecular recognition of caffeine by shell molecular imprinted core-shell polymer particles in aqueous media. *Advanced Materials* **2002**, 14, (9), 667-670.

158. Takagi, M.; Maeda, M.; Hijiya, S.; Murata, M., Template-Dependant Selectivity in Metal Adsorption on Phosphoric Diester-Carrying Resins Prepared by Surface Template Polymerization Technique. *Bulletin of the Chemical Society of Japan* **1996,** 69, 637-642.
159. Carter, S. R.; Rimmer, S., Surface molecularly imprinted polymer core-shell particles. *Advanced Functional Materials* **2004,** 14, (6), 553-561.
160. Carter, S.; Lu, S.-Y.; Rimmer, S., Core-shell Molecular Imprinted Polymer Colloids. *Supramolecular Chemistry* **2003,** 15, (3), 213-220.
161. Hjerten, S.; Liao, J.-L.; Nakazato, K.; Wang, Y.; Zamaratskaia, G.; Zhang, H.-X., Gels mimicking antibodies in their selective recognition of proteins. *Chromatographia* **1997,** 44, (5/6), 227-234.
162. Bacskay, I.; Takatsy, A.; Vegvari, A.; Elfwing, A.; Ballagi-Pordany, A.; Kilar, F.; Hjerten, S., Universal method for synthesis of artificial gel antibodies by the imprinting approach combined with a unique electrophoresis technique for detection of minute structural differences of proteins, viruses, and cells (bacteria). III: Gel antibodies against cells (bacteria). *Electrophoresis* **2006,** 27, 4682-4687.
163. Takatsy, A.; Kilar, A.; Kilar, F.; Hjerten, S., Universal method for synthesis of artificial gel antibodies by the imprinting approach combined with a unique electrophoresis technique for detection of minute structural differences of proteins, viruses, and cells (bacteria): II. gel antibodies against virus (Semliki Forest Virus). *Journal of separation science* **2006,** 29, (18), 2810-2815.
164. Takatsy, A.; Kilar, A.; Kilar, F.; Hjerten, S., Universal method for synthesis of artificial gel antibodies by the imprinting approach combined with a unique electrophoresis technique for detection of minute structural differences of proteins, viruses, and cells (bacteria): La. gel antibodies against proteins (transferrins) *Journal of separation science* **2006,** 29, (18), 2802-2809.
165. Ou, S. H.; Wu, M. C.; Chou, T. C.; Liu, C. C., Polyacrylamide gels with electrostatic functional groups for the molecular imprinting of lysozyme. *Analytica Chimica Acta* **2004,** 504, 163-166.
166. Pang, X.; Cheng, G.; Lu, S.; Tang, E., Synthesis of polyacrylamide gel beads with electrostatic functional groups for the molecular imprinting of bovine serum albumin. *Analytical and Bioanalytical Chemistry* **2006,** 384, 225-230.
167. Byrne, M. E.; Salian, V., Molecular imprinting within hydrogels II: Progress and analysis of the field. *International Journal of Pharmaceutics* **2008,** 364, 188-212.
168. Karmalkar, R. N.; Kulkarni, M. G.; Mashelkar, R. A., Molecularly Imprinted Hydrogels Exhibit Chymotrypsin-like Activity. *Macromolecules* **1995,** 29, (4), 1366-1368.
169. Watanabe, M.; Akahoshi, T.; Tabata, Y.; Nakayama, D., Molecular Specific Swelling Change of Hydrogels in Accordance with the Concentration of Guest Molecules. *Journal of the American Chemical Society* **1998,** 120, (22), 5577-5578.
170. Uysal, A.; Demirel, G.; Turan, E.; Caykara, T., Hemoglobin recognition of molecularly imprinted hydrogels prepared at different pHs. *Analytica Chimica Acta* **2008,** 625, 110-115.
171. Hua, Z.; Chen, Z. Y.; Li, Y.; Zhao, M., Thermosensitive and Salt-Sensitive Molecularly Imprinted Hydrogel for Bovine Serum Albumin. *Langmuir* **2008,** 24, (11), 5773-5780.
172. Miyata, T.; Jige, M.; Nakaminami, T.; Uragami, T., Tumor marker-responsive behaviour of gels prepared by biomolecular imprinting. *Proceedings of the National Academy of Sciences* **2006,** 103, (5), 1190-1193.
173. Guo, T. Y.; Xia, Y. Q.; Hao, G. J.; Song, M. D.; Zhang, B. H., Adsorptive separation of hemoglobin by molecularly imprinted chitosan beads. *Biomaterials* **2004,** 25, 5905-5912.
174. Glad, M.; Norrlow, O.; Sellergren, B.; Siegbahn, N.; Mosbach, K., Use of silane monomers for molecular imprinting and enzyme entrapment in polysiloxane-coated porous silica. *Journal of Chromatography* **1985,** 347, 11-23.
175. Zhang, Z.; Long, Y.; Nie, L.; Yao, S., Molecularly imprinted thin film self-assembled on piezoelectric quartz crystal surface by the sol-gel process for protein recognition. *Biosensors and Bioelectronics* **2006,** 21, 1244-1251.

176. Wang, Y.; Zhou, Y.; Sokolov, J.; Rigas, B.; Levon, K.; Rafailovich, M., A potentiometric protein sensor built with surface molecular imprinting method. *Biosensors and Bioelectronics* **2008,** 24, 162-166.
177. Shnek, D. R.; Pack, D. W.; Sasaki, D. Y.; Arnold, F. H., Specific Protein Attachment to Artificial Membranes via Coordination to Lipid-Bound Copper(II). *Langmuir* **1994,** 10, 2382-2388.
178. Bossi, A.; Piletsky, S. A.; Piletska, E. V.; Righetti, P. G.; Turner, A. P. F., Surface-grafted molecularly imprinted polymers for protein recognition. *Analytical Chemistry* **2001,** 73, (21), 5281-5286.
179. Ramanaviciene, A.; Ramanavicius, A., Molecularly imprinted polypyrrole-based synthetic receptor for direct detection of bovine leukemia virus glycoproteins. *Biosensors and Bioelectronics* **2004,** 20, 1076-1082.
180. Britt, D. W.; Mobius, D.; Hlady, V., Ferritin adsorption to multicomponent monolayers: Influence of lipid charge density, miscibility and fluidity. *Physical Chemistry Chemical Physics* **2002,** 2, 4594-4599.
181. Chou, P.-C.; Rick, J.; Chou, T.-C., C-reactive protein thin-film molecularly imprinted polymers formed using a micro-contact approach. *Analytica Chimica Acta* **2005,** 542, (1), 20-25.
182. Lin, H.-Y.; Hsu, C.-Y.; Thomas, J. L.; Wang, S.-E.; Chen, H.-C.; Chou, T.-C., The microcontact imprinting of proteins: The effect of cross-linking monomers for lysozyme, ribonuclease A and myoglobin. *Biosensors and Bioelectronics* **2006,** 22, 534-543.
183. Chen, Y.-W.; Rick, J.; Chou, T.-C., A systematic approach to forming micro-contact imprints of creatine kinase. *Organic and Biomolecular Chemistry* **2009,** 7, 488-494.
184. Su, W.-X.; Rick, J.; Chou, T.-C., Selective recognition of ovalbumin using a molecularly imprinted polymer. *Microchemical Journal* **2009,** Article in Press.
185. Shi, H.; Tsai, W.-B.; Garrison, M. D.; Ferrari, S.; Ratner, B. D., Template-imprinted nanostructured surfaces for protein recognition. *Nature* **1999,** 398, (6728), 593-597.
186. Shiomi, T.; Matsui, M.; Mizukami, F.; Sakaguchi, K., A method for the molecular imprinting of hemoglobin on silica surfaces using silanes. *Biomaterials* **2005,** 26, 5564-5571.
187. Li, Y.; Yang, H.-H.; You, Q.-H.; Zhuang, Z.-X.; Wang, X.-R., Protein Recognition via Surface Molecularly Imprinted Polymer Nanowires. *Analytical Chemistry* **2006,** 78, (1), 317-320.
188. Matsunaga, T.; Takeuchi, T., Crystallized Protein-imprinted Polymer Chips. *Chemistry Letters* **2006,** 35, (9), 1030-1031.
189. Tan, C. J.; Chua, H. G.; Ker, K. H.; Tong, Y. W., Preparation of Bovine Serum Albumin Surface-Imprinted Submicrometer Particles with Magnetic Susceptibility through Core-Shell Miniemulsion Polymerization. *Analytical Chemistry* **2008,** 80, 683-692.
190. Rachkov, A.; Minoura, N., Towards molecularly imprinted polymers selective to peptides and proteins. The epitope approach. *Biochimica et Biophysica Acta, Protein Structure and Molecular Enzymology* **2001,** 1544, (1-2), 255-266.
191. Titirici, M.; Sellergren, B., Peptide recognition via hierarchical imprinting. *Analytical and Bioanalytical Chemistry* **2004,** 378, 1913-1921.
192. Emgenbroich, M.; Borrelli, C.; Shinde, S.; Lazraq, I.; Vilela, F.; Hall, A. J.; Oxelbark, J.; Lorenzi, E. D.; Courtois, J.; Simanova, A.; Verhage, J.; Irgum, K.; Karim, K.; Sellergren, B., A Phosphotyrosine-Imprinted Polymer Receptor for the Recognition of Tyrosine Phosphorylated Peptides. *Chemistry - A European Journal* **2008,** 14, 9516-9529.
193. Nishino, H.; Huang, C.-S.; Shea, K. J., Selective Protein Capture by Epitope Imprinting. *Angewandte Chemie International Edition* **2006,** 45, 2392-2396.
194. Tai, D.-F.; Lin, C.-Y.; Wu, T.-Z.; Chen, L.-K., Recognition of Dengue Virus Protein Using Epitope-Mediated Molecularly Imprinted Film. *Analytical Chemistry* **2005,** 77, (16), 5140-5143.
195. Xue, X.; Pan, J.; Xie, H.; Wang, J.; Zhang, S., Specific recognition of staphylococcus aureus by staphylococcus aureus protein A-imprinted polymers. *Reactive and Functional Polymers* **2009,** 69, (3), 159-164.

196. Wichterle, O.; Lim, D., Hydrophilic Gels for Biological Use. *Nature* **1960,** 185, 117-118.
197. Peppas, N. A.; Mikos, A. G., Preparation Methods and Structure of Hydrogels. *Hydrogels in Medicine and Pharmacy. Volume I Fundamentals* **1986,** Peppas, N. A. Boca Raton, Florida, CRC Press, 1-25.
198. Peppas, N. A.; Bures, P.; Leobandung, W.; Ichikawa, H., Hydrogels in pharmaceutical formulations. *European Journal of Pharmaceutics and Biopharmaceutics* **2000,** 50, 27-46.
199. Hoffman, A. S., Hydrogels for biomedical applications. *Advanced Drug Delivery Reviews* **2002,** 43, 3-12.
200. Lin, C.-C.; Metters, A. T., Hydrogels in controlled release formulations: Network design and mathematical modeling. *Advanced Drug Delivery Reviews* **2006,** 58, 1379-1408.
201. Duncan, E., What Is a Biomaterial? *Medical Device and Diagnostic Industry* **1990,** 12, (1), 138-142.
202. Marchant, R. E., The Cage Implant System for Determining *in Vivo* Biocompatibility of Medical Device Materials. *Fundamental and Applied Toxicology* **1989,** 13, (2), 217-227.
203. Gupta, P.; Vermani, K.; Garg, S., Hydrogels: from controlled release to pH-responsive drug delivery. *Drug Discovery Today* **2002,** 7, (10), 569-579.
204. Hoare, T. R.; Kohane, D. S., Hydrogels in drug delivery: Progress and challenges. *Polymer* **2008,** 49, 1993-2007.
205. Ganji, F.; Vasheghani-Farahani, E., Hydrogels in Controlled Drug Delivery Systems. *Iranian Polymer Journal* **2009,** 18, (1), 63-88.
206. Jen, A. C.; Wake, M. C.; Mikos, A. G., Review: Hydrogels for Cell Immobilization. *Biotechnology and Bioengineering* **1996,** 50, 357-364.
207. Nicodemus, G. D.; Bryant, S. J., Cell Encapsulation in Biodegradable Hydrogels for Tissue Engineering Applications. *Tissue Engineering: Part B* **2008,** 14, (2), 149-165.
208. Lee, K. Y.; Mooney, D. J., Hydrogels for Tissue Engineering. *Chemical Reviews* **2001,** 101, (7), 1869-1880.
209. Van Tomme, S. R.; Storm, G.; Hennink, W. E., In situ gelling hydrogels for pharmaceutical and biomedical applications. *International Journal of Pharmaceutics* **2008,** 355, (1-2), 1-18.
210. Menaker, G. M., Wound Dressings at the Turn of the Millenium. *Current Problems in Dermatology* **2001,** 13, (2), 86-89.
211. Lionelli, G. T.; Lawrence, W. T., Wounds dressings. *Surgical Clinics of North America* **2003,** 83, 617-638.
212. Helfman, T.; Ovington, L.; Falanga, V., Occlusive Dressings and Wound Healing. *Clinics in Dermatology* **1994,** 12, 121-127.
213. Jones, A.; Vaughan, D., Hydrogel dressings in the management of a variety of wound types: A review. *Journal of Orthopaedic Nursing* **2005,** 9, S1-S11.
214. Morgan, D., Wounds - what should a dressings formulary include? *Hospital Pharmacist* **2002,** 9, 261-266.
215. Qiu, Y.; Park, K., Environment-sensitive hydrogels for drug delivery. *Advanced Drug Delivery Reviews* **2001,** 53, 321-339.
216. Baldwin, S. P.; Saltzman, W. M., Materials for protein delivery in tissue engineering. *Advanced Drug Delivery Reviews* **1998,** 33, 71-86.
217. Silva, A. K. A.; Richard, C.; Bessodes, M.; Scherman, D.; Merten, O. W., Growth Factor Delivery Approaches in Hydrogels. *Biomacromolecules* **2009,** 10, (1), 9-18.
218. Hamidi, M.; Azadi, A.; Rafiei, P., Hydrogel nanoparticles in drug delivery. *Advanced Drug Delivery Reviews* **2008,** 60, 1638-1649.
219. George, M.; Abraham, T. E., pH sensitive alginate-guar gum hydrogel for the controlled delivery of protein drugs. *International Journal of Pharmaceutics* **2007,** 335, 123-129.
220. Xiao, Y.; Xu, W.; Zhu, Q.; Yan, B.; Yang, D.; Yang, J.; He, X.; Liang, S.; Hu, X., Preparation and characterization of a novel pachyman-based pharmaceutical aid. II: A pH-sensitive, biodegradable and biocompatible hydrogel for controlled release of protein drugs. *Carbohydrate Polymers* **2009,** Article in Press.

221. Wu, J.-Y.; Liu, S.-Q.; Heng, P. W.-S.; Yang, Y.-Y., Evaluating proteins release from, and their interactions with, thermosensitive poly(*N*-isopropylacrylamide) hydrogels. *Journal of controlled release* **2005,** 102, 361-372.
222. Tae, G.; Kornfield, J. A.; Hubbell, J. A., Sustained release of human growth hormone from in situ forming hydrogels using self-assembly of fluoroalkyl-ended poly(ethylene glycol). *Biomaterials* **2005,** 26, 5259-5266.
223. Huynh, D. P.; Nguyen, M. K.; Pi, B. S.; Kim, M. S.; Chae, S. Y.; Lee, K. C.; Kim, B., S.; Kim, S. W.; Lee, D. S., Functionalized injectable hydrogels for controlled insulin delivery. *Biomaterials* **2008,** 29, 2527-2534.
224. Piantino, J.; Burdick, J. A.; Goldberg, D.; Langer, R.; Benowitz, L. I., An injectable, biodegradable hydrogel for trophic factor delivery enhances axonal rewiring and improves performance after spinal cord injury. *Experimental Neurology* **2006,** 201, 359-367.
225. Carvalho, J. M.; Coimbra, M. A.; Gama, F. M., New dextrin-vinylacrylate hydrogel: Studies on protein diffusion and release. *Carbohydrate Polymers* **2009,** 75, 322-327.
226. Nochos, A.; Douroumis, D.; Bouropoulos, N., In vitro release of bovine serum albumin from alginate/HPMC hydrogel beads. *Carbohydrate Polymers* **2008,** 74, 451-457.
227. Hori, K.; Sotozono, C.; Hamuro, J.; Yamasaki, K.; Kimura, Y.; Ozeki, M.; Tabata, Y.; Kinoshita, S., Controlled-release of epidermal growth factor from catonized gelatin hydrogel enhances corneal epithelial wound healing. *Journal of controlled release* **2007,** 118, 169-176.
228. Lee, F.; Chung, J. E.; Kurisawa, M., An injectable hyaluronic acid-tyramine hydrogel system for protein delivery. *Journal of controlled release* **2009,** 134, 186-193.
229. Everett, D. H., Manual of Symbols and Terminology for Physiochemical Quantities and Units, Appendix II: Definitions, Terminology and Symbols in Colloid and Surface Chemistry. *Pure and Applied Chemistry* **1972,** 31, (4), 577-638.
230. Odian, G. G., Emulsion Polymerization. *Principles of polymerization. Ed 4* **2004,** 4th Ed., John Wiley and Sons, 350-371.
231. Schork, F. J.; Luo, Y.; Smulders, W.; Russum, J. P.; Butte, A.; Fontenot, K., Miniemulsion Polymerization. *Advances in Polymer Science* **2005,** 175, 129-255.
232. O'Shannessy, D.; Ekberg, B.; Mosbach, K., Molecular Imprinting of Amino Acid Derivatives at Low Temperature (O°C) Using Photolytic Homolysis of Azobisnitriles. *Analytical Biochemisty* **1989,** 177, 144-149.
233. Gafurov, A., Kh; Yakubov, N. I.; Asamov, M. K., Kinetics of emulsion copolymerization of vinyl fluoride and trifluoroethylene. *Polymer Science USSR* **1987,** 29, (2), 363-369.
234. Chow, P. Y.; Gan, L. M., Microemulsion Polymerization and Reactions. *Advances in Polymer Science* **2005,** 175, 257-298.
235. Moad, G.; Solomon, D. H., Chain Transfer. *The Chemistry of Radical Polymerisation. Ed. 2.* **2006,** Elsevier Ltd, 279-331.
236. Goddard, J. M.; Hotchkiss, J. H., Polymer surface modification for the attachment of bioactive compounds. *Progress in Polymer Science* **2007,** 32, 698-725.
237. Faust, S. D.; Aly, O. M., *Chemistry of Water Treatment, Ed. 2* **1998,** CRC Press, 220-222.
238. Hunter, R. J., *Zeta Potential in Colloid Science. Principles and Applications.* **1981,** Academic Press Inc. London, U.K., 1-7.
239. Heurtault, B.; Saulnier, P.; Pech, B.; Proust, J.-E.; Benoit, J.-P., Physico-chemical stability of colloidal lipid particles. *Biomaterials* **2003,** 24, 4283-4300.
240. Fasman, G. D., *Prediction of Protein Structure and the Principles of Protein Conformation* **1989,** Springer, 48.
241. Luger, K.; Maeder, A., W.; Richmond, R. K.; Sargent, D. F.; Richmond, T. J., Crystal structure of the nucleosome core particle at 2.8A resolution. *Nature* **1997,** 389, 251-260.
242. Schug, K. A.; Lindner, W., Noncovalent Binding between Guanidinium and Anionic Groups: Focus on Biological- and Synthetic-Based Arginine/Guanidinium Interactions with Phosph(on)ates and Sulf(on)ate Residues. *Chemical Reviews* **2005,** 105, (1), 67-114.
243. Hames, B. D.; Hooper, N. M., *Instant Notes: Biochemistry. Ed. 2* **2000,** BIOS Scientific Publishers Limited

244. Fromm, J. R.; Hileman, R. E.; Caldwell, E. E. O.; Weiler, J. M.; Linhardt, R. J., Differences in the Interaction of Heparin with Arginine and Lysine and the Importance of these Basic Amino Acids in the Binding of Heparin to Acidic Fibroblast Growth. *Archives of Biochemistry and Biophysics* **1995,** 323, (2), 279-287.
245. Hu, X.; An, Q.; Li, G.; Tao, S.; Liu, J., Imprinted Photonic Polymers for Chiral Recognition. *Angewandte Chemie International Edition* **2006,** 45, 8145-8148.
246. Takeuchi, T.; Mukawa, T.; Mutsui, J.; Higashi, M.; Shimizu, K. D., Molecularly Imprinted Polymers with Metalloporphyrin-Based Molecular Recognition Sites Coassembled with Methacrylic Acid. *Analytical Chemistry* **2001,** 73, (16), 3869-3874.
247. Turkewitsch, P.; Wandelt, B.; Darling, G. D.; Powell, W. S., Fluorescent Functional Recognition Sites through Molecular Imprinting. A Polymer-Based Fluorescent Chemosensor for Aqueous cAMP. *Analytical Chemistry* **1998,** 70, (10), 2025-2030.
248. Piletsky, S. A.; Terpetschnig, E.; Andersson, H. S.; Nicolls, I. A.; Wolfbeis, O. S., Application of non-specific fluorescent dyes for monitoring enantio-selective ligand binding to molecularly imprinted polymers. *Fresenius Journal of Analytical Chemistry* **1999,** 364, 512-516.
249. Chow, C.-F.; Lam, M. H. W.; Leung, M. K. P., Fluorescent sensing of homocysteine by molecular imprinting. *Analytica Chimica Acta* **2002,** 466, (1), 17-30.
250. Graefe, A.; Haupt, K.; Mohr, G. J., Optical sensor materials for the detection of amines in organic solvents. *Analytica Chimica Acta* **2006,** 565, 42-47.
251. Henry, O. Y. F.; Cullen, D. C.; Piletsky, S. A., Optical interrogation of molecularly imprinted polymers and development of MIP sensors: a review. *Analytical and Bioanalytical Chemistry* **2005,** 382, 947-956.
252. Manesiotis, P.; Hall, A. J.; Emgenbroich, M.; Quaglia, M.; Lorenzi, E. D.; Sellergren, B., An enantioselective imprinted receptor for Z-glutamate exhibiting a binding induced colour change. *Chemical Communications* **2004,** 2278-2279.
253. Bisset, A.; Dines, T. J., Resonance Raman Spectroscopic Study of Methyl Red and Ethyl Red adsorbed on Silica. *Journal of the Chemistry Society Faraday Transactions* **1995,** 91, (3), 499-505.
254. Bell, S.; Bisset, A.; Dines, T. J., Ab Initio and Density Functional Study of the Resonance Raman Spectra of Methyl Red, Ethyl Red and Their Protonated Derivatives. *Journal of Raman Spectroscopy* **1998,** 29, 447-462.
255. Park, S.-K.; Lee, C.; Min, K.-C.; Lee, N.-S., Structural and Conformational Studies of ortho-, meta-, and para-Methyl Red upon Proton Gain and Loss. *Bulletin of the Korean Chemical Society* **2005,** 26, (8), 1170-1176.
256. Tawarah, K. M.; Khouri, S. J., The Tautomeric and Acid-Base Equilibria of p-Methyl Red in Aqueous Solutions. *Dyes and Pigments* **1992,** 20, 261-270.
257. Kuwabara, T.; Nakajima, H.; Nanasawa, M.; Ueno, A., Color Change Indicators for Molecules Using Methyl Red-Modified Cyclodextrins. *Analytical Chemistry* **1999,** 71, 2844-2849.
258. Ueno, A.; Kuwabara, T.; Nakamura, A.; Toda, F., A modified cyclodextrin as a guest responsive colour-change indicator. *Nature* **1992,** 356, 136-137.
259. Huang, M.; Vitharana, S. N.; Peek, L. J.; Coop, T.; Berkland, C., Polyelectrolyte Complexes Stabilize and Controllably Release Vascular Endothelial Growth Factor. *Biomacromolecules* **2007,** 8, 1607-1614.
260. Alvarez-Lorenzo, C.; Yanez, F.; Barreiro-Iglesias, R.; Concheiro, A., Imprinted soft contact lenses as norfloxacin delivery systems. *Journal of controlled release* **2006,** 113, 236-244.
261. Umpleby, R. J.; Baxter, S. C.; Rampey, A. M.; Rushton, G. T.; Chen, Y.; Shimizu, K. D., Characterization of the heterogeneous binding site affinity distributions in molecularly imprinted polymers. *Journal of Chromatography B, Analytical technologies in the biomedical and life sciences* **2004,** 804, 141-149.
262. Brown, M. E.; Puleo, D. A., Protein binding to peptide-imprinted porous silica scaffolds. *Chemical Engineering Journal* **2008,** 137, 97-101.

263. Qin, L.; He, X.-W.; Zhang, W.; Li, W.-Y.; Zhang, Y.-K., Surface-modified polystyrene beads as photografting imprinted polymer matrix for chromatographic separation of proteins. *Journal of Chromatography A* **2009,** 1216, 807-814.
264. Tan, C. J.; Wangrangsimakul, S.; Bai, R.; Tong, Y. W., Defining the Interactions between Proteins and Surfactants for Nanoparticle Surface Imprinting through Miniemulsion Polymerization. *Chemistry of Materials* **2008,** 20, 118-127.
265. Okutucu, B.; Zihnioglu, F.; Telefoncu, A., Shell-core imprinted polyacrylamide crosslinked chitosan for albumin removal from plasma. *Journal of Biomedical Materials Research Part A* **2008,** 84, (3), 842-845.
266. Robinson, B. V.; Sullivan, F. M.; Borzelleca, J. F.; Schwartz, S. L., *PVP: A Critical Review of the Kinetics and Toxicology of Polyvinylpyrrolidone* **1990,** Lewis Publishers, Michigan, USA.
267. Monfardini, C.; Veronese, F. M., Stabilization of Substances in Circulation. *Bioconjugate Chemistry* **1998,** 9, (4), 418-450.
268. Zelikin, A.; Such, G. K.; Postma, A.; Caruso, F., Poly(vinylpyrrolidone) for Bioconjugation and Surface Ligand Immobilization. *Biomacromolecules* **2007,** 8, 2950-2953.
269. Kaneda, Y.; Tsutsumi, Y.; Yoshioka, Y.; Kamada, H.; Yamamoto, Y.; Kodaira, H.; Tsunoda, S.-i.; Okamoto, T.; Mukai, Y.; Shibata, H.; Nakagawa, S.; Mayumi, T., The use of PVP as a polymeric carrier to improve the plasma
half-life of drugs. *Biomaterials* **2004,** 25, 3259-3266.
270. Vijayasekaran, S.; Chirila, T. V.; Hong, Y.; Tahija, S. G.; Dalton, P. D.; Constable, I. J.; McAllister, I. L., Poly(1-vinyl-2-pyrrolidinone) hydrogels as vitreous substitutes: Histopathological evaluation in the animal eye. *Journal of Biomaterials Science, Polymer Edition* **1996,** 7, (8), 685-696.
271. Hong, Y.; Chirila, T. V.; Fitton, J. H.; Ziegelaar, B. W.; Constable, I. J., Effect of crosslinked poly(1-vinyl-2-pyrrolidinone) gels on cell growth in static cell cultures. *Bio-Medical Materials and Engineering* **1997,** 7, 35-47.
272. Hong, Y.; Chirila, T. V.; Vijayasekaran, S.; Shen, W.; Lou, X.; Dalton, P. D., Biodegradation *in vitro* and retention in the rabbit eye of crosslinked poly(1-vinyl-2-pyrrolidinone) hydrogel as a vitreous substitute. *Journal of Biomedical Materials Research* **1998,** 39, (4), 650-659.
273. Francois, P.; Vaudaux, P.; Nurdin, N.; Mathieu, H. J.; Descouts, P.; Lew, D. P., Physical and biological effects of a surface coating procedure on polyurethane catheters. *Biomaterials* **1996,** 17, (7), 667-678.
274. Liu, Z.; Fullwood, N.; Rimmer, S., Synthesis of allyloxycarbonyloxymethyl-5-fluouracil and copolymerizations with N-vinylpyrrolidinone. *Journal of Materials Chemistry* **2000,** 10, 1771-1775.
275. Liu, Z.; Rimmer, S., Studies on the Free Radical Polymerization of N-Vinylpyrrolidinone in 3-Methylbutan-2-one. *Macromolecules* **2002,** 35, (4), 1200-1207.
276. Liu, Z.; Rimmer, S., Synthesis and release of 5-fluorouracil from poly(N-vinylpyrrolidinone) bearing 5-fluorouracil derivatives. *Journal of controlled release* **2002,** 81, 91-99.
277. Luo, L.; Lessard, D. G.; Garrec, D. L.; Gori, S.; Leroux, J. C.; Rimmer, S.; Smith, D., Novel amphiphilic diblock copolymer of low molecular weight poly(N-vinylpyrrolidone)-block-poly(D,L-lactide): Synthesis, characterization, and micellization *Macromolecules* **2004,** 37, (11), 4008-4013.
278. Smith, L. E.; Rimmer, S.; MacNeil, S., Examination of the effects of poly(vinylpyrrolidinone) hydrogels in direct and indirect contact with cells. *Biomaterials* **2006,** 27, 2806-2812.
279. Powell, A. K.; Yates, E. A.; Fernig, D. G.; E., T. J., Interactions of heparin/heparan sulfate with proteins: Appraisal of structural factors and experimental approaches. *Glycobiology* **2004,** 14, (4), 17R-30R.
280. Mulloy, The specificity of interactions between proteins and sulfated polysaccharides. *Annals of the Brazilian Academy of Sciences* **2005,** 77, (4), 651-664.

281. Cardin, A. D.; Weintraub, H. J. R., Molecular modeling of protein-glycosaminoglycan interactions. *Arteriosclerosis, Thrombosis and Vascular Biology* **1989,** 9, 21-32.
282. Sobel, M.; Soler, D. F.; Kermode, J. C.; Harris, R. B., Localisation and characterization of a heparin binding domain peptide of human von Willebrand factor. *Journal of Biological Chemistry* **1992,** 267, 8857-8862.
283. Hileman, R., E.; Fromm, J., R.; Weiler, J. M.; Linhardt, R. J., Glycosaminoglycan-protein interactions: definition of consensus sites in glycosaminoglycan binding proteins. *BioEssays* **1998,** 20, 156-167.
284. Caldwell, E. E. O.; Nadkarni, V. D.; Fromm, J., R.; Linhardt, R. J.; Weiler, J. M., Importance of specific amino acids in protein binding sites for heparin and heparan sulfate. *International Journal of Biochemistry and Cell Biology* **1996,** 28, 203-216.
285. Ikada, Y., Surface modification of polymers for medical applications. *Biomaterials* **1994,** 15, 725-736.
286. Smith, L. E., *PhD Thesis: Development of poly(vinylpyrrolidinone) networks for treatment of skin graft contracture* **2007.**
287. Steffens, G. C. M.; Nothdurft, L.; Buse, G.; Thissen, H.; Hoeker, H.; Klee, D., High density binding of proteins and peptides to poly(D,L-lactide) grafted with polyacrylic acid. *Biomaterials* **2002,** 23, 3523-3531.
288. Lopez, L. C.; Gristina, R.; Ceccone, G.; Rossi, F.; Favia, P.; d'Agostino, R., Immobilisation of RGD peptides on stable plasma-deposited acrylic acid coatings for biomedical devices. *Surface & Coatings Technology* **2005,** 200, 1000-1004.
289. Ebara, M.; Yamato, M.; Aoyagi, T.; Kikuchi, A.; Sakai, K.; Okano, T., Temperature-Responsive Cell Culture Surfaces Enable "On-Off" Affinity Control between Cell Integrins and RGDS Ligands. *Biomacromolecules* **2004,** 5, (2), 505-510.
290. Yamaoka, T.; Hotta, Y.; Kobayashi, K.; Kimura, Y., Synthesis and properties of malic acid-containing functional polymers. *International Journal of Biological Macromolecules* **1999,** 25, 265-271.
291. Oh, J.-T.; Nam, J.-H.; Jung, Y. M., Molecular miscible blend of poly(2-cyano-1,4-phenyleneterephthalamide) and polyvinylpyrrolidone characterized by two-dimensional correlation FTIR and solid state 13C NMR spectroscopy. *Vibrational Spectroscopy* **2009,** 51, (1), 15-21.
292. Lau, C.; Mi, Y., A study of blending and complexation of poly(acrylic acid)/poly(vinyl pyrrolidone). *Polymer* **2002,** 43, 823-829.
293. Flory, P. J.; Rehner, J. J., Statistical mechanics of cross-linked polymer networks II. Swelling. *Journal of Chemical Physics* **1943,** 11, 521-526.
294. Wong, J., Y.; Bronzino, J. D., *Biomaterials* **2007,** CRC Press.
295. Snyder, S. L.; Sobocinski, P. Z., An Improved 2,4,6-Trinitrobenzenesulfonic Acid Method for the Determination of Amines. *Analytical Biochemistry* **1975,** 64, 284-288.
296. Weber, C. J., A Modification of Sakaguchi's Reaction for the Quantitative Determination of Arginine. *Journal of Biological Chemistry* **1930,** 86, 217-222.
297. Sakaguchi, S., Ueber eine neue Farbenreaktion von Protein und Arginin. *Journal of Biochemistry* **1925,** 5, 25-31.
298. Parniak, M. A.; Lange, G.; Viswanatha, T., Quantitative determination of monosubstituted guanidines: A comparative study of different procedures. *Journal of Biochemical and Biophysical Methods* **1983,** 7, 267-276.
299. Buergel, T.; Fedtke, M., Reactions of cyclic carbonates with amines: Model studies for curing process. *Polymer Bulletin* **1991,** 27, 171-177.
300. Blomberg, E.; Claesson, P. M.; Froeberg, J. C., Surfaces coated with protein layers: a surface force and ESCA study. *Biomaterials* **1998,** 19, (371-386).
301. McArthur, S. L., Applications of XPS in bioengineering. *Surface and Interface Analysis* **2006,** 38, 1380-1385.
302. Ma, Z.; Mao, Z.; Gao, C., Surface modification and property analysis of biomedical polymers used for tissue engineering. *Colloids and Surfaces B: Biointerfaces* **2007,** 60, 137-157.

303. Wagner, M. S.; Pasche, S.; Castner, D. G.; Textor, M., Characterization of Poly (L-lysine)-graft-Poly(ethylene glycol) Assembled Monolayers on Niobium Pentoxide Substrates Using Time-of-Flight Secondary Ion Mass Spectrometry and Multivariate Analysis. *Analytical Chemistry* **2004,** 76, 1483-1492.
304. Belu, A. M.; Graham, D. J.; Castner, D. G., Time-of-flight secondary ion mass spectrometry: techniques and applications for the characterization of biomaterial surfaces. *Biomaterials* **2003,** 24, 3635-3653.
305. Samuel, N. T.; Wagner, M. S.; Dornfeld, K. D.; Castner, D. G., Analysis of Poly(amino acids) by Static Time-of-Flight Secondary Ion Mass Spectrometry (TOF-SIMS). *Surface Science Spectra* **2001,** 8, (3), 163.
306. Scott, J. E.; Harbinson, R. J., Periodate Oxidation of Acid Polysaccharides Inhibition by the Electrostatic Field of the Substrate. *Histochemie* **1968,** 14, 215-220.
307. Hermanson, G. T., *Bioconjugate Techniques. Ed. 2* **2008,** Academic Press, 412-413.
308. West, R. H.; Paul, A. J.; Hibbert, S., Correlation of the surface chemistries of polymer bioactive coatings, with their biological performances. *Journal of Materials Science: Materials in Medicine* **1995,** 6, 63-67.
309. Steffen, H. J.; Schmidt, J.; Gonzalez-Elipe, A., Biocompatible surfaces by immobilization of heparin on diamond-like carbon films deposited on various substrates. *Surface and Interface Analysis* **2000,** 29, 386-391.
310. Nakayama, Y.; Okahashi, R.; Iwai, R.; Uchida, K., Heparin Bioconjugate with a Thermoresponsive Cationic Branched Polymer: A Novel Aqueous Antithrombogenic Coating Material. *Langmuir* **2007,** 23, 8206-8211.
311. Meng, S.; Rouabhia, M.; Shi, G.; Zhang, Z., Heparin dopant increases the electrical stability, cell adhesion and growth of conducting polypyrrole/poly(L,L-lactide) composites. *Journal of Biomedical Materials Research - Part A* **2008,** 87, (2), 332-344.
312. Aksoy, A. E.; Hasirci, V.; Hasirci, N., Surface modification of polyurethanes with covalent immobilisation of heparin. *Macromolecular Symposia* **2008,** 269, (1), 145-153.
313. Robinson, D., *PhD Thesis: Investigating glycosaminoglycan-protein interactions: the "sugar chip"* **2009.**
314. Gu, F.; Neufeld, R.; Amsden, B., Sustained release of bioactive therapeutic proteins from a biodegradable elastomeric device. *Journal of controlled release* **2007,** 117, 80-89.
315. Elcin, A. E.; Elcin, Y. M., Localized Angiogenesis Induced by Human Vascular Endothelial Growth Factor-Activated PLGA Sponge. *Tissue Engineering* **2006,** 12, (4), 959-968.
316. Zhang, L.; Furst, E. M.; Kiick, K. L., Manipulation of hydrogel assembly and growth factor delivery via the use of peptide-polysaccharide interactions. *Journal of controlled release* **2006,** 114, 130-142.
317. Mosmann, T., Rapid Colorimetric Assay for Cellular Growth and Survival: Application to Proliferation and Cytotoxicity Assays. *Journal of Immunological Methods* **1983,** 65, 55-63.
318. Scudiero, D. A.; Shoemaker, R. H.; Paull, K. D.; Monks, A.; Tierney, S.; Nofziger, T. H.; Currens, M. J.; Seniff, D.; Boyd, M. R., Evaluation of a Soluble Tetrazolium/Formazan Assay for Cell Growth and Drug Sensitivity in Culture Using Human and Other Tumor Cell Lines. *Cancer Research* **1988,** 48, 4827-4833.
319. Haigh, R.; Fullwood, N.; Rimmer, S., Synthesis and properties of amphiphilic networks 2: a differential scanning calorimetric study of poly(dodecyl methacrylate-*stat*-2,3-propandiol-1-methacrylate-*stat*-ethandiol dimethacrylate) networks and adhesion and spreading of dermal fibroblasts on these materials. *Biomaterials* **2002,** 23, 3509-3516.
320. Nuttelman, C. R.; Mortisen, D. J.; Henry, S. M.; Anseth, K. S., Attachment of fibronectin to poly(vinyl alcohol) hydrogels promotes NIH3T3 cell adhesion, proliferation, and migration. *Journal of Biomedical Materials Research - Part A* **2001,** 57, (2), 217-223.
321. Hynd, M. R.; Frampton, J. P.; Dowell-Mesfin, N.; Turner, J. N.; Shain, W., Directed cell growth on protein-functionalized hydrogel surfaces. *Journal of Neuroscience Methods* **2007,** 162, 255-263.

322. Sun, Y.; Maughan, J.; Haigh, R.; Hopkins, S. A.; Wyman, P.; Johnson, C.; Fullwood, N. J.; Ebdon, J.; MacNeil, S.; Rimmer, S., Polymethacrylate Networks as Substrates for Cell Culture. *Macromolecular Symposia* **2007,** 256, 137-148.
323. Rimmer, S.; Johnson, C.; Zhao, B.; Collier, J.; Gilmore, L.; Sabnis, S.; Wyman, P.; Sammon, C.; Fullwood, N. J.; MacNeil, S., Epithelialization of hydrogels achieved by amine functionalization and co-culture with stromal cells. *Biomaterials* **2007,** 28, 5319-5331.
324. Kim, S.; English, A. E.; Kihm, K. D., Surface elasticity and charge concentration-dependent endothelial cell attachment to copolymer polyelectrolyte hydrogel. *Acta Biomaterialia* **2009,** 5, 144-151.
325. Haxhinasto, K. B.; English, A. E.; Moy, A. B., Equilibrium and non-equilibrium charge-dependent quantification of endothelial cell hydrogel scaffolds. *Journal of Materials Science: Materials in Medicine* **2008,** 19, 1999-2008.
326. Akhtar, N.; Dickerson, E. B.; Auerbach, R., The sponge/Matrigel angiogenesis assay. *Angiogenesis* **2002,** 5, 75-80.
327. Nguyen, M.; Shing, Y.; Folkman, J., Quantitation of Angiogenesis and Antiangiogenesis in the Chick Embryo Chorioallantoic Membrane. *Microvascular Research* **1994,** 47, 31-40.
328. Presta, M.; Rusnati, M.; Belleri, M.; Morbidelli, L.; Ziche, M.; Ribatti, D., Purine Analogue 6-Methylmercaptopurine Riboside Inhibits Early and Late Phases of the Angiogenesis Process. *Cancer Research* **1999,** 59, 2417-2424.
329. Dudar, T. E.; Jain, R. K., Microcirculatory Flow Changes during Tissue Growth. *Microvascular Research* **1983,** 25, 1-21.
330. Serbedzija, G. N.; Flynn, E.; Willett, C. E., Zebrafish angiogenesis: A new model for drug screening. *Angiogenesis* **1999,** 3, 353-359.
331. Doumont, G.; De Visser, K. E.; Derksen, P. W. B.; Jonkers, J., Models for angiogenesis: From fundamental mechanisms to anticancer treatment research. *Drug Discovery Today: Disease Models* **2008,** 4, (2), 75-82.
332. Staton, C. A.; Stribbling, S. M.; Tazzyman, S.; Hughes, R.; Brown, N. J.; Lewis, C. E., Current methods for assaying angiogenesis in vitro and in vivo. *International Journal of Experimental Pathology* **2004,** 85, 233-248.
333. Zhu, W.-H.; Lurlaro, M.; MacIntyre, A.; Fogel, E.; Nicosia, R. F., The mouse aorta model: Influence of genetic background and aging on bFGF- and VEGF-induced angiogenic sprouting. *Angiogenesis* **2003,** 6, (3), 193-199.
334. Feraud, O.; Cao, Y.; Vittet, D., Embryonic Stem Cell-Derived Embryoid Bodies Development in Collagen Gels Recapitulates Sprouting Angiogenesis. *Laboratory Investigation* **2001,** 81, (12), 1669-1681.
335. Deckers, M.; Van der Pluijm, G.; Dooijewaard, S.; Kroon, M.; Van Hinsbergh, V.; Papapoulos, S.; Loewik, C., Effect of Angiogenic and Antiangiogenic Compounds on the Outgrowth of Capillary Structures from Fetal Mouse Bone Explants. *Laboratory Investigation* **2001,** 81, (1), 5-15.
336. Liekens, S.; De Clercq, E.; Neyts, J., Angiogenesis: regulators and clinical applications. *Biochemical Pharmacology* **2001,** 61, 253-270.
337. Goodwin, A. M., In vitro assays of angiogenesis for assessment of angiogenic and anti-angiogenic agents. *Microvascular Research* **2007,** 74, 172-183.
338. Yamashita, Y.; Nakagomi, K.; Takeda, T.; Hasegawa, S.; Mitsui, Y., Effect of heparin on pulmonary fibroblasts and vascular cells. *Thorax* **1992,** 47, 634-639.
339. Weatherford, D. A.; Sackman, J. E.; Reddick, T. T.; Freeman, M. B.; Stevens, S. L.; Goldman, M. H., Vascular endothelial growth factor and heparin in a biologic glue promotes human aortic endothelial cell proliferation with aortic smooth muscle cell inhibition. *Surgery* **1996,** 433-439.
340. Saksela, O.; Moscatelli, D.; Sommer, A.; Rifkin, D. B., Endothelial Cell-derived Heparan Sulfate Binds Basic Fibroblast Growth Factor and Protects It from Proteolytic Degradation. *The Journal of Cell Biology* **1988,** 107, 743-751.
341. Gospodarowicz, D.; Cheng, J., Heparin Protects Basic and Acidic FGF from Inactivation. *Journal of Cellular Physiology* **1986,** 128, 475-484.

342. Brandner, B.; Kurkela, R.; Vihko, P.; Kungl, A. J., Investigating the effect of VEGF glycosylation on glycosaminoglycan binding and protein unfolding. *Biochemical and Biophysical Research Communications* **2006,** 340, 836-839.
343. Saksela, O.; Rifkin, D. B., Release of Basic Fibroblast Growth Factor-Heparan Sulfate Complexes from Endothelial Cells by Plasminogen Activator-mediated Proteolytic Activity. *The Journal of Cell Biology* **1990,** 110, 767-775.
344. Ishai-Michaeli, R.; Eldor, A.; Vlodavsky, I., Heparanase activity expressed by platelets, neutrophils, and lymphoma cells releases active fibroblast growth factor from extracellular matrix. *Cell Regulation* **1990,** 1, 833-842.
345. Salbach, P. B.; Brueckmann, M.; Turovets, O.; Kreuzer, J.; Kuebler, W.; Walter-Sack, I., Heparin-mediated selective release of hepatocyte growth factor in humans. *British Journal of Clinical Pharmacology* **2000,** 50, 221-226.
346. Yayon, A.; Klagsbrun, M.; Esko, J. D.; Leder, P.; Ornitz, D. M., Cell Surface, Heparin-like Molecules Are Required for Binding of Basic Fibroblast Growth Factor to Its High Affinity Receptor. *Cell* **1991,** 64, 841-848.
347. Hamma-Kourbali, Y.; Vassy, R.; Starzec, A.; Le Meuth-Metzinger, V.; Oudar, O.; Bagheri-Yarmand, R.; Perret, G.; Crepin, M., Vascular Endothelial Growth Factor 165 ($VEGF_{165}$) Activities Are Inhibited by Carboxymethyl Benzylamide Dextran That Competes for Heparin Binding to $VEGF_{165}$ and $VEGF_{165}$-KDR Complexes. *The Journal of Biological Chemistry* **2001,** 276, (43), 39748-39754.
348. Rouet, V.; Hamma-Kourbali, Y.; Petit, E.; Panagopoulou, P.; Katsoris, P.; Barritault, D.; Canielle, J.-P.; Courty, J., A Synthetic Glycosaminoglycan Mimetic Binds Vascular Endothelial Growth Factor and Modulates Angiogenesis. *The Journal of Biological Chemistry* **2005,** 280, (38), 32792-32800.
349. Davies, P. F.; Robotewskyj, A.; Griem, M. L., Quantitative Studies of Endothelial Cell Adhesion: Directional Remodeling of Focal Adhesion Sites in Response to Flow Forces. *Journal of Clinical Investigations* **1994,** 93, 2031-2038.
350. Jockusch, B. M.; Bubeck, P.; Giehl, K.; Kroemker, M.; Moschner, J.; Rothkegel, M.; Ruediger, M.; Schlueter, K.; Stanke, G.; Winkler, J., The Molecular Architecture of Focal Adhesions. *Annual Review of Cell and Developmental Biology* **1995,** 11, 379-416.
351. Burridge, K.; Chrzanowska-Wodnicka, M., Focal Adhesions, Contractility, and Signaling. *Annual Review of Cell and Developmental Biology* **1996,** 12, 463-519.
352. Bacakova, L.; Filova, E.; Rypacek, F.; Svorcik, V.; Stary, V., Cell Adhesion on Artificial Materials for Tissue Engineering. *Physiological Research* **2004,** 53, S35-S45.
353. Oezyuerek, Z.; Franke, K.; Nitschke, M.; Schulze, R.; Simon, F.; Eichhorn, K.-J.; Pompe, T.; Werner, C.; Voit, B., Sulfated glyco-block copolymers with specific receptor and growth factor binding to support cell adhesion and proliferation. *Biomaterials* **2009,** 30, 1026-1035.
354. Kubota, Y.; Kleinman, H. K.; R., M. G.; Lawley, T. J., Role of laminin and basement membrane in the morphological differentiation of human endothelial cells into capillary-like structures. *Journal of Cell Biology* **1988,** 107, 1589-1598.
355. Lawley, T. J.; Kubota, Y., Induction to morphologic differentiation of endothelial cells in culture. *Journal of Investigative Dermatology* **1989,** 93, 59S-61S.
356. Kanzawa, S.; Endo, H.; Shioya, N., Improved *in vitro* angiogenesis model by collagen density reduction and the use of type III collagen. *Annals of Plastic Surgery* **1993,** 30, 244-251.
357. Donovan, D.; Brown, N. J.; Bishop, E. T.; Lewis, C. E., Comparison of three in vitro human "angiogenesis" assays with capillaries formed in vivo. *Angiogenesis* **2001,** 4, (2), 113-121.
358. Yarrow, J. C.; Perlman, Z. E.; Westwood, N. J.; Mitchison, T. J., A high-throughput cell migration assay using scratch wound healing, a comparison of image-based readout methods. *BMC Biotechnology* **2004,** 4, 21-30.
359. Boyden, S., The chemotactic effect of mixtures of antibody and antigen on polymorphonuclear leukocytes. *Journal of Experimental Medicine* **1962,** 115, 453-466.

360. Soga, N.; Namba, N.; McAllister, S.; Cornelius, L.; Teitelbaum, S. L.; Dowdy, S. F.; Kawamura, J.; Hruska, K. A., Rho Family GTPases Regulate VEGF-Stimulated Endothelial Cell Motility. *Experimental Cell Research* **2001,** 269, 73-87.
361. Mastyugin, V.; McWhinnie, E.; Labow, M.; Buxton, F., A Quantitative High-Throughput Endothelial Cell Migration Assay. *Journal of Biomolecular Screening* **2004,** 9, (8), 712-718.
362. Shamloo, A.; Ma, N.; Poo, M.-m.; Sohn, L. L.; Heilshorn, S. C., Endothelial cell polarization and chemotaxis in a microfluidic device. *Lab on a Chip* **2008,** 8, 1292-1299.
363. Barkefors, I.; Le Jan, S.; Jokobsson, L.; Hejll, E.; Carlson, G.; Johansson, H.; Jarvius, J.; Park, J. W.; Jeon, N. L.; Kreuger, J., Endothelial cell migration in stable gradients of VEGFA and FGF2: Effects on chemotaxis and chemokinesis. *The Journal of Biological Chemistry* **2008,** 283, (20), 13905-13912.
364. Burdick, J. A.; Khademhosseini, A.; Langer, R., Fabrication of Gradient Hydrogels Using a Microfluidics/Photopolymerization Process. *Langmuir* **2004,** 20, 5153-5156.
365. Smith, J. T.; Tomfohr, J. K.; Wells, M. C.; Beebe, T. P.; Kepler, T. B.; Reichert, W. M., Measurement of Cell Migration on Surface-Bound Fibronectin Gradients. *Langmuir* **2004,** 20, 8279-8286.
366. Liu, L.; Ratner, B. D.; Sage, E. H.; Jiang, S., Endothelial Cell Migration on Surface-Density Gradients of Fibronectin, VEGF, or Both Proteins. *Langmuir* **2007,** 23, 11168-11173.
367. Gerhardt, H.; Golding, M.; Fruttiger, M.; Ruhrberg, C.; Lundkvist, A.; Abramsson, A.; Jeltsch, M.; Mitchell, C.; Alitalo, K.; Shima, D.; Betsholtz, C., VEGF guides angiogenic sprouting utilizing endothelial tip cell filopodia. *The Journal of Cell Biology* **2003,** 161, (6), 1163-1177.
368. Benndorf, R. A.; Schwedhelm, E.; Gnann, A.; Taheri, R.; Kom, G.; Didie, M.; Steenpass, A.; Erguen, S.; Boeger, R. H., Isoprostanes Inhibit Vascular Endothelial Growth Factor Induced Endothelial Cell Migration, Tube Formation, and Cardiac Vessel Sprouting In Vitro, As Well As Angiogenesis In Vivo via Activation of the Thromboxane A 2 Receptor: A Potential Link Between Oxidative Stress and Impaired Angiogenesis. *Circulation Research* **2008,** 103, 1037-1046.
369. Tufro, A., VEGF Spatially Directs Angiogenesis during Metanephric Development *in Vitro*. *Developmental Biology* **2000,** 227, 558-566.